Carbon dynamics in deeply weathered forest and cropland soils of the humid African Tropics – A geochemical perspective

2025 | Mario Reichenbach

Universität
Augsburg
University

Universität
Augsburg
University

Universität Augsburg

Fakultät für Angewandte Informatik – Institut für Geographie

Carbon dynamics in deeply weathered forest and cropland soils of the humid African Tropics – A geochemical perspective

Kumulative Dissertation zur Erlangung des akademischen Grades "doctor rerum naturalium" (Dr. rer. nat.) in der Wissenschaftsdisziplin Klima- & Umweltwissenschaften am Institut für Geographie der Fakultät für Angewandte Informatik der Universität Augsburg

vorgelegt von:

Mario Reichenbach, M.Sc.

geboren in Heppenheim a. d. Bergstraße, Deutschland

2025

Gutachter:

Prof. Dr. Peter Fiener
Boden- & Wasserressourcenforschung
Institut für Geographie
Universität Augsburg

Prof. Dr. Sebastian Dötterl
Professur für Bodenressourcen
Departement Umweltsystemwissenschaften
ETH Zürich

Ort und Tag der Disputation:
Augsburg: 31.03.2025

Mario Reichenbach

Carbon dynamics in deeply weathered forest and cropland soils of the humid African Tropics – A geochemical perspective, 2025

“Omuganda agamba tosobola ku kulugusa ttaka kwo yimilidde atte nosigala nga okya yimiridde.”
("The baganda say that you can’t erode the land you are standing on and remain standing.")

Bagandian proverb from Uganda

Preface

"Okay guys, good luck and see you in a few months!" This was the farewell of our supervisor before he drove away leaving us behind on the road somewhere in Nyungwe Forest in Rwanda. It was heavily raining and not the most comfortable moment. "Well", one of my colleagues said, "we should walk along the road until we see other people waiting for a bus which will pass by... maybe." So, we walked along the road and eventually found some people waiting for something and after a while – to my surprise – a small bus arrived. We were heading towards the border to the Democratic Republic of the Congo where we would start our field campaign in the mountain rainforests of Kahuzi-Biega. The bus ride was quite an experience as the bus driver took the serpentines full speed on a wet and slippery road. I felt a bit uncomfortable and so did the guy sitting behind me who unfortunately started puking. That was the start of my PhD journey, which was by far one of the toughest yet most amazing experiences. It led me to the forests and croplands of the DR Congo, Rwanda and Uganda, where I got to know the people and their way of life. This PhD tries to contribute more knowledge about the soil under our feet, especially in a region ridden by armed conflicts where people are heavily dependent on the land for their livelihoods and, at the same time, face rapid environmental and societal changes that threaten soil health and food security. My motivation pursuing a PhD stems from the desire to do my part – as little as it is – to raise awareness for the need to protect Africa's soil resources and to face the environmental challenges of the 21st century.

Acknowledgements

"There is no such thing as a self-made man. You will reach your goals only with the help of others." – George Shinn

I realized during the past 5 – 6 years that earning a PhD is like running a marathon on uneven ground. You fall flat on your face multiple times but you get back on your feet and carry on to reach the finish line little by little. While I brought the stubbornness with me, other way smarter people than me helped me with their expertise, ressources, guidance and friendship to head into the right direction. This PhD is the result of teamwork and many people helped me to actually accomplish this incredible milestone.

First of all, I'd like to thank my supervisors Peter Fiener and Sebastian Dötterl for all your immense mentorship, feedback and constructive criticism during field campaigns, lab work and writing science. I learned a lot from you, which helped me tremendously to cultivate my critical thinking and grow as a scientist. I highly appreciate that both of you have kept a door open for me to finish my PhD, while I wandered off to arctic and antarctic regions. Thank you!

This thesis was funded in the framework of Deutsche Forschungsgemeinschaft (DFG) Emmy Noether group through TROPSOC (project no. 387472333).

Next, I would like to thank the team of the Soil Resources Group at ETH Zürich, especially Marco Griepentrog, who helped me analyze my samples.

I´d like to express my deepest gratitude to my colleagues and friends Benjamin Bukombe, Laurent Kidinda and Daniel Muhindo. Guys, without you nothing of this would have been possible and we have some stories to tell. We did it! A thesis never reflects the ups and downs of such a journey but you can relate. A special thanks and my deepest respect to you Benji. We shared the academic foxhole and kept each other going. Also, a big hug to your lovely mom for her warm welcome and delicious food in Kigali.

A big thank you to all the colleagues at Augsburg University and the "after-work beer meetings" at Unikum. It always paid off to spend more time in the pub sharing our thoughts than we did working in the lab that day as we would bump into each other in the lab again anyway and wonder what the heck we were doing here on sundays. Thank you Alessandro Fabrizi, Ana Carolina Cugler, Annette Dietmaier, Raphael Rehm, Jake Simpson, Silvia Schrötter, Kathi Öttl, Florian Wilken and Tabea Zeyer. Especially a big thank you to Joseph Tamale for sharing the house and discussing science while drinking a “kühles Helles”.

Next, I´d like to give a huge thanks to the TropSOC team at Augsburg University. Thank you Anna Stegmann, Julia Mayrock, Moritz Mainka, Annina Maier and Robin Unseld. Without your outstanding help in the lab and with logistical and administrative work, it would have been impossible. You were fantastic!

In the same sense, I´d like to show my utmost respect to all the people during the field campaigns, especially Fernando Bamba and the helpers and rangers contributing with their local expertise and immense man and woman power to the success of the campaign. To my shame I can’t remember all your names, but rest assured that without your help the sampling campaign would have failed.

On a personal note I‘d like to express my deepest gratitude towards my wife Nana. I can’t put it into words and if I did, it wouldn’t do justice to how you supported me. All the patience and encouragement and taking care of our kids Lotte and Luise while I was hiding away in the jungle, lab or behind the desk. I don´t take it for granted having all your support. Thank you Lotte and Luise for reminding me that there is more than chasing the PhD in life. I love you!

Finally, yet importantly, I´d thank my mum and dad for all the traveling we did during my childhood. All those early experiences fostered my genuine curiosity for the world around me and still keeps me exploring. Lastly, a big thanks to my brother Domi, who reminded me that playing video games, enjoying gin and whiskey and going to Rammstein concerts is also important in life.

Dedication

I dedicate this work to my wife Nana and our two lovely daughters Lotte and Luise and to all the mind-like people who take actions grounded in reason when it comes to climate change, biodiversity loss and sustainability.

Summary

African tropical soils play a pivotal role in global biogeochemical cycles due to the carbon (C) they store and their support of one of the most productive terrestrial ecosystems worldwide. Multiple socio-economic factors (e.g. rapid population growth, increase in income and consumption per person, expansion of road infrastructure to explore resources, arable land producing for the international market) in tropical Africa has led to a hotspot of modern-day land use change from old-growth forest to cropland, with potentially irreversible changes to soil geochemical properties and health. These properties, in turn, influence the conditions under which C is stabilized in soils. Our understanding of the relationships between C stabilization and geochemical properties is largely derived from studies conducted in temperate regions and tropical regions of America and Asia. However, due to profound differences in climate, landform, local parent material and soil development, the applicability of this knowledge to tropical Africa is limited. This gap in knowledge of the relationship between mineral C stabilization and geochemical properties and the mechanistic controls on C cycling in these soils constrains our ability to predict C cycling. This thesis aims to present new insights on this topic and provide directions on where future research can focus.

The thesis is based on experimental (field and laboratory) studies conducted at various sites within the Eastern Congo Basin and along the Albertine Rift Valley System. It has three major parts: (i) Understanding how the geochemical properties of soil, originating from diverse parent material along a natural forest catena, influence soil organic carbon (SOC) stocks, soil C fractions, and the mechanisms involved in C stabilization; (ii) analyzing how parent material mineralogy and its weathering status impact SOC stocks and soil C turnover after land conversion from tropical forest to cropland on stable landscape positions; and (iii) understanding the impact of lateral soil fluxes on SOC stocks and turnover in sloping and geochemically diverse cropland systems. Specifically, the thesis focused on three contrasting geochemical regions (mafic magmatic rocks, felsic magmatic and metamorphic rocks together with volcanic ashes and a mixture of sedimentary rocks).

The first major part, presented in chapter 3, assessed SOC stocks, soil C fractions and the soil $\Delta^{14}C$ across geochemical and topographic gradients in pristine rainforests. The findings indicated minimal topographical impact on SOC variables regarding soil fluxes along slopes. However, geochemical soil properties emerged as key explanatory factors. The influence of these variables on SOC is closely linked to reactive mineral surfaces dependent on parent material composition. The greater availability of reactive surfaces favors sorptive C stabilization and the formation of stable aggregates, consequently leading to higher SOC stocks. Variations in the distribution of C associated with microaggregates and the free silt and clay fractions were notably different across geochemical regions and correlated with pedogenic oxide content. This underscores the role of pedogenic oxides in tropical soil aggregate formation, linking two of the most important mineral-related carbon stabilization mechanisms to geochemical variability inherited from parent material.

The second major part, presented in chapter 4, evaluated the factors influencing SOC dynamics across geochemical gradients and different land uses (forest versus cropland) at stable plateau positions without erosion. While the controls on SOC stocks and turnover vary across geochemical regions, the overall SOC stocks remain similar despite land use change. Due to the prolonged weathering of these tropical soils, they lack sufficient reactive minerals to stabilize the higher C inputs from forests. This highlights the absence of SOC losses related to land conversion and the prevalence of weakly bound, relatively young, and accessible SOC in these soils.

The third major part, presented in chapter 5, focused on the influence of lateral soil fluxes on SOC stocks and turnover in sloping and geochemically diverse cropland systems. This study demonstrates that the distribution of SOC stocks in cropland does not consistently align with the conventional topography-driven patterns that are typically attributed to soil redistribution. SOC stocks in eroding positions are similar to those in non-eroding landscape positions and the recent accumulation of eroded topsoil material at footslopes only slightly increases SOC stocks but presents a potentially substantial yet fragile C sink. In parallel, soil degradation initiates a disruption of the C cycle on numerous hillslopes in the region, although not all.

Overall, the results of the thesis demonstrate that, even in deeply weathered tropical soils, parent material has a long-lasting effect on soil geochemistry that can affect (i) SOC stocks, mineral C stabilization and soil microaggregation under natural forest systems. However, the same endmember mineralogy (ii) limits the potential of the investigated soils to stabilize plant C inputs as SOC for long-term and (iii) and minimizes effects of soil erosion on SOC stocks and stabilization. Therefore, soil parent material and its controls on soil geochemistry needs to be taken into account to predict SOC stocks and turnover and to understand mineral C stabilization mechanisms across disturbance gradients of land conversion and soil erosion in the humid African Tropics.

Zusammenfassung

Die tropischen Böden Afrikas spielen eine zentrale Rolle im globalen biogeochemischen Kreislauf, da sie Kohlenstoff (C) speichern und eines der produktivsten terrestrischen Ökosysteme weltweit unterstützen. Mehrere sozioökonomische Faktoren (z. B. rasches Bevölkerungswachstum, Anstieg des Einkommens und des Pro-Kopf-Verbrauchs, Ausbau der Straßeninfrastruktur zur Erschließung von Ressourcen, Anbauflächen für den internationalen Markt) in den tropischen Regionen Afrikas haben zu einem Hotspot des modernen Landnutzungswandels von Regenwäldern hin zu Ackerland geführt, der potenziell irreversiblen Veränderungen der geochemischen Eigenschaften und der Gesundheit der hiesigen Böden zur Folge hat. Die genannten Eigenschaften wirken sich wiederum auf die Stabilisierungsbedingungen von C in Böden aus. Unser Wissen über die Zusammenhänge zwischen der Stabilisierung von C und den geochemischen Eigenschaften stammt weitgehend aus Studien, die in gemäßigten und tropischen Regionen Amerikas und Asiens durchgeführt wurden. Aufgrund der signifikanten Unterschiede in Bezug auf Klima, Landform, lokales Ausgangsmaterial und Bodenentwicklung ist die Anwendbarkeit dieses Wissens auf das tropische Afrika jedoch begrenzt. Diese Wissenslücke bezüglich der Beziehung zwischen mineralischer C-Stabilisierung und geochemischen Eigenschaften sowie über die mechanistische Steuerung des C-Kreislaufs in diesen Böden schränkt unsere Möglichkeiten zur Vorhersage des C-Kreislaufs stark ein. Das Ziel dieser Arbeit besteht in der Gewinnung neuer Erkenntnisse hinsichtlich der C-Stabilisierung an reaktiven Mineralen in stark verwitterten Böden sowie der Aufzeigung von möglichen zukünftigen Forschungsschwerpunkten.

Die vorliegende Arbeit basiert auf umfassenden empirischen Feld- und Laborarbeiten an unterschiedlichen Standorten im östlichen Kongobecken und entlang des Albertine-Grabensystems, die sich durch unterschiedliche geochemische und topographische Standortbedingungen auszeichnen. Im Rahmen der vorliegenden Studien werden folgende Aspekte untersucht: (i) Es wird untersucht, wie die geochemischen Eigenschaften des Bodens, die aus unterschiedlichem Ausgangsmaterial entlang einer Waldkatena stammen, den Bestand an organischem Kohlenstoff (SOC) im Boden, die C-Fraktionen im Boden und die an der C-Stabilisierung beteiligten Mechanismen beeinflussen. (ii) Es wird untersucht, wie sich die Mineralogie des Ausgangsmaterials und dessen Verwitterungsstatus auf den SOC-Bestand und den C-Umsatz im Boden nach der Umwandlung von Tropenwald in Ackerland an stabilen Landschaftspositionen auswirkt. (iii) Zudem wird der Einfluss der lateralen Bodenverlagerung auf den SOC-Bestand und den Umsatz in steilen und geochemisch vielfältigen Ackerlandschaften analysiert. Im Fokus dieser Arbeit stehen drei geochemisch unterschiedliche Regionen: Mafische magmatische Gesteine, felsische magmatisch-metamorphe Gesteine zusammen mit vulkanischen Aschen sowie ein Gemisch aus Sedimentgesteinen.

In Kapitel 3 wurden die SOC-Vorräte, die C-Fraktionen im Boden und das Δ^{14}C im Boden über geochemische und topographische Gradienten in unberührten Regenwäldern untersucht. Die Resultate legen nahe, dass die Topographie nur einen geringen Einfluss auf die SOC-Variablen in Bezug auf Bodenverlagerung entlang der Hänge ausübt. Allerdings konnten geochemische Bodeneigenschaften als wichtige Erklärungsfaktoren identifiziert werden. Der Einfluss dieser Variablen auf den SOC-Bestand steht in engem Zusammenhang mit reaktiven mineralischen Oberflächen, deren Zusammensetzung maßgeblich von der Ausgangsmaterialzusammensetzung und dem Verwitterungszustand abhängt. Die größere Verfügbarkeit reaktiver Oberflächen fördert die sorptive C-Stabilisierung sowie die Bildung stabiler Aggregate, was letztlich zu einer Zunahme der SOC-Vorräte führt. Die Verteilung von C, das mit Mikroaggregaten und den freien Schluff- und Tonfraktionen assoziiert ist, wies in den verschiedenen geochemischen Regionen bemerkenswert unterschiedliche Variationen auf, welche mit dem pedogenen Oxidgehalt korrelierten. Dies unterstreicht die Relevanz pedogener Oxide bei der Bildung tropischer Bodenaggregate und verknüpft zwei der wichtigsten mineralischen Kohlenstoffstabilisierungsmechanismen mit der geochemischen Variabilität des Ausgangsmaterials.

In Kapitel 4 wurden die Faktoren bewertet, die die SOC-Dynamik an erosionsfreien Plateaustandorten über geochemische Gradienten und kontrastierende Landnutzungen (Wald- und Ackerland) hinweg beeinflussen. Während die Einflussfaktoren auf die SOC-Bestände und den SOC-Umsatz in den verschiedenen geochemischen Regionen unterschiedlich sind, bleiben die SOC-Bestände trotz der veränderten Landnutzung insgesamt ähnlich. Aufgrund der fortgeschrittenen Verwitterung dieser tropischen Böden fehlt es ihnen an ausreichenden reaktiven Mineralen, um die höheren C-Einträge aus den Wäldern zu stabilisieren. Dies unterstreicht das Fehlen von SOC-Verlusten im Zusammenhang mit der Landumwandlung und das Vorherrschen von schwach gebundenem, relativ jungem und mikrobiell zugänglichem SOC in diesen Böden.

In Kapitel 5 wurde der Einfluss von lateralen Bodenverlagerungen auf den SOC-Bestand und -Umsatz in steilen und geochemisch vielfältigen Ackerlandschaften untersucht. Die vorliegende Studie demonstriert, dass die Verteilung der SOC-Bestände in Ackerland nicht durchgängig mit den konventionellen, durch die Topographie bedingten Mustern übereinstimmt, die üblicherweise der lateralen Umverteilung des Bodens zugeschrieben werden. Die SOC-Bestände in erodierten Lagen zeigen eine ähnliche Tendenz wie in nicht erodierten Landschaftslagen. Die jüngste Akkumulation von erodiertem Oberbodenmaterial an den Fußhängen führt zu einer geringfügigen Erhöhung der SOC-Bestände, stellt jedoch eine potenziell beträchtliche, wenn auch fragile C-Senke dar. Gleichzeitig führt die Bodendegradation zu einer Unterbrechung des C-Zyklus in zahlreichen, wenn auch nicht allen, Hanglagen der Region.

Die Ergebnisse dieser Arbeit zeigen, dass das Ausgangsmaterial selbst in tief verwitterten tropischen Böden einen lang anhaltenden Einfluss auf die Bodengeochemie hat. Dieser Einfluss (i) kann die SOC-Vorräte, die mineralische C-Stabilisierung und die Mikroaggregation des Bodens in natürlichen Waldsystemen beeinflussen. Die Mineralogie des Ausgangsmaterials limitiert jedoch (ii) das Potenzial der untersuchten Böden, pflanzliche C-Einträge als SOC langfristig zu stabilisieren, und (iii) minimiert die Auswirkungen der Bodenerosion und -akkumulation auf die SOC-Bestände und die mineralische Kohlenstoffstabilisierung. Daher ist es erforderlich, das Ausgangsmaterial des Bodens und dessen Einfluss auf die Bodengeochemie zu berücksichtigen, um die SOC-Bestände und deren Umsatzrate vorherzusagen und die Stabilisierungsmechanismen von organischem Kohlenstoff entlang Störungsgradienten der Landumwandlung und Bodenerosion in den afrikanischen Feuchttropen zu verstehen.

Contents

Chapter 1

General introduction and theoretical background

1.1 The relevance of tropical soils in the global carbon cycle

"Human activity on the African continent will potentially cause irreversible changes to soil properties and the services they provide to the global biosphere on the scale of centuries and millennia." – (Doetterl *et al.*, 2021c)

With storing more organic carbon (OC) than the atmosphere and plants combined (global SOC stock at depths of 3 m: ~2770 Pg C) (Jackson *et al.*, 2017), soils represent the largest biogeochemically active terrestrial soil organic carbon (SOC) pool on earth (Amundson, 2001). The ability to sequester CO_2 is a key function of soils (Bossio *et al.*, 2020; Köchy *et al.*, 2015; Kpemoua *et al.*, 2023; Rodríguez-Albarracín *et al.*, 2023; Rumpel *et al.*, 2020; Wiesmeier *et al.*, 2019). Small changes of global SOC fluxes can substantially alter atmospheric CO_2 concentration therefore mitigating or amplifying anthropogenic climate change (Luo *et al.*, 2020b; Wang *et al.*, 2019b). However, increasing global pressure on soil resources are threatening their ecosystem functions and pertubating the global carbon (C) cycle (Jackson *et al.*, 2017; Naipal *et al.*, 2018; Sanderman *et al.*, 2017) leading to a downward spiral towards degraded soils and to severe consequences for climate, food security and socio-economic circumstances (Kraamwinkel *et al.*, 2021).

Especially tropical forest ecosystems are considered as potential tipping points for the climate – carbon feedback due to their significant impact on continental precipitation patterns (Kumagai *et al.*, 2004; Lan *et al.*, 2016) and their substantial C storage in the biosphere, fast C turnover and its potential loss to the atmosphere (Schimel *et al.*, 2015). Tropical soils account for more than one-third of the world's land area (Palm *et al.*, 2007), are estimated to contain one-third of global SOC (Köchy *et al.*, 2015) and serve as a substrate for one of the most productive ecosystems worldwide (Cusack and Marín-Spiotta, 2019). At the same time, the African Tropics together with the Amazonian rainforest are among the most dynamic regions worldwide characterized by modern day land use change (Ren *et al.*, 2020) and deforestation both advancing at a fast pace (Hansen *et al.*, 2013), which potentially changes soil´s ability to store C (Veldkamp *et al.*, 2020). As a consequence, tropical soils account for almost 50 % of total global C loss (Padarian *et al.*, 2022) while associated CO_2 fluxes to the atmosphere are fueling global warming (Berkowitz, 2020; Cusack and Marín-Spiotta, 2019; Nottingham *et al.*, 2020).

Despite their key relevance for the cycling of C and nutrients between plants, soils and the atmosphere, deeply weathered tropical soils, especially in tropical Africa, are also the least studied regarding the biogeochemical drivers of SOC stocks and stabilization (Castillo-Figueroa, 2021; Doetterl *et al.*, 2016; Nottingham *et al.*, 2022; Schimel *et al.*, 2015). Therefore, a comprehensive understanding of how C stabilization drives C stocks and soil C turnover and how this interacts with land conversion in a landscape context covering geomorphic, geochemical and pedological factors is essential. It is not clear to what extent deeply weathered soils developed from contrasting parent material differ in their impact on soil mineral reactivity let alone mineral C stabilization mechanisms. The response of tropical soils to disturbances by erosion and land conversion remains another great uncertainty in explaining and predicting global C cycling. Such insights will improve our mechanistic understanding of C stabilization in rapidly changing soil ecosystems of Tropical Africa.

1.2 Understanding tropical soils

1.2.1 Stabilization of organic carbon in mineral soils

> *"The vast majority of organic carbon in the biosphere (...) occurs at solid earth interfaces in close spatial proximity to some form of mineral matter. For this reason, carbon flowing through the biosphere will, at some point, almost inevitably come into contact with mineral surfaces, as it undergoes the many transformations inherent in the carbon cycle."* – (Kleber *et al.*, 2021)

The prevailing environmental conditions within the soil matrix provide the framework in which all other interactions between SOC, microorganisms and soil minerals occur (Doetterl *et al.*, 2016). For example, soil water content and aeration conditions determine the amount of mineralizable C (Barcellos *et al.*, 2018; Chen *et al.*, 2020; Thompson *et al.*, 2006). Especially soil temperature (Davidson and Janssens, 2006; Feng *et al.*, 2017) is a key control on soil microbial activity with higher decomposition rates of SOC generally driven by increasing temperature (Liu *et al.*, 2018; Nottingham *et al.*, 2018; Nottingham *et al.*, 2022; Nottingham *et al.*, 2020). The environmental controls together with substrate quality further controls microbial activity and the amount of microbial biomass (Jagadamma *et al.*, 2014; Xu *et al.*, 2014). Consequently, these conditions modulate the rate of C turnover and mineralization, ultimately governing C sequestration (Angers *et al.*, 2022).

The potential of soils to sequester C relies on a spectrum of soil geochemical attributes, such as mineralogical composition, texture and nutrients. In general, SOC is stabilized against microbial decomposition on a decadal up to a millennial timescale (Trumbore, 2009; Trumbore, 2000) by several interacting mechanisms (Basile-Doelsch *et al.*, 2020): Certain C compounds like pyrogenic or aliphatic C are resistant against decomposition due their complex molecular structure and can remain stable over decades to centuries (Knicker, 2011; Mikutta *et al.*, 2006; Singh *et al.*, 2012). Also, the decomposition of fossil organic carbon (FOC) found in subsoils overlaying sedimentary rocks is an energy-demanding process for microbes, resulting in long turnover times (Grant *et al.*, 2023; Kalks *et al.*, 2021; Voort *et al.*, 2019).

However, recent studies challenge the assumption that the chemical structure alone implies slower turnover times (Kleber *et al.*, 2011). Instead, studies highlight the interaction between the mineral phase and SOC as another important stabilization process (Finke *et al.*, 2019; Heckman *et al.*, 2018; Hemingway *et al.*, 2018; Mainka *et al.*, 2022; Rodríguez-Albarracín *et al.*, 2023; Weng *et al.*, 2018). Especially the availability of reactive mineral surfaces drives the formation of organo − mineral associations (Kleber *et al.*, 2021; Mikutta *et al.*, 2019; Possinger *et al.*, 2020). Clay minerals primarily provide these reactive minerals (Islam *et al.*, 2022; Singh *et al.*, 2019; Six *et al.*, 2002a; Six *et al.*, 2002b) alongside secondary hydro (oxy) oxides (Kramer and Chadwick, 2018). The adsorption of SOC onto hydro (oxy) oxides is regulated by the specific surface area (Feng *et al.*, 2014; Guggenberger and Kaiser, 2003; Kaiser and Guggenberger, 2007; Song *et al.*, 2022) and crystallinity (Hall *et al.*, 2018) of minerals, creating diverse interactions with minerals that adsorb C onto their surface, fostering conditions for subsequent organic reactions and stabilization mechanisms (Kleber *et al.*, 2021).

Reactive and adsorptive surfaces not only contribute to mineral C stabilization but also promote the formation of soil aggregates (Chenu and Plante, 2006; Lehmann *et al.*, 2007; Ozlu and Arriaga, 2021; Torres-Sallan *et al.*, 2017) via chemical processes (e.g. adsorption, co-precipitation and complexation) together with biological (e.g. bioturbation by soil flora and fauna) and physical processes (e.g. shrinking and swelling of clay minerals) (Totsche *et al.*, 2018). These soil aggregates show a hierarchical spatial organization (Waters and Oades, 1991), wherein SOC is physically stabilized within macroaggregate (>250 µm) through encapsulation. Simultaneously, microaggregates (20 – 250 µm) form within macroaggregates, featuring incrustations of SOC with clay-sized minerals and microbial products, facilitating long-term stabilization (Arachchige *et al.*, 2018; Simpson *et al.*, 2004; Six *et al.*, 2000a; Six *et al.*, 2000b).

1.2.2 Mineral C stabilization in deeply weathered tropical soils – Profoundly different to temperate soils

> *"A third of global soil C is held in the tropics and is distributed among a very wide range of parent materials, ages, geomorphology and landforms (...). Tropical soils are, however, often generalised as being strongly weathered, a result of a warm humid climate and because they were largely unaffected by recent glaciation (...)."* – (Nottingham *et al.*, 2022)

Given that most of the research on C stabilization is derived from temperate soils of the Northern Hemisphere (Schimel *et al.*, 2015), there's legitimate skepticism regarding the direct applicability of these mechanisms to tropical soils. This doubt arises from substantial differences in their formation and weathering history (Denef *et al.*, 2004; Six *et al.*, 2002a; Six *et al.*, 2002b). Temperate soils often originate from young (peri)glacial sediments of Pleistocene age and relatively unweathered bedrock (approximately 15,000 years old). In contrast, tropical soils have often experienced chemical weathering for millions of years without significant environmental disturbances (Finke and Hutson, 2008; Porder *et al.*, 2005).

Consequently, most temperate soil systems are primarily characterized by minerals at intermediate weathering stages that show high capacities for absorbing water, nutrients, and SOC (Begill *et al.*, 2023; Georgiou *et al.*, 2022; Schneider *et al.*, 2010). Additionally, these systems are dominated by primary minerals as the soil approaches the weathering front towards the parent material, typically located between 1 to 3 meters below the surface in well-developed soils (Hunter *et al.*, 2023; Šamonil *et al.*, 2020).

Conversely, deeply weathered tropical systems are dominated by end-member minerals such as 1 : 1 clays (e.g., kaolinite) and highly crystalline iron (Fe) oxyhydroxides and Fe oxides. These minerals show lower potential for organic matter sorption, reduced reactivity to induce further weathering, and subsequently lower fertility indicators (Ashida *et al.*, 2021; Barré *et al.*, 2014; Doetterl *et al.*, 2018; Ito and Wagai, 2017). These deeply weathered minerals often prevail across several meters of subsoil (Schaefer *et al.*, 2022), resulting in a more extensive expanse of infertile soil above the remaining saprolite and bedrock layers compared to most temperate systems.

While the general types of stabilization against microbial decomposition in tropical soils are likely similar to those in temperate soils, their relative importance and prevalence may significantly differ. In kaolinitic tropical soils, organomineral complexes, particularly those linked with amorphous short-range-ordered (SRO) pedogenic oxides, stand out as the primary mechanism for mineral C stabilization (Coward *et al.*, 2017; Fromm *et al.*, 2021; Fromm *et al.*, 2024b; Heckman *et al.*, 2018; Heckman *et al.*, 2009; Martinez and Souza, 2020). These complexes play a crucial role, considered an intermediary step pivotal for long-term C stabilization (Coward *et al.*, 2018; Heckman *et al.*, 2018) and in slowing down C turnover (Heckman *et al.*, 2018; Heckman and Rasmussen, 2018; Kramer *et al.*, 2012). Conversely, pyrophosphate extractable oxides are often regarded as weak agents in stabilizing C against microbial decomposition (Heckman *et al.*, 2018; Lawrence *et al.*, 2015; Paul *et al.*, 2008), representing a readily available C pool for microorganisms (Bukombe *et al.*, 2021; Heckman *et al.*, 2009). Consequently, differences in mineralogy not only impact key soil fertility parameters but also influence how C is stabilized onto minerals, thereby influencing the interplay among mineral reactivity, microbial community structures, and nutrient dynamics (Doetterl *et al.*, 2018; Kidinda *et al.*, 2023; Kidinda *et al.*, 2022; Six *et al.*, 2002a; Six *et al.*, 2002b).

For instance, Fe-oxides like hematite can incorporate substantial amounts of alumina (Al) within a kaolinite-rich soil matrix through substitution (Tardy and Nahon, 1985). Such (hydro)oxides of Al and Fe serve as cementing agents in forming pseudosands and microaggregates (Kirsten *et al.*, 2021a; Kirsten *et al.*, 2021b), with their chemical composition regulated by the geochemistry of the parent material. Within these pseudosand structures and highly stable soil aggregates, the concurrent and efficient stabilization of SOC takes place through mineral-organic complexes (Martinez and Souza, 2020; Quesada *et al.*, 2020). Kaolinitic soils have the ability to rapidly form aggregates independent of biological processes owing to electrostatic interactions between $1:1$ clay minerals and oxides. Additionally, soils in humid tropical regions experience fluctuating redox potential due to alternating dry and wet seasons (Barcellos *et al.*, 2018; Liptzin *et al.*, 2011). This, coupled with high Fe content, further promotes the formation of stable aggregates (Giannetta *et al.*, 2022; Thompson *et al.*, 2006; Tong *et al.*, 2016). These stable Fe and Al-rich concretions and aggregations are prominent physico-chemical features observed and identified in numerous tropical soils (Cooper *et al.*, 2005; Zotarelli *et al.*, 2005).

Consequently, based on the local edaphic settings and the stage of soil development, similar proxies for mineral C stabilization may represent a varying mix of mechanisms (Kleber *et al.*, 2021). Minerals can act as a sorbent or reactant for associated SOC resulting in diverse bonding mechanisms with varying strength of absorptive interactions (Cusack *et al.*, 2013; Kleber *et al.*, 2021). The distinct different mineralogy and reactivity of tropical soils (Doetterl *et al.*, 2015b; Tang and Riley, 2015) compared to temperate soils may result in different responses to environmental disturbances such as land conversion and soil erosion, particularly concerning mineral C stabilization. In addition to contrasting soil mineralogical settings, markedly different environmental conditions between tropical and temperate ecosystems (e.g. temperature, precipitation, net primary production, microbial activity, vegetation patterns) result in divergent SOC stocks and turnover (Luyssaert *et al.*, 2007). However, the mechanistic processes beyond these interacting factors are poorly understood primarily due to data scarcity.

1.2.3 Impact of land conversion on tropical soil systems

> *"Loss of SOC is a well-known consequence of converting natural forest to agricultural land (...). Nevertheless, the magnitude, rates, and even the direction of the changes in SOC depend on the type of conversion and are still unclear (...)." –*
> (Guillaume *et al.*, 2015)

Increasing deforestation in the African Tropics is mainly driven by cropland expansion, especially by smallholder farmers (Tyukavina *et al.*, 2018), which accounts for 70 % to 80 % of Africa's total forest loss (Olorunfemi *et al.*, 2022). Practices like crop harvesting without applying fertilizer to replenish the nutrients removed during the process frequently lead to the degradation of nutrient-rich topsoil layers, often culminating in field abandonment after as little as a decade of cultivation (Hattori *et al.*, 2019; Heinrich *et al.*, 2021). This accelerated degradation intensifies the demand for more land and significantly contributes to the increasing trend of deforestation (Megevand, 2013). Deforestation leads to profound changes in physico-chemical soil properties and the degradation of most soil (ecosystem) functions, eventually extending its effects to deep subsoil, even decades after land conversion (Veldkamp *et al.*, 2020).

However, the response of tropical soils to land conversion depends on several interacting factors such that the magnitude, rates and direction of SOC changes differ across tropical regions (Guillaume *et al.*, 2015). Some studies show no significant changes (Kukla *et al.*, 2019; Sayer *et al.*, 2019; Tamale *et al.*, 2022) or even an increase (Kirsten *et al.*, 2019; Kirsten *et al.*, 2021b) in SOC while other studies state that in the initial years following the conversion from forest to cropland, most tropical soils experience considerable losses of SOC, ranging between 30 % and 70 % (Don *et al.*, 2011; Gregorich *et al.*, 1998; Guillaume *et al.*, 2015; Wei *et al.*, 2014). Notably, these SOC losses are not limited to topsoil and merely labile C sources, but extend to subsoil where C is predominately stabilized by minerals (Don *et al.*, 2011; Luo *et al.*, 2020a). For example, deforestation mobilizes and releases deeply stored SOC upon transitioning from natural tropical forest to agriculture, which had remained stable for millennia (Drake *et al.*, 2019; Veldkamp *et al.*, 2003).

Efforts to mitigate C loss in cropland soils, even with significant fertilizer input, cannot completely halt the decline (Laub *et al.*, 2023). The diminishing soil quality (Kihara *et al.*, 2020; Obidike-Ugwu *et al.*, 2023), coupled with alterations in soil environmental conditions (You *et al.*, 2010) and C input (Luo *et al.*, 2015), impact microbial activity (Malik *et al.*, 2018) and the chemical composition of C (Assunção *et al.*, 2019). These changes, in turn, modify the contribution of plant and microbial derived compounds and eventually the conditions necessary for C stabilization (Angst *et al.*, 2021).

The dynamics of SOC depend on a complex interplay of factors such as mineralogy, crop and soil types, management practices, and land use history (Don *et al.*, 2011; Fujisaki *et al.*, 2015). As such, predicting presumed SOC losses upon conversion from forest to cropland remains challenging across larger scales, with only a limited number of studies investigating the combined effect of geochemical properties (Kirsten *et al.*, 2021a; Kirsten *et al.*, 2019; Kirsten *et al.*, 2021b) and land use (Fromm *et al.*, 2021) on C stabilization in deeply weathered tropical soils.

Given that soil mineralogical properties, which significantly impact C stabilization and nutrient release, are largely influenced by the parent material, it's reasonable to expect that soils originating from parent materials with different mineralogy and weathering histories may respond differently to land use changes.

1.2.4 Erosional disturbances in tropical soil systems

> *"Because of the large amount and high intensity of rainfall (...) soil erosion can potentially reach dramatic levels in this region (...)."* – (Labrière *et al.*, 2015)

Lateral soil redistribution resulting from erosion changes the functionality of landscape compartments. For instance, soil erosion on hillslopes correlates with sediment accumulation in valley bottoms, where C and nutrient-rich topsoil becomes buried beneath new sediments. This process extends the residence time of C as buried soil experiences slower microbial turnover (Alcántara *et al.*, 2017; Doetterl *et al.*, 2012; Voort *et al.*, 2019). However, the erosional loss of nutrients is reducing biomass productivity (Veldkamp *et al.*, 2020) and contributing to the general degradation of tropical soils.

Soil redistribution also alters the spatio-temporal patterns of soil weathering thus reshaping the biogeochemical stage on which C stabilization takes place. Erosion not only removes weathered (top)soil from slopes but also brings the soil weathering front into closer contact with the C cycle, affecting C, nitrogen (N), and phosphorus (P) cycling, as well as the mineral-mediated stabilization of C (Berhe, 2012; Berhe *et al.*, 2012; Doetterl *et al.*, 2016; Park *et al.*, 2014).

Regarding feedback on biogeochemical cycles between soil weathering and erosion, differences arise not only between natural and disturbed systems but also among systems with varying soil mineral reactivity (Figure 1.1). While climate remains a key control on SOC dynamics on the global scale and across pedo-climatic regions (Fromm *et al.*, 2024a; Fromm *et al.*, 2024b; Georgiou *et al.*, 2022; Wasner *et al.*, 2024), recent findings emphasize that mineral reactivity, primarily dictated by soil weathering and parent material mineralogy, directly governs SOC dynamics, with climate exerting only an indirect influence through biogeochemical processes and matter fluxes (Doetterl *et al.*, 2015b; Tang and Riley, 2015; Zhao *et al.*, 2022) at least on the regional scale with less climatic variation. However, in how far soil erosion on hillslopes and accumulation in valleys in tropical soil landscapes impact biogeochemical cycling and mineral-mediated C stabilization remain unclear.

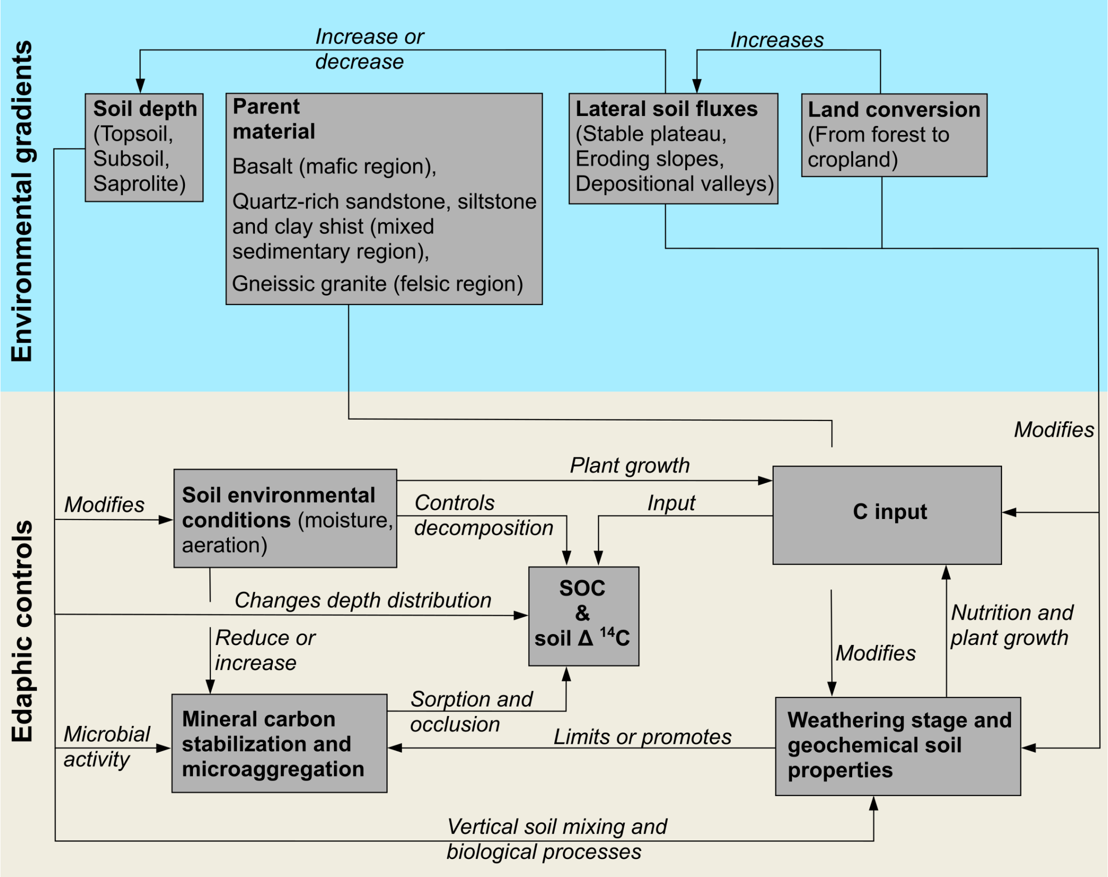

Figure 1.1: Conceptual model for investigating the links between SOC stabilization and biogeochemical properties. Interacting factors of land conversion, topography and geochemistry resulting in a complex interplay of direct and indirect relationships affecting SOC dynamics.

1.3 Research gaps in tropical soil organic carbon cycling

"We know nothing about changes in chemical weathering rates [and] biogeochemical flux rates (...)." – (Amundson, 2021)

"Tropical regions are grossly undersampled (...)." – (Schimel *et al.*, 2015)

Our understanding of the geochemical factors influencing C stabilization and turnover predominantly stems from research in temperate regions, as well as tropical South American and Asian regions. However, transferring this knowledge to tropical Africa encounters challenges due to distinct differences in climate, topography, geotectonic settings, and soil development. Consequently, despite its crucial role in global biogeochemical cycles, Tropical Africa remains one of the least explored regions, contributing to gaps in our understanding.

In detail, there is a need to understand how deeply weathered tropical soils, shaped by different parent materials and with varying mineralogical compositions, influence the mechanisms of C stabilization. While studies have highlighted the role of mineral-organic associations in temperate soils, the direct applicability and prevalence of these mechanisms in deeply weathered tropical soils remain unclear.

The effects of land conversion, especially deforestation for cropland expansion, on the stabilization of C in deeply weathered tropical soils need further investigation. Understanding the alterations in soil properties and the subsequent changes in C stabilization following land use change is crucial to give advice on how to sustainably manage these soils regarding fertility and C sequestration.

Soil erosion alters soil distribution and changes the spatio-temporal patterns of soil weathering, potentially affecting biogeochemical cycling and mineral-mediated C stabilization. However, the specific impact of erosional disturbance on these mechanisms within tropical soil systems is not yet fully understood. In a nutshell, the combined effect of geochemistry, land use and topography on mineral C stabilization needs to be further explored to fill the gap in our process-understanding of deeply weathered soils.

1.4 Research objectives, questions and hypothesis

The main objective of this research is to develop a mechanistic understanding of SOC stocks, turnover and stabilization in deeply weathered tropical African forest and cropland soils across gradients of geochemistry and geomorphology. To achieve this, the thesis is divided into three work packages focusing on specific objectives:

1.4.1 Objectives

i. To understand the influence of topography and geochemical properties of soils derived from different parent material on SOC stocks, soil C fractions and mechanisms for C stabilization within natural tropical forest soil systems. Objective 1 will be addressed in study I (see Chapter 3).

ii. To identify the effect of parent material mineralogy and its weathering status on SOC stocks and soil C turnover following land conversion from tropical forest to subsistence cropland on stable landscape positions. Objective 2 is the topic of study II (see Chapter 4).

iii. To analyze the impact of lateral soil fluxes on geochemical soil properties, SOC stocks and soil C turnover along geochemical diverse and sloping tropical landscapes characterized by small-scale subsistence farming. This will be addressed in study III (see Chapter 5).

1.4.2 Overarching research questions and hypothesis

This research addresses following questions and hypothesis:

i. How does soil parent mineralogy and its weathering stage shape the soil geochemical conditions driving SOC dynamics and how is this controlled or modified by the interaction between soil erosion and land conversion? The hypothesis was that *H1.1: Soil geochemical properties will be driven by soil parent mineralogy even in deeply weathered tropical soils since the distribution and quantity of minerals released into the soil by weathering processes depend on the initial mineralogical composition and texture of the bedrock. H1.2: Soil geochemistry will be modified by soil disturbances as weathered (top)soil is removed from slopes thus bringing the soil weathering front into closer contact with the C cycle, which will affect mineral-mediated stabilization of C.*

ii. How does soil geochemistry interact with the effect of soil erosion and land conversion on SOC stocks and turnover? The hypothesis was that *H2.1: SOC stocks and turnover will be driven by geochemical soil properties as a function of parent material composition. H2.2: These controls will be modified by soil erosion and land conversion since they change the geochemical and environmental conditions under which mineral C stabilization takes place.*

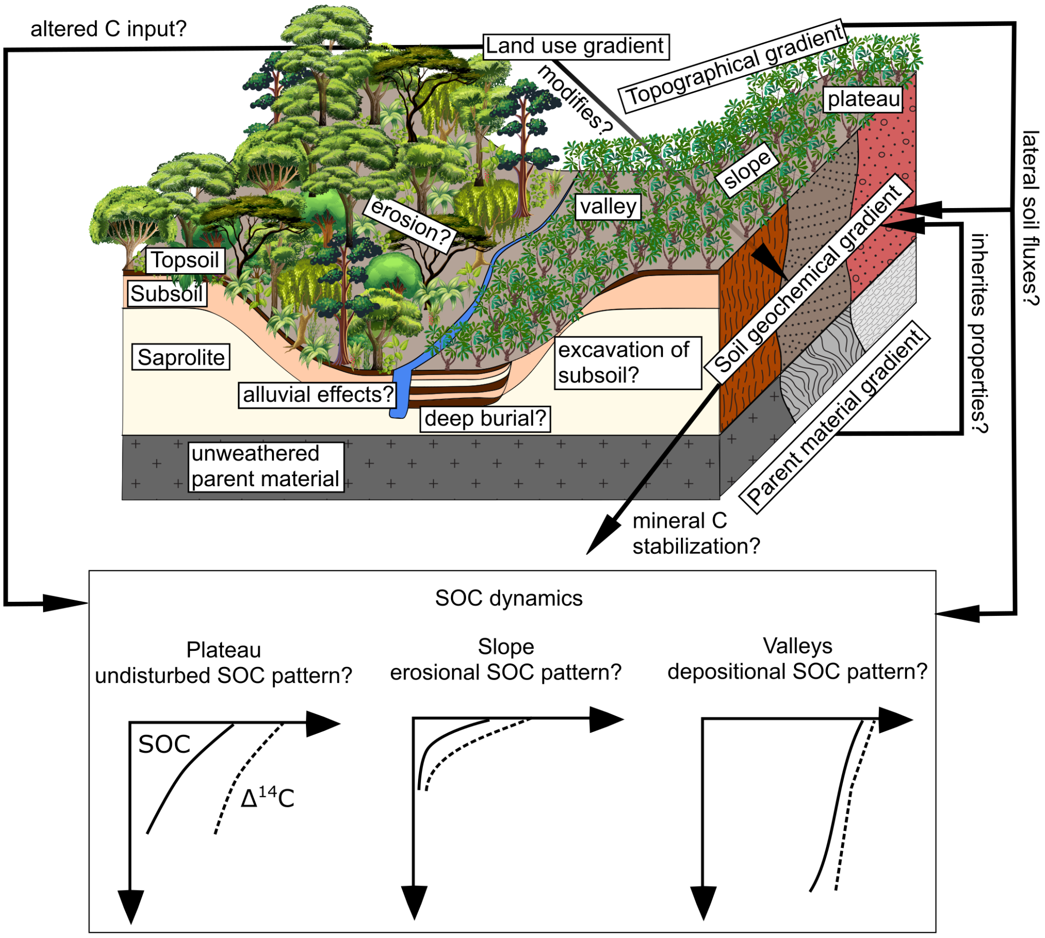

Figure 1.2: Schematic representation of the overarching research questions. Please refer to Figure 1.1 for more details about the hypothetical effects between the different environmental gradients. Please refer to Figure 6.1 to see a synthesis on the investigated controls and gradients.

1.5 Outline

This research is divided into six main sections (Figure 1.3). The first chapter (Chapter 1) reviews current knowledge on the role of C stabilization on C cycling, the relationships between C stabilization and geochemical soil properties and their interactions with land conversion and associated lateral soil fluxes. Next, the research objectives, questions and hypothesis are presented. In the second chapter (Chapter 2), the study sites (location, vegetation, geology and soil types) suitable for addressing the research questions are described, along with the study design, sampling approach and the experimental set-up for analyzing soil C fractions, C stocks and its turnover and soil mineralogy.

Moving on to the third chapter (Chapter 3) that focuses on the first research article, describing patterns and controls of mineral C stabilization, soil C fractions and turnover in deeply weathered tropical montane forest soils, answering the first research questions of this dissertation. The study shows that despite advanced degree of soil weathering, parent material remains an important driver of geochemical properties and their strong influence on soil C fractions, including FOC, and C turnover in C-depleted soils. These findings were independent of topography in the absence of detectable erosion processes.

The fourth chapter (Chapter 4) presents the second research article, which addresses the second question of this dissertation. The objective was to assess if the effect of parent mineralogy and its weathering status on C stocks and turnover is modified by land conversion from forest to cropland. The findings point to a lack of reactive minerals for the stabilization of C input in either high-input (tropical forest) or low-input (cropland) systems due to their long weathering history.

The fifth chapter (Chapter 5) addresses the research question of the third research article, which analyzes the impact of erosion-induced lateral soil fluxes on SOC stocks and turnover in geomorphologically and geochemically diverse tropical landscapes under small-scale subsistence farming systems. The study's outcome shows that cropland SOC stocks and turnover do not consistently adhere to classical topography-driven patterns caused by soil redistribution due to the low SOC persistence of deposited SOC even in subsoils and the generally low mineral C stabilization potential of the investigated soils. The results indicate the rather recent accumulation of eroded C in many valleys which can create a potentially large but vulnerable C sink, while soil degradation initiates a decline in the C cycle on many -but not all- hillslopes in the region.

Finally, the sixth chapter (Chapter 6) places the findings of this research within the broader context of the state-of-the-art knowledge and develops it further, emphasizing the implications of geochemical soil properties for mineral C stabilization, C stocks and soil C turnover in tropical ecosystems and gives directions for further research.

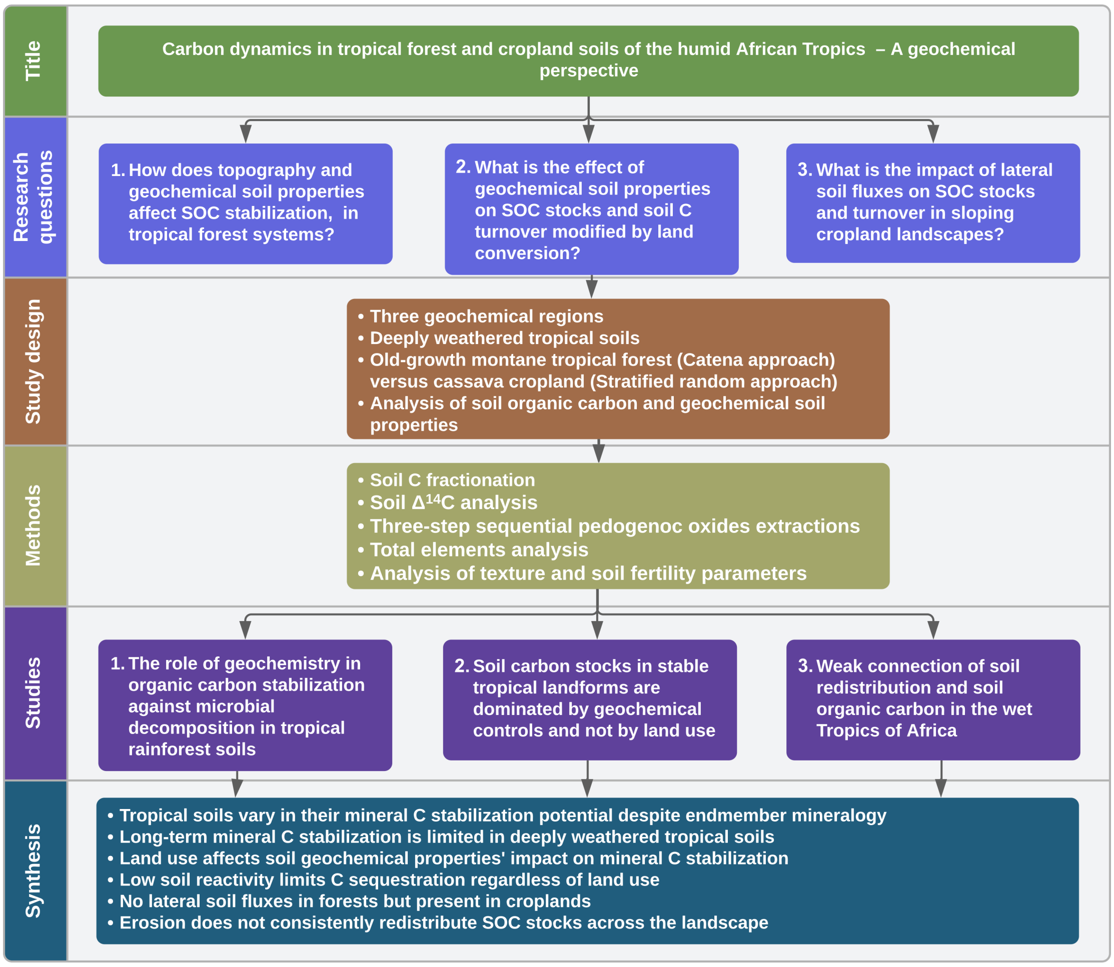

Figure 1.3: Flowchart showing the main sections of the dissertation.

Chapter 2

Materials and methods

2.1 Study area

The study area lies in the eastern regions of the Democratic Republic of the Congo (DRC), Rwanda, and Uganda, bordering the Congo and Nile Basin (Figure 2.1). Despite its critical importance in the global climate system (Amundson *et al.*, 2015; Jobbágy and Jackson, 2000), this area has been notably understudied (Schimel *et al.*, 2015). Furthermore, it faces rapid land conversion and forest degradation (Hansen *et al.*, 2013).

2.1.1 Climate and vegetation

The region has a tropical humid climate (Köppen Af – Am) characterized by monsoonal dynamics and is divided into four seasons: a weak dry period from December to February, heavy rains from March to May, a strong dry season from June to August, and lighter rains from September to November (Bukombe *et al.*, 2022; Doetterl *et al.*, 2021b). The mean annual temperature (MAT) ranges from 15.3 °C to 19.2 °C, while mean annual precipitation (MAP) varies between 1697 mm and 1924 mm (Fick and Hijmans, 2017). Generally, MAP is greater in forested study sites compared to croplands. MAT and potential evapotranspiration (PET) are marginally higher in cropland sites than in forests.

The predominant natural vegetation in the area consists of tropical montane forests (Bukombe *et al.*, 2022; Doetterl *et al.*, 2021b). Based on available data, all forest stands within the test sites are over 300 years old (Besnard *et al.*, 2021). However, extensive logging of the surrounding area has rapidly converted from this natural vegetation to croplands in recent decades (Curtis *et al.*, 2018; Tyukavina *et al.*, 2018). Today, the majority of the region is characterized by low-input, manually cultivated croplands managed by subsistence farmers (Friedl *et al.*, 2013; Verdoodt and Ranst, 2003). Local agricultural practices typically involve rotations of cassava and maize, alongside various legumes and vegetables, with minimal to no fertilizer application (Mangaza *et al.*, 2021; Ordway *et al.*, 2017; Tyukavina *et al.*, 2018).

2.1.2 Parent material geochemistry and soil types

As a part of the East African Rift mountain system, the active tectonism produced a steep terrain with smaller plateaus and ridges, steep slopes (up to 60 % steepness) and various valley shapes. The study area comprises three distinct regions, each representing different geochemical parent materials contributing to soil formation. The first region primarily consists of mafic magmatic rocks, predominantly alkali basalts resulting from volcanic activities — both extinct (Mount Kahuzi) and active (Mount Nyiragongo) between Bukavu and Goma, Kivu, DRC. The second region features felsic magmatic and metamorphic rocks, mainly gneissic granites together with volcanic ashes near Fort Portal, at the base of the Rwenzori Mountains, Uganda. The third region shows a mix of sedimentary rocks, including quartz-rich sandstone, siltstone, and dark clay schists, distributed across Rwanda's western province, particularly around the Rusizi district.

The prevailing soil types in the study area are various types of deeply weathered tropical soils (FAO, 2014). Active volcanoes in the region lead to periodic ash deposition, contributing to varying degrees of soil rejuvenation. According to World Reference Base (WRB) soil classification (FAO, 2014), soils in the mafic region can be categorized as umbric, vetic, and geric Ferralsol, along with ferralic vetic Nitisol (Figure D.2). Meanwhile, soils in the mixed sedimentary and felsic region align with geric and vetic Ferralsol classifications. Valley bottoms may exhibit gleyic features or consist of fluvic Gleysols.

There are pronounced differences in elemental composition among the three parent materials (Figure D.1) (Doetterl *et al.*, 2021b). The mafic region's bedrock show high iron (Fe) and aluminum (Al) content, along with abundant rock-derived nutrients such as base cations and phosphorus (P). In contrast, the felsic and mixed sedimentary regions exhibit lower Fe and Al contents, reduced rock-derived nutrient levels, and higher silicon (Si) content. Notably, the mixed sedimentary region contains FOC in parent material soils ranging between 1.29 % and 4.03 % C. This organic C shows a high C : N ratio (mean ± standard deviation: 153.9 ± 68.5), is N-depleted, and depleted of ^{14}C (attributed to the high age of sedimentary rock formation).

In summary, the study region offers a distinctive mixture of: (i) encompassing both near-pristine forest and agricultural land, (ii) characterized by steep terrain and substantial tropical rainfall, amplifying erosion risks, and (iii) featuring diverse geological parent materials shaping soil formation. These factors collectively make the study region an ideal setting for exploring the significance of diverse controls on biogeochemical cycles within tropical soils.

2.2 Study design and soil sampling

Soil sampling and analysis were conducted as part of the comprehensive research initiative Tropical Soil Organic Carbon (TropSOC), designed to establish a detailed understanding of how organic C, plants, and microbial processes respond to shifting soil properties in the African Tropics. This project culminated in the initial release of a database presenting measurement and monitoring data on soil and vegetation parameters across the African Tropics, exploring various land use types, topographic positions, and geochemical gradients at the landscape scale. These extensive data were collected over multiple years of fieldwork and numerous laboratory experiments, representing the most comprehensive project database to date on plant-microbe-soil systems in the Congo Basin. A detailed description of the database can be found in Doetterl *et al.* (2021c) and accessed at https://doi.org/10.5880/fidgeo.2021.009.

Plots were established along geomorphic gradients in old-growth closed-canopy forest, as well as in cropland, in all three geochemical regions (Figure 2.2). Field campaigns took place from March 2018 to July 2020, involving soil sampling at 36 forest (using a catena approach) and 100 cropland plots (using a stratified random approach). These plots were strategically positioned across stable, eroding, and depositional landforms, spanning plateaus (slope <5 %), slopes (9 % to 60 %), and valley positions (slope <5 %).

In each geochemical region, forest study sites were set within 40 m × 40 m plots (three replicates per topographic position) following standardized tropical forest analysis protocols (Marthews *et al.*, 2014). Additionally, within each topographic position, a soil profile pit was dug to a depth of 100 cm in one of the three replicate plots per region, adhering to FAO guidelines (FAO, 2006). Cropland study sites were established within 3 m × 3 m plots specifically cultivated with cassava. For each study site, four forest cores, respectively two cropland soil cores, were combined to form depth-specific composite samples. Prior to drilling, leaf litter (L horizon) and partially decomposed organic soil material (O horizon) were removed. Percussion drilling equipment was used to obtain undisturbed 1 m deep soil cores at 9 cm diameter. Soil bulk density samples were collected using known volume Kopecky cylinders (9.81 cm^3) or derived from drilled soil volume and weight.

From a total of 36 forest and 100 cropland sites, we generated 136 composite soil cores, divided into 10 cm depth increments, resulting in 1266 samples for analysis (since not all cores reached 1 m soil depth). Collected samples were promptly cooled and transported to the laboratory within 48 hours. In the lab, samples were oven-dried at 40 °C for 48 – 72 hours, followed

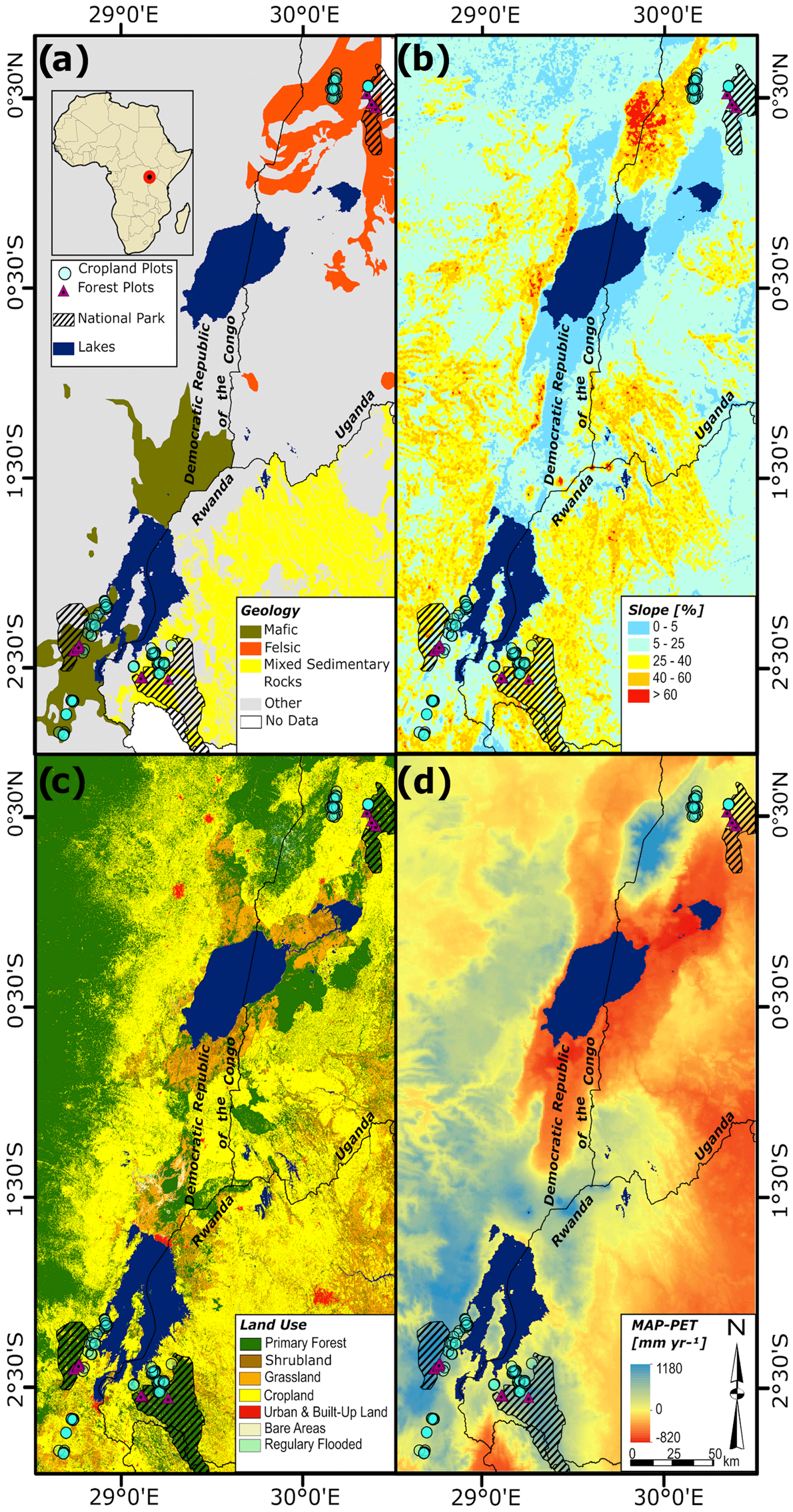

Figure 2.1: Overview map of the study region in respect to (a) geochemical regions, (b) slope steepness, (c) land use and (d) climate (Doetterl *et al.*, 2021b).

by precision weighing (accuracy: ± 0.01 g).

For forest study sites, the L and O horizons were sampled at eight points along the border and in the center of each forest plot. At each sampling point, the thickness of the L and O horizon layer was measured with a ruler and then sampled within a 5 cm × 5 cm square. When the litter layer was too thin (no closed coverage of forest floor with litter), the sampling square was expanded to a 10 cm × 10 cm to retrieve enough sample material. The 9 samples of each layer per plot were combined to one composite sample. Additionally, unweathered bedrock samples were collected from soil pits, quarries, or roadcuts near the forest plots (within 15 km) to characterize the parent material's chemical composition.

2.3 Soil analysis

As part of the TropSOC project (Doetterl *et al.*, 2021a; Doetterl *et al.*, 2021b), a comprehensive array of soil physical and chemical parameters were analyzed. Within this dissertation, specific parameters covering soil fertility and geochemical soil properties were considered as potential covariates for driving SOC dynamics (Figure 2.3).

Briefly, total carbon (TC) and total nitrogen (TN) were analyzed using dry combustion (Vario EL Cube CNS Elementar Analyzer, Germany) and C : N ratio used as a measure of soil organic matter (SOM) quality. In the absence of carbonates, all C and N sources were considered of organic nature. Note that rock content of all samples was negligible due to the generally deep weathering and long, relatively undisturbed period of soil development (Doetterl *et al.*, 2021a; Doetterl *et al.*, 2021b). Thus, SOC stocks of the bulk soil were calculated by multiplying the SOC concentration by soil bulk density and the thickness of the depth increment (10 cm). A microaggregate isolator was used to isolate soil C fractions associated with distinct stabilization mechanisms and soil C turnover (Doetterl *et al.*, 2015a; Six *et al.*, 2000a; Stewart *et al.*, 2008). These fractions consisted of >250 µm representing unprotected C, 53 – 250 µm representing occluded C in microaggregates and <53 µm representing C associated with free-silt-and-clay-sized particles. The C content of each soil C fraction was determined by multiplying the C concentration by the respective fraction mass. Bulk soil $\Delta^{14}C$ was analyzed for selected depth increments using AMS (accelerator mass spectrometry) at the Max Planck Institute for Biogeochemistry (Jena, Germany) and conventional radiocarbon age following the conventions of Stuiver and Polach (1977). The total amount of rock-derived nutrients in soils was characterized by the total reserve in base cations (TRB) and total P. Soil fertility was assessed by analyzing base saturation, exchangeable base cations of calcium (Ca), magnesium (Mg) and potassium (K) and bioavailable P (bray-P). The general physico-chemical soil environment was assessed by analyzing soil texture and soil pH (KCl). Concentrations of pedogenic aluminum (Al), iron (Fe)

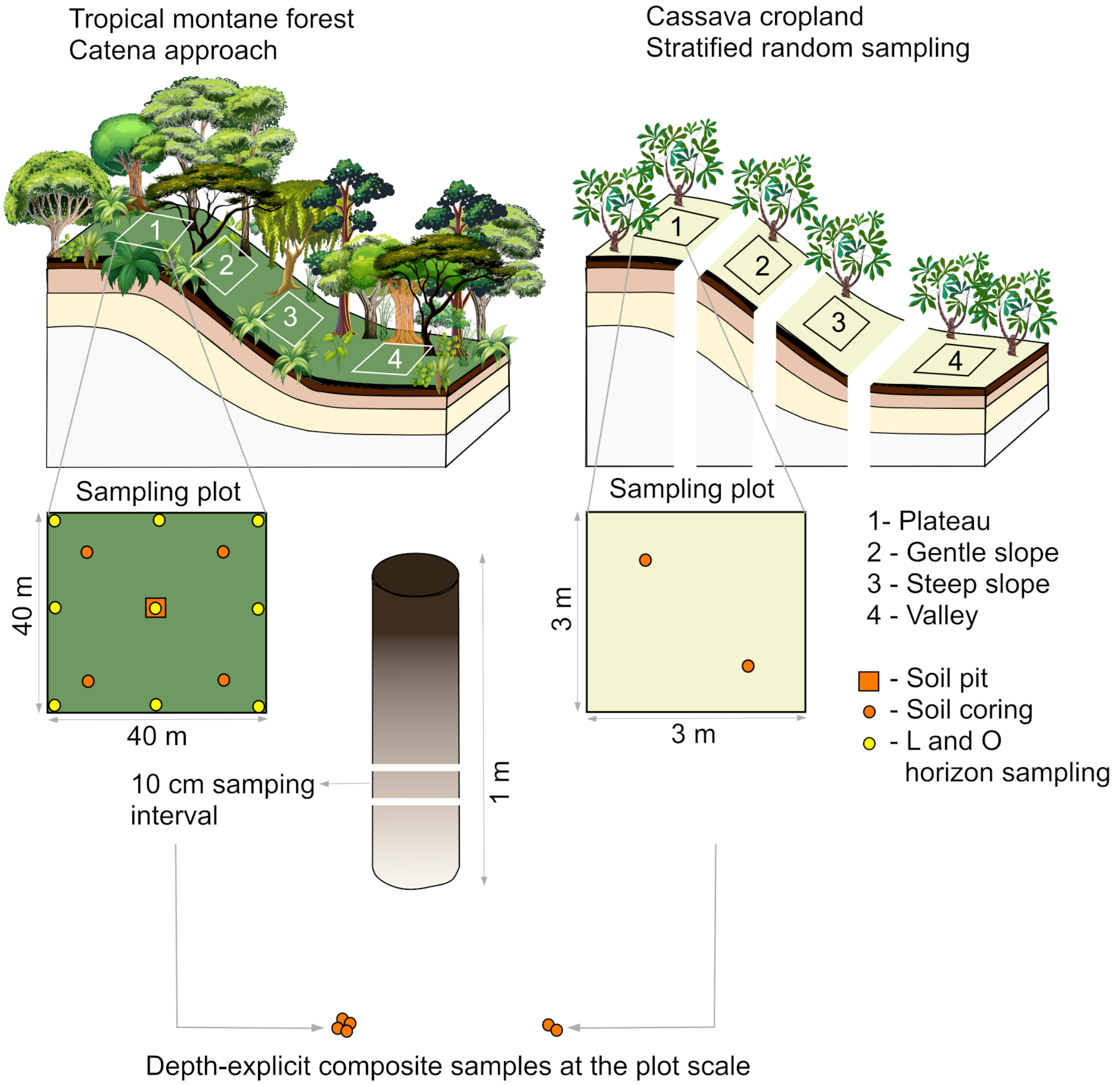

Figure 2.2: Soil sampling approach applied in forest and cropland in each geochemical region.

and manganese (Mn) bearing mineral phases relevant for mineral C stabilization were assessed by a three-step sequential extraction scheme of pedogenic oxy-hydroxides (Stucki *et al.*, 1988) and by aqua-regia extraction for the total metal content.

All values for the presented variables have been analyzed using a Bruker Vertex 70, (Hanau, Germany) near and mid-infrared (NIR-MIR) Fourrier Transform FT-IR spectrometer (Doetterl *et al.*, 2021b; Summerauer *et al.*, 2021). As part of the calibration of the spectrometer, 20 % of all samples (n = 253) were analyzed with traditional wet-chemistry methods before predicting all samples (n = 1266) following the workflow of Summerauer *et al.* (2021).

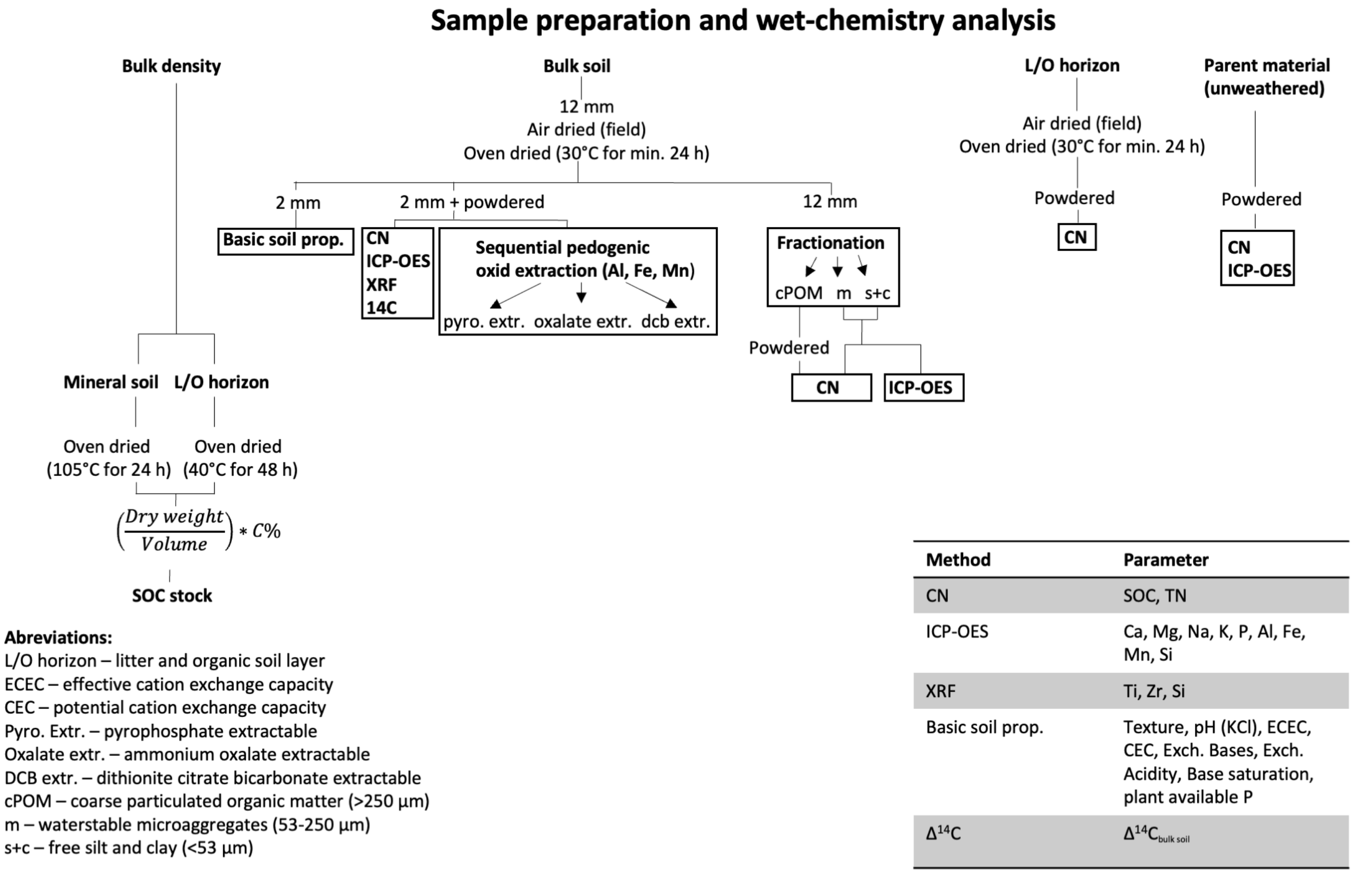

Abreviations:
L/O horizon – litter and organic soil layer
ECEC – effective cation exchange capacity
CEC – potential cation exchange capacity
Pyro. Extr. – pyrophosphate extractable
Oxalate extr. – ammonium oxalate extractable
DCB extr. – dithionite citrate bicarbonate extractable
cPOM – coarse particulated organic matter (>250 µm)
m – waterstable microaggregates (53-250 µm)
s+c – free silt and clay (<53 µm)

Method	Parameter
CN	SOC, TN
ICP-OES	Ca, Mg, Na, K, P, Al, Fe, Mn, Si
XRF	Ti, Zr, Si
Basic soil prop.	Texture, pH (KCl), ECEC, CEC, Exch. Bases, Exch. Acidity, Base saturation, plant available P
$\Delta^{14}C$	$\Delta^{14}C_{\text{bulk soil}}$

Figure 2.3: Schematic overview of the sample preparation and wet-chemistry analysis prior to mid-infrared (NIR-MIR) Fourier Transform FT-IR spectrometer measurements.

Chapter 3

The role of geochemistry in organic carbon stabilization against microbial decomposition in tropical rainforest soils

---

The content of this chapter has been published as: Reichenbach, M., Fiener, P., Garland, G., Griepentrog, M., Six, J., and Doetterl, S.: The role of geochemistry in organic carbon stabilization against microbial decomposition in tropical rainforest soils, SOIL, 7, 453–475, https://doi.org/10.5194/soil-7-453-2021, 2021.

Author contributions: Sebastian Doetterl and Peter Fiener designed the research. Mario Reichenbach conducted the sampling campaign and collected the data. All authors analyzed and interpreted the data. All authors contributed to the writing of the paper.

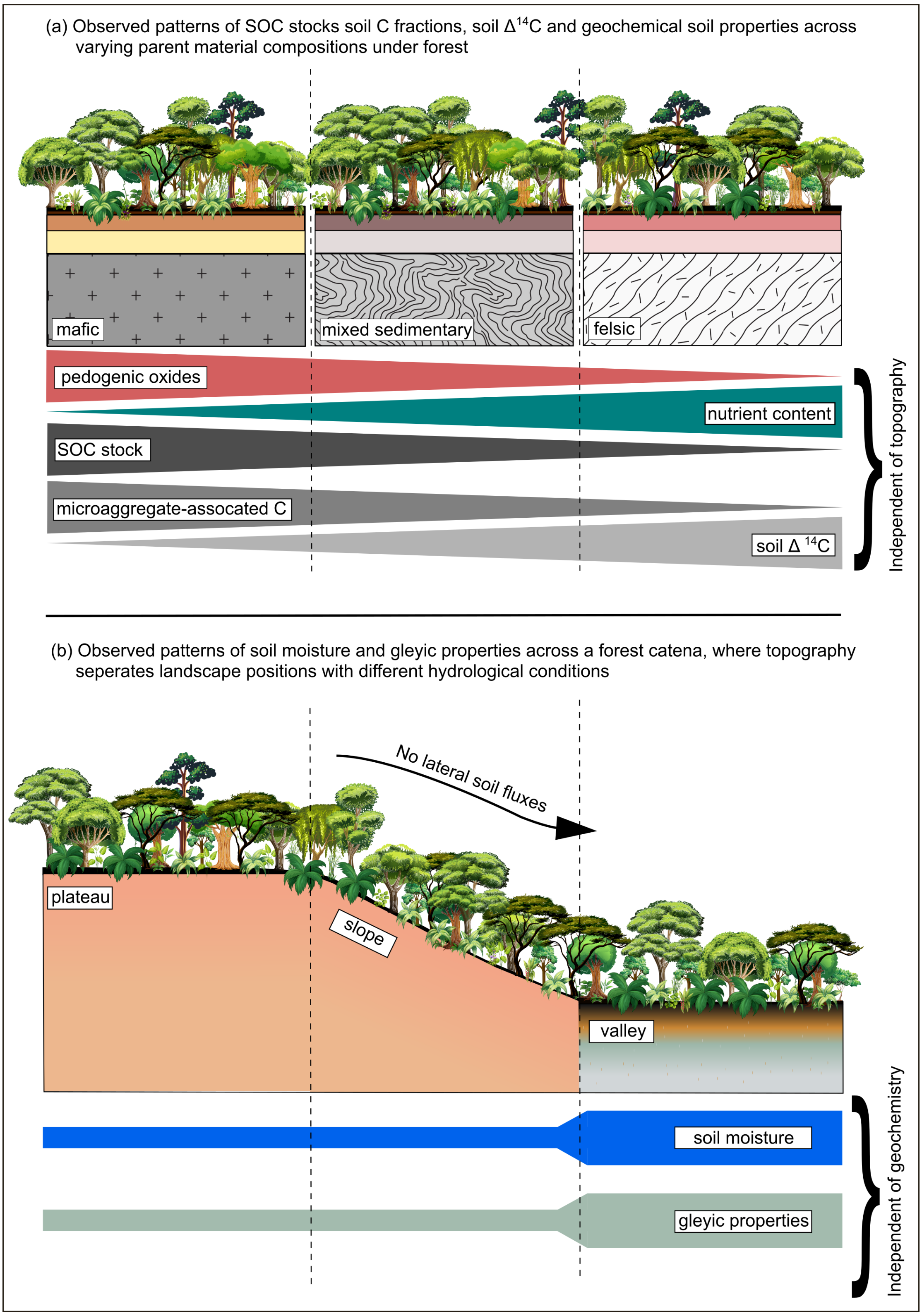

Figure 3.1: Graphical abstract – Pattern and controls of mineral C stabilization across geochemical test sites under forest.

3.1 Abstract

Stabilization of soil organic carbon (SOC) against microbial decomposition depends on several soil properties, including the soil weathering stage and the mineralogy of parent material. As such, tropical SOC stabilization mechanisms likely differ from those in temperate soils due to contrasting soil development. To better understand these mechanisms, we investigated SOC dynamics at three soil depths under pristine tropical African mountain forest along a geochemical gradient from mafic to felsic and a topographic gradient covering plateau, slope and valley positions. To do so, we conducted a series of soil C fractionation experiments in combination with an analysis of the geochemical composition of soil and a sequential extraction of pedogenic oxides. Relationships between our target and predicting variables were investigated using a combination of regression analyses and dimension reduction. Here, we show that reactive secondary mineral phases drive SOC properties and stabilization mechanisms together with, and sometimes more strongly than, other mechanisms such as aggregation or C stabilization by clay content. Key mineral stabilization mechanisms for SOC were strongly related to soil geochemistry, differing across the study regions. These findings were independent of topography in the absence of detectable erosion processes. Instead, fluvial dynamics and changes in soil moisture conditions had a secondary control on SOC dynamics in valley positions, leading to higher SOC stocks there than at the non-valley positions. At several sites, we also detected fossil organic carbon (FOC), which is characterized by high ratios and depletion of N. FOC constitutes up to 52.0 ± 13.2 % of total SOC stock in the C-depleted subsoil. Interestingly, total SOC stocks for these soils did not exceed those of sites without FOC. Additionally, FOC decreased strongly towards more shallow soil depths, indicating decomposability of FOC by microbial communities under more fertile conditions. Regression models, considering depth intervals of 0 − 10, 30 − 40 and 60 − 70 cm, showed that variables affiliated with soil weathering, parent material geochemistry and soil fertility, together with soil depth, explained up to 75 % of the variability of SOC stocks and Δ^{14}C. Furthermore, the same variables explain 44 % of the variability in the relative abundance of C associated with microaggregates vs. free-silt- and-clay-associated C fractions. However, geochemical variables gained or retained importance for explaining SOC target variables when controlling for soil depth. We conclude that despite long-lasting weathering, geochemical properties of soil parent material leave a footprint in tropical soils that affects SOC stocks and mineral-related C stabilization mechanisms. While identified stabilization mechanisms and controls are similar to less weathered soils in other climate zones, their relative importance is markedly different in the tropical soils investigated.

3.2 Introduction

3.2.1 SOC research in the Tropics

The Tropics are considered potential tipping points for the climate – carbon (C) feedback due to their substantial C storage in the biosphere, fast C turnover and the associated potential C losses to the atmosphere. Despite this key relevance in the terrestrial C cycle and climate regulation, the tropics remain highly underrepresented in research (Schimel *et al.*, 2015). This is especially true for tropical soils, which are estimated to contain approximately one-third of global soil organic carbon (SOC) (Köchy *et al.*, 2015). Many interacting soil processes, both in temperate and tropical soils, are not adequately represented in C turnover models, such as the effect of soil aggregation on soil biota and SOC dynamics (Keulen, 2001; Vereecken *et al.*, 2016; Wood *et al.*, 2012). Studies analyzing the effect of soil geochemistry on SOC dynamics and stabilization against microbial decomposition combined are also rare (Denef and Six, 2005; Quesada *et al.*, 2020; Wattel-Koekkoek *et al.*, 2003; Zotarelli *et al.*, 2005), and such effects are not included in large-scale C cycle modeling approaches (Vereecken *et al.*, 2016). Most of these geochemical effect studies focus on midlatitudes in the Northern Hemisphere, while the specific conditions under tropical conditions with highly weathered soils remain relatively unknown (Schimel *et al.*, 2015) and can differ greatly compared to temperate soils (Denef and Six, 2006; Denef *et al.*, 2007). Thus, findings from midlatitudes are not easily transferable to tropical soils, since the potential in stabilizing SOC depends on geochemical soil properties that differ fundamentally between geo-climatic zones as a function of pedogenesis. The lack of mechanistic understanding regarding SOC dynamics and their controlling factors creates substantial uncertainties when predicting the future of SOC stocks in the tropics (Schmidt *et al.*, 2011; Shi *et al.*, 2020).

3.2.2 Environmental and geochemical controls on SOC dynamics in tropical forests

SOC dynamics in tropical rainforests are characterized by high C input and fast C turnover rates (Pan *et al.*, 2011; Wang *et al.*, 2018). Carbon input to soils is mainly driven by root growth and litter production (Raich *et al.*, 2006), both of which are often driven by climatic and hydrological variables that govern vegetation dynamics. Climatic factors such as temperature and precipitation are strong drivers of soil environmental conditions, which can greatly influence soil microbial activity and hence C mineralization and turnover (Davidson and Janssens, 2006; Feng *et al.*, 2017; Zhang *et al.*, 2011). For example, decomposition rates increase in general with temperature, but soil microbial communities adapted to high temperatures are less sensitive to warming (Blagodatskaya *et al.*, 2016). However, climate-driven factors can also influence SOC dynamics indirectly through the interaction with soil factors (Doetterl *et al.*, 2015a). For example, C-depleted tropical subsoils contain small but metabolically active microbial communities contributing to C cycling (Kidinda *et al.*, 2022; Stone *et al.*, 2014). Low soil pH in combination with high clay content dominated by pedogenic oxides can stabilize enzymes on mineral surfaces, which will affect microbial C acquisition (Allison and Vitousek, 2005; Dove *et al.*, 2020; Liu *et al.*, 2020). The accessibility of C for mineralization is predominantly driven by several interacting mechanisms that can stabilize C in soils against microbial decomposition on a decadal up to a millennial timescale (Trumbore, 2009; Trumbore, 2000). For example, certain C compounds such as pyrogenic or aromatic C show biochemical resistance since the decomposition of its complex molecular structure is an energy-demanding process and microbes will preferentially consume more easily available organic C forms (Czimczik and Masiello, 2007; Knicker, 2011). Another C fraction that is characterized by long turnover times is fossil organic carbon (FOC), deposited during the formation of sedimentary rocks and often hard to decompose (Kalks *et al.*, 2021; Voort *et al.*, 2019). Carbon can also be protected physically against decomposition by encapsulation within soil aggregates. Minerals can also increase the energetic barrier for microorganisms to overcome by forming organo–mineral associations (Cotrufo *et al.*, 2013; Lehmann *et al.*, 2007; Lützow *et al.*, 2007; Oades, 1988; Oades, 1984). In particular, it has been shown that the availability of reactive mineral surfaces influences the formation of organo–mineral associations as well (Angst *et al.*, 2018; Eusterhues *et al.*, 2003; Jagadamma *et al.*, 2014). Furthermore, reactive and adsorptive surfaces not only contribute to chemical C stabilization, but also favor the formation of soil aggregates (Chenu and Plante, 2006; Lehmann *et al.*, 2007; Simpson *et al.*, 2004; Six *et al.*, 2004).

While these general types of stabilization against microbial decomposition in the Tropics are similar to those in temperate soils, their relative importance and abundance differ greatly due to contrasting weathering history (Denef *et al.*, 2004; Six *et al.*, 2002b). Most temperate soils have developed from young (peri)glacial sediments and relatively unweathered bedrock (∼15 000 years old). Tropical soils have often been exposed to chemical weathering for millions of years if landforms are stable (Finke and Hutson, 2008; Porder *et al.*, 2005). The resulting soil geochemistry in the Tropics is therefore often composed of end-members of weathering products such as secondary minerals (i.e., 1 : 1 low-activity clays, kaolinite) and highly crystalline, pedogenic oxides (West and Dumbleton, 1970). Clay-sized mineral fractions in tropical soils are composed of up to 15 % pedogenic oxides, which is usually much higher than in temperate soils (Ito and Wagai, 2017). While some studies in tropical regions have shown that variation in clay content explains SOC stocks in kaolinitic soils (Quesada *et al.*, 2020), others have shown that SOC stabilization is not affected by clay quantity but instead by the clay mineralogy (Bruun *et al.*, 2010). The most important identified stabilization mechanisms in kaolinitic tropical soils are mineral – organic associations with short-range-ordered (SRO) pedogenic oxides (Bruun *et al.*, 2010; Kleber *et al.*, 2005; Martinez and Souza, 2020), which stabilize 47 % to 63 % of the bulk SOC stocks in tropical forests (Kramer and Chadwick, 2018). Hence, differences in mineralogy affect a number of key soil fertility parameters and also the way C is stabilized onto minerals, ultimately impacting the interplay between mineral reactivity, microbial community structures and nutrient dynamics (Denef and Six, 2005; Doetterl *et al.*, 2018; Six *et al.*, 2002a). For example, SOC stabilization by mineral – organic complexes in tropical soils is highly efficient as they appear in parallel and within highly stable soil aggregates and pseudosand structures (Martinez and Souza, 2020; Quesada *et al.*, 2020). Furthermore, kaolinitic soils can form aggregates rapidly independent from biological processes due to electrostatic interactions between 1 : 1 clay minerals and oxides. But biological processes can lead to stronger organic bonds in soils with 1 : 2 clays, promoting long-term stability (Denef and Six, 2005). This finding relates to the observation that SOC stabilized in kaolinitic 1 : 1 clay soils turns over faster compared to SOC associated with 1:2 clay soils (Wattel-Koekkoek *et al.*, 2003). Hence, interactions between geochemistry, aggregation and mineral surface, governed by soil weathering, need to be considered more prominently to understand SOC dynamics in temperate vs. tropical soils.

3.2.3 Topographical controls on SOC dynamics in tropical forests

In addition to larger-scale biogeochemical and climatic controls of C dynamics, in undulating landscapes soil redistribution processes can highly influence SOC dynamics (Doetterl *et al.*, 2016; Hemelryck *et al.*, 2010; Wilken *et al.*, 2017). Excessive erosion of topsoils on hillslopes often results in exposure of subsoils with low C contents, which on the one hand can lead to dynamic C replacement (Harden *et al.*, 1999) and on the other hand may stimulate the decomposition of older SOC due to priming with fresh C inputs (Fontaine *et al.*, 2004; Keiluweit *et al.*, 2015). Thereby, removal of weathered topsoils brings new mineral surfaces in contact with fresh C input, which could favor C sequestration due to organo – mineral associations (Doetterl *et al.*, 2016), especially in highly weathered tropical landscapes (Porder *et al.*, 2005; Vitousek *et al.*, 2003). These processes are of potentially great importance for tropical soil systems, as an erosional rejuvenation of land surfaces can bring an entirely different soil mineral composition in touch with the biological C cycle and provide a geochemically entirely different environment for C stabilization against microbial decomposition. Similarly, fossil organic carbon that is brought to the surface might become increasingly decomposed when brought in contact with more active microbial communities compared to subsoil environments. Parallel to these processes of soil denudation, at depositional sites in valleys and at footslopes, former topsoil SOC can become buried by colluvial and alluvial sediments, potentially greatly decreasing microbial decomposition. However, the fate of buried SOC depends greatly on the prevailing environmental conditions in the depositional sites and the sedimentation rates (Berhe *et al.*, 2012; Berhe *et al.*, 2007; Gregorich *et al.*, 1998). Topography can control hydrological patterns in tropical rainforests (Detto *et al.*, 2013; Silver *et al.*, 1999). For example, high water tables lead to lower soil oxygen levels in valley positions, which in turn reduce microbial C decomposition and potentially result in the accumulation of labile SOC. Furthermore, changes in soil water content can cause reductive dissolution of iron oxides, which ultimately affects organo – mineral associations (Berhe *et al.*, 2012). Thus, the interplay between environmental, geochemical and topographic conditions sets the stage for C stabilization and will most likely differ from temperate to tropical soils.

3.2.4 Study aims

In summary, our current understanding of how geochemistry and topography in highly weathered tropical soils affects SOC stocks and stabilization mechanisms against microbial decomposition is still limited. This study thus aimed to better understand the influence of topography and geochemical properties of soils developed from different parent materials on (i) SOC stocks, (ii) SOC fractions and (iii) SOC stabilization mechanisms in tropical forest soil systems. In addition, (iv) we assessed the contribution of FOC to SOC stocks in sedimentary-rock-derived soils using Δ^{14}C. Within this context, the following hypotheses were tested:

(i) SOC stocks and geochemical soil properties sensitive to soil redistribution will vary as a function of a soil's topographic position.

(ii) C stabilization mechanisms against microbial decomposition in highly weathered tropical soils, indicated by the amount of C associated with minerals (stable microaggregates and free silt and clay), will be driven by geochemical soil properties as a function of parent material composition.

(iii) Fossil organic carbon content in C-bearing parent material will vary as a function of soil depth because it may become accessible for microbial decomposition under surface conditions.

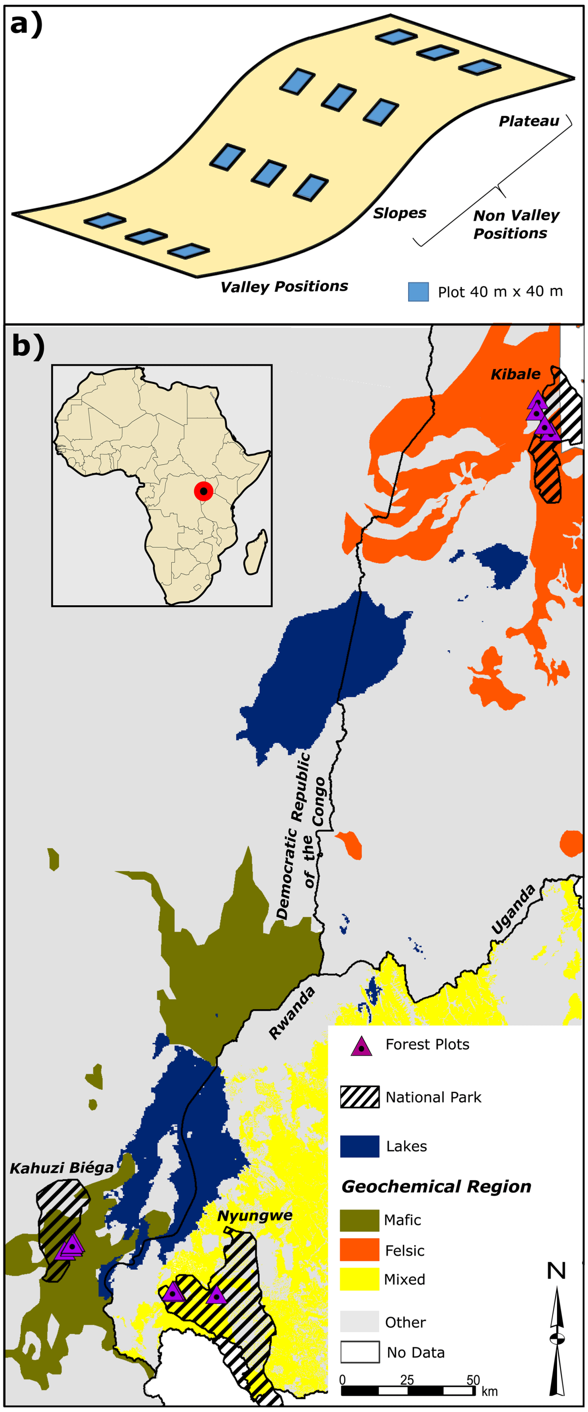

Figure 3.2: (a) Study design used in each geochemical region. (b) Overview of study area with respect to soil parent material geochemistry (modified from Doetterl *et al.* (2021b).

3.3 Materials and methods

3.3.1 Study region

The study region is located in the eastern part of the Congo basin and the western part of the Blue Nile basin, with study sites located along the East African Rift Mountain System. Vegetation at all sites is dominated by primary tropical mountain forests (Figure 3.2b). Climate of the region is characterized as humid tropical (Köppen Af – Am) with a short dry season (i.e., only 2 months per year with <50 mm precipitation). The tectonically active rift system resulted in geochemically diverse parent material and in a heterogeneous hilly landscape. The study area consists of parent material ranging from mafic to felsic magmatic bedrock as well as sedimentary rocks of mixed geochemical composition. The undulating landscape resulted in a variety of hydrological conditions at plateau, slope and valley positions. In combination, this makes the study area ideal to analyze the effect of soil geochemistry and topography on SOC stabilization mechanisms against microbial decomposition and stocks in a variety of tropical soils.

Kahuzi-Biega

The study region consisted of three main sites. The Kahuzi-Biega site (from here on called mafic site) is located in the South Kivu province of the Democratic Republic of the Congo (DRC) (-2.31439°S; 28.75246°E) with an altitude of 2220 ± 38 m.a.s.l. and slopes ranging between 1 % – 60 %. The parent material consists of mafic alkali basalts with an age ranging between 9 – 13 Ma (Schlüter and Trauth, 2006). According to FAO soil classification (FAO, 2014), typical soils in this region are Ferralic Nitisols and Geric Ferralsols. Vegetation is described as a closed broad-leaved semi-deciduous mountain forest (Verhegghen et al., 2012). Mean annual precipitation (MAP) is 1924 mm yr^{-1}, and the mean annual temperature (MAT) is 15.3 °C (Fick and Hijmans, 2017).

Nyungwe

The Nyungwe site (from here on called mixed sedimentary site) is situated in the southwestern part of Rwanda (-2.463088°S; 29.103834°E) at 1909 ± 22 m.a.s.l. and with slopes ranging between 1 % – 60 %. The parent material consists of mixed sedimentary rocks showing alternating layers of quartz-rich sandstone, siltstone and dark clay schists with an age between 1000 – 1600 Ma(Schlüter and Trauth, 2006). A specific feature of the sedimentary site is the presence of

FOC in the parent material of soils ranging between 1.29 % – 4.03 % C. FOC in these sediments is further characterized by a high C : N ratio (153.9 ± 68.5), depleted in N and free of ^{14}C (due to the high age of sedimentary rock formation). Typical soils are Geric Ferralsols and Fluvic Gleysols. Vegetation is classified as an afromontane rainforest (van Breugel et al., 2020). MAP is 1702 mm yr^{-1}, and MAT is 16.7 °C (Fick and Hijmans, 2017).

Kibale

The Kibale site (further called felsic site) is located in western Uganda (0.46225° N; 30.37403 °E) with an altitude of 1324 ± 60 m.a.s.l. and slopes between 3 % – 55 %. The parent material consists of felsic gneissic granites with an age between 1600 – 2500 Ma (Schlüter and Trauth, 2006). Dominant soils are Geric Ferralsols. Vegetation is classified as Lake Victoria drier peripheral semi-evergreen Guineo – Congolian rainforest (Breugel *et al.*, 2020). The MAP is 1697 mm yr^{-1} and the MAT is 19.2 °C (Fick and Hijmans, 2017).

3.3.2 Study design and soil sampling

In the framework of the project TropSOC (Doetterl *et al.*, 2021a; Doetterl *et al.*, 2021b), soil sampling took place from March to June 2018, applying a stratified random sampling design with triplicate plots of 40 m × 40 m across three topographic positions (i.e., plateau, slope and valley; Figure 3.2a) in each geochemical region. Note that because hillslopes were much larger landscape features, we sampled at both topslope and midslope positions. Slope steepness was measured at the center of each plot using a clinometer. Slope length at each plot was derived from a shuttle radar topography mission digital elevation model (SRTM-DEM) (JPL, 2013) with a 30 m × 30 m resolution using the flow direction and flow length tool in ArcMap 10.6.1 (ESRI, USA). Slope length in Kahuzi-Biéga was 70 ± 56 m (max. 170 m), in Nyungwe 101 ± 103 m (max. 339 m) and in Kibale 149 ± 125 m (max. 374 m). No evidence of soil erosion could be observed during the field survey within the plots, and all soil samples were free of carbonates and inorganic C. Attention was paid to install the study plots in areas that are affected by landslides as little as possible. Note that the occurrence of natural landslides cannot be excluded with certainty. However, the vegetation patterns were fairly regular across landforms and replicates. Thus, landslide events can be excluded for the time needed to establish the current vegetation coverages. Additionally, landforms and sampled soils did not show signs of larger erosional events in the recent past. All soils were deeply weathered and showed no signs that would indicate a disturbance event in the past outside of valleys and fluvial systems. Soils were described for every topographic position per geochemical region following WRB classification (FAO, 2014).

To describe the chemical composition of the parent material, unweathered bedrock samples were collected in each study area from soil pits, quarries or roadcuts near the plots (maximum distance 15 km). Rock samples from the plots were compared to rock samples from the roadcuts and quarries where possible to ensure that the samples were taken from the same geology.

Each plot was subdivided into four 20 m × 20 m subplots, in which soil profiles were sampled in 10 cm increments down to 1 m soil depth and combined to get depth-explicit composite samples. We then selected three soil layers for further analyses as they represent distinct sections in a soil profile that differ in C input and biogeochemical soil factors: 0 – 10 cm (topsoil, TS), 30 – 40 cm (shallow subsoil, SS) and 60 – 70 cm (deep subsoil, DS). Field-moist samples were sieved to 12 mm to get a homogenous substrate still containing the inherent aggregate structure. Samples were then air-dried for 3 – 5 d. Soil bulk density samples were taken using Kopecky cylinders. Litter (L) and decomposed organic (O) layers on top of the mineral soil were sampled within a 20 cm × 20 cm square in the center of each subplot and combined to composite samples for the L and O layers, respectively. In total, 36 composite soil cores were sampled on which the soil analysis was conducted (4 cores per plot, combined to one composite, resulting in 12 soil cores per geochemical region distributed across 4 topographic positions in triplicate). In addition, one soil pit of variable depth but always deeper than 100 cm dug in the center in one of three replicate plots per topographic position in each region was described according to FAO guidelines (FAO, 2006). The soils were classified according to the World Reference Base (WRB) soil classification (FAO, 2006). Soils in the mafic region can be described as Umbric, Vetic and Geric Ferralsols and Ferralic Vetic Nitisols. Soils in the felsic regions are classified as Geric and Vetic Ferralols. The mixed sedimentary region shows Geric and Vetic Ferralsols along plateaus and slopes, whereas soils at the valley bottoms are described as Fluvic Gleysols.

3.3.3 Soil analysis

A wide range of soil physical and chemical parameters were analyzed in the framework of project TropSOC (Doetterl *et al.*, 2021a; Doetterl *et al.*, 2021b), from which the following were used in this study as potential covariates for controls on SOC: bulk density, total elements of base cations (Ca, Mg, K, Na), total phosphorus, metal oxides with relevance to C stabilization against microbial decomposition (Al, Fe, Mn), elements where concentrations relate strongly to weathering (Si, Ti, Zr) and additional soil properties that relate to soil fertility (texture, pH, effective and potential cation exchange capacity, base saturation, bioavailable phosphorus). Generally, each analysis was performed with 20 % of the samples analyzed in triplicate to assess analytical error. Prior to analyses, all samples were oven-dried at 30 °C for 48 – 72 h until dry.

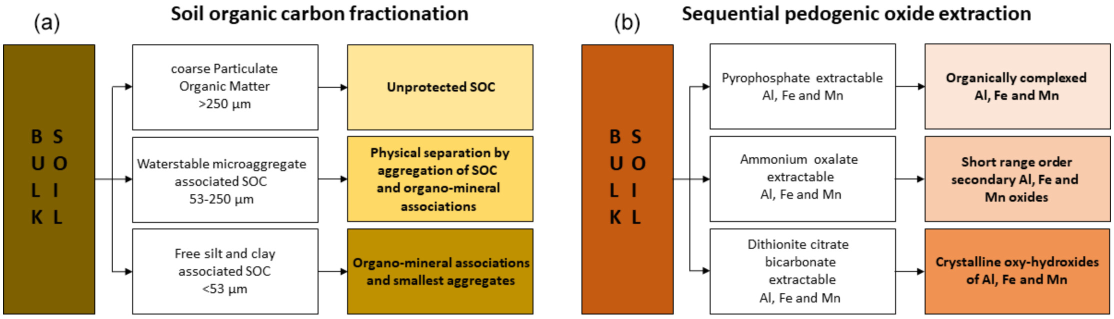

Figure 3.3: (a) Applied SOC fractionation scheme after Stewart *et al.* (2008) and Doetterl *et al.* (2015a) and its interpretation in terms of functional SOC pools and C stabilization mechanisms. (b) Applied sequential extraction scheme following Stucki *et al.* (1988) and its interpretation in terms of oxide phases relevant for C stabilization.).

Soil C fractionation and nutrient analysis

Three soil size fractions representing different stabilization mechanisms against microbial decomposition associated with varying SOC turnover times were isolated using a microaggregate isolator (Doetterl *et al.*, 2015a; Six *et al.*, 2000a; Stewart *et al.*, 2008). These fractions consisted of (i) >250 µm, i.e., unprotected C; (ii) 53 – 250 µm, i.e., occluded C in microaggregates; and (iii) <53 µm, i.e., C associated with free-silt- and-clay-sized particles (Figure 3.3a). Briefly, 20 g of 12 mm sieved bulk soil was submerged under water for 24 h to break up non-water stable aggregates. Next, the slaked soil sample was wet-sieved through a 250 µm sieve using the microaggregate isolator mounted on a sample shaker. The sample was shaken for 20 ± 11 min with 50 glass beads to break up any remaining macroaggregates. The remaining material was then wet-sieved through a 53 µm sieve by moving the sieve 50 times up and down within 2 min by hand. The isolated soil fractions were then analyzed for carbon and nitrogen (SOC and total nitrogen, TN). To ensure sample homogeneity, the >250 µm fraction was powdered with a ball mill (Mixer Mill MM 200, Retsch, Germany) prior to C and N analysis. The carbon mass of each soil C fraction ($\mathrm{SOC}_{>250 \mu m}$, $\mathrm{SOC}_{53-250 \mu m}$ and $\mathrm{SOC}_{<53 \mu m}$) was calculated by multiplying the SOC concentration by the corresponding fraction mass. The ratio of the C mass of microaggregate-associated C to free-silt- and-clay-associated C (m / s+c ratio) was calculated as a proxy to distinguish between soils in which mineral – C protection, which takes place in both fractions, is amplified by the physical protection through aggregation. It is generally interpreted that the higher this ratio, the more C is occluded within stable microaggregates, on top of being stabilized by mineral-organic interactions (and vice versa for low rations). SOC and TN for all samples were analyzed using dry combustion (Vario EL Cube CNS Elementar Analyzer, Germany). Since the content of rock fragments of all samples was negligible, the SOC stock of the bulk soil (SOC_{bulk}) was calculated by multiplying the SOC concentration by the bulk density and the thickness of the depth increment (10 cm).

Sequential pedogenic oxide extraction

To assess the abundance of Al-, Fe- and Mn-bearing phases and their correlation with SOC$_{bulk}$, a three-step sequential extraction of pedogenic oxyhydroxides (Stucki *et al.*, 1988) was performed on powdered bulk soil (Figure 3.3b). First, sodium pyrophosphate at pH 10 was used for extracting organically complexed metals (Bascomb, 1968). Second, ammonium oxalate – oxalic acid at pH 3 was used for extracting amorphous, short-range-order (SRO) secondary oxides and poorly crystalline alumnosilicates (Dahlgren, 1994). Note that results of pyrophosphate extraction must be interpreted with caution, since Al from Al hydroxide phases and poorly crystalline alumnosilicates can also be partially extracted using this reagent (Kaiser and Zech, 1996; Schuppli *et al.*, 1983). Third, dithionite – citrate – bicarbonate (DCB) at pH 8 was used for extracting crystalline oxyhydroxides (Mehra and Jackson, 1958). All extracts including the calibration standards were filtered through 41 grade Whatman filters, diluted (1 : 1000) and then analyzed for elemental concentrations using inductively coupled plasma optical emission spectroscopy (ICP-OES) (5100 ICP-OES Agilent Technologies, USA).

Calculation of FOC contribution to total SOC$_{bulk}$

The radioisotopic signature (Δ^{14}C) of bulk soil was assessed using AMS (accelerator mass spectrometry) at the Max Planck Institute for Biogeochemistry (Jena, Germany) and conventional radiocarbon age following the conventions of Stuiver and Polach (1977). ^{14}C radiocarbon dating was used to estimate the relative age differences of C between samples and to estimate the potential contribution of FOC to the total SOC in soils developed from mixed sedimentary rocks. Following Cerri *et al.* (1985) and Kalks *et al.* (2021), we assume that the biogenic carbon in the different soil depths of all sites was relatively similar and overall several orders of magnitude younger than the FOC. The baseline values for this assumption are the depth-explicit mean values of Δ^{14}C of the mafic and felsic sites as they are free of FOC. Based on this assumption, the mean depth-specific percent modern carbon (PMC) values for those regions were calculated as follows:

$$f_{\text{bio}} = \left(\frac{F}{F_{\text{bio}}}\right) \times 100, \tag{3.1}$$

where F is the PMC in a sample, f_{bio} (%) is the proportion of biogenic organic carbon in the total amount of organic carbon and F_{bio} is the fraction PMC averaged from the plateau and slope sites and depths of the mafic and felsic sites.

In a second step, the amount of FOC at the mixed sedimentary site was assessed as follows:

$$f_{\text{FOC}} = 100 - f_{\text{bio}}, \tag{3.2}$$

where f_{FOC} is the proportion of fossil organic carbon as a fraction of the total amount of soil organic carbon (%).

Calculation of the chemical index of alteration and elemental differences between parent material and soil

Based on results of the analyses of total element concentrations (see Doetterl *et al.* (2021a) for details), the chemical index of alteration (CIA, in %) (Fiantis *et al.*, 2010) was calculated to assess the weathering stage of the soil as follows:

$$\text{CIA} = \left(\frac{\text{Al}_2\text{O}_3}{\text{Al}_2\text{O}_3 + \text{CaO} + \text{Na}_2\text{O} + \text{K}_2\text{O}}\right) \times 100, \tag{3.3}$$

To illustrate gains and losses of nutrients in the soil column compared to the underlying parent material, the relative and absolute difference in element concentration for key elements that enrich or deplete with weathering (ΔCa, ΔK, ΔMg, ΔNa, ΔP, ΔFe, ΔAl,ΔMn, ΔSi) were assessed using unweathered bedrock samples and soil collected from 30 – 40 cm depth at the plateau position in each geochemical region. This location and depth was chosen as it (i) represents the most weathered part of the soil column, (ii) excludes any potential influence by lateral fluxes and (iii) reduced the likelihood of biogenic disturbance through root growth, which is concentrated in our sites in organic layers and topsoil (Doetterl *et al.*, 2021a).

3.3.4 Statistical analysis

The significance level for all statistical analysis was set at $p < 0.05$. Differences with depth, topography and geochemistry of the region for the various SOC fractions and SOC-related variables described above were assessed by testing for equality of means using one-way and Welch analysis of variance (ANOVA) ($n = 3$ for plateaus, $n = 6$ for slopes and $n = 3$ for valleys). To avoid type I errors in ANOVA caused by heteroscedasticity (Moder, 2016), we performed Levene's test (Levene, 1960) for all ANOVA. Based on the outcome of the Levene's test, the result of either one-way ANOVA (no heteroscedasticity) or of the Welch ANOVA (heteroscedasticity present) was used. To compare the means of multiple groups, post hoc pairwise comparison was applied using Bonferroni correction (Day and Quinn, 1989) or Tamhane T2 in the case of unequal variances (Tamhane, 1979).

For dimension reduction of independent potential predictors of SOC, to illustrate the variance of these predictors across the dataset, and to minimize multicollinearity in regression analyses, we performed a varimax-rotated principal component analysis (rPCA) (n = 27) using all non-SOC-derived chemical and physical soil variables described above. Only predictor variables with a loading factor of >0.5 or <-0.5 were interpreted for each rotated component (RC). Because of differences in units and ranges of predictor variables, prior to the rPCA, a Z-score standardization (Lacrose, 2004) was applied as follows:

$$X^* = \frac{X - \text{mean}(X)}{\text{SD}(X)}, \tag{3.4}$$

where X^* is the standardized value, X is the original value and SD is the standard deviation.

Only RCs with an eigenvalue >1 and explaining >5 % variances were kept for further statistical analyses. A mechanistic interpretation of the identified RCs was provided based on the loading of each RC.

The remaining RCs were used as explanatory variables in multiple linear stepwise regressions to the most important predictors explaining differences in SOC variables. We focused our analyses on predicting SOC_{bulk} and Δ^{14}C, as well as m / s+c ratios for non-valley positions (n = 27). Valley positions were excluded due to the small sample size (n = 9). As most of these variables naturally show strong depth trends (Minasny *et al.*, 2016), we added soil depth as an additional explanatory variable in our models to avoid over-interpretation of variables, which were cross-correlated with soil depth. After assessing the predictive model strength of our multi-RC models on SOC target variables, we assessed the relative importance of explanatory variables using the R package Relaimpo (Grömping, 2006). In a final step, to disentangle the effect of soil depth and RCs to predict our SOC target variables, partial correlation was used by controlling correlations of RCs to explore whether SOC variables were directly controlled by the rPCs after controlling for soil depth. IBM SPSS Statistics 26 (IBM, 2019) was used for the ANOVA and partial correlation. The rPCA, regressions and relative importance analysis were realized using R 3.6.1 (RCoreTeam, 2020).

3.4 Results

Note that we have pretested for correlations between SOC stocks, mean annual temperature (MAT) and mean annual precipitation (MAP) across our study sites. No significant correlations were found with the included climatic variables (Table A.1), indicating no significant effect of climatic variation between sites on SOC dynamics. Hence, we focused our further analyses on the impact of local geochemistry and topography on SOC stocks and stabilization against microbial decomposition.

For all tested SOC variables, significant differences in the means of different topographic positions within each geochemical region were found between valley and non-valley positions (plateaus and slopes) with higher SOC stocks in valley positions compared to non-valley positions. No significant differences were found between plateau and slope positions (Table A.2). Even though valley positions are of the same geochemistry as the non-valley positions, geochemical soil properties in valleys were significantly different than at non-valley positions, as fluvial activity and sedimentation unrelated to hillslope processes were dominant (see Supplement A.1 for additional results and discussion on valley positions). Consequently, for all follow-up analyses on differences with soil depth and geochemistry, the dataset was split into valley positions vs. non-valley positions. Due to the limited sample size for the valley positions ($n = 1 - 3$), no further statistical analysis was applied. However, all valley data are available in a short supplementary result and discussion section attached to this paper (see Supplement A.1).

3.4.1 Soil chemical weathering stage and pedogenic oxides

Parent material geochemistry and weathering stage

Parent material, from which soils in the three geochemical regions have developed, showed distinct differences in elemental composition (Doetterl *et al.*, 2021a; Doetterl *et al.*, 2021b), with generally low concentrations of Ca, Mg and Na base cations (0.01 − 0.58 wt%). Al and Fe concentrations were significantly higher in the mafic (Al: 6.27 ± 2.84; Fe: 8.98 ± 1.84 mass%) than sedimentary rocks region (Al: 0.62 ± 0.41; Fe: 2.32 ± 1.73 mass%) and the felsic region (Al: 0.52 ± 1.21; Fe: 1.09 ± 1.58 mass%). Similarly, total P was highest in the mafic region (P: 0.37 ± 0.14 mass %) compared to the mixed sedimentary (P: 0.02 ± 0.02 mass%) and the felsic region (P: 0.01 ± 0.1 mass%). In contrast, Si content was lowest in the mafic region (Si: 14.22 ± 2.01 mass%) compared to the mixed sedimentary rocks region (Si: 36.11 ± 7.01 mass%) and the felsic region (Si: 37.29 ± 5.92 mass%). Across geochemical regions, soils were highly weathered, as indicated by high CIA values of 78 % − 99 % at all three soil depths (data not shown). Soils developed from mafic parent material were depleted in Ca, Mg and Na base cations compared to parent material (Ca: -38 % to -100 %; Mg: -72 % to -87 %; Na: -90 % to 375 %). Soils developed in the mixed sedimentary region were depleted in Ca (-100 ± 172 %) compared to parent material but not for Mg or Na. Soils developed from felsic parent material showed a substantial increase in all base elements (Ca: up to 1240 %; Mg: up to 1015 %; Na: up to 677 %). All soils were enriched in Al compared to parent material (mafic: up to 307 %; felsic: up to 6859 %; mixed sedimentary: up to 1514 %). Similarly, all soils were enriched in Fe compared to parent material (mafic: up to 85 %; felsic: up to 1482 %; mixed sedimentary: up to 3486 %). Soils developed from mafic parent material showed depletion in P (-72 % to 14 %) compared to the parent material. In contrast, we observed an enrichment in P for soils developed from mixed sedimentary (up to +2583 %) and felsic parent material (up to 6671 %) compared to parent material. Note that the extraordinarily high differences in P between soil and parent material in the latter regions are mainly related to the fact that P concentrations in parent material of the felsic and sediment region were extremely small to begin with but did accumulate in soil through fixation in the biosphere and plant uptake (Wang *et al.*, 2010; Wilcke *et al.*, 2002). This interpretation is supported by the observations that P mass in all three geochemical regions for the investigated soil layers used for comparison to parent material converges (mafic: 0.15 ± 0.002 mass%; felsic: 0.05 ± N/A mass%; mixed sedimentary: 0.08 ± 0.01 mass%), while other less critical elements for biological processes leached during soil development. For example, all soils were depleted in Si compared to the parent material (mafic: -27 % to 8 %; felsic: -62 % to -26 %; mixed sedimentary: -71 % to -58 %), which is indicative of long-term weathering.

Pedogenic oxides

For non-valley positions, pyrophosphate-extractable oxides (0.02 to 1.93 mass%) and oxalate-extractable oxides (0.32 to 2.33 mass%) were low compared to DCB-extractable oxides (2.74 to 13.63 mass%) (Figure 3.4). Pyrophosphate-extractable oxides showed no significant differences across geochemical regions. Oxalate-extractable oxides were significantly higher across all soil depths in mafic (1.68 to 2.33 mass%) and mixed sedimentary (0.32 to 2.28 mass%) soils compared to soils developed from felsic parent material (0.35 to 0.91 mass%). DCB-extractable oxides across all soil depths were significantly higher in mafic soils (9.54 to 13.63 mass%) compared to soils developed from felsic (2.74 to 7.03 mass%) and mixed sedimentary parent material (3.55 to 8.44 mass%).

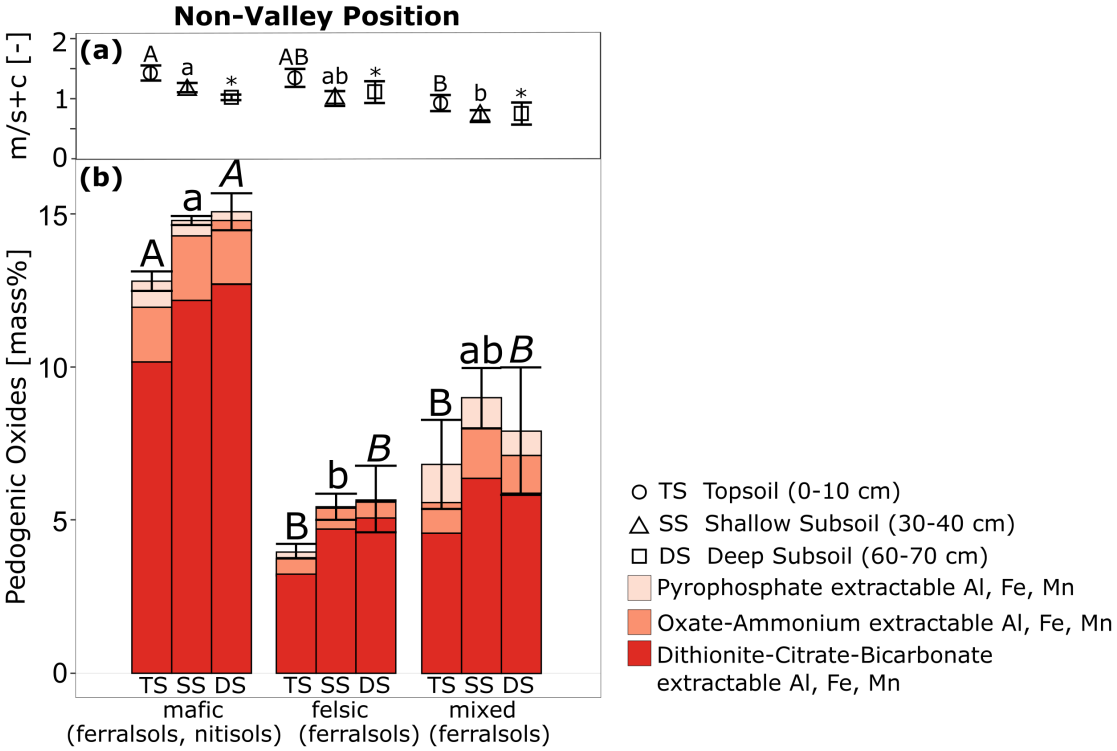

Figure 3.4: (a) m/s + c ratio (n = 9 per bar) and (b) pedogenic oxide fractions (n = 3 per bar) of the sequential extraction across geochemical regions in non-valley positions. Where letters share the same font type, means were compared to each other, with letters indicating significant differences between geochemical regions per soil depth for m/s + c ratio (a) and total pedogenic oxide mass (b). Asterisks indicate no significant differences in means ($p > 0.05$). The error bar represents standard error.

3.4.2 Variation in SOC properties with geochemistry

SOC$_{bulk}$

SOC$_{bulk}$ in topsoil did not differ across geochemical regions (mafic: 50.6 ± 13.9 tC ha^{-1}; felsic: 45.3 ± 3.9 tC ha^{-1}; mixed sedimentary: 44.0 ± 3.9 tC ha^{-1}), whereas subsoil SOC$_{bulk}$ was significantly smaller in the felsic region (shallow subsoil: 16.3 ± 2.5 tC ha^{-1}; deep subsoil: 10.1 ± 1.9 tC ha^{-1}) compared to the mafic (shallow subsoil: 28.3 ± 3.3 tC ha^{-1}; deep subsoil: 22.9 ± 7.2 tC ha^{-1}) and mixed sedimentary region (shallow subsoil: 30.4 ± 2.8 tC ha^{-1}; deep subsoil: 23.9 ± 4.7 tC ha^{-1}). Note that while SOC$_{bulk}$ decreased strongly with depth in the mafic and felsic region, only a weak decrease in SOC$_{bulk}$ with depth was observed in the mixed sedimentary region (Figure 3.5).

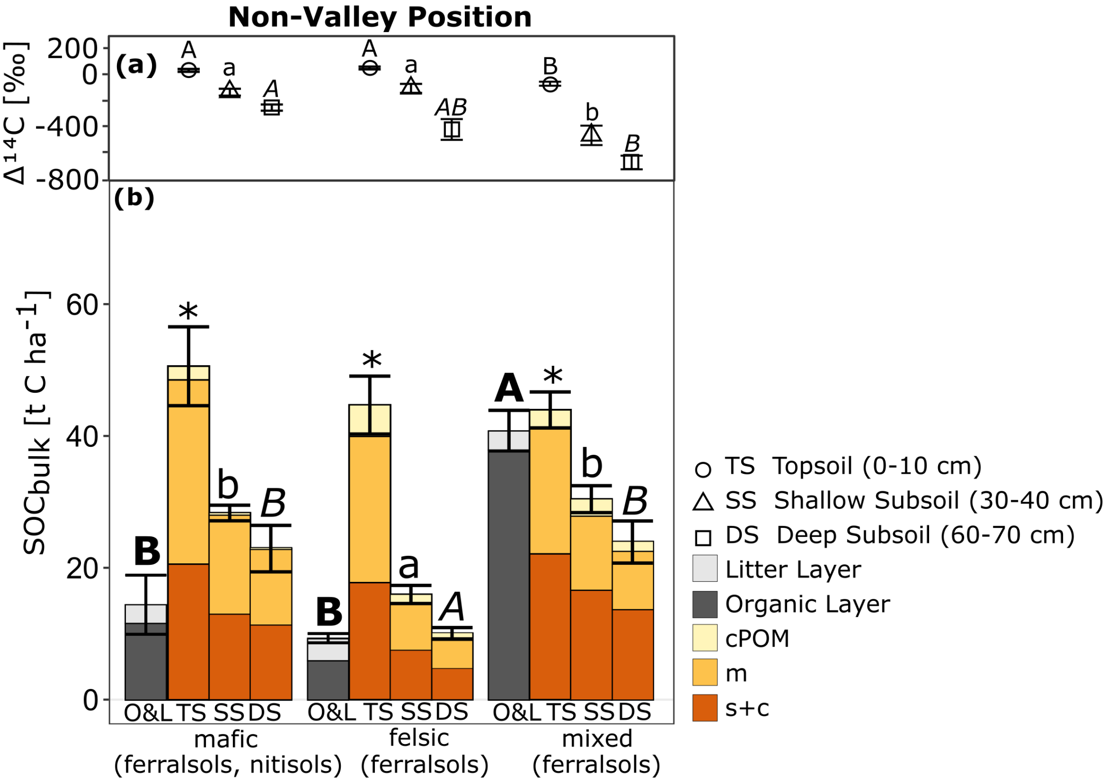

Figure 3.5: (a) Δ^{14}C across geochemical regions in non-valley positions (n = 3 per bar). (b) SOC$_{bulk}$ and fractions across geochemical regions in non-valley positions (n = 9 per bar). Where letters share the same font type, means were compared to each other, with letters indicating significant differences between geochemical regions per soil layer for Δ^{14}C (a) and SOC$_{bulk}$ (b). Asterisks indicate no significant differences in means (p >0.05). For Δ^{14}C values, error bars are smaller than symbols. cPOM – coarse particulate organic matter, m – stable microaggregates, s+c – free silt and clay fraction.

Abundance of C fractions

At all sites and soil depths, fractions were dominated by microaggregate-associated C (SOC$_{53-250\mu m}$), contributing 32.6 ± 9.9 % to 55.2 ± 1.4 % of SOC$_{bulk}$, and free-silt-and clay-associated C (SOC$_{<53\mu m}$), contributing 40.3 ± 4.8 % to 54.5 ± 2.4 % of SOC$_{bulk}$. Coarse particulate organic carbon (SOC$_{>250\mu m}$) contributed 1.4 ± 0.2 % to 11.1 ± 1.5 % of SOC$_{bulk}$. Microaggregate-associated C and m / s+c ratios were generally higher in topsoils (SOC$_{53-250\mu m}$: 43.19 ± 6.77 % to 55.23 ± 1.43 %; m / s+c: 0.93 ± 0.17 to 1.42 ± 0.04) compared to subsoils (SOC$_{53-250\mu m}$: 32.64 ± 9.88 % to 49.65 ± 1.84 %; m / s+c: 0.75 ± 0.2 to 1.07 ± 0.35) (Figure 3.4a). For topsoil and shallow subsoil, the m / s+c ratio was significantly higher in the mafic region than in the sediment region, meaning more microaggregate-associated C in mafic than in mixed sediments compared to free-s+c-associated C. The felsic region ranges between the other two geochemical regions in this regard and was not significantly different to either one. Deep subsoil m / s+c indicated the same trends but was not statistically different across regions

(Figure 3.4a). Note that the relative abundance of microaggregate-associated and free silt and clay associated with C was not significantly different with topographic positions (Table A.2).

Changes in ^{14}C signature

Soils from all geochemical regions at non-valley positions were significantly more depleted in Δ^{14}C with increasing soil depth (Figure 3.5a and b). The Δ^{14}C ranged from 31.2 ± 11.5 ‰ (mafic) to -78.7 ± 26.6 ‰ (mixed sedimentary) in the topsoil and -257.8 ± 32.8 ‰ (mafic) to -675.2 ± 89.6 ‰ (mixed sedimentary) in subsoil. While there were no significant differences between Δ^{14}C of comparable samples of the felsic and mafic region, their counterparts from the mixed sedimentary region were significantly more depleted in Δ^{14}C. The contribution of FOC to soil C in the mixed sedimentary region increased significantly with soil depth for non-valley positions, ranging from 11.3 ± 2.6 % FOC in topsoils to 52.0 ± 13.2 % in subsoils (Table 3.1).

Table 3.1: Proportion of biogenic- vs. fossil-derived organic carbon (OC) in soils developed from mixed sedimentary rocks in non- valley positions (n = 3). FOC values in felsic and mafic soils were 0 % (data not shown).

Depth increment	Amount of biogenic OC (%)	Amount of fossil OC (%)
0 – 10 cm	88.7 ± 2.6	11.3 ± 2.6
30 – 40 cm	60.7 ± 14.5	39.3 ± 14.5
60 – 70 cm	48.0 ± 13.2	52.0 ± 13.2

3.4.3 Rotated principal component explained variance and loadings

Four rPCs were determined (rPC_{nv}) explaining 78.1 % of the variance in the non-valley position subset (Figure 3.6; Table A.4). $rPC1_{nv}$(eigenvalue 9.34, explaining 33.4 % of the variance) represents solid-phase mineralogy, in which total metal oxide concentration (ΣFe, Al, Mn), DCB-extractable oxide concentration and the Al / Si ratio had strong positive loadings (variable loading >0.9), while Si, the pH / clay ratio and sand content had strong negative loadings (<-0.7). $rPC2_{nv}$ (eigenvalue 9.15, explaining 32.7 % of the variance) represents the chemistry of the soil solution where exchangeable bases, the cation exchange capacity (CEC) base saturation / clay ratio and the Ca / Ti ratio showed strong positive loadings (≥0.87), and exchangeable acidity, CIA and $SOC_{organic}$ showed strong negative loadings (<-0.5). $rPC3_{nv}$ (eigenvalue 1.82, explaining 6.5 % of the variance) represents silt content and the C stock of organic layers ($SOC_{organic}$), both having a strong negative loading (<-0.5). $rPC4_{nv}$ (eigenvalue 1.57, explaining 5.6 % of the variance) represents organo–mineral complexes, with pyrophosphate-extractable oxide concentration showing a strong positive loading (<0.8).

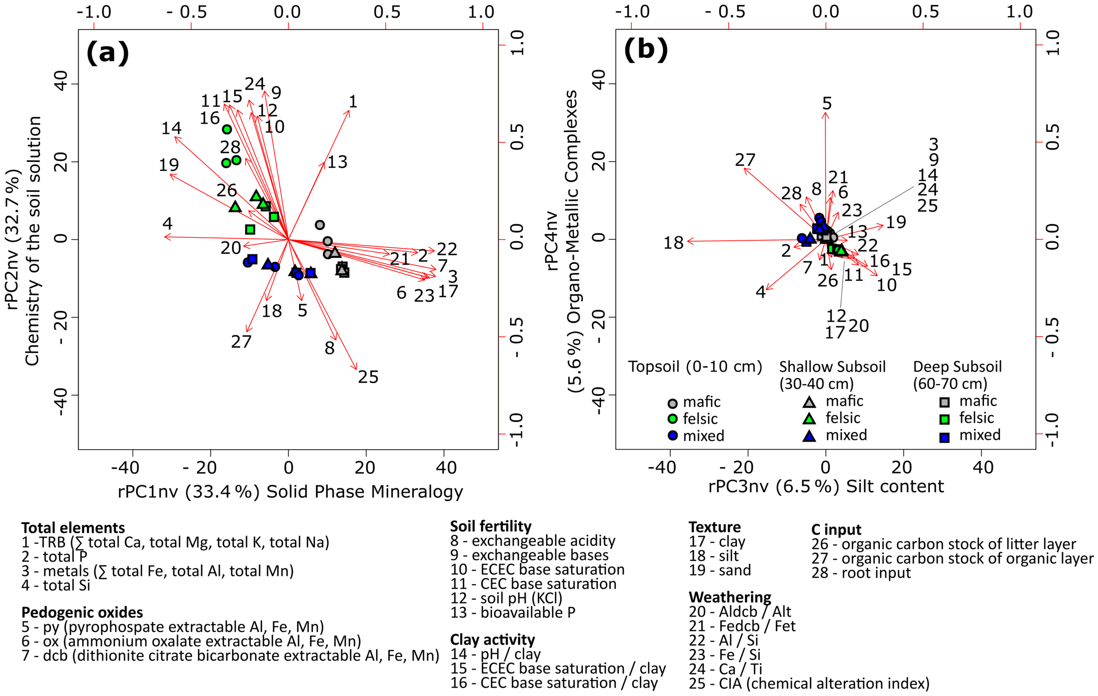

Figure 3.6: Biplots of the varimax-rotated principal component analysis. (a) $rPC1_{nv}$ and $rPC2_{nv}$ and (b) $rPC3_{nv}$ and $rPC4_{nv}$ of non-valley positions ($n = 27$). Observations cluster together based on similarities within geochemical regions and their distinction to other geochemical regions. Vector length indicates how strongly variables influence a specific rPC. The angles between vectors display the degree of auto- correlation between variables. Small angles represent positive correlations and high degree of autocorrelation, diverging angles represent negative correlations and a high degree of autocorrelation, and high angles indicate no correlations between variables and / or rPCs.

3.4.4 Explained variability and relative importance of predictors (non-valley soils)

Soil depth and $rPC4_{nv}$ explained 73 % of variability (R^2) in SOC_{bulk} ($p < 0.01$). Soil depth contributed 82 % to the explanatory power of the model (Table 3.2). The second most important explanatory variable in our model was $rPC4_{nv}$, which represented organo – mineral complexes ($p < 0.01$) and contributed 18 % to the explanatory power of the model. Soil depth and $rPC1_{nv}$, $rPC3_{nv}$ and $rPC4_{nv}$ could explain 75 % of variability (R^2) in $\Delta^{14}C$ data ($p < 0.01$). Soil depth contributed 75 % to the explanatory power of the model, followed by $rPC3_{nv}$ (silt content, 16 % explanatory power), $rPC4_{nv}$ (organo–mineral complexes, 5 % explanatory power) and rPC1nv (solid-phase mineralogy, 4 % explanatory power). Soil depth, $rPC1_{nv}$ and $rPC2_{nv}$ could explain 44 % of variability (R^2) in the m / s+c ratio ($p < 0.01$). $rPC2_{nv}$ contributed 46 % to the explanatory power of the model, followed by rPC1$_{\mathrm{nv}}$ (solid-phase mineralogy, 31 % explanatory power) and soil depth (23 % explanatory power), making m / s+c ratios the only SOC target variable not highly correlated with soil depth.

Table 3.2: Multiple linear stepwise regression analysis (beta coefficients) and relative importance analysis in brackets for non-valley soils. SOC$_{\mathrm{bulk}}$, Δ^{14}C and the m / s + c ratio are explained by soil depth and the extracted rPCs. Adjusted R^2 displays the goodness of fit, and the root mean square error (RMSE) assesses the model quality.

Response	Soil depth	rPC1$_{\mathrm{nv}}$ – solid phase mineralogy	rPC2$_{\mathrm{nv}}$ – chemistry of the soil solution	rPC3$_{\mathrm{nv}}$ – silt content	rPC4$_{\mathrm{nv}}$ – organo-mineral complexes	Adjusted R^2	RMSE
SOC$_{\mathrm{bulk}}$	-0.77^{c} (82 %)				0.31^{c} (18 %)	0.73	0.46
Δ^{14}C	-0.87^{c} (75 %)	0.39^{b} (4 %)		0.24^{a} (16 %)	-0.32^{a} (5 %)	0.75	0.47
m / s+c	-0.29^{a} (23 %)	0.74^{c} (31 %)	0.8^{c} (46 %)			0.44	0.39

^{a} $p < 0.1$. ^{b} $p < 0.05$. ^{c} $p < 0.01$.

3.4.5 Partial correlations controlled for soil depth

When controlling for soil depth, correlations between SOC$_{bulk}$ and the identified rPCs became significant, with changes in correlation coefficients ranging from 0.01 to 0.44 (Table 3.3). Solid-phase mineralogy explained 16.8 %, chemistry of the soil solution 15.2 %, silt content 16.8 % and organo – mineral complexes 28.1 % of the variability (R^2) in SOC$_{bulk}$. Correlation between Δ^{14}C and the chemistry of the soil solution became insignificant and declined by 0.13, whereas the correlation of silt content and organo – mineral complexes improved by 0.16 and 0.22, respectively. Silt content explained 32.5 %, and organo – mineral complexes explained 12.3 % of the variability (R^2) in Δ^{14}C. Correlation between the m / s+c ratio and chemistry of the soil solution decreased by 0.09, with only silt content left with a significant correlation. Silt content explained 22.1 % of the variability (R^2) in the m / s+c ratio.

Table 3.3: Partial correlation analysis between SOC variables (SOC_{bulk}, $\Delta^{14}C$ and m/s+c ratio) and extracted rPCs controlling for soil depth. Zero-order correlation displays the Pearson r value when including no control variable. The controlled correlation shows the Pearson r value when controlling for soil depth.

Response	Control	$rPC1_{nv}$ – solid phase mineralogy		$rPC2_{nv}$ – chemistry of the soil solution		$rPC3_{nv}$ – silt content		$rPC4_{nv}$ – organo – mineral complexes	
		Pearson r	R^2	Pearson r	R^2	Pearson r	R^2	Pearson r	R^2
SOC_{bulk}	zero-order	0.06	0.00	0.05	0.00	-0.19	0.04	$0.41^{b,d}$	0.17
	soil depth	$0.41^{b,d}$	0.17	$-0.39^{b,f}$	0.15	$-0.41^{b,g}$	0.17	$0.53^{c,d}$	0.28
$\Delta^{14}C$	zero-order	-0.05	0.00	$0.44^{b,d}$	0.19	$0.41^{b,d}$	0.17	-0.13	0.02
	soil depth	0.19	0.04	0.31^{e}	0.10	$0.57^{c,d}$	0.32	$-0.35^{a,f}$	0.12
m / s+c	zero-order	0.13	0.02	$0.38^{a,e}$	0.14	$0.46^{b,d}$	0.21	-0.22	0.05
	soil depth	0.23	0.05	0.29	0.08	$0.47^{b,d}$	0.22	-0.30f	0.09

[a] *$p < 0.1$.* [b] *$p < 0.05$.* [c] *$p < 0.01$. Pearson's r and R^2 values derive from simple linear regression between the individual rPCA and the respective SOC variable.* [d] *$r > 0.4$.* [e] *$r > 0.3$.* [f] *$r < -0.3$.* [g] *$r < -0.4$.*

3.5 Discussion

3.5.1 Soil C stabilization against microbial decomposition driven by soil chemistry and parent material

In contrast to our initial hypothesis that topography affects C stabilization in tropical forest soils through lateral material movements, we found no indication of this in our analysis (see the Supplement and Short discussion A.1 therein). Despite prolonged chemical weathering, parent material leaves an identifiable, long-lasting footprint in the chemical properties of tropical forest soils (Figure 3.6). Overall, the differences in elemental composition between parent materials in each geochemical region, together with enrichment and depletion processes of elements during weathering, have resulted in soils with specific properties and prerequisites for SOC stabilization against microbial decomposition (Table A.3). In particular, stabilization mechanisms related to pedogenic oxides (Figure 3.4) and the formation of organo – mineral associations are relevant for SOC stabilization at our sites, as illustrated by the strong correlation of variables representing organo – mineral complexes with SOC_{bulk} and $\Delta^{14}C$ (Table 3.3). The influence of parent material geochemistry and weathering on the pattern of physically separated soil C fractions, in particular on stabilizing C in microaggregates, was smaller across soil geochemical regions than across soil depths. (Figures 3.4 and 3.5 and Table 3.3). The most important variables for explaining m / s+c ratios were found to be soil depth, solid-phase mineralogy and the chemistry of the soil solution, which could in total explain 44 % of m / s+c variance (Table 3.2). We interpret the high m / s+c ratios in topsoils as indicative for the formation of stable microaggregates promoted by the higher abundance of C, which functions as a binding agent (Denef and Six, 2005) and the generally more fertile conditions in tropical topsoil compared to subsoil favoring microbial activity (Kidinda *et al.*, 2022). The abundance of pedogenic oxides further promotes aggregation by providing reactive mineral surfaces (Oades, 1988). In this study, pedogenic oxides are determined by geochemistry with higher contents in mafic compared to felsic and mixed sedimentary soils (Figure 3.4b). Therefore, mafic soils also stabilize more C in microaggregates. It is likely that the high amount of pedogenic oxides usually measured in microaggregates (Doetterl *et al.*, 2015b) and the low amount of particulate organic matter (POM) measured in our study overall suggests that predominantly mineral-complexed SOC accumulated within the isolated aggregates. This is supported by studies showing that microaggregate-sized particles in deeply weathered tropical soils are rich in Fe and Al concretions (Cooper *et al.*, 2005; Denef *et al.*, 2007; Martinez and Souza, 2020; Zotarelli *et al.*, 2005). Fe oxides like hematite can incorporate large amounts of Al in their crystal structure by substitution, especially within a kaolinite-rich soil matrix (Tardy and Nahon, 1985). Such (hydro)oxides of Al and Fe act as a cementing agent in the formation of pseuosands, and their chemical composition is controlled by parent material geochemistry. In general, (hydro)oxides dominated by Fe are more abundant on mafic rocks, whereas Al is more abundant on rocks with low amounts of Fe (e.g., quartz-rich sedimentary rocks) (Martinez and Souza, 2020). In our study, both the parent material and soil geochemistry show considerable amounts of Al, even though the Fe content exceeds that of Al. The dominating soils are Ferralsols and Nitisols, which are dominated by kaolinitic clays. Given the above-mentioned observations, it is likely that Fe and Al concretions are present in the studied soils, even though the elemental composition of the concretions was not directly measured. In light of this finding, aggregation is an important means to promote the complexation of C with minerals (Martinez and Souza, 2020) but also the result of the tendency of pedogenic oxides to form stable aggregates (Doetterl *et al.*, 2015b), which lends additional protection of soil C. When controlling for soil depth, our geochemical predictors ($\mathrm{rPC1_{nv}}$, $\mathrm{rPC2_{nv}}$, $\mathrm{rPC3_{nv}}$, $\mathrm{rPC4_{nv}}$) gained or retained similar prediction power (Table 3.3), showing the importance for predicting SOC target variables at all soil depths. Geochemical predictors were also more important to stabilize C in shallow and deep subsoils compared to topsoils, as indicated by the absence of correlations in topsoils but significant correlations in subsoils (data not shown).

3.5.2 Fossil organic carbon contributions to SOC_{bulk} and driving Δ^{14}C

While depth trends in Δ^{14}C were similar across geochemical regions (Figure 3.5a), soils developed on mixed sedimentary rocks were significantly depleted in Δ^{14}C for all topographic positions. A significant amount between 11.3 ± 2.6 and 52.0 ± 13.2 % FOC was found to contribute to

SOC_{bulk} in soils developed on mixed sedimentary rocks (Table 3.1), thus supporting our initial hypothesis (iii) that FOC-bearing parent material will strongly impact SOC_{bulk}. Despite contributions of FOC of up to 52 %, SOC_{bulk} did not differ to the same extent between the geochemical regions (Figure 3.5b). Two potential explanations could be found for this observation. First, fertility conditions and stabilization mechanisms against microbial decomposition in soils developed from mixed sedimentary parent material reduce the amount of SOC with modern biogenic origin drastically due to slower C cycling (Trumbore, 2009). However, neither $\Delta^{14}C$ nor the analyzed distribution of soil C fractions support this explanation. Biologically active topsoil $\Delta^{14}C$ in the mixed sediment region was less depleted than the subsoil counterparts when being compared across regions (Figure 3.5). Additionally, auxiliary data on the overall net primary productivity of the investigated systems (Doetterl *et al.*, 2021a; Doetterl *et al.*, 2021b) point towards relatively comparable C inputs across the three regions, at least in topsoil. Subsoils of the sediment region, however, may receive significantly less C input, which is the subject of future investigations. A second explanation could be the decomposition of FOC once it enters more biologically active zones (i.e., topsoils), where climatic and edaphic conditions are more suitable for microbial decomposer communities. Findings on $\Delta^{14}C$ signatures of respired C indicate the presence of FOC contributing to CO_2 release (Bukombe *et al.*, 2021). Here, on average only 6.7 ± 2.5 % of the respired CO_2 showed a fossil origin in the non-valley positions. Hence, the fact that FOC content increases with depth (Table 3.1) but is nearly depleted in topsoils indicates that these sources of fossil C, even though a poor source of nutrients and energy for microorganisms (Hemingway *et al.*, 2018), can become available to microbial decomposition under more suitable conditions. Statistically, differences in $\Delta^{14}C$ were best explained by soil depth (Table 3.2) but between regions by the presence of FOC in soils developed from mixed sedimentary parent material and when controlling for soil depth with geochemical variables (Table 3.2). Further, our model identified silt content as a strong predictor for $\Delta^{14}C$. It is possible that tropical soils form very stable silt-sized microaggregates (Six *et al.*, 2000b), in which FOC is potentially stabilized. However, the low pedogenic oxide content in the mixed sedimentary region, important for microaggregate formation (Denef *et al.*, 2007; Doetterl *et al.*, 2015b; Martinez and Souza, 2020; Zotarelli *et al.*, 2005), is not entirely supportive of this interpretation. There is also no statistically significant relationship between fine soil texture classes and the C associated with microaggregates or the free silt and clay fraction in our investigated sites in the sediment region (data not shown). We argue, therefore, that no mechanistic relationship exists between $\Delta^{14}C$ and silt content, and the observed relationship is to be interpreted as an autocorrelation between the high amounts of ^{14}C-depleted FOC in the mixed sedimentary region and the fact that these sediments have a higher silt content than their felsic and mafic counterparts.

3.5.3 Interpreting soil controls for predicting SOC dynamics

Our regression analyses revealed that a wide variety of soil variables contribute to predicting SOC and its turnover in a quantitative and qualitative way (Tables 3.2 and A.4). An exact mechanistic interpretation is difficult due to the relatively small number of observations compared to potential predictor variables. However, in general a set of variables related to soil fertility and the chemistry of the solid phase and soil solution contributed to predicting our three target variables: (1) SOC_{bulk}, (2) $\Delta^{14}C$ and (3) m / s+c (Tables 3.2 and A.4). Furthermore, some interpretation of the included rotated components is possible because their respective loading is clearly distinct from each other (Table A.4, Figure 3.6). Notably, the prediction power of our models was dominated by soil depth (Table 3.2) for all three target variables. However, partial correlation revealed that soil depth covered relationships between the target variables and our predictors (Table 3.3), indicating that soil depth is autocorrelated with variability in soil mineralogy and soil fertility. For example, solid-phase mineralogy and organo − mineral complexes reflect the amount of total elements in the soil and their transformation into secondary minerals and thus the amount of reactive mineral surfaces, which are highly relevant in the sorptive protection of SOC (Evanko and Dzombak, 1998; Kleber *et al.*, 2015; Oades, 1984). Similarly, the chemistry of the soil solution represents properties that are relevant for C stabilization against microbial decomposition. Here, low pH levels can mobilize Al^{3+}, which eventually sorbs onto reactive mineral surfaces, preventing C stabilization (Smith, 1999). In our mafic soils, sorptive C stabilization created by pedogenic oxides leads to high SOC_{bulk} (Figures 3.4 and 3.5 and Table 3.2) and supports the formation of aggregates. Conversely, felsic soils are low in pedogenic oxides and thus have low sorption potential and consequently also the lowest SOC_{bulk}. Clay content, identified as a major factor for stabilizing SOC in temperate soils (Angst *et al.*, 2018) and also in tropical soil systems (Quesada *et al.*, 2020; Souza *et al.*, 2017), was not identified as a major control for our soils. This illustrates the importance of understanding soil geochemical preconditions when identifying controls of C dynamics and that findings are not necessarily transferable, even between comparable soil types and climates. Overall, we found that chemical stabilization of SOC, especially by organo − mineral complexation, contributed the most to explaining differences in SOC_{bulk} in the analyzed soils, while aggregation, profiting from the abundance of pedogenic oxides and stable Fe and Al structures in soils, added additional C stabilization potential. Hence, under similar climatic conditions and similar C input through vegetation (Doetterl *et al.*, 2021a), our data indicate that C stabilization mechanisms in soil control SOC stocks and turnover in deeply tropical weathered soils more so than soil fertility conditions and drive patterns of SOC stocks across geochemical regions (Figures 3.4 and 3.5). Our results are comparable to other studies investigating the impact of reactive mineral surfaces on SOC_{bulk} in tropical kaolinitic soils (Bruun *et al.*, 2010) and the importance of sorptive processes to C on mineral surfaces (Jagadamma *et al.*, 2014). These processes have been identified to be important for soil C stabilization in a variety of ecosystems and climate zones (Evanko and Dzombak, 1998; Fang *et al.*, 2019; Kögel-Knabner *et al.*, 2008; Murphy *et al.*, 1992)). However, they stand out in tropical soils due to the high amounts of Fe and Al oxides in the system overall and the advanced stage of weathering of soils that led to the formation of low-activity clays and other end-member minerals with low potential for C sorption (Ito and Wagai, 2017).

3.6 Conclusion and outlook

Overall, we found a minimal impact of topography on SOC variables as a function of soil fluxes along slopes but observed higher SOC stocks in valleys compared to non-valley positions due to varying hydrological conditions and alluvial processes. Instead, chemical soil properties, derived from parent material geochemistry, were identified as major explanatory factors. We argue that the strong role of geochemical variables in explaining SOC is a function of reactive mineral surfaces dependent on the composition of the parent material and its weathering status. More available reactive surfaces will favor sorptive C stabilization and the formation of stable aggregates, thus leading to higher SOC_{bulk}. In the deeply weathered tropical soil systems investigated, the formation of organo–mineral complexes of Al, Fe and Mn was most important for explaining SOC_{bulk} across geochemical regions, and the impact of clay content was minimal. Differences in the relative abundance of C associated with microaggregates and with free silt and clay fractions differed significantly between geochemical regions and soil depth, indicating that despite long-lasting weathering, mafic soils can protect C better than their felsic and mixed sediment counterparts. Aggregate formation in tropical soils seems to profit from the abundance of pedogenic oxides in soils, linking two of the most important mineral-related C stabilization mechanisms against microbial decomposition in soil with geochemical variability retained from parent material. Differences in Δ^{14}C were best explained by soil depth as a proxy for factors limiting microbial respiration, which are more pronounced in subsoils than in topsoils. While following similar depth trends, the presence of fossil organic carbon contributed to significantly explain the Δ^{14}C pattern when comparing across regions. It is recommended to repeat our analyses in other tropical soil and land use systems, where external drivers such as soil redistribution, weathering stages or stabilization mechanisms against microbial decomposition might differ. This way, a more spatially explicit picture of C stabilization mechanisms will contribute to understanding future tropical SOC dynamics in light of ongoing climatic and land use changes, as well as the representation of SOC stabilization and destabilization in land surface models.

Chapter 4

Soil carbon stocks in stable tropical landforms are dominated by geochemical controls and not by land use

---

The content of this chapter has been published as: Reichenbach, M., Fiener, P., Hoyt, A., Trumbore, S., Six, J., and Doetterl, S.: Soil carbon stocks in stable tropical landforms are dominated by geochemical controls and not by land use. Global Change Biology, 29, 2591–2607, https://doi.org/10.1111/gcb.16622, 2023.

Author contributions: Sebastian Doetterl and Peter Fiener designed the research. Mario Reichenbach conducted the sampling campaign and collected the data. All authors analyzed and interpreted the data. All authors contributed to the writing of the paper.

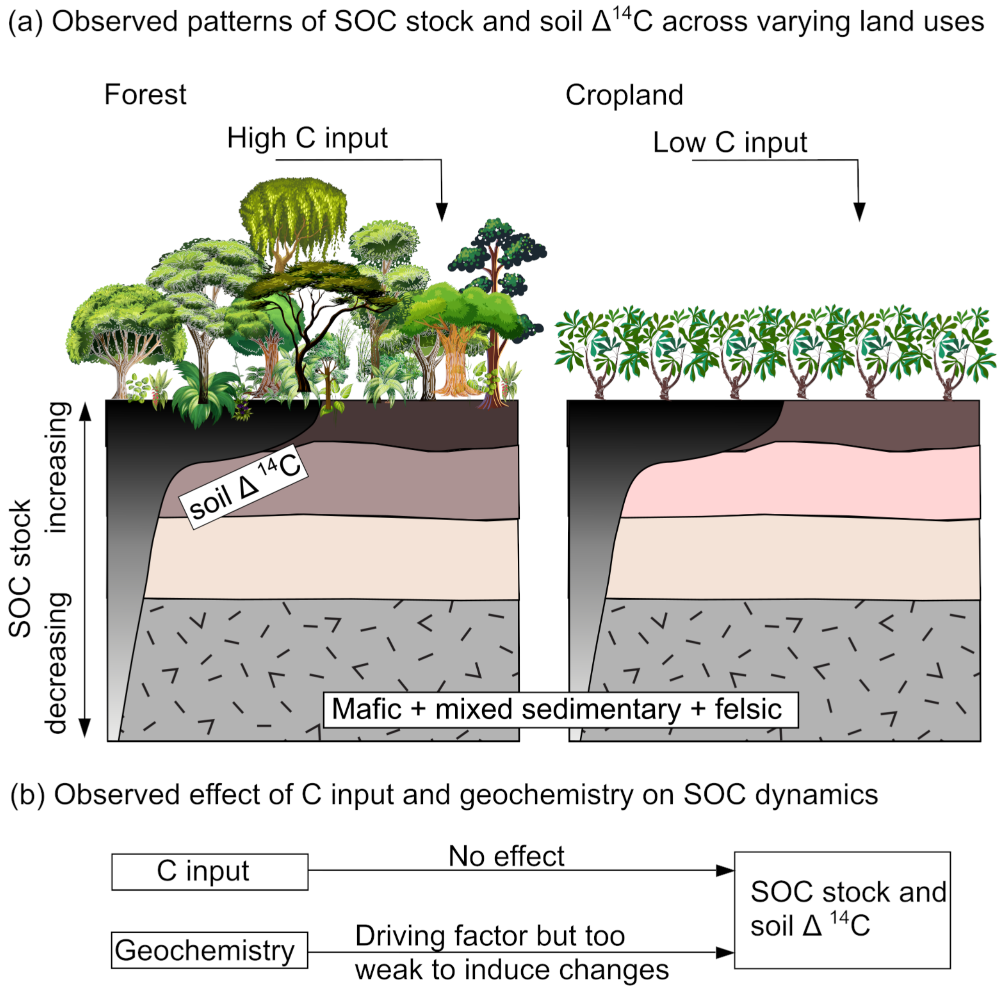

Figure 4.1: Graphical abstract – Pattern and controls of mineral C stabilization across land uses.

4.1 Abstract

Soil organic carbon (SOC) dynamics depend on soil properties derived from the geoclimatic conditions under which soils develop and are in many cases modified by land conversion. However, SOC stabilization and the responses of SOC to land use change are not well constrained in deeply weathered tropical soils, which are dominated by less reactive minerals than those in temperate regions. Along a gradient of geochemically distinct soil parent materials, we investigated differences in SOC stocks and SOC (Δ^{14}C) turnover time across soil profile depth between montane tropical forest and cropland situated on flat, non-erosive plateau landforms. We show that SOC stocks and soil Δ^{14}C patterns do not differ significantly with land use, but that differences in SOC can be explained by the physicochemical properties of soils. More specifically, labile organo – mineral associations in combination with exchangeable base cations were identified as the dominating controls over soil C stocks and turnover. We argue that due to their long weathering history, the investigated tropical soils do not provide enough reactive minerals for the stabilization of C input in either high input (tropical forest) or low-input (cropland) systems. Since these soils exceeded their maximum potential for the mineral related stabilization of SOC, potential positive effects of reforestation on tropical SOC storage are most likely limited to minor differences in topsoil without major impacts on subsoil C stocks. Hence, in deeply weathered soils, increasing C inputs may lead to the accumulation of a larger readily available SOC pool, but does not contribute to long-term SOC stabilization.

4.2 Introduction

The loss of forests driven by cropland expansion and deforestation for timber, agriculture, or charcoal production is a global problem, with great consequences for terrestrial carbon cycling. The vast majority of research analyzing the effect of land conversion on SOC dynamics focuses on geochemically less altered and more intensively managed soils of the temperate zone (Cotrufo *et al.*, 2019; Degryze *et al.*, 2004; Gregorich *et al.*, 1998; Lugato *et al.*, 2018). In these younger, often more productive soils of the temperate zone, land conversion from forest to cropland accelerates SOC decomposition by enhancing biological activity (e.g., by changing soil moisture, aeration, and temperature), paired with lower C inputs from plant primary productivity and the removal of biomass through harvesting. Studies on the effects of land conversion on SOC dynamics in geochemically more altered soils in low intensity management systems of the Tropics, however, are still rare (Köchy *et al.*, 2015; Schimel *et al.*, 2015), despite their importance for the global C cycle and high rates of deforestation (Amundson *et al.*, 2015; Curtis *et al.*, 2018; Gerland *et al.*, 2014; Tyukavina *et al.*, 2018). The consequences of this accelerated land conversion for biogeochemical cycles are unclear, particularly for tropical Africa. Limited observations of processes controlling SOC dynamics in critical regions of the African Tropics with growing land pressure lead to substantial uncertainties in predicting SOC stocks after conversion and limit our ability to upscale local experimental findings to larger scales (Fromm *et al.*, 2021; Sanderman and Chappell, 2013; Vereecken *et al.*, 2016). Thus, land use change effects on soils remain poorly constrained for Africa, despite their importance (Cusack *et al.*, 2013; Don *et al.*, 2011; Kirsten *et al.*, 2021b; Perrin *et al.*, 2014).

Previous studies show that tropical land conversion from forest to cropland may drive substantial SOC losses just as observed in temperate zones (Don *et al.*, 2011). According to the literature, most tropical soils lose between 30 % and 70 % of SOC during the first few years after conversion from forest to cropland (Don *et al.*, 2011; Gregorich *et al.*, 1998; Guillaume *et al.*, 2015; Wei *et al.*, 2014). These SOC losses are not limited to topsoil and the loss of labile C sources alone, but are also detectable in subsoil where C is predominately sorbed to and stabilized by minerals (Don *et al.*, 2011; Luo *et al.*, 2020a). Despite these reported general trends, presumed SOC losses upon conversion to cropland are difficult to predict across larger scales. Data are often derived from regions under seasonal climate or geomorphologically and geologically active zones where soils are generally younger and less weathered. Additionally, SOC dynamics depend on several interacting factors like mineralogy, crop and soil types, management practices, and land use history (Don *et al.*, 2011; Fujisaki *et al.*, 2015). The combination of these factors is usually not assessed across regions, catchments, or even fields. Recent studies do indicate that substantial variability in the potential of tropical soils to stabilize C is more governed by geochemical properties (i.e., pedogenic metal phases, clay mineralogy, texture) derived from its soil parent material (Doetterl *et al.*, 2021b; Reichenbach *et al.*, 2021), as well as the degree of soil weathering (Kirsten *et al.*, 2021b) than by land use (Fromm *et al.*, 2021).

In mineral soils, the dominant long-term C stabilization mechanism is the sorption of functional C groups to mineral surfaces (Dick *et al.*, 2005; Herold *et al.*, 2014; Kramer *et al.*, 2012; Lawrence *et al.*, 2015). However, the quantity of secondary, pedogenic minerals is not always indicative of better C stabilization (Bruun *et al.*, 2010; McNally *et al.*, 2017; Rasmussen *et al.*, 2018). Instead, mineralogical properties of the soil parent material and its weathering stage govern long-term C stabilization (Heckman *et al.*, 2009). Due to their environmental boundary conditions and their extensive weathering history, most tropical soils are dominated by end member minerals such as 1 : 1 clays (e.g., kaolinite) as well as highly crystalline Fe oxyhydroxides and Fe oxides, which have a lower potential for the sorption of organic matter (Barré *et al.*, 2014; Doetterl *et al.*, 2018; Ito and Wagai, 2017; Six *et al.*, 2002a). Thus, the reduced mineral reactivity of tropical soils (Doetterl *et al.*, 2018; Mendez *et al.*, 2022) compared to temperate soils leads to a lower potential to store C despite higher inputs in natural (tropical forest) ecosystems.

In this study, we aimed to analyze and understand the effect of geochemical properties and weathering status of soil parent material on SOC stocks and soil C turnover time following land conversion from tropical forest to subsistence cropland in tropical central Africa. We postulated that geochemical properties of parent material and the weathering status of soils govern SOC loss and soil C turnover time following conversion from forest to cropland. More specifically, we hypothesized that deeply weathered and less reactive soils would be less responsive to changes in C input when C inputs exceed the capacity of soils to store C. Consequently, tropical SOC dynamics may be less sensitive to land use change and be more governed by soil geochemistry.

4.3 Material and methods

4.3.1 Study region — Geoclimatic characterization

This study is embedded in the larger framework of project TropSOC (Doetterl *et al.*, 2021a; Doetterl *et al.*, 2021b) which aims to study the effects of soil geochemistry, weathering and erosion on tropical forest, and cropland C cycles. Our study sites are located along the Albertine Rift, a part of the East African Rift System in the border region between the Democratic Republic of the Congo (DRC), Rwanda and Uganda (Figure 4.2). The region was chosen due to its large variety of soil parent material (geological units), while the environmental conditions are similar. The region is characterized by tropical humid climate (Köppen Af – Am) with monsoonal dynamics. The regional climate is subdivided into four seasons (weak dry in December – February; strong rains in March – May; strong dry in June – August; and weak rains in September – November) each covering three months (Bukombe *et al.*, 2022; Doetterl *et al.*, 2021b). The mean annual temperature (MAT) varies between 15.3 °C and 19.2 °C and mean annual precipitation (MAP) varies between 1697 mm and 1924 mm (Fick and Hijmans, 2017). In general, MAP is higher in study sites under forest compared to cropland. MAT and PET are slightly higher in the study sites under cropland compared to forest, at least in the mafic and mixed study regions (Table 4.1).

Soils in DRC are developed from mafic magmatic rocks and are classified as alic Nitisols (ochric), alic Nitisols (vetic), and mollic Nitisols (ochric) (Doetterl *et al.*, 2021b) (this region is further called mafic region). Soils in Uganda are developed from felsic magmatic and metamorphic rocks: they are classified as sederalic Nitisols (ochric), haplic Lixisols (nitic), and luvic Nitisols (endogleyic) (Doetterl *et al.*, 2021b) and this region is further called felsic region. Since the region is tectonically active, re-fertilization of soils with rock-derived nutrients by pyroclastica occurs to various degrees at a local scale (Bailey *et al.*, 2005; Barker and Nixon, 1989; Eby *et al.*, 2009). Study sites in Rwanda consist of mixed sedimentary rocks dominated by quartz-rich sandstone and schists and the soils are classified as haplic Acrisols (nitic), acric Ferralsols (vetic), and acric Ferralsols (gleyic) (Doetterl *et al.*, 2021b). This region is further called mixed sedimentary region. A specific feature of soils in this region is the presence of fossil, geogenic organic carbon free of radiocarbon in the parent material (dark clay-silt schists). For further details on the soil mineralogy of the study region, please refer to Bukombe *et al.* (2022), Bukombe *et al.* (2021), Doetterl *et al.* (2021b), and Reichenbach *et al.* (2021).

Table 4.1: Climatic parameters for land uses within test regions. Data show mean and standard deviation and are compiled from the WorlClim 2 database (Fick and Hijmans, 2017).

		MAT [°C]	MAP [mm]	PET [mm]
mafic	forest	15.5 ± 0.3	1928 ± 3	1124 ± 16
	cropland	18.2 ± 0.7	1606 ± 88	1303 ± 80
felsic	forest	19.2±0	1697 ± 0	1486 ± 0
	cropland	18.9 ± 0.3	1465 ± 13	1371 ± 20
mixed sedimentary	forest	17.3 ± 0.1	1691 ± 0	1242 ± 8
	cropland	18.2 ± 0.2	1499 ± 46	1296 ± 25

Abbreviations: MAP, mean annual precipitation; MAT, mean annual temperature; PET, potential evapotranspiration.

4.3.2 Study region — Land use and vegetation

The dominant natural vegetation in the area is tropical montane forest (Bukombe *et al.*, 2022; Doetterl *et al.*, 2021b). Based on available information, all forest stands within our study sites are >300-year-old growth forests (Besnard *et al.*, 2021). For most of the surrounding area, however, this natural vegetation did undergo a rapid conversion to cropland during recent decades (Gerland *et al.*, 2014; Tyukavina *et al.*, 2018). Today, most of the area is dominated by low-input, hand-hoed cropland managed by subsistence farmers (Figure 4.2) (Dewitte *et al.*, 2013; Dressée and Lepersonne, 1949; Friedl *et al.*, 2013; Verdoodt and Ranst, 2003). Local agriculture is characterized by rotations of cassava and maize, as well as various legumes and vegetables with little to no fertilizer input (Mangaza *et al.*, 2021; Ordway *et al.*, 2017; Tyukavina *et al.*, 2018).

Before analyzing our soil data, we assessed potential differences in the time since land conversion from forest to cropland in our study sites, to determine its potential influence on SOC stocks. To understand the history of land conversion throughout the study regions, historical satellite images (1985 – 2022) based on Landsat 4 – 8 satellite data providing multi-band surface reflectance properties were analyzed using the Google Earth Engine time-lapse function (Gorelick *et al.*, 2017). The results of the satellite data analyses were additionally evaluated through farmer questionnaires collected in 2018 – 2020 (Doetterl *et al.*, 2021b) where we acquired information on the time since deforestation. This analysis revealed that all cropland sites in this study area

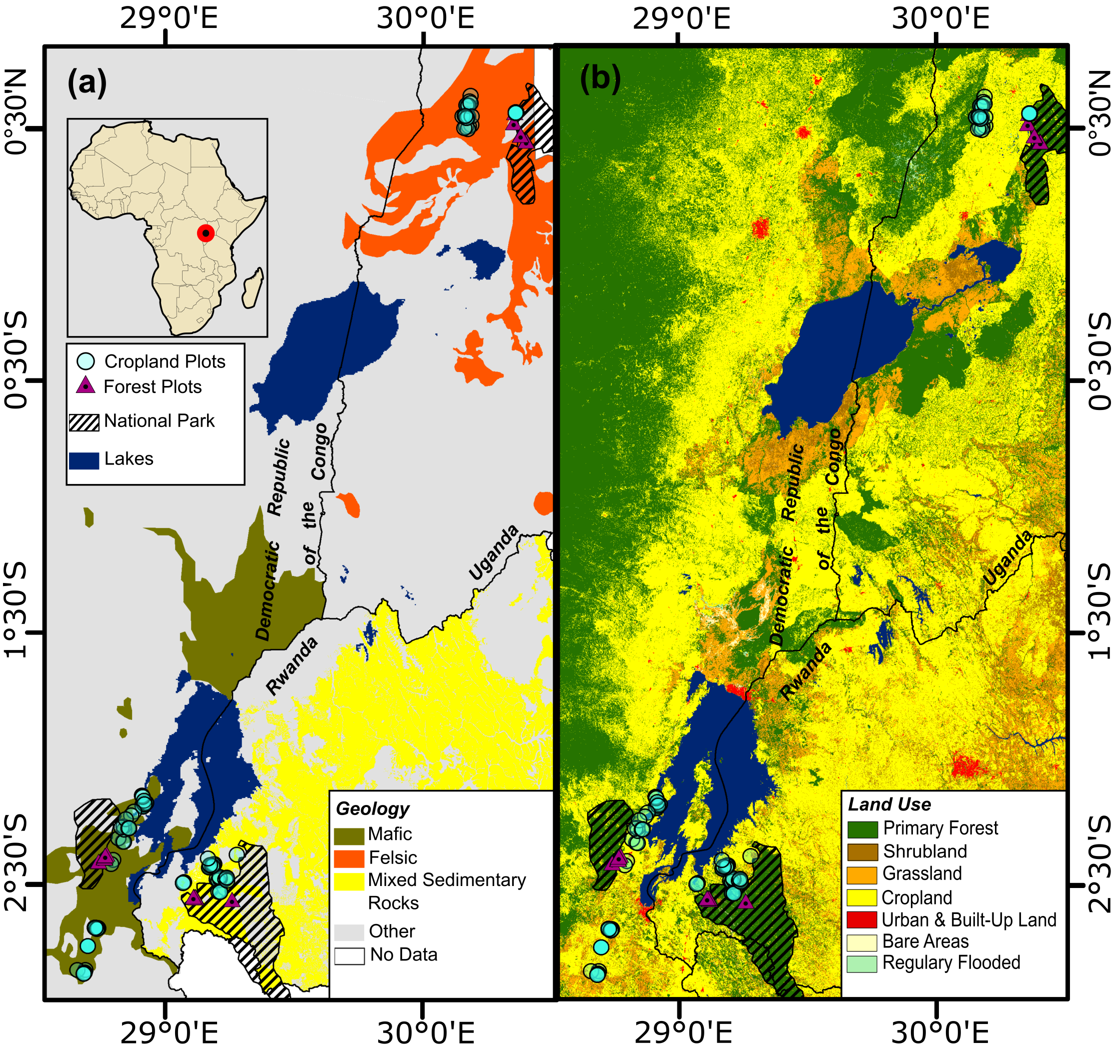

Figure 4.2: Overview of the study region with respect to (a) geology and (b) land use (modified from Doetterl *et al.* (2021b) with line features delineating national parks.

were converted before 1985. Other studies have found that the largest effects on SOC dynamics occur in the first three decades after conversion (Don *et al.*, 2011; Guillaume *et al.*, 2015). Thus, we concluded that differences in conversion timing were unlikely to impact our results, as all cropland sites should have had sufficient and similar amounts of time for SOC stocks to equilibrate to the new land use and land cover.

4.3.3 Study design and soil sampling

A total of 29 study sites were established consisting of eight forest sites (two to three replicates in each geochemical region) and 21 cropland sites (five to nine replicates in each geochemical region). Forest study sites within each geochemical region were established within 40 m × 40 m plots following an international, standardized protocol for tropical forest analysis (Marthews *et* *al.*, 2014). Cropland study sites were established within 3 m × 3 m plots cultivated with cassava only. Only study sites located on morphodynamically stable plateau positions were considered in this study to exclude the effect of soil redistribution with soil losses through erosion on slopes and soil gains through deposition in valleys after conversion of natural forest to cropland. Within each study site, four soil cores from forest and two soil cores from cropland were taken and combined to one depth-explicit composite sample representing one study site. Leaf litter (L horizon) and organic soil material (O horizon) were removed prior to drilling. Cores were taken using percussion drilling and soil column sampling equipment allowing for undisturbed sampling of 1 m deep soil cores at 9 cm diameter. Soil bulk density samples were taken with Kopecky cylinders of known volume (98.13 cm^3) or derived from the known volume and weight of the soils sampled by percussion drilling. From the eight forest and 21 cropland sites, we overall produced 29 composite soil cores (to 1 m soil depth), which were subdivided in 10 cm depth increments. As some drillings could not reach 1 m soil depth, this resulted in 282 samples for analysis. Please refer to Doetterl *et al.* (2021b) for a more detailed description of the study and sampling design.

4.3.4 Soil analysis

As this study is part of an extensive sampling and analysis campaign of project TropSOC, previous work has analyzed a wide range of soil physical and chemical properties that are published in a project-specific database (Doetterl *et al.*, 2021a; Doetterl *et al.*, 2021b), where details of the methods used are described. Therefore, we only provide a brief overview of the analytical methods in the following sections. Importantly, for sample analyses, a two-step approach was followed. First, 20 % of all soil samples in project TropSOC covering a wide range of geoclimatic as well as geochemical conditions and land uses were analyzed based on classical wet chemistry methods. These were then used to calibrate a spectroscopic database (Summerauer *et al.*, 2021).

Key reference methods

Soil bulk density samples were oven-dried at 105 °C for 24 h and weighed subsequently. Note that rock content (>2 mm) of all samples was negligible due to the generally deep weathering and long, relatively undisturbed period of soil development (Doetterl *et al.*, 2021a; Doetterl *et al.*, 2021b). Soil texture (clay, silt, sand) was analyzed using the Bouyoucos hydrometer method (Bouyoucos, 1962) modified following Beretta *et al.* (2014). A three-step sequential extraction scheme of Al, Fe, and Mn bearing pedogenic organo − mineral associations and oxyhydroxides (Stucki *et al.*, 1988) was performed in the following order: (i) extraction with sodium pyrophosphate at pH 10 following procedures by Bascomb (1968), (ii) extraction with ammonium oxalate-oxalic acid at pH 3 following Dahlgren (1994) and (iii) extraction with dithionite – citrate – bicarbonate (DCB) at pH 8 following Mehra and Jackson (1958). All extracts, including the calibration standards, were filtered through a grade 41 Whatman filter and diluted (1 : 1000) prior to analysis on the inductively coupled plasma optical emission spectrometry (ICP-OES; 5100 ICP-OES Agilent Technologies). In our sequential extraction of pedogenic metal phases, the pyrophosphate extraction was assumed to primarily retrieve Al, Fe, Mn from dissolution of labile organo-metal complexes and associations but may dissolve some non-crystalline short-range order (SRO) minerals and/or promote limited dispersion of ferrihydrite and goethite colloids. It is therefore more accurate to interpret them as both organo – mineral nanoparticles and organo-metal complexes (pyrophosphate extractable complexes (ΣAl, Fe, Mn)) (Rennert, 2019). The oxalate extraction of residual soil (following the pyrophosphate extraction) is interpreted to retrieve Al, Fe, and Mn from the complete dissolution of non-crystalline SRO minerals and ferrihydrite that form more stable organo – mineral complexes (oxalate extractable complexes (ΣAl, Fe, Mn)). It is also assumed that the oxalate extraction partially dissolves magnetite, hematite, and gibbsite (Rennert, 2019). The DCB method is interpreted to release highly crystalline forms of Al, Fe, and Mn from the complete dissolution of ferrihydrite, and goethite as well as partial dissolution of hematite, magnetite, and gibbsite (DCB extractable complexes (ΣAl, Fe, Mn)) (Rennert, 2019) that showed no strong role for the stabilization of C in soil (Mikutta *et al.*, 2009). However, recent studies in a tropical context document C accumulation with larger amounts of DCB extractable oxides, but did not employ sequential extraction as performed in our study (Kirsten *et al.*, 2021b).

Total elemental composition was determined by ICP-OES for analyzing calcium (Ca), magnesium (Mg), sodium (Na), potassium (K), phosphorous (P), aluminum (Al), iron (Fe), and manganese (Mn). One gram of powdered sample material was placed in digestion tubes and boiled for 90 min at 120 °C in aqua regia (2 mL bi-distilled water, 2 mL 70 % nitric acid (HNO_3), 6 ml 37 % hydrochloric acid (HCl)) using a DigiPREP digestion system (DigiPREP MS SCP Science, Canada). All extracts, including the calibration standards, were filtered through a grade 41 Whatman filter and diluted with a ratio of 1 : 2 for Ca, Mg, Na, K, P, and 1 : 1000 for A, Fe, Mn using a dilution system (Hamilton 100). All extracted elements (aqua regia, sequential oxide extraction) are reported by mass.

Soil pH (KCl) was determined potentiometrically with a glass electrode using a portable multiparameter (Meter HI9828, Hanna Instruments US Inc.) following the protocol by Black (1965) on 20 g of 2 mm sieved bulk soil samples. Plant available P was analyzed on 2 mm sieved bulk soil using the Bray 2 method (Okalebo *et al.*, 2002). Exchangeable bases were measured on 2 mm sieved bulk soil by percolation with $BaCl_2$ at pH 8.1. The percolate was then analyzed via flame photometry and atomic absorption spectrophotometry (Pauwels *et al.*, 1992).

Total carbon (TC) and total nitrogen (TN) were analyzed using dry combustion (Vario EL

Cube CNS Elementar Analyzer, Germany) with the C : N ratio used as an indicator for soil organic matter (SOM) quality. None of the samples showed any reaction when treated with 10 % HCl and thus all C and N sources were considered of organic nature. SOC stocks of the bulk soil were calculated by multiplying the SOC concentration by soil bulk density and the thickness of the depth increment (10 cm). Please note that we focused on mineral C stocks and excluded C stocks from litter and organic soil horizons from forest to ensure comparability with cropland soils. Bulk soil $\Delta^{14}C$ was analyzed for selected depth increments (0 – 10, 30 – 40, 60 – 70 cm) on graphite prepared from purified CO_2 released on combustion (Steinhof *et al.*, 2017) using AMS (accelerator mass spectrometry) at the Max Planck Institute for Biogeochemistry (Jena, Germany) and are reported using the conventions of Stuiver and Polach (1977).

Soil spectroscopy

All values for the presented variables (Table 4.2) have been analyzed using a Bruker Vertex 70, near and mid-infrared (NIR-MIR) Fourier transform FT-IR spectrometer (Doetterl *et al.*, 2021b) following the workflow of Summerauer *et al.* (2021). Please note that the intercept calculated in the predictive regression models is not forced through zero. Therefore, predicted values based on low calibration values near zero can result in slightly negative values due to the uncertainty of the predictive model. We tested if statistical outcomes would differ when using the dataset including negative values from the dataset using zeros. The results and conclusions did not change and thus we decided to set all negative values to zero since negative elemental contents do not exist in nature. NIR-MIR predictions resulted in high to very high performance in explaining the observed variability ($R^2 = 0.69 - 0.93$) for all assessed values, except for soil bulk density ($R^2 = 0.43$; Table 4.2). Thus, we used the soil bulk density derived from Kopecky cylinders instead of FT-IR spectrometry derived values to calculate SOC stocks.

Table 4.2: Soil property calibrations with near- and mid-infrared spectroscopy (Summerauer *et al.*, 2021).

parameter	unit	mid-infrared spectroscopy prediction		sample size	reference method	reference
		R^2	RMSE			
SOC variables						
SOC	wt%	0.92	0.53	282	dry combustion	(Nelson and Sommers, 1996)
soil $\Delta^{14}C$	‰	0.69	103.54	282	Elementar Analyzer coupled to an IRMS, AMS spectrometer	(Stuiver and Polach, 1977)
soil organic matter (SOM) quality						
C : N	-	0.84	11.73	282	dry combustion	(Nelson and Sommers, 1996)
soil physical variables						
bulk density	g cm^{-3}	0.43	0.27	282	Kopecky cylinder	(Blake and Hartge, 1986)
clay	%	0.93	4.43	282	Bouyoucos hydrometer	(Bouyoucos, 1962)
silt	%	0.80	4.02	282	Bouyoucos hydrometer	(Bouyoucos, 1962)
sand	%	0.90	5.28	282	Bouyoucos hydrometer	(Bouyoucos, 1962)
mineral C stabilization potential						
pyro. extr. oxides (Al, Fe, Mn)	wt%	0.71	0.08	282	three-step sequential extraction	(Stucki *et al.*, 1988)
oxalate. extr. oxides (Al, Fe, Mn)	wt%	0.66	0.30	282	three-step sequential extraction	(Stucki *et al.*, 1988)
DCB. extr. oxides (Al, Fe, Mn)	wt%	0.93	0.34	282	three-step sequential extraction	(Stucki *et al.*, 1988)
metals ($\sum$total Al, Fe, Mn)	wt%	0.88	0.45	282	ICP-OES	(Hossner, 1996)
soil fertility						
soil pH (KCl)	-	0.87	0.27	282	potentiometrically with a glass electrode	(Black, 1965)
bray-P	mg kg^{-1}	0.81	29.96	282	Bray 2	(Okalebo *et al.*, 2002)
total P	wt%	0.74	0.06	282	ICP-OES	(Hossner, 1996)
exchangeable bases cations	meq 100g^{-1}	0.72	0.81	282	flame photometry and AAS spectrophotometry	(Pauwels *et al.*, 1992)
TRB	wt%	0.73	2.00	282	ICP-OES	(Hossner, 1996)

Abbreviations: ANOVA, analysis of variance; DCB extr. oxides ($\sum$Al, Fe, Mn), dithionite–citrate–bicarbonate extractable oxides of Al, Fe, and Mn; oxalate extr. oxides ($\sum$Al, Fe, Mn), oxalate extractable oxides of Al, Fe, and Mn; pyro. extr. complexes ($\sum$Al, Fe, Mn), pyrophosphate extractable organo - mineral complexes of Al, Fe, and Mn; VIF, variation inflation factor.

4.3.5 Statistical data analysis

Standardization and cluster analyses

In a first step, prior to all statistical analyses, (except for analysis of variances (ANOVAs)), due to the differences in units and ranges of the target and predictor variables, Z-score standardization was applied to increase the comparability of effect sizes between predictors following Lacrose (2004). In a second step, (unrotated) principal component analysis (PCA) and cluster analysis using K-means partitioning clustering were performed to structure the dataset based on (geo)chemical characteristics with relation to fertility and mineralogy derived from soil parent material. Our reasoning for this choice is that tropical plant growth can be limited by rock-derived nutrients that can be partly depleted in deeply weathered tropical soils (Augusto *et al.*, 2017; Vitousek *et al.*, 2010). Similarly, mineral C stabilization in tropical soils is often directly or indirectly driven by its pedogenic metal content because chemical soil weathering of primary minerals results in the formation of minerals that can sorb C (Fromm *et al.*, 2021; Reichenbach *et al.*, 2021). Thus, we interpret the sum of total Al, Fe, and Mn (metals (Σtotal Al, Fe, Mn)) as a proxy for soil mineral C stabilization (PC 2, Figure 4.3). To limit the effects of biological disturbance (root growth, bioturbation etc.) on the assessed geochemical — parent material derived — soil variables, we considered only deeper subsoil samples for the cluster analyses (70 – 80, 80 – 90, and 90 – 100 cm; n = 82). Cluster analysis was realized using the R-package Factoextra (Kassambara and Mundt, 2020) following Han *et al.* (2012)).

Comparing mean values / ANOVA analyses

In a third step, depth-explicit patterns of SOC stocks and soil Δ^{14}C were assessed across both land use types and the identified geochemical clusters (see Section 4.4.1) using one-way ANOVA analyses (Crawley, 2009). Differences across geochemical clusters and land use for SOC variables (SOC stock, soil Δ^{14}C) were assessed by testing for equality of means. Please note that the study design resulted in a larger sample size of cropland sites than forest sites, varying group sizes (n = 7 – 21 per group with generally more cropland than forest plots within groups), as well as varying distances between cropland sites compared to forest sites of the same group. Thus, standard deviations of groups with cropland plots are generally larger than those of groups with little to no cropland. Therefore, before performing any mean value comparison, we conducted Levene's test to avoid type I error in ANOVA caused by heteroscedasticity (Moder, 2016). Based on the outcome, either one-way ANOVA (equal variances) or Welch-statistic (unequal variances) was used. Similarly, to compare the means of multiple groups, post-hoc testing was applied either with Bonferroni correction (equal variances) or Tamhane T2 (unequal variances) based on the outcome of the Levene's test (Day and Quinn, 1989).

Regression analyses and minimizing multicollinearity effects

Stepwise linear regression analyses were used to build depth-explicit prediction models for SOC stocks and soil $\Delta^{14}C$. An overview of ranges of soil properties considered for regression analyses is given in Table 4.3. To minimize multicollinearity effects and to prevent overfitting in the regression analysis, we assessed the variation inflation factor (VIF) for our model structures before analyzing model outcomes, starting with nine geochemical variables and samples stemming from all investigated geochemical clusters and land uses ($n = 282$; Table B.1). After calculating the VIF for each run, the geochemical variable with the highest VIF and the lowest correlation (Pearson r) with SOC variables was excluded iteratively until the VIF of each of the remaining variables was <2.5 (Senaviratna and Cooray, 2019). Pearson correlation was used to assess the cross-correlation between retained and removed variables (Figure B.1). Thus, a subset of geochemical variables was created that can be used as covariates in the prediction models without losing information from the initial dataset. The following variables remained after four runs of the VIF assessment: The sum of pyrophosphate extractable organo − mineral complexes of Al, Fe, and Mn (pyrophosphate extractable complexes (ΣAl, Fe, Mn)), sum of oxalate extractable Al, Fe, and Mn oxides (oxalate extractable oxides (ΣAl, Fe, Mn)), clay content, silt content, the sum of exchangeable bases (Ca, Mg, K), $C : N$ ratio, and soil depth. Clay content was highly correlated with the removed sum of dithionite–citrate–bicarbonate extractable Al, Fe, and Mn oxides (DCB extractable oxides (ΣAl, Fe, Mn)). The sum of exchangeable bases correlated highly with several other removed soil fertility proxies (soil pH, bray-P; Figure B.1). Finally, the VIF-assessed geochemical variables were used as explanatory variables in multiple linear stepwise regression to explain differences in SOC variables. Relative importance analysis of each explanatory variable was used to assess their predictive power.

Table 4.3: Ranges of soil properties in each geochemical cluster including samples from all soil depth (0 – 100 cm).

			used for regression	low fertility / low stabilization potential		low fertility / high stabilization potential		high fertility / low stabilization potential	
	parameter	unit		MIN – MAX	n	MIN – MAX	n	MIN – MAX	n
target	SOC variables								
	SOC	tC ha^{-1}	yes	1.1 – 62.0	125	0.0 – 66.0	90	4.0 – 64.0	67
	soil Δ^{14}C	‰	yes	-477.5 – 160.9	125	-437.6 – 152.3	90	-512.4 – 119.1	67
explanatory	soil organic matter (SOM) quality								
	C : N	-	no	1.8 – 35.5	125	0.0 – 30.7	90	0.0 – 34.3	67
	texture								
	clay	%	yes	21.9 – 82.6	125	26.5 – 83.9	90	13.9 – 46.1	67
	silt	%	yes	1.6 – 22.2	125	2.6 – 15.8	90	8.3 – 25.7	67
	sand	%	no	8.4 – 65.2	125	13.5 – 52.4	90	39.8 – 65.7	67
	mineral C stabilization potential								
	pyro. extr. oxides (Al, Fe, Mn)	wt%	yes	0.0 – 1.4	125	0.0 – 1.1	90	0.1 – 0.8	67
	oxalate. extr. oxides (Al, Fe, Mn)	wt%	yes	0.0 – 2.3	125	1.0 – 4.0	90	0.7 – 4.5	67
	DCB. extr. oxides (Al, Fe, Mn)	wt%	no	1.0 – 12.1	125	9.1 – 17.7	90	0.0 – 8.0	67
	metals ($\sum$total Al, Fe, Mn)	wt%	no	4.1 – 18.8	125	16.0 – 27.1	90	3.5 – 14.3	67
	soil fertility								
	soil pH (KCl)	-	no	3.2 – 6.2	125	2.8 – 4.8	90	4.4 – 6.4	67
	bray-P	mg kg -1	no	0.0 – 78.2	125	0.0 – 30.7	90	47.0 – 300.6	67
	total P	wt%	no	0.0 – 0.2	125	0.1 – 0.3	90	0.2 – 0.7	67
	exchangeable bases (Ca, Mg, K)	meq 100g^{-1}	yes	0.0 – 23.8	125	0.0 – 12.0	90	6.0 – 27.9	67
	TRB	wt%	no	0.0 – 0.9	125	0.1 – 0.8	90	0.9 – 2.1	67

4.4 Results

4.4.1 Geochemical dataset structure

The principal component analyses resulted in two distinct principal components (PCs; Figure 4.3a). PC 1 explains 64.8 % variability in the data with significant positive loadings of total P (0.99) and TRB (0.99) and was thus interpreted as the axis representing "soil fertility." PC 2 explains 33.8 % variability in the data with significant loadings of the sum of total metal concentration of Al, Fe, and Mn and was thus interpreted as the axis for "mineral C stabilization potential." The following cluster analyses yielded three distinct clusters based on TRB, total P, and total metal concentrations (Figure 4.3b and c) which roughly followed the investigated geochemical regions mafic, felsic, and mixed sedimentary as the main divide for structuring the data. The first cluster reflects geochemistry with low fertility and low mineral C stabilization potential. It contains 36 samples from both land use types and all geochemical regions but is dominated by samples from the mixed sedimentary region. The second cluster represents low fertility but high mineral C stabilization potential. This cluster contains 27 samples from both land use types of the mafic region. The third cluster represents high fertility and low mineral C stabilization potential. This cluster contains 19 samples from croplands of the felsic region and no forest samples. The lack of forest sites in this cluster is explained through the preferential use of fertile land for cropping in an otherwise less fertile tropical soil landscape with deeply weathered soils (Ordway et al., 2017). An overview of ranges of soil properties grouped by the identified clusters are given in Table 4.3. Note that clay content was also identified to correlate with both soil fertility (Kome *et al.*, 2019) and mineral C stabilization (Quesada *et al.*, 2020). Here, due to this mixed role, it is hard to interpret its mechanistic role clearly, and we thus excluded it from informing the cluster formation (Figure 4.3a).

4.4.2 SOC stocks and Δ^{14}C across land use and geochemical regions

SOC stocks

Across geochemical clusters, no significant difference was found between land use types in means of SOC stocks for the upper meter of soil for any depth increment, except for an insignificant trend of higher SOC stocks in topsoils (0 – 10 cm) under forest in the low fertility / high stabilization potential cluster (Figure 4.4). Across both land uses, in the low fertility / high stabilization potential cluster, depth-explicit SOC stocks ranged from 43.6 ± 15.3 tC ha^{-1} at the soil surface (0 – 10 cm) to 15.3 ± 8.3 tC ha^{-1} in subsoil (90 – 100 cm). In the low fertility /

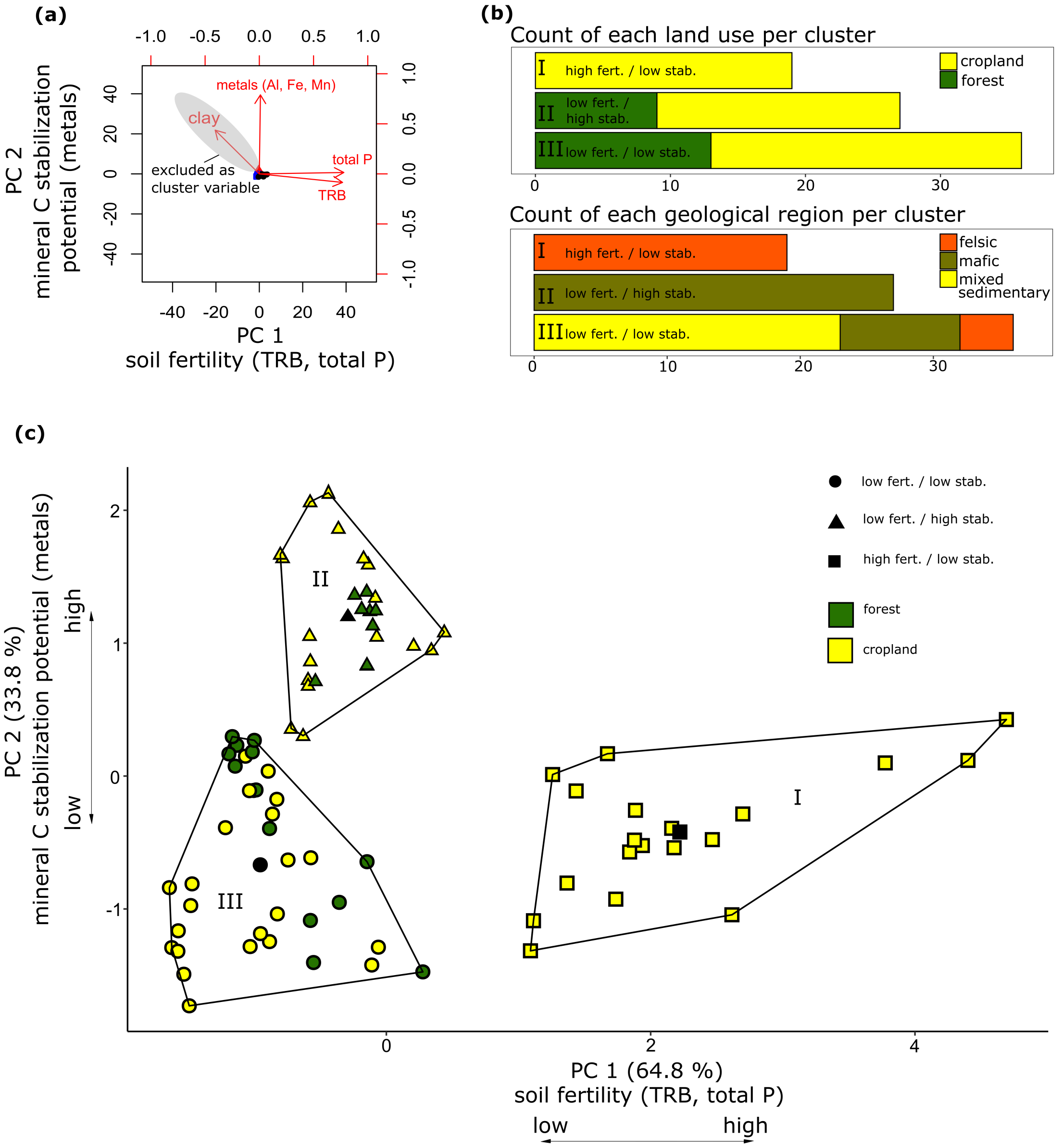

Figure 4.3: Cluster analysis considering TRB, total P, and the sum of total Al, Fe, and Mn concentrations of deeper subsoil samples (70 − 80, 80 − 90, and 90 − 100 cm; n = 82). Panel (a) Principal components that structure the dataset. Note the mixed role of clay, which was consecutively excluded to build clusters. Panel (b) Loading of clusters concerning data from varying land use and geochemical regions. Panel (c) Outcome of the K-mean clustering, resulting in three distinct clusters with respect to pairing of soil fertility and mineral C stabilization potential. The black symbol in each cluster shows the center point. Note that available rock-derived nutrients and pedogenic metal phases generally followed the same patterns as outlined here for total concentrations of rock-derived elements.

low stabilization potential cluster, SOC stocks range from 40.8 ± 11.7 tC ha^{-1} at the soil surface to 18.9 ± 11.7 tC ha^{-1} in subsoil. In the high fertility / low stabilization cluster, SOC stocks range from 46.4 ± 11.0 tC ha^{-1} at the soil surface to 17.2 ± 4.6 tC ha^{-1} in subsoil. Similarly, no significant differences in SOC stocks across geochemical clusters were detected under forest (Figure 4.4a) and cropland. SOC stocks ranged from 52.5 ± 17.6 tC ha^{-1} in topsoil (highest in forest) to 13.3 ± 9.3 tC ha^{-1} in subsoil (lowest in cropland).

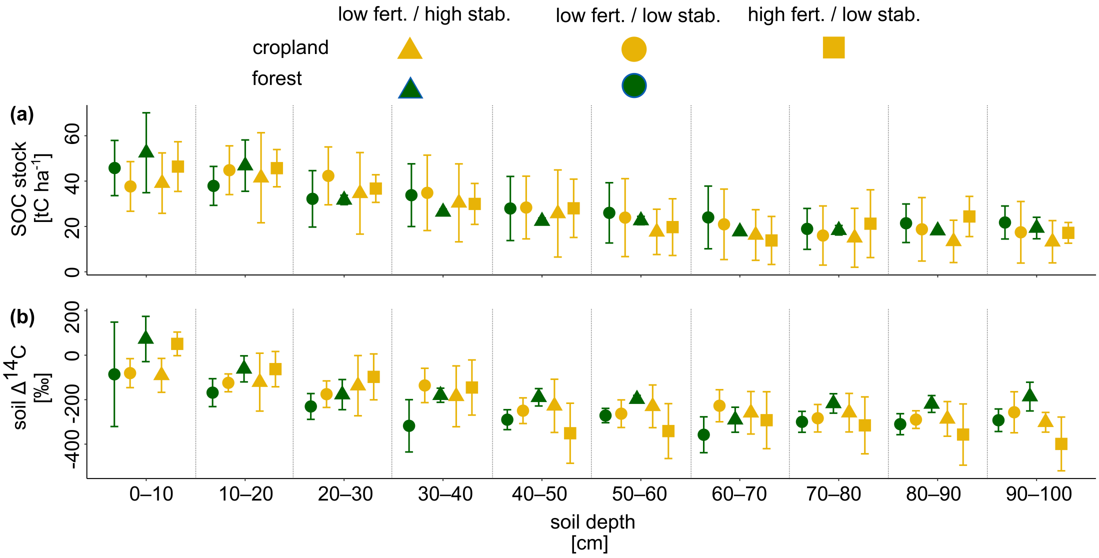

Figure 4.4: Comparison of (a) SOC stocks and (b) soil Δ^{14}C across land use types and geochemical clusters (n = 3 – 8). Symbols show means and error bars represent standard deviation. Where not visible, standard deviation bars were smaller than the symbol of the means. fert: soil fertility; stab: mineral stabilization potential.

Soil Δ^{14}C

Differences in bulk soil Δ^{14}C across land use types were non-significant and no patterns with depth could be observed, except for higher soil Δ^{14}C in topsoil (0 – 30 cm) versus low values in subsoil (30 – 100 cm). However, soil Δ^{14}C for specific depth layers were significantly different when analyzing the data across geochemical clusters.

When comparing soil Δ^{14}C across geochemical clusters for each land use separately, differences were more pronounced between geochemical clusters under forest compared to cropland (Figure 4.4b). Under forest, the low fertility / low stabilization potential cluster (-86.0 ± 234.8 ‰ to -357.8 ± 80.6 ‰) shows lower soil Δ^{14}C signatures compared to the low fertility / high stabilization potential cluster (+72.9 ± 101.8 ‰ to -290.0 ± 56.0 ‰). This difference was significant for the 40 – 50, 50 – 60, 70 – 80, and 80 – 90 cm depth increments. Under cropland, the high fertility / low stabilization potential cluster shows significantly higher soil Δ^{14}C signatures in the 0 – 10 cm (+51.0 ± 53.1 ‰) and lower values in the 90 – 100 cm depth increment (-399.0

± 121.0 ‰) compared to both other clusters (Figure 4.4b).

4.4.3 Geochemical drivers of SOC stocks and soil $\Delta^{14}C$

Predictors for SOC stocks

Based on the stepwise regression analysis, the included soil geochemical properties and soil depth explained between 71 % and 90 % of the variance in SOC stocks across land use types and geochemical clusters (Figure 4.5). While the structure of the regression models for cropland and forest was similar, model structures differed significantly between geochemical clusters. The most important predictors across all clusters were pyrophosphate extractable organo – mineral complexes (ΣAl, Fe, Mn), which explained nearly half of the variance when using samples from both land use types and geochemical clusters combined. However, the importance of the latter reduced from 55 % in the low fertility / low stabilization potential cluster to 32 % in the high fertility / low stabilization potential cluster. The importance of soil depth remained fairly constant (19 % – 32 %). Exchangeable base cations (Ca, Mg, K) were identified as a secondary control with prediction power ranging from 6 % to 24 % and were particularly important for the low fertility / high stabilization potential cluster and high fertility / low stabilization potential cluster. Silt and clay content ranked as tertiary controls between 1 % and 15 %, with higher predictive power for silt (6 % – 18 %) only in the low fertility / high stabilization potential cluster and high fertility / low stabilization potential cluster. SOM quality (C : N ratio) contributed as a minor control, between 2 % and 12 %, on the explanatory power of the different models. Similarly, in contrast to the importance of pyrophosphate extractable organo – mineral complexes (ΣAl, Fe, Mn), oxalate extractable oxides — extracted sequentially after using pyrophosphate — were of only minor importance (3 % – 7 %).

Predictors for soil $\Delta^{14}C$ patterns

The same set of predictors used for predicting SOC stocks explained between 45 % and 81 % of variance in soil $\Delta^{14}C$ across land use types and geochemical clusters (Figure 4.6). The explanatory power of models built for specific geochemical clusters was generally similar or slightly higher (4 5 % – 81 % of total explained variance) than the explanatory power of land use type differentiated models (57 % – 63 % of total explained variance). However, the explanatory power over all data points was lower (46 % of explained variance) compared to most of the submodels. Model structures across land use types were similar but with a generally lower importance of geochemical soil variables (3 % – 39 %) than of soil depth (23 % – 61 %), particularly in crop-

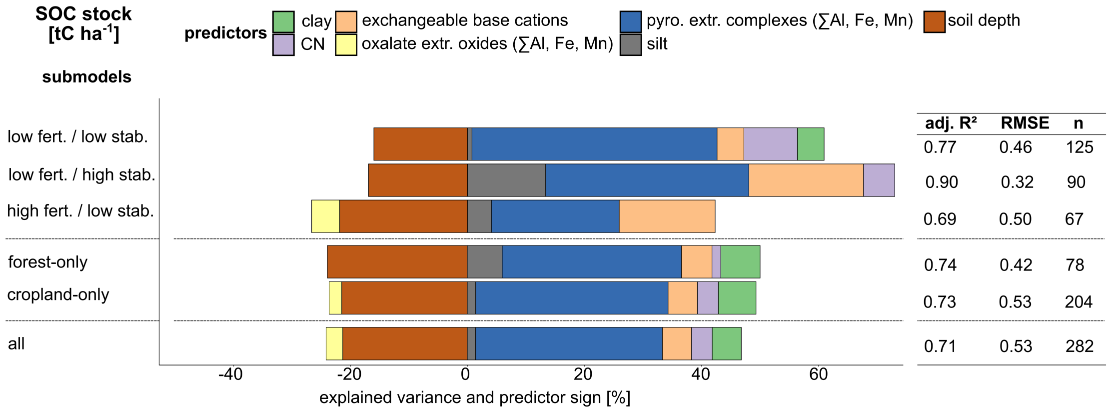

	adj. R^2	RMSE	n
low fert. / low stab.	0.77	0.46	125
low fert. / high stab.	0.90	0.32	90
high fert. / low stab.	0.69	0.50	67
forest-only	0.74	0.42	78
cropland-only	0.73	0.53	204
all	0.71	0.53	282

Figure 4.5: Regression analysis between SOC stocks and soil variables with relative importance and explained variance of predictors using observations from all increments until 1 m soil depth for different submodels (selected by geochemical cluster or land use) and all data points. Adjusted R^2 displays the goodness of fit. Root mean square error (RMSE) assesses the model quality. The length of the total bar for each plots represent the adj. R^2. The length of the colored sections in each plot represents the relative importance [%] of a respective explanatory variable, normalized to the adj. R^2. fert: soil fertility; stab: mineral stabilization potential.

land. An exception was observed for exchangeable bases being more important in forest (38 %) than soil depth (29 %). Among the included soil variables and in contrast to the predictions of the SOC stocks, pyrophosphate extractable organo – mineral complexes (ΣAl, Fe, Mn) and oxalate extractable oxides (ΣAl, Fe, Mn) were ranked at the same importance (3 % – 38 %) as soil texture (4 % – 39 %). Included proxies for soil fertility (exchangeable base cations, 7 % – 38 %), were important in both high and low fertility clusters. As observed in the SOC stock models, soil organic matter quality (C : N ratio) was also of minor importance across all soil $\Delta^{14}C$ models (2 % – 13 %), with highest predictive power in the high fertility / low stabilization cluster. Notably, while overall important, soil depth was the weakest explanatory variable in the cluster with low fertility / high stabilization potential.

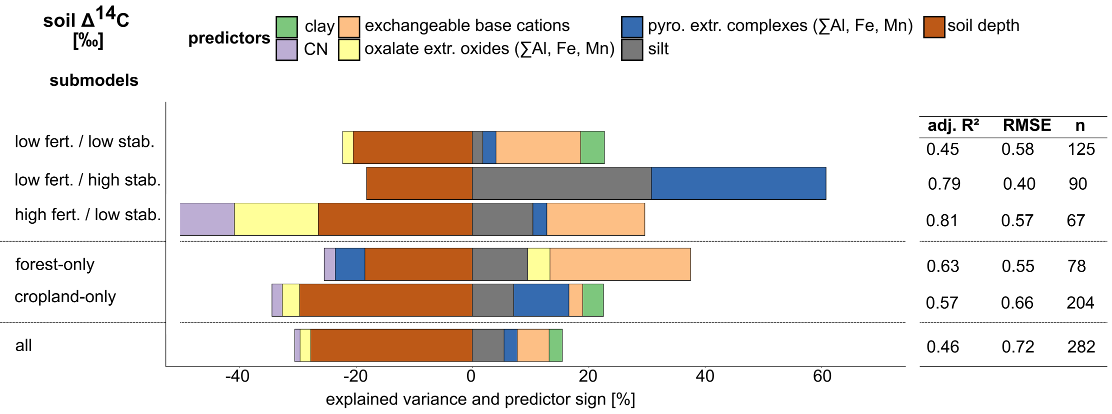

adj. R²	RMSE	n
0.45	0.58	125
0.79	0.40	90
0.81	0.57	67
0.63	0.55	78
0.57	0.66	204
0.46	0.72	282

Figure 4.6: Regression analysis between soil Δ^{14}C and soil variables with relative importance and explained variance of predictors using observations from all increments to 1 m soil depth for different submodels (selected by geochemical cluster or land use) and all data points. Adjusted R^2 displays the goodness of fit. Root mean square error (RMSE) assesses the model quality. The length of the total bar for each plots represent the adj. R^2. The length of the colored sections in each plot represents the relative importance [%] of a respective explanatory variable, normalized to the adj. R^2. fert: soil fertility; stab: mineral stabilization potential.

4.5 Discussion

4.5.1 Data representativeness and caveats

Spectroscopy and landforms

Our dataset (n = 282) represents a wide range of geochemical soil conditions including different land uses (forest, cropland) that were predicted using novel NIR-MIR spectrometry methods across a wide range of soil types with distinct properties. High variance in the SOC data (Figure 4.4) is therefore not an artifact caused by our statistical approach but reflects the natural variability in a highly complex soil landscape. In agreement with other large-scale environmental data analyses (Baumann *et al.*, 2021; Summerauer *et al.*, 2021) an R^2 of 0.93 is to be considered very good in terms of spectroscopic estimates for predicting SOC. Similarly, the spectroscopic estimates of the geochemical predictor variables (Table 4.2) are considered to be good to very good compared to other studies (Baumann *et al.*, 2021). Thus, the data quality and robustness of our SOC and geochemical data as well as its sample size enables us to interpret correlations across a variety of tropical soil and environmental conditions.

Similarly, an R^2 of 0.69 is sufficient to identify broad trends of soil Δ^{14}C across our regional-scale dataset. This indirect application of FT-IR spectroscopy to estimate soil Δ^{14}C is possible due to the availability of calibration data representing the range of environmental conditions (parent material, land use) within a spatially limited study region (Trumbore, 2009). However, several factors can affect soil Δ^{14}C besides measurable soil conditions and therefore, extrapolation of spectroscopic estimates of soil Δ^{14}C across larger spatial scales is not possible with the applied method. Additionally, note that the lowest model performance for explaining Δ^{14}C is in the low fertility / low stabilization potential cluster (Figure 4.6). This cluster contains samples with geogenic fossil organic carbon (Reichenbach *et al.*, 2021). However, since the spectroscopic models are not calibrated for geogenic, fossil organic carbon, the estimated depth distribution is not able to identify their presence or absence. Note also that, since we focused on stable, non-eroding landforms, only the direct effects on SOC of land conversion and the pedogenetic variation of soil profiles along geochemical gradients were investigated. Effects of soil relocation through erosion and deposition would lead to substantial additional alteration of the soil C cycle (Doetterl *et al.*, 2016) and is the subject of future work.

Climatic variation

Overall, like many other field studies in underrepresented regions of the Tropics, our analysis lacks long-term data on differences in climatic factors affecting SOC stocks and soil Δ^{14}C, and measurements of site specific precipitation, soil moisture, and temperature dynamics would provide helpful additional insights. The coarser resolved global climate data available for the region (MAP, MAT, PET) (Fick and Hijmans, 2017) is associated with substantial errors at the level of individual raster cells (Beck *et al.*, 2020). However, given this range, estimates regarding the importance of climatic variables for analyses on SOC stocks and dynamics across land use and geochemistry are possible. Overall, we assume that climatic differences between study sites do not have a substantial effect on SOC dynamics. While one would expect forest soils to be generally cooler than cultivated soils due to the removal of the shading canopy, changes in C cycling due to soil temperature profiles between forests and croplands are likely limited to topsoils (Tian *et al.*, 2017) and litter layers (not considered here). In addition, with the exception of the forest sites in the mafic region (ΔMAT to highest: -3.7 °C), differences in MAT between the sites are relatively small (with a total range of 15.5 – 19.2 °C). In the case of MAP, all forest sites have higher rainfall than the respective cropland site in each geochemical region (differences between study regions ranging from 192 to 322 mm, totals of 1465 – 1928 mm yr^{-1}) with similar values in PET (1124 – 1486 mm yr^{-1}). Taking into account the observed difference in MAT and MAP and the fact that tropical rainforests have a substantial interception potential (Rosalem *et al.*, 2019), the slightly higher rainfall amount seems not to have substantially affected soil moisture or temperature conditions enough to strongly alter SOC dynamics. Otherwise, the lower MAT and higher MAP values in forest compared to cropland should lead to higher SOC stocks (Wagai *et al.*, 2008), which we did not observe.

4.5.2 Responses of SOC stocks and turnover across land use

Meta-analysis studies covering (tropical) soils across all continents recognize land conversion as a major driver of SOC stock changes both in top- and subsoils from primary forest to cropland (Don *et al.*, 2011). In our study across distinct geochemical regions and focusing on deeply weathered and developed (non-eroded) soils, no effect of land conversion from forest to cropland on SOC stocks and soil Δ^{14}C could be detected, neither in topsoil nor in subsoil layers (Figure 4.4). To explain this observation, we argue that our findings point toward a limitation of C storage in deeply weathered soils that is independent of C inputs, which differ significantly between tropical forests and cropland (Bukombe *et al.*, 2022; Kaiser *et al.*, 2016). Rather, soil C storage seems to depend more strongly on a soil's ability to stabilize C inputs with the mineral matrix. In temperate soils of intermediate weathering stages, which are usually characterized by an abundance of highly reactive minerals that can sorb C, the soil (mineral) matrix allows for stabilizing larger amounts of C over longer timescales in aerated (not water-logged) soils (Doetterl *et al.*, 2018; Eusterhues *et al.*, 2003; Torn *et al.*, 1997). There, organo − mineral association can form stable complexes that represent an effective energetic barrier against microbial decomposition of organic matter. In the deeply weathered tropical soils investigated in our study, minerals have lost a significant amount of their reactivity toward C sorption during their long development history (Coward *et al.*, 2017). Accordingly, labile pyrophosphate extractable complexes were far more important than the more commonly assessed oxalate extractable pedogenic oxides or soil clay content (Figure 4.5). Pyrophosphate extractable organo − mineral complexes can be attached to larger minerals (Wagai *et al.*, 2020), but are usually interpreted as only weak agents for stabilizing C against microbial decomposition (Heckman *et al.*, 2018; Lawrence *et al.*, 2015; Paul *et al.*, 2008). Thus, the C associated with them represents an easily available pool of C for microorganisms (Bukombe *et al.*, 2021; Heckman *et al.*, 2009). Overall, this means that organic matter cannot be efficiently stabilized in these soils and is more easily decomposed by microbial communities, leading to the observed limited differences in SOC stocks across land use with very different C inputs. Our data support this interpretation in several ways.

First, despite differences in C input and rooting patterns across geochemical regions in our study (Bukombe *et al.*, 2022; Doetterl *et al.*, 2021b), SOC depth curves are similar between forest and cropland soils (Figure 4.4a, Figure B.2). Importantly, the identified relationships between predictor variables and SOC content or soil Δ^{14}C do not change with soil depth or for separate depth increments (Table B.2). Moreover, SOC stocks and soil Δ^{14}C show only weak depth trends due to sharp differences between top- and subsoil (Figure B.2). This finding may be indicative of some disconnection between fast cycling C in topsoil versus C cycling in subsoil with slower turnover times. Second, soil Δ^{14}C patterns and the derived turnover time estimates for SOC at greater depths are still rather short compared to temperate soil systems and geochemically less altered (more reactive) soil systems in the (Sub)tropics (Marín-Spiotta *et al.*, 2008; Mathieu *et al.*, 2015) (Figure 4.4b). This indicates a shorter average turnover time of stored SOC in deeply weathered tropical soils compared to less weathered temperate soils, also at greater depth (Shi *et al.*, 2020). The faster turnover of soil C at our study sites is also supported by results from laboratory incubations in recent studies conducted on samples from the same forest gradients as analyzed here. In these incubations, both top as well as subsoil C sources decomposed (Bukombe *et al.*, 2021), and decomposer communities adapted their strategies to access nutrients according to specific nutrient limitations (Kidinda *et al.*, 2022). Thus, mineral-bound organic matter may still sorb onto secondary minerals in deeply weathered soils, but Δ^{14}C data show that the turnover time of C remains short due to the limited ability to stabilize SOC in the long term because of the weakening of mineral-related protection of SOC against decomposition. Third, despite strong differences in pedogenic metal phases and clay content controlling mineral C stabilization and the amount of rock-derived cations between geochemical regions (Doetterl *et al.*, 2021b; Reichenbach *et al.*, 2021), only the (statistically) identified controls between geochemical clusters differed. SOC stocks and soil Δ^{14}C patterns remain similar (Figures 4.4, 4.5 and 4.6).

Taken together, variations in controls on SOC dynamics between the investigated geochemical regions seem not to be strong enough to induce quantitative changes in SOC stocks and soil C turnover time in deeply weathered tropical soils. Consequently, efforts to increase soil carbon storage by improving land management and C inputs, or conversion of cropland into forests may only lead to limited responses in tropical SOC stocks in deeply weathered soils. Positive effects in terms of increasing SOC stocks by these measures might be restricted to the accumulation of labile organic matter in near surface horizons where they remain sensitive to future alterations in climate (Knorr *et al.*, 2005; Wang *et al.*, 2018) and land use (Sheng *et al.*, 2015; Silva Oliveira *et al.*, 2017). Suggested efforts in this direction might therefore overestimate the potential increases in the C sink function of tropical soils that is achievable by reforestation, with positive effects limited to biomass C accumulation (Lewis *et al.*, 2019; Silver *et al.*, 2001; Silver *et al.*, 2004).

4.6 Conclusion and outlook

We demonstrate that similar SOC stocks and SOC turnover times can be found in deeply weathered soils across tropical forest and cropland as well as geochemical regions. Differences in SOC dynamics between the investigated soils can be predicted predominantly by biogeochemical soil properties, and less by land use. Soils across geochemical regions differ in controls on SOC dynamics, but little in quantity of SOC and its distribution with soil depth. Across land use types and geochemical regions, a small selection of easy to measure soil mineral properties together with soil depth can explain between 69 % and 90 % of the variation in SOC stocks and between 46 % and 81 % of the variation in soil Δ^{14}C at the regional scale. The formation of labile organo – mineral complexes and the presence or absence of exchangeable base cations drive the observed variation in SOC stocks, but do not contribute to long-term SOC stability. In conclusion, the specific mineralogical properties and reactivity of tropical soils related to parent material and weathering status are an important factor to determine the potential impact that land conversion may or may not have on tropical soil C stocks. This information can help to guide efforts and identify regions where reforestation and the protection of intact plant – soil systems in the Tropics are most efficient, and where the potential to store more C in soils will be constrained by soil mineralogy.

Chapter 5

Weak connection of soil redistribution and soil organic carbon in the wet Tropics of Africa

---

A revised version of this chapter has been published as: Reichenbach, M., Doetterl, S., Van Oost, K., Wilken, F., Muhindo, D., Bamba, F., and Fiener, P.: Low but highly variable soil organic carbon stocks across deeply weathered eroding and depositional tropical landforms, Catena, 254, 108971, https://doi.org/10.1016/j.catena.2025.108971, 2025.

Author contributions: Sebastian Doetterl (SD) and Peter Fiener (PF) designed the research. Mario Reichenbach (MR) conducted the sampling campaign and collected the data. Daniel Muhindo (DH) and Fernando Bamba (FB) were technical contributors and participated via data collection. SD, PF and MR analyzed and interpreted the data and framed the writing process. All authors contributed to the writing of the paper.

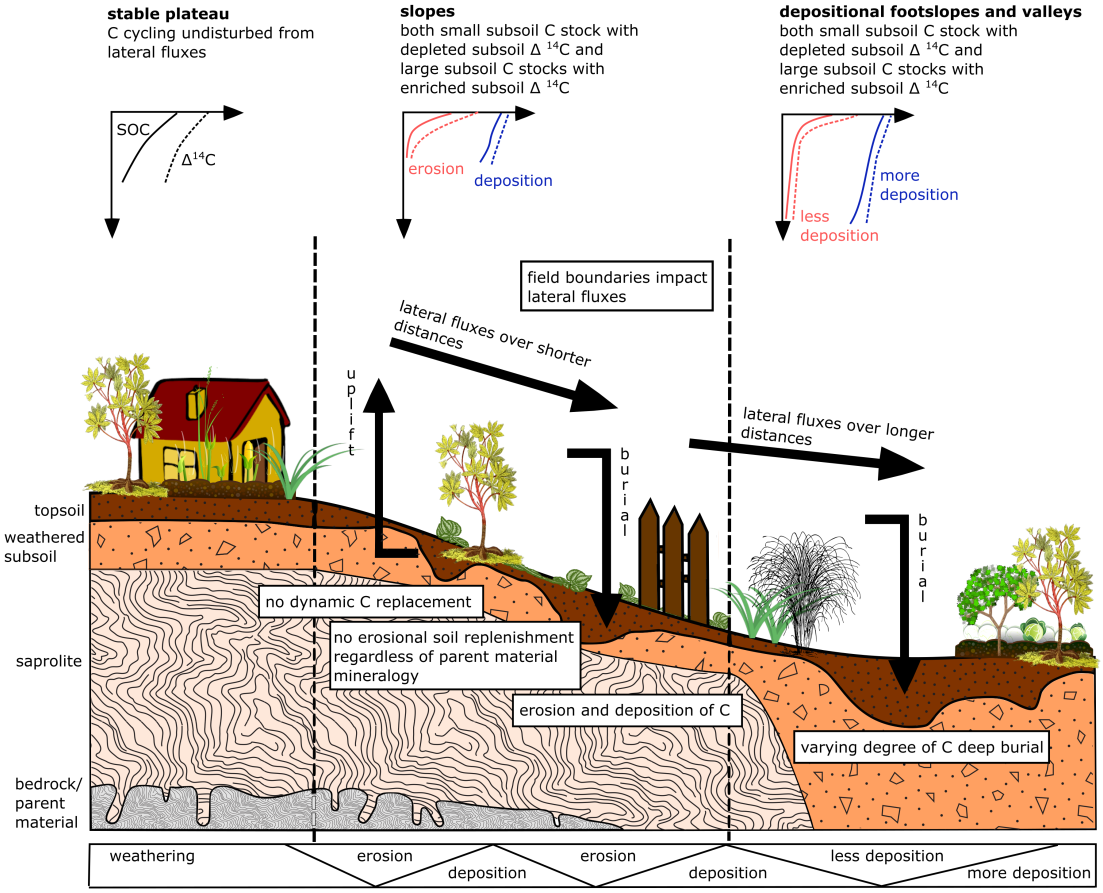

Figure 5.1: Graphical abstract – Pattern and controls of SOC stocks and soil Δ^{14}C across sloping cropland.

5.1 Abstract

Soil organic carbon (SOC) dynamics in sloping agricultural landscapes are highly affected by lateral soil fluxes induced by soil redistribution. SOC dynamics in fast eroding tropical cropland systems characterized by deeply weathered soils and heterogeneous small-scale subsistence farming structures, however, are not well understood. Along topographic gradients in the East African Albertine rift region, we investigated the differences in SOC stocks and SOC persistence for the upper meter of tropical cropland soils developed from geochemically distinct parent materials and cultivated by subsistence farmers. We show that cropland SOC stocks and persistence do not always follow topography-driven patterns expected from research on less weathered, more fertile soils of temperate climate zones and more large-scale farming systems (larger fields and machinery). At all investigated topographic positions, the variability of SOC stocks was high in both top- and subsoil. Independent of soil parent material and unless situated on very steep slopes (>15 % slope steepness), SOC stocks in eroding positions are similar to those in non-eroding landscape positions, capable of replacing SOC losses to stabilize generally low SOC stocks. Our results further suggest that deposition of eroded topsoil material at footslopes only slightly increases SOC stocks, as SOC persistence of deposited SOC is low even in subsoils indicating the generally limited potential of the investigated soils to stabilize buried or deposited former topsoil SOC. Therefore, the rapidly eroding and not yet fully consolidated tropical cropland systems appear to act as a potential C source at the regional and slope scale investigated here.

5.2 Introduction

Agricultural erosion represents a disturbance to the soil system that can have an impact on soil systems and biogeochemical cycles (Doetterl *et al.*, 2016; Nadeu *et al.*, 2015; Oost *et al.*, 2007; Quinton *et al.*, 2010; Wang *et al.*, 2017). Specifically, lateral soil fluxes result in the horizontal and vertical redistribution of SOC in different quantities and quality across the landscape (Berhe *et al.*, 2007; Gregorich *et al.*, 1998; Oost *et al.*, 2005). On eroding slopes, soils are generally truncated resulting in the exposure of SOC depleted subsoils at the soil surface. Following truncation, exposed subsoils receive fresh plant C inputs through litter and roots, and this process brings carbon-unsaturated reactive minerals from the subsoil into contact with fresh organic materials. This leads to a process generally described as dynamic C replacement (Dialynas *et al.*, 2016a; Dialynas *et al.*, 2016b; Harden *et al.*, 1999; Kirkels *et al.*, 2014; Stallard, 1998). At the same time, fresh C input can provide a readily available energy source for microbes that can speed up decomposition of older and formerly stabilized SOC, a process generally understood as C priming (Blagodatskaya and Kuzyakov, 2008; Chen *et al.*, 2019; Fontaine *et al.*, 2003; Fontaine *et al.*, 2004; Kuzyakov and Blagodatskaya, 2015), which will change the SOC compositions in these soils. Whether soil erosion creates local C sinks or sources depends on the interactions between processes of SOC priming (Blagodatskaya and Kuzyakov, 2008; Chen *et al.*, 2019; Kuzyakov and Blagodatskaya, 2015), dynamic replacement (Doetterl *et al.*, 2016; Harden *et al.*, 1999; Nadeu *et al.*, 2012) and C conservation through soil burial. These processes have been described in detail but with a strong bias towards temperate systems (Oost and Six, 2023; Van Oost *et al.*, 2012). However, process interactions and rates at which they operate are likely different in tropical soils due to their pronounced differences in chemico-physical soil features (Bukombe *et al.*, 2022; Bukombe *et al.*, 2021; Doetterl *et al.*, 2021b; Kidinda *et al.*, 2023; Kidinda *et al.*, 2022; Reichenbach *et al.*, 2021; Reichenbach *et al.*, 2023).

In most mineral soils, the dominant long-term C stabilization mechanism is the sorption of functional C groups to mineral surfaces (Hemingway *et al.*, 2019; Kleber *et al.*, 2021; Possinger *et al.*, 2020) reducing C turnover, respective enhancing C persistence in soil (Heckman *et al.*, 2022; Schrumpf *et al.*, 2021). Together with environmental factors that control microbial C decomposition (Basile-Doelsch *et al.*, 2020), the mineralogical properties of the soil parent material and its weathering stage are the main factors for governing long-term C stabilization (Roering *et al.*, 2023; Slessarev *et al.*, 2022). Many tropical regions have undergone long lasting chemical weathering for millions of years resulting in decameter thick and deeply weathered saprolite layers (Porder *et al.*, 2005) reducing the capacity of C sequestration by reactive minerals. Relatively thin (8 – 25 cm) (Doetterl *et al.*, 2012; Sæther *et al.*, 1997) fertile topsoil layers, often overlay extremely thick (up to >50 m meters) (Zauyah *et al.*, 2010) nutrient-depleted subsoil layers. Thus, in how far dynamic replacement of C on hillslopes and accumulation in valleys can actually occur in tropical soil landscapes remains unclear as fertile topsoils are easily eroded and excavated subsoils show limited mineral reactivity. However, this is a question of the local biogeochemical and hydrological conditions.

Soil redistribution by water erosion in the Tropics differs greatly from temperate cropland systems for several reasons: (i) regular heavy tropical rainfall events result in a high frequency and severity of erosive events (Panagos *et al.*, 2017), (ii) due to increasing pressure on land resources (Hansen *et al.*, 2013; Karamage *et al.*, 2016b; UNESCO and WHC, 2010), even very steep slopes are clear cut (Karamage *et al.*, 2016b; Kroese *et al.*, 2020; Tyukavina *et al.*, 2018) for arable cultivation by smallholder farmers, (iii) subsistence farming without mineral fertilization is not leaving substantial amounts of plant residues after harvest (Castellanos-Navarrete *et al.*, 2015; Kim *et al.*, 2021; Valbuena *et al.*, 2015). Apart from the high water erosion potential, tillage erosion also plays a crucial role, especially on very steep slopes, where farmers are only plowing down slopes using hand held tools (Fatumah *et al.*, 2020; Nyakudya and Stroosnijder, 2015; Ziegler and Sutherland, 2009). This results in similar tillage erosion potential as compared to mechanized agriculture in temperate zones (Öttl *et al.*, 2024; Zhao *et al.*, 2024; Ziegler and Sutherland, 2009), where tillage erosion rates are often found to be similar or even higher than water erosion rates (Oost *et al.*, 2006; Öttl *et al.*, 2021; Wilken *et al.*, 2020).

Beside limited knowledge regarding water and tillage erosion rates in case of subsistence farming in the Tropics, our biogeochemical understanding of accelerated agricultural soil erosion and deposition processes is also strongly biased towards large-scale mechanized cropping systems in fertile soil settings that have been successfully cultivated for centuries (Borrelli *et al.*, 2021; Oost and Six, 2023; Öttl *et al.*, 2024; Ren *et al.*, 2020; Schimel *et al.*, 2015). Despite the fact that large-scale mechanized farming exists also in tropical settings, for example in South America, (Giller *et al.*, 2021), smallholder farming still dominates many tropical regions in which farming is conducted on deeply weathered soils. This is in particular the case for tropical sub-Saharan Africa (Lowder *et al.*, 2016), where large parts of the population (52 %) (Lowder *et al.*, 2016) conduct subsistence agriculture on smallholder farms and produce about 30 % (farm size <2 ha) to 77 % (farm size ≤50 ha) of local food commodities (Giller *et al.*, 2021). Such smallholder farming structures often result in small field sizes and a high degree of land use patchiness. These features can potentially impact lateral soil fluxes due to creating a complex hydro-sedimentological connectivity between fields (Baartman *et al.*, 2020; Nunes *et al.*, 2018) and breaking the flow of water from hillslopes into valleys, substantially affecting the resulting transport mechanisms and patterns of soil redistribution after erosive rainfall events (Wilken *et al.*, 2021).

Additionally, a large amount of eroded soil material is deposited in alluvial and colluvial settings in footslope and valley positions (Wang *et al.*, 2015). Eventually, long-term gains from additional C sequestered through replacement of eroded C may be created by conservation of this deposited SOC in valley sediments resulting in a net C sink on decadal timescales (Oost *et al.*, 2007; VandenBygaart *et al.*, 2015). The effectiveness of this depositional valley soil C sink can be assessed by analyzing patterns of SOC stock (more effective C sink results in higher SOC stocks) and SOC persistence using radiocarbon analyses (more effective C sink results in more depleted soil Δ^{14}C) (Fromm *et al.*, 2024a; Grant *et al.*, 2023; Grant *et al.*, 2022; Shi *et al.*, 2020). The replacement of eroded C and conversion of deposited C depend on the (i) the type of deposited soil material (e.g. C rich or C depleted soil from hillflanks or the stability of organo-mineral complexes) (Nijs and Cammeraat, 2020), (ii) the speed of soil burial (faster burial contributing to more conservation) (Zhao *et al.*, 2022) and (iii) the environmental conditions (water-saturation and oxygen limitations) that may reduce or promote microbial decomposition to conserve labile SOC (Davidson and Janssens, 2006; Feng *et al.*, 2017; Li *et al.*, 2017; Moyano *et al.*, 2012). Since many tropical regions experience rapid land use change in upland regions, leading to uneven promotion of erosion across catchments (Wilken *et al.*, 2021), depositional settings may therefore accumulate both C-enriched and practically unaltered former topsoil, as well as C-depleted subsoil. This has implications for the assessment of the future size and stability of buried SOC stocks.

In summary, to date, the impact of erosion-induced lateral soil fluxes on SOC stocks across tropical landscapes, characterized by smallholder farming structures on deeply weathered and rapidly eroding soils systems, has not been sufficiently studied and the consequences for C cycling in sloping tropical land are unclear. Three hypotheses on the effects of soil redistribution on SOC quality and quantity at the landscape scale were tested using soil data from different test sites representing distinctly different geochemical conditions along topographic gradients located in the Albertine Rift region of the East African Rift System in the border region between the Democratic Republic of the Congo (DRC), Rwanda and Uganda. We hypothesize that: (i) Any loss or gain of soil due to redistribution processes has little effect on total SOC stocks at different landscape positions since the investigated soils show limited reactivity of mineral surfaces. (ii) Thus, differences between deposited topsoil SOC contents and subsoil SOC contents will be small (iii) and deep burial of topsoil at footslopes will be limited.

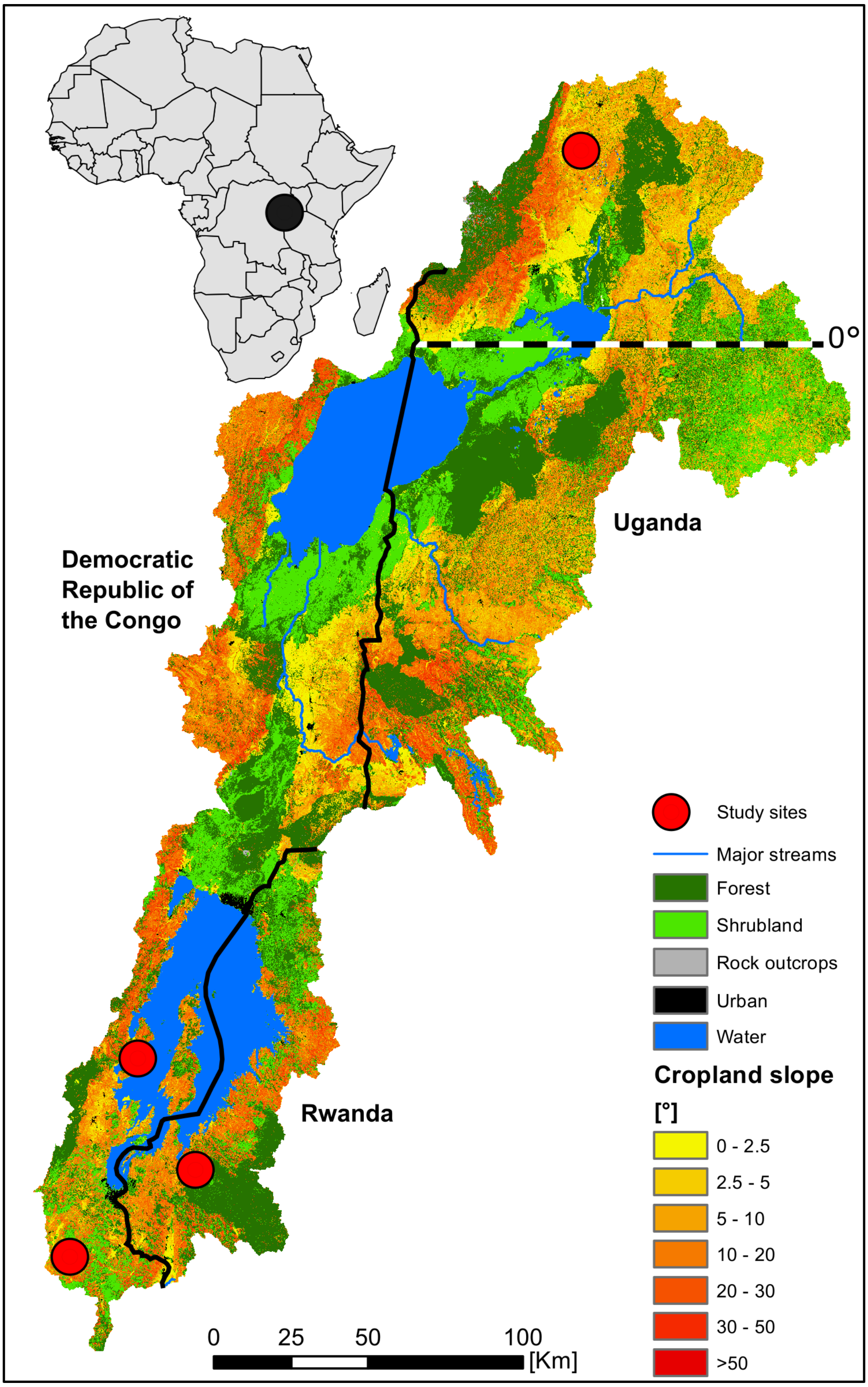

Figure 5.2: Overview regarding land use and slopes and the location of the test sites along the headwater catchments of the Nile and Congo (Kivu and Edward catchments), a part of the East African Rift. System in the border region between the Democratic Republic of the Congo (DRC), Rwanda and Uganda.

5.3 Materials and Methods

5.3.1 Study sites

The study area and test sites are located along the Albertine Rift, a part of the East African Rift System in the border region between the Democratic Republic of the Congo (DRC), Rwanda and Uganda (Figure 5.2). The test sites were chosen to represent soils that have developed from geochemically contrasting parent materials within a region with similar climate, topography and agricultural land management, thus similar starting conditions regarding lateral soil fluxes.

The region is characterized by tropical humid climate (Köppen Af-Am) with monsoonal dynamics and is subdivided into four seasons (weak dry in December–February; strong rains in March – May; strong dry in June – August; and weak rains in September – November) each covering three months (Bukombe *et al.*, 2022). The mean annual temperature (MAT) varies between 15.3 °C and 19.2 °C and mean annual precipitation (MAP) varies between 1697 mm and 1924 mm (time period between 1970 – 2000) (Fick and Hijmans, 2017). The active tectonism within the study region produced a steep terrain with smaller plateaus and ridges, steep slopes (up to 60 %) and various valley shapes. Cropland can be found across all hillslope positions. To represent this variable topographic situation, the test sites were sorted into stable plateaus (low / non eroding positions with slopes <5 %), slopes up to 50 % slope steepness (highly eroding at slope steepness >15 %), and footslope positions (low-eroding / accumulating positions), representing a transition zone between slope and valley bottom with a drop in transport capacity (Figure 5.3).

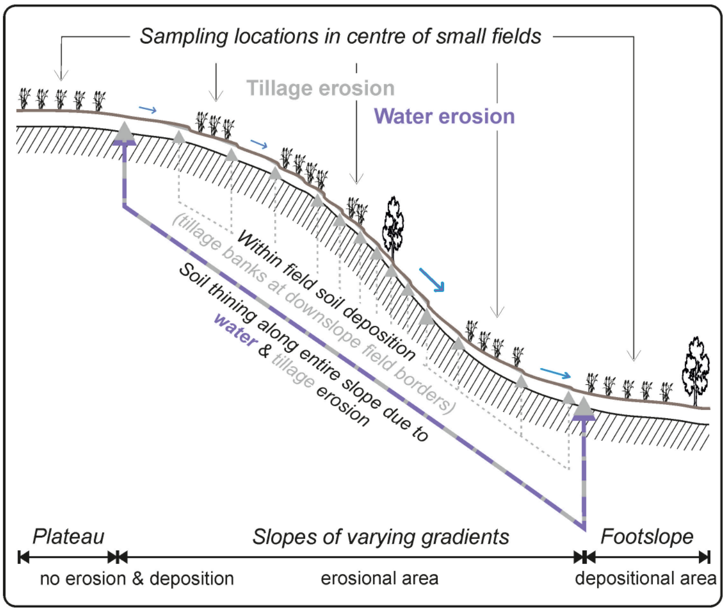

Figure 5.3: Schematic figure of land use patchiness, slopes of different gradients and landscape positions as well as locations of soil sampling at the different study sites all under small scale farming (field sizes <5 ha).

All study sites were converted from forest to cropland before 1985 (Reichenbach *et al.*, 2023). Thus, differences in conversion timing were (i) unlikely to impact our results, as all cropland sites should have had sufficient time for SOC stocks to equilibrate to the new land cover (Don *et al.*, 2011; Guillaume *et al.*, 2015), and (ii) similar time to equilibrate to the new conditions of accelerated soil redistribution, which reaches values of about 80 Mg ha^{-1} yr^{-1} erosion as well as deposition (Wilken *et al.*, 2021) as a response to land conversion from forest to cropland. The investigated fields are situated on farms that are generally small (<5 ha) and hence represent the vast majority of farmland in the region (>90 % of total cropland area) (Lowder *et al.*, 2016). The average field parcel size at the study sites is 450 m^2 (Wilken *et al.*, 2021) with crop rotations of cassava and maize as well as various legumes and vegetables with little to no fertilizer input (Mangaza *et al.*, 2021; Ordway *et al.*, 2017; Tyukavina *et al.*, 2018). Fertilizer use is rare and very limited and restricted to manure and fallow application. Pest management is done by manual weeding and soil management by hand plows (Doetterl *et al.*, 2021b). Multicropping is generally dominating over monocultures (Munyakazi *et al.*, 2022). The individual field parcels are highly dynamic in terms of sowing and harvest time which results in a high patchiness of land cover and selective harvest of planted multicropping fields, which can result in alternating areas of bare soil and full crop cover within the same field parcel (Wilken *et al.*, 2021). This leads to a high intra-slope variability with many different field conditions and connectivity properties.

At the time of sampling, the study sites are characterized by cassava and cassava intercropped with beans and crop rotations of (soy-) bean, maize, onion, pea, and (sweet-) potato. Farmers aim for one or two seasons of cassava followed by one or two seasons with alternative crops or fallow, if soil fertility is limited. Some study sites in the DRC also show cassava-only rotations which can be a sign of extremely poor soil quality in terms of nutrient availability and Al-toxicity (Doetterl *et al.*, 2021b). While on steep slopes predominantly cassava is planted, cassava intercropped with legumes is more often found at footslope positions (oral communication IITA, 2018).

Soils investigated in the DRC are developed from mafic magmatic rocks and are classified as alic Nitisols (ochric), alic Nitisols (vetic), and mollic Nitisols (ochric) (Doetterl *et al.*, 2021b). Soils in Uganda are developed from felsic magmatic and metamorphic rocks and are classified as sederalic Nitisols (ochric), haplic Lixisols (nitic), and luvic Nitisols (endogleyic) (Doetterl *et al.*, 2021b). Since the region is tectonically active, re-fertilization of soils with rock-derived nutrients by pyroclastica occurs to various degrees at a local scale (Bailey *et al.*, 2005; Barker and Nixon, 1989; Eby *et al.*, 2009). Study sites in Rwanda consist of mixed sedimentary rocks dominated by quartz-rich sandstone and schists and soils are classified as haplic Acrisols (nitic), acric Ferralsols (vetic), and acric Ferralsols (gleyic) (Doetterl *et al.*, 2021b). A specific feature of soils in this region is the presence of fossil, geogenic organic carbon free of radiocarbon in the parent material (dark clay-silt schists) (Bukombe *et al.*, 2021; Reichenbach *et al.*, 2021).

Soils on plateaus without erosion in the test regions have both similar and different biogeochemical properties. (Figure 5.4; Data taken from Doetterl *et al.* (2021b) and Reichenbach *et al.* (2023). Overall, the depth trends of all soil properties across the test sites are similar, and the differences between topsoil and subsoil are minimal. However, there is one exception, which is the subsoil C : N ratio in Rwanda. The C : N ratio increases with depth (ranging from 12.5 to 24.5) and exhibits higher variance as a result of the geogenic carbon influence of soil parent material there. This trend is the opposite for other test regions (ranging from 6.8 to 13.6) where C : N ratios decrease with depth. Similar, SOC content decreases with depth in all test regions (ranging from 12.9 tC ha^{-1} to 44.8 tC ha^{-1}). Soils in Uganda have a higher content of pedogenic oxides (ranging from 2.4 wt% to 3.0 wt%) compared to soils from the DRC and Rwanda (ranging from 0.7 wt% to 1.9 wt%). The clay content generally increases with depth in all test regions. Soils from the DRC exhibit the highest content, ranging from 49.0 % to 65.5 %, followed by soils from Rwanda, ranging from 39.0 % to 53.1 %, and Uganda, ranging from 23.0 % to 36.0 % clay content. There is no pronounced depth trend for bioavailable phosphorus (Bray-P) and exchangeable bases (Ca, Mg, K). However, soils from Uganda show higher contents (Bray-P ranging from 187.6 mg kg^{-1} to 137.7 mg kg^{-1}, exchangeable bases (Ca, Mg, K) ranging from 10.8 meq 100 g^{-1} to 18.3 meq 100 g^{-1}) and variability in fertility proxies compared to soil from DRC (Bray-P ranging from 4.2 mg kg^{-1} to 15.1 mg kg^{-1}, exchangeable bases (Ca, Mg, K) ranging from 3.1 meq 100 g^{-1} to 7.5 meq 100 g^{-1}) and Rwanda (Bray-P ranging from 0.0 mg kg^{-1} to 20.8 mg kg^{-1}, exchangeable bases (Ca, Mg, K) ranging from 0.7 meq 100 g^{-1} to 4.4 meq 100 g^{-1}).

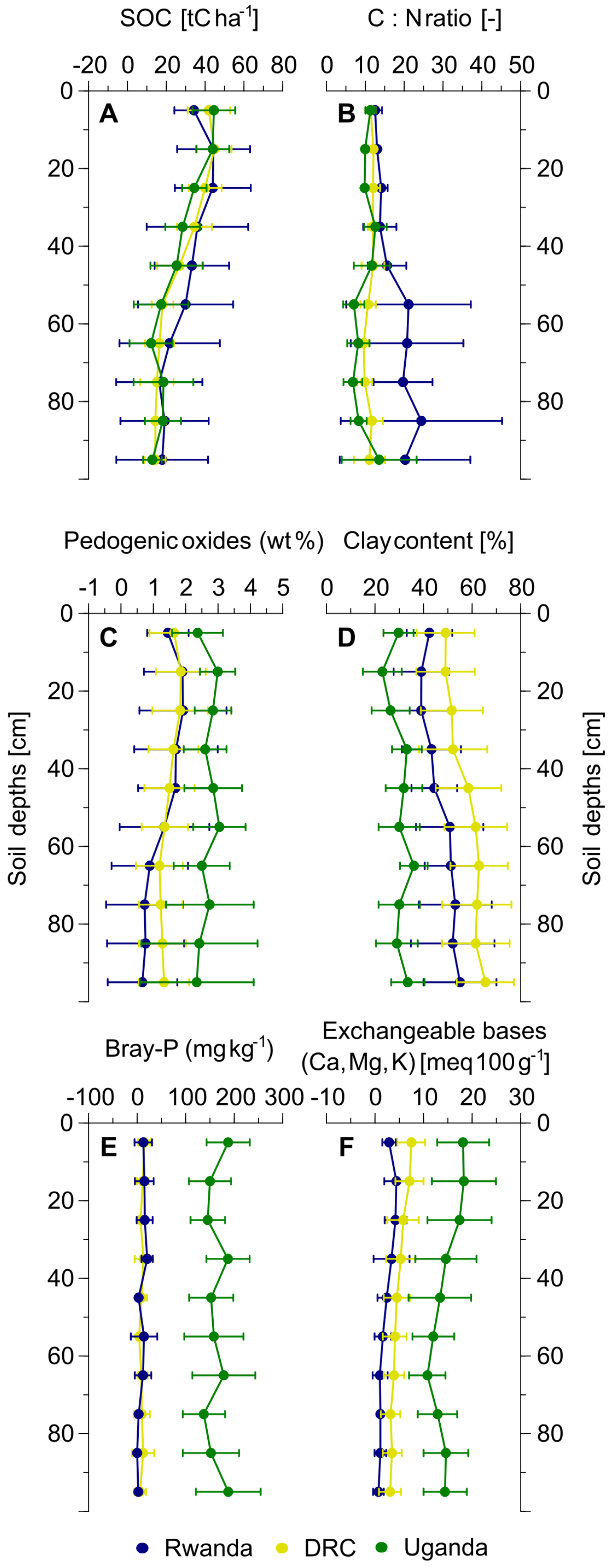

Figure 5.4: Mean soil organic carbon stocks as well as important other properties at plateaus positions without erosion in the different test regions in Rwanda (n = 6), Uganda (n = 5) and DRC (n = 8). Error bars give 95 %-confidence intervals of the mean (data taken from Doetterl *et al.* (2021b) and Reichenbach *et al.* (2023)).

5.3.2 Soil sampling

Overall, 99 plots with a dimension of 3 m x 3 m within each test site (= one single field), cultivated with cassava at the time of sampling, were analyzed (40, 25, and 34 sites in DRC, Uganda, and Rwanda, respectively). To represent the soils within fields with partly extreme slope, plots were always located in the center of the fields to avoid strong effects of tillage erosion, most pronounced at upslope and downslope field borders (Figure 5.3). Within each plot, two soil cores were taken and combined to one depth-explicit composite sample. Cores were taken using percussion drilling and soil column sampling equipment allowing for undisturbed sampling of 1 m deep soil cores at 9 cm diameter. Soil bulk density samples were taken with Kopecky cylinders of known volume (98.13 cm^3) or derived from the known volume and weight of the soils sampled by percussion drilling. Thus, we overall produced 99 composite soil cores (to 1 m soil depth), which were subdivided in 10 cm depth increments. As some drillings could not reach 1 m soil depth due to reaching the underlying saprolite and bedrock, this resulted in 914 samples for analysis. Please refer to Doetterl *et al.* (2021b) for a more detailed description of the study and sampling design.

5.3.3 Soil analysis

Details of the following methods are described in a published project-specific database (Doetterl *et al.*, 2021b) of project TropSOC. We refer to the following publications that analyzed a wide range of soil physical and chemical properties (Bukombe *et al.*, 2022; Bukombe *et al.*, 2021; Kidinda *et al.*, 2023; Kidinda *et al.*, 2022; Reichenbach *et al.*, 2021; Reichenbach *et al.*, 2023; Wilken *et al.*, 2021).

Soil bulk density samples were oven-dried at 105 °C for 24 h and weighted subsequently. Note that rock content (>2 mm) of all samples was negligible. Soil texture (clay, silt, sand) was analyzed using the Bouyoucos hydrometer method (Bouyoucos, 1962) modified following Beretta *et al.* (2014). Soil fertility was assessed by analyzing exchangeable base cations of calcium (Ca), magnesium (Mg) and potassium (K) and bioavailable phosphorus (bray-P) following Okalebo *et al.* (2002) and Pauwels *et al.* (1992).

Concentrations of pedogenic aluminum (Al), iron (Fe) and manganese (Mn) bearing mineral phases were assessed by a sequential extraction scheme of pedogenic oxy-hydroxides (Stucki *et al.*, 1988) resulting in pyrophosphate extractable organo-metallic complexes ($\sum$Al, Fe, Mn) and oxalate extractable oxides ($\sum$Al, Fe, Mn). Those two fractions were then summed up to represent pedogenic oxides relevant for mineral C stabilization (Kögel-Knabner *et al.*, 2008; Rennert, 2019; Wagai *et al.*, 2013).

Total carbon (TC) and total nitrogen (TN) were analyzed using dry combustion (Vario EL

Cube CNS Elementar Analyzer, Germany) and C : N ratio used as a measure of soil organic matter (SOM) quality in terms of plant-derived and less decomposed organic matter (high CN) vs. microbio-derived and more decomposed organic matter (low CN) (Cleveland and Liptzin, 2007; Whalen *et al.*, 2022). All C and N sources were considered of organic nature as inorganic carbon is absent in the investigated soils. Thus, SOC stocks of the bulk soil were calculated by multiplying the SOC concentration by soil bulk density and the thickness of the depth increment (10 cm). Bulk soil Δ^{14}C was analyzed for selected depth increments using AMS (accelerator mass spectrometry) at the Max Planck Institute for Biogeochemistry (Jena, Germany) and conventional radiocarbon age following the conventions of Stuiver and Polach (1977).

All values (n = 914) for the presented variables have been analyzed using a Bruker Vertex 70, (Hanau, Germany) near and mid-infrared (NIR-MIR) Fourier Transform FT-IR spectrometer (Doetterl *et al.*, 2021b; Summerauer *et al.*, 2021). As part of the calibration of the spectrometer, 20 % of all samples (n = 183) were analyzed with traditional wet-chemistry methods described above before predicting all samples following the workflow of Summerauer *et al.* (2021). NIR-MIR predictions resulted in high to very high performance in explaining the observed variability ($R^2 = 0.69 - 0.93$) for all assessed values, except for soil bulk density ($R^2 = 0.43$) (Reichenbach *et al.*, 2023; Summerauer *et al.*, 2021). Thus, we used the soil bulk density derived from Kopecky cylinders instead of FT-IR spectrometry derived values to calculate SOC stocks.

5.3.4 Slope gradient and slope position as erosion and deposition proxies

To capture the effect of soil redistribution through erosion on slopes and soil accumulation through deposition at footslopes, we used a random sampling scheme along slopes (potential erosional areas) to account for differences in slope steepness, while locations at plateaus and footslopes (both with slopes <5 %) were determined due to their landscape positions (Figure 5.3), representing areas without erosion and deposition as well as areas representing deposition, respectively. Slopes were determined in the center of each plot using a clinometer. We assume that slope gradient and slope position can act as a proxy for lateral soil fluxes since soil under low vegetation cover, on steep slopes and under high precipitation intensity and downslope tillage are most prone to erosion (see Section 5.5.1).

5.3.5 Exploring micro-scale variability in soil geochemical and SOC properties within topographic landscape positions

Prior to any data analysis, we conducted a series of pre-tests attempting to explain the observed variability (Figure 5.4) and its relation to more complex topographic indices. However, this resulted in a complex statistic (Table C.1) with limited informative value (see Appendix C.1 and Section 5.5.2). Thus, we focused on a more data-driven approach to test our hypothesis (see Section 5.3.4 and 5.3.6).

5.3.6 Data analysis

All data were visualized relative to the mean of the respective plateau positions to highlight potential effects of slope gradient and topographic landscape position on SOC stock and geochemical soil properties. Therefore, we aggregated the data on the plot-level for topsoil (0 – 20 cm) and subsoil (20 – 100 cm). The SOC stock represents the total SOC content of the profile down to 1 m depth, while the mean was calculated for all other variables for the respective depth increments. To calculate the plateau references for all variables, we averaged all plateau plots for each test region and depth increment. The relative differences to the respective plateau depth increments were calculated by dividing each observation with the respective plateau reference mean and then further called "relative SOC stock" in varying context below. The same approach was taken for other chemico-physical soil parameters such as clay content, exchangeable bases, etc. Before running parametric tests, data was tested for normality. Ordinary Least Square (OLS) regression and Pearson correlation analysis tested for relationships between SOC stock, soil fertility (Bray-P, exchangeable bases (Ca, Mg, K)) and stabilization mechanisms (clay content, pedogenic oxides). All statistical analyses were conducted at a significant level of $p < 0.05$ and realized using R 3.6.1 (RCoreTeam, 2020).

5.4 Results

5.4.1 Top-, subsoil and full profile SOC stocks relative to undisturbed plateau positions

Overall, there was a high variability in top-, subsoil, and full profile SOC stocks relative to undisturbed plateau positions across slope positions and test sites (Figure 5.5). Additionally, there were no significant differences in relative cumulative SOC stocks between test sites nor slope gradients, footslopes, and plateau positions. This was also observed for relative top- and subsoil SOC stocks, despite the lower variability in topsoils compared to subsoils.

In detail, relative full profile SOC stocks ranged from 0.3 to 2.0 with the highest values being observed along slope gradients in Ugandan test sites, while the lowest values being observed along slope gradients in DRC test sites. There is a wider spread in variation along slope gradients compared to plateaus and footslopes. Higher values tend to be observed at footslopes, but not consistently so. Relative topsoil SOC stocks ranged from 0.4 to 1.6 with the highest values at footslopes in Ugandan test sites and lowest values located along slope gradients in Rwandese test sites. The variability observed between topographic positions is comparable, and there is no clear trend in the distribution of the highest and lowest values. Relative subsoil SOC stocks ranged from 0.3 to 2.4 with the highest values observed along slope gradients in Ugandan test sites. The lowest values were observed both along slope gradients and footslopes. There were no significant relationships between relative SOC stocks between plateaus and slope gradients for the full profile (0 – 1 m soil depth). However, slope gradient was a significant predictor for relative full profile SOC stocks but could only explain 7 % of the variance (Figure 5.5a). Across the study region, there is a wider spread in variation of SOC stocks both on slope gradients and at footslopes compared to plateau positions with a non-consistent trend of higher values at footslopes.

5.4.2 (Bio)geochemical topsoil properties relative to undisturbed plateau positions

In general, geochemical variables relative to undisturbed plateau positions showed high variance across test regions and slope positions (Figure 5.6). In detail, the relative clay content ranged from 0.5 at plateaus with lowest values in DRC test sites to 1.6 at footslopes with highest values in Ugandan test sites. However, there was a higher variability along the slope gradient ranging from 0.5 and lowest values in DRC test sites to 1.8 and highest values in Ugandan test sites. The relative pedogenic oxides content showed a similar range across slope positions from 0.2 and lowest values in Ugandan test sites to 1.9 and highest values in Rwandese test sites. The relative Bray-P content ranged from 0.0 to 2.1 at plateaus and from 0.4 to 2.7 at footslopes with lowest and highest values both in DRC test sites but showed less variability along the slope gradients ranging from 0.0 and lowest values in DRC and Rwandese test sites to 1.5 and highest values in DRC test sites. The relative exchangeable bases (Ca, Mg, K) ranged from 0.1 to 21 on plateaus and footslopes and lowest values both in DRC and Rwandese test sites but showed a higher variability along slope gradients ranging from 0.2 to 3.1 driven by observations from the Rwandese test region. An exception were the relative C : N ratios with very little variability at

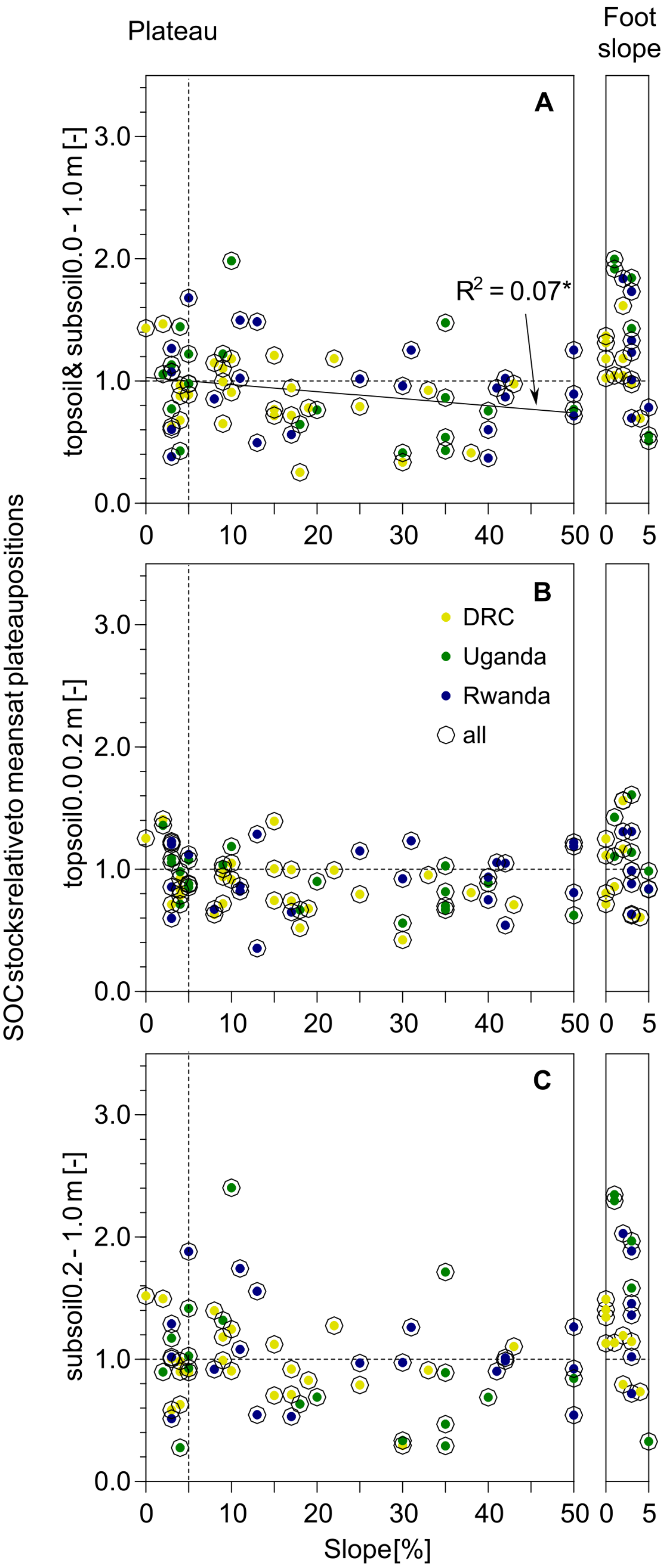

Figure 5.5: SOC stocks relative to mean SOC stocks at undisturbed plateau positions given for the entire profile (A), topsoil (B) and subsoil (C) at different landscape and slope positions. Note the regression line given in (A) is based on all test sites (black circle symbols) excluding the footslopes affected via deposition (assuming that erosion is a continuous process from plateaus to slopes up to 50 %).

different slope positions and slope gradients ranging from 0.8 to 1.5.

Slope gradient explained 24 % of the variance in relative clay content which increased with increasing slope gradient in the clay-rich DRC test sites (Figures 5.4 and 5.6). Relative pedogenic oxides content decreased with increasing slope gradient which explained 45 % of the variance in Ugandan test sites, which showed a high pedogenic oxides content. Slope gradient explained 34 % of variance in relative Bray-P content which decreased with increasing slope gradient. This was observed in Ugandan test sites also characterized by high Bray-P content. There was no significant relationship between slope gradient with relative C : N ratio nor relative exchangeable bases (Ca, Mg, K).

5.4.3 Depth distribution of SOC content and soil Δ^{14}C across slope positions

Please note that for Rwandan test sites soil Δ^{14}C data are only given to a depth of 40 cm as fossil geogenic organic carbon in deeper soil layers can result in misleading values (Figure 5.7). Furthermore, since the goal of this data display here is to represent differences across topographic units, for representing slopes only slopes with a slope steepness >15 % were considered as effects of lateral soil fluxes on SOC stocks soil Δ^{14}C should be more pronounced with steeper slope gradients and less influenced by small-scale land use patterns.

In general, SOC content decreased with depth. This depth trend was more pronounced for test sites in Uganda (higher content in exchangeable bases, Bray-P and pedogenic oxides but lower clay content) compared to DRC test sites (lower content in pedogenic oxides, Bray-P and exchangeable bases but higher clay content). In detail, the decrease with depth is more pronounced on plateaus compared to slopes and footslopes. At plateaus, SOC ranged from 12.2 tC ha^{-1} in subsoil to 44.8 tC ha^{-1} in topsoil, at slopes from 10.2 tC ha^{-1} to 41.1 tC ha^{-1} and at footslopes from 23.2 tC ha^{-1} to 56.8 tC ha^{-1}. Mean differences between the three regions were negligible and not significant due to the high variability within each region. However, some trends in the data can be observed. Most Rwandese subsoils (20 – 100 cm) SOC stocks are higher across all topographic positions compared to DRC and Ugandan test sites, but not consistently so. Topsoil SOC stocks (0 – 20 cm) at plateaus and along slope gradients do not differ across test sites except for footslopes. Here, Ugandan test sites show a non-consistent trend of higher topsoil SOC stocks compared to footslopes in DRC and Rwandese test sites. SOC stocks at Ugandan test sites showed a higher variability compared to test sites in Rwanda or DRC. SOC stocks across all test sites show a higher variability at plateaus and footslopes compared to slope gradients.

In general, the soil Δ^{14}C values followed the patterns observed in SOC, showing a decrease

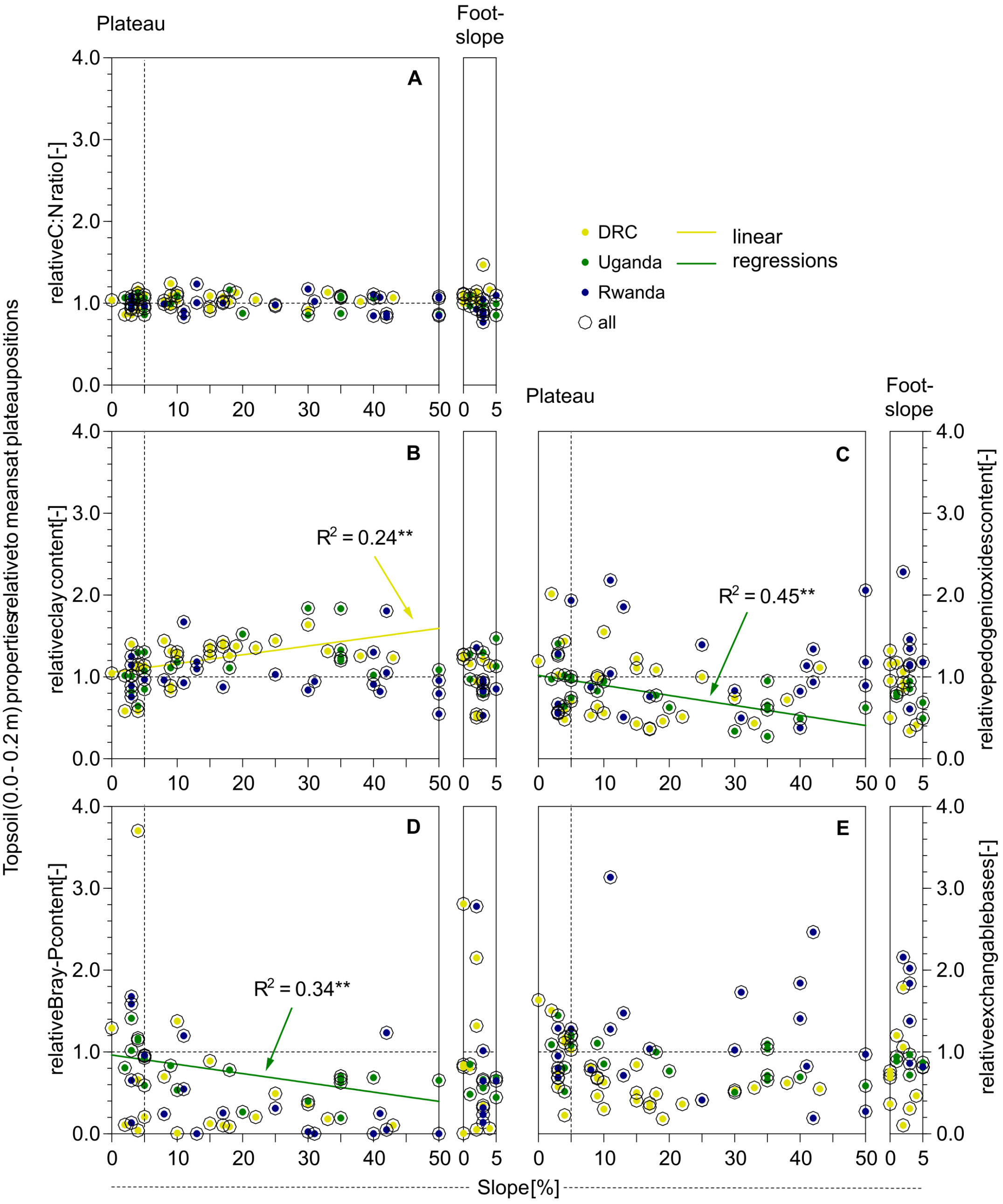

Figure 5.6: Topsoil (0 – 0.2 m) properties at different slope positions and slope gradients. Regression lines are only given if the Person R was significant ($p < 0.05$; whereas ** means $p < 0.01$); Note, in case of the relative exchangeable bases, two outliers from Rwanda were above a ratio of four and hence are not displayed, so that all remaining data can be shown for an easier comparison of the rations with the same y-axis scaling.

with depth. This depth trend was more pronounced for test sites in Uganda compared to DRC test sites. In detail, the decrease with depth is more pronounced on plateaus compared to slopes and footslopes. At plateaus, soil Δ^{14}C ranged from -399.0 ‰ in subsoil to 23.8 ‰ in topsoil, at slopes from -339.0 ‰ to -81.5 ‰ and at footslopes from -244.8 ‰ to 42.4 ‰. However, similar to SOC stocks, due to the high variability within regions, differences between test regions were small. But again, some trends can be described in the data. Soil Δ^{14}C at Ugandan test sites showed a higher variability compared to test sites in Rwanda or DRC. Soil Δ^{14}C across all test sites showed a higher variability at plateaus and footslopes compared to slope gradients. Topsoil Δ^{14}C (0 – 20 cm) was less depleted at plateaus and footslopes in Ugandan compared to DRC and Rwandese test sites but not along slope gradients. Subsoil Δ^{14}C (20 – 100 cm) at plateaus and slope gradients were less depleted in DRC compared to Ugandan test sites but not consistently so. This trend was not observed at footslopes due to the high variability at Ugandan test sites. Footslopes tended to be less Δ^{14}C depleted than other slope positions, especially in subsoils.

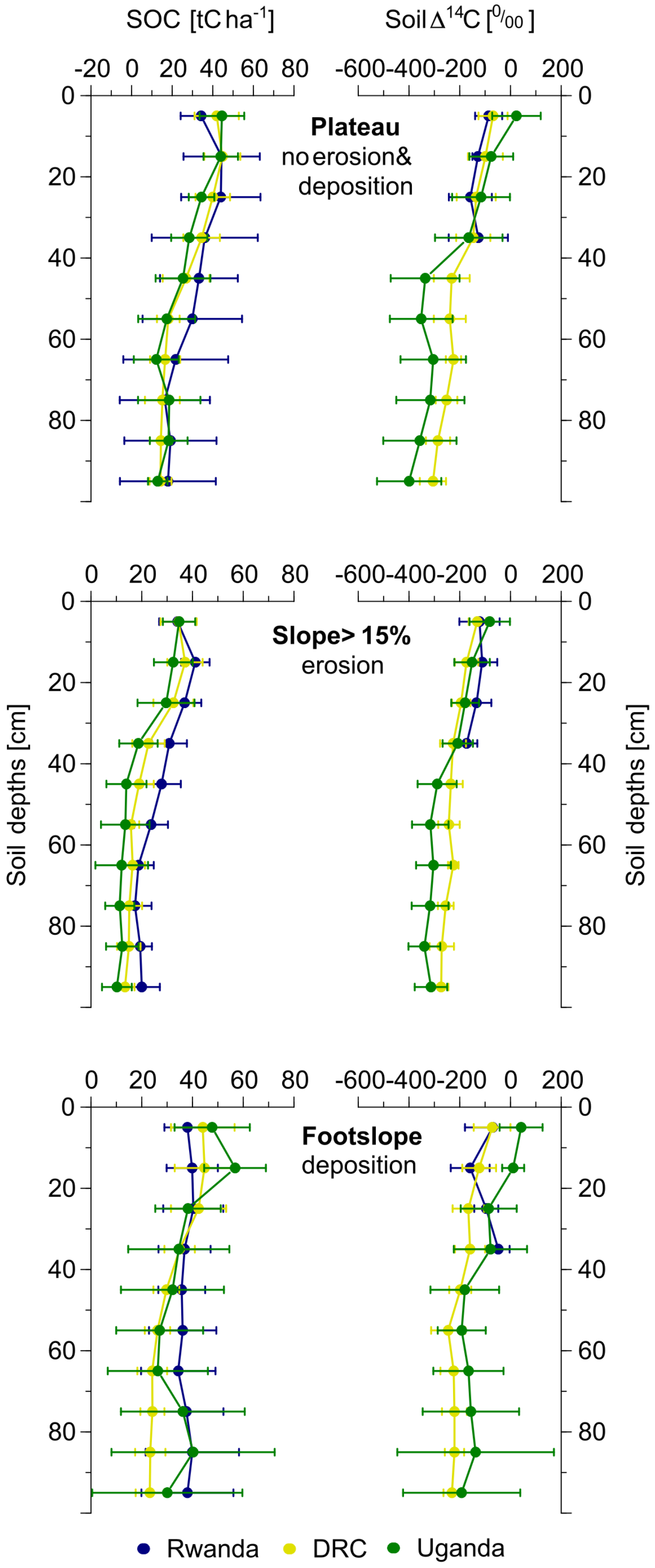

Figure 5.7: Mean Δ^{14}C data for the three different sites in Rwanda, DRC, and Uganda calculated from the sites at the plateaus (no erosion or deposition), sites with slopes >15 %, and the footslopes. Number of samples per site and depths between 5 and 13); Soil Δ^{14}C data for Rwanda are only given to a depth of 0.4 m as fossil geogenic carbon in deeper layers of some plateaus in Rwanda give misleading values. Error bars give 95 %-confidence intervals of the mean.

5.5 Discussion

5.5.1 Representativeness of erosion proxies limited by land use patchiness

Our results indicate that, for the deeply weathered soil landscapes cultivated by smallholder farmers, slope gradient and slope position may only weakly indicate soil redistribution by water and tillage (Figures 5.5, 5.6 and 5.7). This is surprising as not only studies in the temperate zone (Dalzell *et al.*, 2022; Li *et al.*, 2018; Nadeu *et al.*, 2015; Quijano *et al.*, 2021; Wiaux *et al.*, 2014a; Wiaux *et al.*, 2014b; Wilken *et al.*, 2020) but also in the Tropics showed a clear relationship between topography and SOC (Chaplot *et al.*, 2009; Labrière *et al.*, 2015; Rizinjirabake *et al.*, 2023; Sanogo *et al.*, 2023; Tian *et al.*, 2020; Vanacker *et al.*, 2019).

Nevertheless, this does not mean the slopes of the study sites are not affected by soil redistribution. Slope position and gradient should still reflect lateral soil fluxes, at least on the slope-scale, as water and tillage erosion in our study areas is likely to vary significantly depending on these topographical attributes. Correspondingly high rates of water and tillage erosion have been reported in the wider region (Labrière *et al.*, 2015; Symeonakis and Drake, 2010; Tamene and Le, 2015). Typical values for both processes on steep slopes are up to 75 Mg ha^{-1} yr^{-1} (Tamene and Le, 2015) and 81 Mg ha^{-1} yr^{-1} (Wilken *et al.*, 2021). Further, the study areas have been used for arable farming for decades, which has contributed to soil erosion (Ordway *et al.*, 2017; Reichenbach *et al.*, 2023; Tyukavina *et al.*, 2018). Therefore, as slope gradient is a significant driver of erosion processes, we assume that slope gradient and slope position are suitable proxies for redistribution in our analysis (Figure 5.3), since the region experiences high water erosion rates due to steep slopes, low soil cover during certain times of the year, high rainfall erosivity (Karamage *et al.*, 2016a; Karamage *et al.*, 2016b; Panagos *et al.*, 2017; Xiong *et al.*, 2019; Ziegler and Sutherland, 2009) and substantial tillage erosion rates due to the down-slope tillage by hand using a hoe (Zhao *et al.*, 2024; Ziegler and Sutherland, 2009). This is supported by our $\Delta^{14}C$ data indicating erosional and depositional processes (Figure 5.7). Slopes with a gradient greater than 15 % exhibit lower topsoil $\Delta^{14}C$ compared to plateau positions, indicating erosion of topsoil material. In contrast, footslopes exhibit a higher subsoil SOC stocks and higher (less depleted) $\Delta^{14}C$ signatures for both topsoil and subsoil, suggesting the deposition of topsoil material from adjacent slope areas (Doetterl *et al.*, 2016; Trumbore, 2009). However, the use of slopes as erosion predictors introduces significant noise in the combined analysis of SOC and soil redistribution patterns (Figures 5.5 and 5.6). This is also evident from the high variance of the footslope $\Delta^{14}C$ data (Figure 5.7). To better represent water erosion potential at different topographic positions, it may be useful to also consider additional indicators such as slope length or the slope length factor of the Universal Soil Loss Equation (USLE) (Wischmeier and Smith, 1978). However, a recent study by Wilken *et al.* (2021) analyzed the small-scale variability of soil redistribution in the study region using $^{239+240}$Pu fallout radionuclides as a soil redistribution tracer. The study highlights the large influence of smallholder farming on the hydrological and sedimentological connectivity, which is driven by an extremely high landcover patchiness driven by small fields and individual management. Both soil erosion and deposition were in direct proximity to each other (Figure 5.3). Furthermore, the downslope soil redistribution via hand-held tillage significantly impacts the overall soil redistribution patterns. This effect is particularly pronounced on steeper slopes, where tillage is consistently performed in a downslope direction (Blanco and Lal, 2023; Turkelboom *et al.*, 1999; Ziegler and Sutherland, 2009). This spatio-temporal diverse land use pattern results in unexpected patterns of SOC stock and C persistence (soil Δ^{14}C). Hence, lateral soil fluxes in steep landscapes characterized by small-scale subsistence farming systems (high degree of land use patchiness) are apparently driven more by land use patterns in contrast to predominantly topography-driven patterns in large-scale industrial farming systems (homogenous land use pattern). As such, the results of erosion models, relying solely on linear topography effects as the key factor for spatial-temporal SOC distribution and assuming homogeneous land use, will not adequately represent SOC dynamics in steep tropical landscapes with a complex land use pattern and history due to small-scale subsistence farming on deeply weathered soils.

5.5.2 Land use patchiness as a potential driver for microscale-variability

The prevalence of small-scale management practices involving alternating crop rotations of cassava, maize, and various legumes and vegetables (Mangaza *et al.*, 2021; Ordway *et al.*, 2017; Tyukavina *et al.*, 2018) may also explain the considerable (bio)geochemical variability observed in the investigated low SOC soils (Figure 5.4). The individual field parcels are highly dynamic in terms of tillage, manual weeding, sowing and harvest time (Kalyebi *et al.*, 2021; Sisheber *et al.*, 2023), which results in a high patchiness of land cover and selective harvest of planted multi cropping fields. This eventually results in alternating areas of bare soil and full crop cover within the same field parcel (Wilken *et al.*, 2021), which may drive soil variability. The variability in soil properties is not confined to the plateau positions but is also evident in other slope positions (Figure 5.6). This may be indicative of the absence of selective transport processes, whereby erosion and deposition affect only a specific portion of the soil (Heng *et al.*, 2011; Shi *et al.*, 2017; Wang *et al.*, 2019a). Instead, the observed rainfall and related erosion events are of such intensity that all soil fractions are affected. This raises the question of the extent to which slope steepness plays a role in monsoonal systems, given that (bio)geochemical soil properties are unaffected by slope angle (Figure 5.6). However, this spatio-temporal diverse land use pattern and complex hydrological connectivity across slopes (intersecting pathways, hedges, drainage channels, roads, terraces, buildings and various degrees of soil cover ranging from bare soil to full crop cover) most likely results in shifting patterns of erosion and deposition, which further contribute to the microscale-variability of soil (bio)geochemical properties. Therefore, more data on land use history and management practices is needed to provide a coherent explanation for the observed variability in soil characteristics associated with smallholder farming systems.

5.5.3 Weak effects of soil erosion on SOC stocks and stabilization due to deeply weathered soil mineralogy

A large body of literature suggests i) a significant effect of lateral soil fluxes in agricultural landscapes resulting in a topography-driven SOC stock pattern with eroding slopes (SOC losses) and depositional footslopes (SOC gains) (Dalzell *et al.*, 2022; Dlugoß *et al.*, 2010; Doetterl *et al.*, 2016; Hemelryck *et al.*, 2011; Li *et al.*, 2018; Li *et al.*, 2015; Nadeu *et al.*, 2015; Oost and Six, 2023; Quijano *et al.*, 2021; Wiaux *et al.*, 2014a; Wiaux *et al.*, 2014b; Xiao *et al.*, 2018); and ii) an interaction between lateral soil fluxes with geochemical soil properties leading to diverse mineral C stabilization processes across erosional and depositional sites (Chadwick and Asner, 2016; Dialynas *et al.*, 2016a; Dialynas *et al.*, 2016b; Doetterl *et al.*, 2016; Nijs and Cammeraat, 2020; Vitousek *et al.*, 2003; Wiaux *et al.*, 2014a; Wiaux *et al.*, 2014b; Xiao *et al.*, 2018; Zhao *et al.*, 2019). In our study across a steeply sloped tropical landscape with steep slopes focusing on deeply weathered cropland soils, observed spatial and vertical distribution of SOC stocks and C persistence (soil Δ^{14}C) do not follow classical topography-driven patterns resulting from soil redistribution nor are they driven by diverse mineral C stabilization processes as widely observed in slowly eroding arable landscapes in temperate climate zones dominated by large-scale industrial farming systems.

Overall, we verify the first part of hypothesis one that under the tested site conditions only weak effects of soil redistribution on SOC stocks (0.0 – 1.0 m) can be recognized (Figure 5.5). However, it is not as clear if this results from the physicochemical properties and especially their depth distribution in deeply weathered tropical soils or from the uncertain estimates of true soil loss or gain based on the slope gradients and slope position.

In contrast to agriculturally used soils derived from younger (peri) glacial parent material (∼10 000 years old) (Finke and Hutson, 2008), the investigated soils have undergone intense chemical weathering (Porder *et al.*, 2005) depleting also several meters deep subsoils from all primary minerals, leaving behind secondary end-member minerals of low reactivity (Bruun *et al.*, 2010). Consequently, even on heavily eroded slopes, the excavation and surfacing of former deep soil layers do not lead to overcoming limitations in mineral C stabilization since degraded soils on slopes get “stuck” in deeply weathered subsoils and less weathered layers close to the bedrock remain distant to the surface (Tanzito *et al.*, 2020; Thomaz, 2013). This is illustrated by a subsidiary regression analysis where depth-specific correlations between SOC stocks and soil properties do not change significantly (Figure C.1). Thus, the lack of change in controls for SOC content shows that mineral C stabilization mechanisms are not changing with soil depth or slope position. At erosional sites where there is a loss of topsoil, neither the soil properties governing C stabilization nor those governing fertility are changing significantly (Figure 5.6). Only slight decreases in some variables, such as exchangeable bases (Ca, Mg, K) were observed for eroding sites, while others, like clay content, even increase with depth (Figure 5.4). Therefore, truncation of the soil profile does not lead to a significantly different (bio)geochemical environment for SOC stabilization. Thus, if eroded topsoils have only slightly reduced fertility, while C stabilization proxies do not show substantial differences, the most likely reason why eroded sites should have lower SOC content is that the lateral SOC loss cannot be replaced fast enough (Dialynas *et al.*, 2016a; Dialynas *et al.*, 2016b; Oost and Six, 2023). Any input of photosynthetic products to these soils appears to be immediately processed by microorganisms or stabilized to a smaller extent via similar mechanisms as the already existing SOC. This is indicated by the low C : N ratios in topsoils of the plateau positions (Castellanos-Navarrete *et al.*, 2015; Kleber *et al.*, 2021) and generally low SOC values observed in the study region (Figures 5.4 and 5.7). The C : N ratio in topsoils (0 – 0.2 m) of DRC, Uganda, and Rwanda are 11.7±1.4, 10.7±0.9, and 12.8±0.8, respectively (Figure 5.4). This finding is consistent with larger scale studies that report high SOC turnover rates combined with low SOC stocks in highly weathered tropical soils (Fromm *et al.*, 2024a; Fromm *et al.*, 2021).

5.5.4 Fast replacement of eroded SOC but limited storage potential

Overall, we confirm our second hypothesis, which suggests that lateral soil and SOC losses at erosional sites are compensated for within a short period due to rapid SOC turnover and low stabilization mechanisms. Here, older SOC comes closer to the surface but is mixed with younger C input (Trumbore, 2009). In the absence of any fresh C input in the excavated subsoil material, it would be expected that significantly greater depletion of Δ^{14}C would be observed along slopes and in areas of erosion (Figure 5.7). However, this replacement does not seem to be influenced by soil geochemical properties. Despite the pronounced variability in soil mineralogy across test regions (Figure 5.4) and slope positions (Figure 5.6), it does not affect SOC stocks or soil Δ^{14}C (Figure C.1). Thus, as long as the stabilization mechanisms in soils remain unchanged due to erosion (Figures 5.6 and C.1), a small amount of C input to the eroded topsoil is enough to achieve topsoil SOC stocks similar to those found on the plateaus (Figures 5.4 and 5.7). This is supported by similar topsoil SOC content found at plateau sites in nearby forests (Reichenbach *et al.*, 2023), which demonstrate that topsoil SOC stocks are hardly affected by significantly larger plant C inputs under forest compared to arable land. However, it is important to note the overall SOC content of the investigated sites are relatively low (mean topsoil SOC content at plateaus in DRC: 86.7±22.1 tC ha^{-1}, Uganda: 88.5±17.2 tC ha^{-1}, and Rwanda: 78.7±21.2 tC ha^{-1}). This highlights the limited potential for effective SOC replacement in highly weathered soil systems (Figures 5.5 and 5.6). Dynamic C replacement may be fast, but it is not as effective in tropical regions as in the temperate zone due to the limited potential of soil to stabilize SOC.

5.5.5 Weak increase of SOC stocks at depositional sites due to fast mineralization of labile C

Overall, we verify our third hypothesis that depositing topsoil material at footslopes only marginally increases profile SOC stocks. Generally, the deposition at footslopes is primarily driven by water erosion, which transports material along the entire slope to the footslopes (Oost and Six, 2023). Thus, at depositional sites, such as footslopes, soil profiles with higher SOC stocks can be expected to extend to deeper soil layers due to the deposition of SOC-rich topsoil (Fiener *et al.*, 2015; Oost *et al.*, 2007; VandenBygaart *et al.*, 2015; Wang *et al.*, 2015). Although the highest SOC stocks in our study are often found at foot slopes, there appears to be no consistent pattern (Figures 5.5 and 5.7). It is likely that deposition in the vicinity of small fields is often influenced by human interventions, such as creating ditches to drain surface runoff (Labrière *et al.*, 2015; Wilken *et al.*, 2021). Therefore, it is highly variable and eroded soil material can be either translocated only for a few meters and deposited within the same field parcel or transported over longer distances across the entire slope eventually accumulating in more distal depositional sites (Figure 5.3). Consequently, depositional footslopes can receive varying amounts of eroded soil material depending on the hydro-sedimentological connectivity across the agricultural landscape. Additionally, the difference between topsoil and subsoil SOC contents is not pronounced, so the deposited topsoil only slightly alters the SOC content along the soil profile. Finally, it could be argued that the SOC buried below the plough layer is not very stable under the soil and climate conditions in the humid Tropics (Fromm *et al.*, 2024a; Hall *et al.*, 2015)) and that SOC turnover rates are also high in subsoils and quickly mineralize added SOC from deposition.

5.6 Conclusion

This study assessed whether rapidly eroding tropical cropland systems function as a C sink or source. Therefore, it's important to understand which processes impact C dynamics in tropical cropland systems. Our data indicates that replacement of SOC at eroding slope positions is achieved quickly because only a small amount of C is needed to compensate for C losses. This is because SOC stocks are generally low due to advanced weathering of the investigated soils and their low potential for SOC stabilization. In addition, eroded topsoil material is not stabilized long-term at depositional footslopes (Figures 5.5 and 5.7) due to the absence of effective stabilization mechanisms in both topsoil and subsoil (Figure C.1).

Both the variability in soil physicochemical and topographical properties do not strongly affect SOC stocks and persistence (soil Δ^{14}C) compared to observations on soil redistribution effects in less weathered and more reactive soils. Consequently, the resulting patterns of SOC stocks and persistence (soil Δ^{14}C) do not match those characteristic of eroding cropland landscapes in temperate regions. Instead, the high variability in both soil geochemical and SOC data suggests a highly dynamic landscape where rapidly eroding and not yet fully consolidated tropical cropland systems appear to function as a C source, at least at the regional and slope scale investigated here. As such, soil redistribution in deeply weathered tropical landscapes does not necessarily lead to higher SOC stocks with higher C persistence in colluvial and alluvial valley soils but can reduce SOC stocks on highly erosive (steep) landforms.

In conclusion, our data suggests that farm management to retain soil stability and limit erosional soil losses is of even greater importance in deeply weathered tropical soils than in other farmed soils of the planet. It is also likely that due to fast erosional soil losses and limited potential to replace C losses with new plant C inputs, depositional sites along slopes and footslopes will receive increasingly C-depleted material, leading to the collapse of already low and unprotected SOC stocks.

Chapter 6

Synthesis and general conclusions

6.1 Main findings and their relevance for carbon research

Many studies have linked SOC dynamics to soil geochemistry, topography and land use (Berhe *et al.*, 2008; Don *et al.*, 2011; Fromm *et al.*, 2024a; Fromm *et al.*, 2021; Kleber *et al.*, 2021). Up until now, the main findings are: (i) Despite the substantial effect of climate on SOC dynamics, mineralogy is particularly known to affect SOC stock and soil C turnover, through its influence on soil structure and reactivity both regulating sorptive processes with C molecules (Kleber *et al.*, 2021; Mikutta *et al.*, 2019; Possinger *et al.*, 2020; Wasner *et al.*, 2024). In this context, many studies have shown that increasing SOC content together with decelerating C turnover correlates with the amount of poorly crystalline minerals of Fe / Al and Fe / Al oxyhydroxides and high-activity 2 : 1 clay minerals (Islam *et al.*, 2022; Song *et al.*, 2022)) both promoting soil aggregation and the occlusion of SOC (Lehmann *et al.*, 2007; Ozlu and Arriaga, 2021; Torres-Sallan *et al.*, 2017). (ii) The magnitude, rate and even direction of SOC change in tropical soils following land conversion remain unclear (Guillaume *et al.*, 2015). For example, meta-analysis focusing on the Tropics identified land conversion especially from natural forest to cropland systems as a major driver of SOC loss both in top- and subsoils (Don *et al.*, 2011) due to changes in C input and management practices that affect the soil structure (Ozlu and Arriaga, 2021; Veldkamp *et al.*, 2020; Wang *et al.*, 2019c; Wang *et al.*, 2019d) and microbial activity (Kidinda *et al.*, 2023). However, other studies show only minor changes (Kukla *et al.*, 2019; Sayer *et al.*, 2019; Tamale *et al.*, 2022) or even an increase in SOC stocks after land conversion (Kirsten *et al.*, 2019; Kirsten *et al.*, 2021b). (iii) Moreover, many studies show the risk of increased soil erosion in agricultural systems especially in sloping landscapes (Fatumah *et al.*, 2020; Oost and Six, 2023; Öttl *et al.*, 2021) combined with high rainfall intensity (Liu *et al.*, 2022; Zhao *et al.*, 2021). However, most of these studies are analyzing the effect of mineralogy, topography and land use isolated from each other. This PhD study contributes to the holistic understanding of how SOC dynamics in deeply weathered soil of the Afrotropics are linked to interacting factors of geochemistry, topography and land use (Figure 6.1). The main innovations of this thesis and its contributions to the scientific community are as follows:

(i) This thesis comprised one of the first studies conducted in one of the hotspots of global change – the Central African Congo Basin and African Great Lakes region – which is at the same time one of the least studied regions worldwide regarding biogeochemical cycling and SOC dynamics in soils.

(ii) The investigated tropical soils exhibit variations in their mineral C stabilization potential depending on their parent material, despite their overall endmember mineralogy.

(iii) However, long-term mineral C stabilization is limited in deeply weathered tropical soils.

(iv) Land use modifies the impact of soil geochemical properties on mineral C stabilization. Differences in soil properties across test regions lead to significant changes in SOC stocks under forest but not under cropland. However, the overall low soil reactivity sets an upper limit for C sequestration in both land uses, regardless of their differing C inputs and management practices.

(v) Topography-driven lateral soil fluxes are minor under forest but pronounced under cropland. However, erosion-induced gravitational soil fluxes do not impact soil geochemical properties nor result in a consistent spatial and vertical redistribution of SOC stocks with different quantities and turnover across landscape compartments.

Overall, the conducted studies improved our mechanistic understanding of how SOC stabilization reacts to changes in soil properties and its effects on biogeochemical cycles in the African Tropics. In detail, chapter 3 (study I) of this PhD thesis focuses on understanding how the geochemical properties of soils, originating from diverse parent materials in natural forest systems, influence SOC stocks, Δ^{14}C, soil C fractions, and the mechanisms involved in C stabilization. This analysis also explores the interaction of these factors with topography. Previous studies predominantly isolated the effects of parent material and topography on SOC dynamics thus missing potential interaction effects. Moreover, these studies primarily focused on young to intermediate-aged (∼15 000 years) grassland or cropland soils from mid-latitudes, leaving tropical soils comparatively understudied. This third dissertation chapter significantly contributed to filling this research gap by identifying the drivers of SOC stabilization in one of Central Africa's least explored tropical regions. The findings indicated minimal topographical

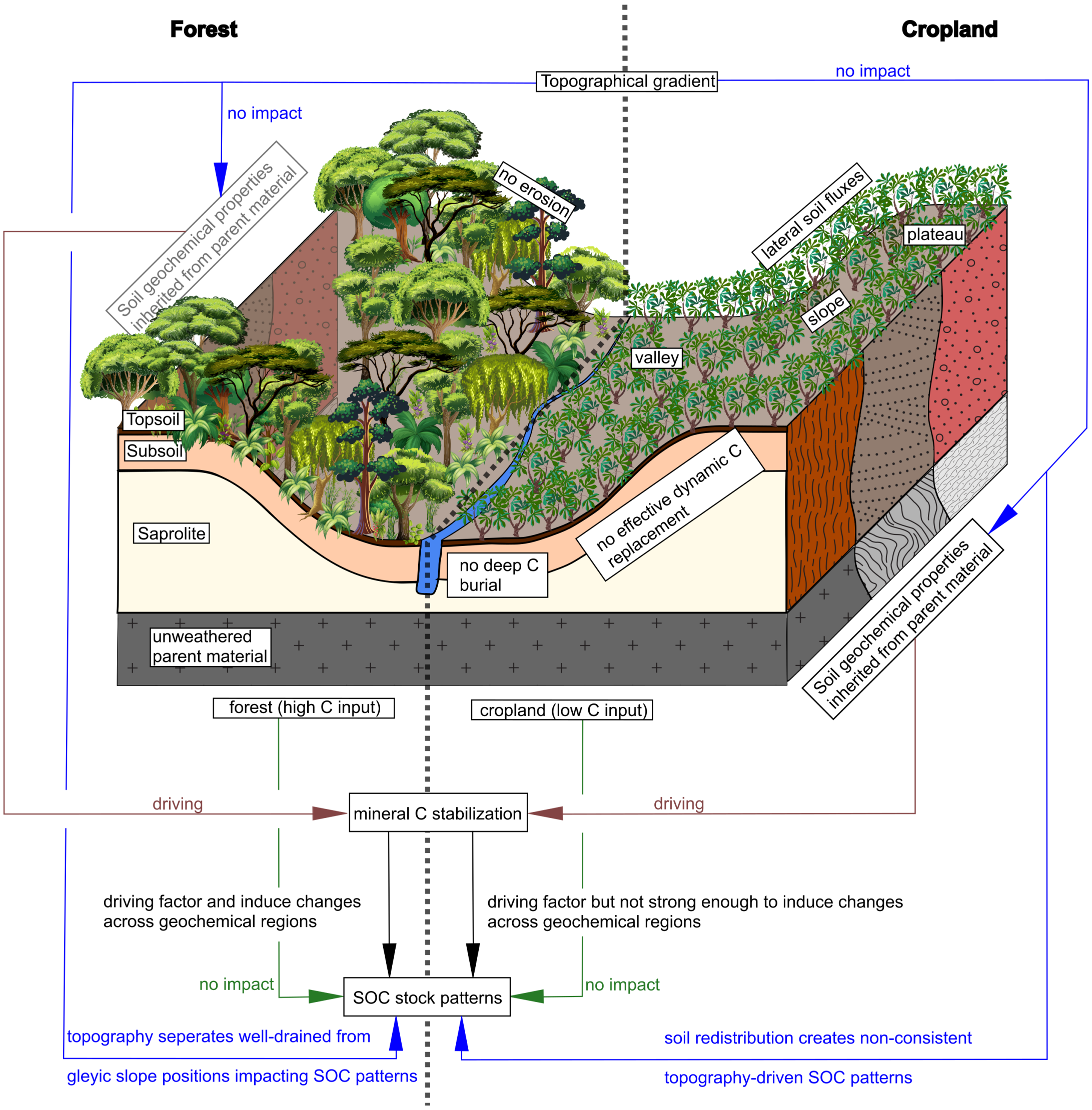

Figure 6.1: Graphical synthesis showing (bio)geochemical controls on SOC stock patterns and mineral C stabilization across gradients of soil geochemistry, land use and topography. Please refer to Figure 1.2 for the related research questions and hypothesis (see H1.1, H1.2, H2.1 and H2.2).

impact on SOC variables regarding soil fluxes along slopes. However, geochemical soil properties emerged as key explanatory factors. The influence of these variables on SOC stocks is closely linked to reactive mineral surfaces dependent on parent material composition and its weathering status. Greater availability of reactive surfaces favors sorptive C stabilization and the formation of stable aggregates, consequently leading to higher SOC stocks. Variations in the distribution of C associated with microaggregates and the free silt and clay fractions were notably different across geochemical test regions and soil depth. This underscores the role of pedogenic oxides in tropical soil aggregate formation, linking two of the most important mineral-related C stabilization mechanisms to geochemical variability inherited from soil parent material. These new insights of organo – metallic complexes and mineral-driven C stabilization mechanisms in a complex tropical setting, along with the influence of fossil organic carbon on SOC dynamics, holds potential for refining future C turnover models.

Following the assessment of undisturbed systems, the following chapter 4 (study II) analyzed how soil parent material mineralogy and its weathering status impact SOC stocks and soil C persistence (Δ^{14}C) following land conversion from tropical forest to cropland. SOC dynamics depend on soil properties derived from the geo-pedo-climatic conditions under which soils develop and are modified by land conversion. However, SOC stabilization and the responses of SOC to land use change are not well constrained across soil types. Especially deeply weathered and often less reactive tropical soils are understudied and SOC dynamics therefore poorly constrained. Thus, this study investigated the drivers of SOC dynamics across geochemical gradients and different land uses (forest versus cropland). While the controls on SOC stocks and persistence change across geochemical regions, overall, SOC stocks remain similar despite land use change. Due to prolonged weathering, these tropical soils lack sufficient reactive minerals to stabilize higher C inputs from forests. This highlights the absence of SOC losses related to land conversion and the prevalence of weakly bound, relatively young, and accessible SOC in these soils. This new understanding of specific parent material and weathering-derived mineralogical properties governing tropical soil reactivity underscores their control over SOC stabilization. It challenges the comprehension of how land conversion may or may not impact SOC stocks in tropical regions experiencing massive land cover changes. This knowledge can guide strategies, pinpointing regions where reforestation and forest protection in the Tropics would be most effective in storing additional C in soils while highlighting areas where soil mineralogy might constrain these efforts.

Continuing from land conversion effects on SOC dynamics, chapter 5 (study III) focused on the impact of lateral soil fluxes on SOC stocks and turnover in sloping and geochemically diverse cropland systems. Current biogeochemical understanding, largely drawn from data of high input cropping systems in the Global North, tends to overlook the complexities of soil erosion and deposition in smallholder-managed tropical landscapes. The traditional depiction of eroding hillflanks and accumulating valleys does not uniformly apply in these settings due to perturbed C inputs and lateral soil fluxes resulting from intricate land use patterns. This study shows that cropland SOC stocks and persistence do not consistently adhere to conventional topography-driven patterns caused by soil redistribution. Soils with high SOC stocks and rapid turnover, particularly in subsoil, are mainly, but not exclusively, found in valley positions, while soils with lower SOC stocks and slower turnover prevail on slopes. The heterogeneous land use by tropical subsistence farmers creates complex hydro-sedimentological settings that can either facilitate or impede soil redistribution on slopes and in valleys. The recent accumulation of eroded C in valleys presents a potentially substantial but labile C sink. Simultaneously, soil degradation initiates a disruption of the C cycle on many, though not all, hillslopes in the region. This new understanding, which states that the pronounced variability in soil physicochemical and topographical properties does not strongly affect SOC stocks and turnover, suggests that farm management practices aimed at retaining soil stability and limiting erosional soil losses are of even greater importance in deeply weathered tropical soils than in other farmed soils worldwide. It thus seems likely that, due to the rapid erosion of soil and the limited potential for replenishing C losses with new plant inputs, depositional sites along slopes and foot-slopes will receive increasingly C-depleted material, which will lead to the collapse of already low and unprotected SOC stocks. Therefore, the rapidly eroding and not yet fully consolidated tropical cropland systems appear to act as a potential C source at the regional and slope scale investigated here.

6.2 The link between geochemistry, land use and topography in driving carbon dynamics

6.2.1 The diverse nature of tropical soils – Setting the stage for mineral carbon stabilization

Historically, tropical soils were regarded as the most infertile soils worldwide despite their highly variable geochemistry and fertility (Sanchez and Logan, 1992). However, this oversimplified depiction has already been challenged by earlier studies (Eswaran *et al.*, 1992; Greenland *et al.*, 1992; Mokwunye and Hammond, 1992) and further disproved by recent studies (Bukombe *et al.*, 2022; Bukombe *et al.*, 2021; Kidinda *et al.*, 2023; Kidinda *et al.*, 2022). These studies demonstrate, similar to our studies, that tropical soils exhibit considerable variability in their geochemical behavior (Figures 3.4, 3.6, 4.3 and 5.4; Table 4.3) and impact on SOC dynamics (Figures 3.5, 4.5, 4.6 and C.1; Tables 3.2 and 3.3), given their extensive range of geotectonic and pedogenetic settings (Figures 3.2, 4.2 and 3.5.2). Our study indicates that despite prolonged chemical weathering (Table A.3), the mineralogical composition of the soil parent material has left an identifiable physico-chemical footprint in the investigated soils (Figures 3.4 and D.1; Table 4.3). The elemental composition of the soil parent material exhibits great variation, which is also reflected in distinct differences in rock-derived nutrient content across soils from different geochemical test regions (Doetterl *et al.*, 2021b). Thus, weathering-related enrichment and depletion processes of elements result in diverse soils, which are distinctly different in their geochemical properties opposed to homogeneous and nutrient-poor (Doetterl *et al.*, 2021b; Grau *et al.*, 2017). Consequently, the investigated soils exhibited variations in their mineral C stabilization potential, despite their overall endmember mineralogy (Figures 3.4, 3.6, 4.3 and 5.4; Tables A.3 and 4.3). This is corroborated by recent studies conducted at the same test sites, which demonstrate that microbial properties (Kidinda *et al.*, 2022) and respiration rates (Bukombe *et al.*, 2021) are also influenced by the inherited chemical soil properties of the parent material. Overall, this sets the geochemical stage providing specific prerequisites for mineral C stabilization against microbial decomposition.

6.2.2 Long-term mineral carbon stabilization is limited in deeply weathered tropical soils

Organomineral complexes, especially those associated with amorphous minerals, are considered the dominant mineral C stabilization mechanism in tropical soils (Coward *et al.*, 2017; Fromm *et al.*, 2021; Heckman *et al.*, 2009). They are also considered an intermediate step crucial for long-term C stabilization (Heckman *et al.*, 2018). However, in our study on SOC stocks and turnover in deeply weathered soils both under forest and cropland, pyrophosphate-extractable pedogenic oxides were far more important than the more commonly assessed oxalate-extractable pedogenic oxides (Figures 3.4 and 4.5; Tables 3.2, 3.3 and B.2). Pyrophosphate-extractable oxides dominated also in subsoils, even though, there, more secondary (clay) minerals as well as more amorphous and crystalline oxy-hydroxides were available as partners for complexation of C inputs (Figure 5.4; Table B.2). In addition, for soil Δ^{14}C, under both land uses, soil fertility parameters were generally more important than the included proxies for mineral C stabilization potential (Figure 4.6) and soil Δ^{14}C indicated comparably young soil C ages (Figures 3.5, 4.4 and 5.7). Thus, our findings raise the question in how far soil C is stabilized effectively in the investigated forest and cropland soils against microbial decomposition. Pyrophosphate-extractable oxides are usually interpreted as only weak forms for stabilizing C against microbial decomposition (Heckman *et al.*, 2018; Lawrence *et al.*, 2015; Paul *et al.*, 2008), and represent still an easily available pool of C for microorganisms (Bukombe *et al.*, 2021; Heckman *et al.*, 2009). In contrast, oxalate-extractable oxides are interpreted as a strong form of mineral-related

C stabilization (Coward *et al.*, 2018) reducing C turnover (Heckman *et al.*, 2018; Heckman and Rasmussen, 2018; Kramer *et al.*, 2012) and stabilizing C long-term. Similarly, even though clay content varies from 14 % to 84 % across our study area (Doetterl *et al.*, 2021b)(Figure 5.4; Table 4.3), it is not an important predictor in our regression models (Figures 4.5 and 4.6; Table B.2). The dominance of low reactivity endmember clays such as kaolinite may explain the low explanatory power of clay content in our study (Fromm *et al.*, 2024b), which is in contrast to other studies on tropical soils where increasing clay content resulted in higher SOC stocks (Quesada *et al.*, 2020). However, an in-depth analysis of clay phases is beyond the scope of this study and subject of future work. We argue that the dominance of pyrophosphate-extractable organo – mineral complexes as a form of organo – mineral interaction in the investigated tropical soils is evidence for the notion that deeply weathered soils do not provide efficient mineral C stabilization given the dominance of endmember minerals (Fromm *et al.*, 2024b; Ito and Wagai, 2017). This interpretation is in agreement with studies on tropical soils that show minor relationships between short-range-ordered minerals and C accumulation (Coward *et al.*, 2017; Wagai *et al.*, 2013). Non-sequential extraction schemes that focus on using oxalate only might therefore integrate oxides that are bond in organo – mineral complexes (pyrophosphate-extractable) and amorphous oxides (oxalate-extractable) into the same pool and lead of a misinterpretation of the potential resilience of mineral stabilized C in old tropical soils (Khomo *et al.*, 2017; Rasmussen *et al.*, 2018). However, while pyrophosphate-extractable organo – mineral complexes dominate as a reservoir and represent an easily available C source, amorphous and crystalline (DCB-extractable) pedogenic oxides can still play a vital role in the mineral stabilization of C indirectly by supporting the formation of stable microaggregates, which protect C via spatial separation to decomposers and occlusion (Figure 3.4; Table A.2) (Denef *et al.*, 2007; Martinez and Souza, 2020; Oades, 1988). The role of minerals to stabilize C might therefore be more indirect (through occlusion of C) than direct (through forming energetic barriers or co-precipitation) in tropical soils compared to younger temperate soils.

6.2.3 The modifying role of land use – Differences in the effect of geochemical controls on carbon dynamics

The impact of soil geochemical properties on SOC stocks and stabilization varies across land use. In forests, changes in the quantity of pedogenic oxides and clay favored microaggregation (Figure 3.4) thus providing additional protection of C against microbial decomposition (Martinez and Souza, 2020; Quesada *et al.*, 2020), which eventually led to significant differences in SOC stocks across geochemical regions (Figure 3.5). Conversely, the influence of geochemical controls was considerably less pronounced under cropland and was insufficient to induce significant changes in SOC stocks (Figures 4.4 and B.2). This observation is may be explained by previous studies which have demonstrated that agricultural management practices can reduce the specific surface area of soil minerals, thereby reducing their capacity for sorptive C processes (Ozlu and Arriaga, 2021; Veldkamp *et al.*, 2020; Wang *et al.*, 2019c; Wang *et al.*, 2019d). Another potential reason for the differing impact of soil geochemistry on SOC stocks is the enhanced protection of soil aggregates against physical disruption under forest compared to cropland. The thick litter and organic soil layers under forest minimize the kinetic energy of rain drops thus reducing the disruption of soil aggregates. Conversely, the seasonally varying crop cover, in conjunction with tillage practices, even those conducted manually with hoes, facilitates the disintegration of soil aggregates, thereby leaving previously occluded SOC unprotected against microbial decomposition (Bailey *et al.*, 2019; Denef *et al.*, 2004; Zotarelli *et al.*, 2005). It should be noted that differences in soil environmental conditions across land uses due to the impact of land cover on soil temperature and moisture strongly impact SOC dynamics (Hao *et al.*, 2016; Sheng *et al.*, 2010). This demonstrates that the quantity of proxies for mineral C stabilization, such as pedogenic oxides and clay, is not necessarily indicative of more effective stabilization and prone to land use effects and possibly modified by environmental controls.

In addition, more fertile soils are found in cropland (Figure 4.3). This indicates that farmers have a purposeful selection of agricultural sites towards more fertile soils, whereas less fertile soils remain forested. This is supported by studies conducted in the same region, which demonstrate that farmers select soils based on their indigenous knowledge about soil fertility (soil color, soil depth) (Kayani *et al.*, 2021). However, the intricate situation of insecure land ownership and armed conflicts, particularly in the DRC, also dictates where agriculture is possible and land conversion takes place, stands in stark contrast to land selection according to soil fertility parameters (Baumann and Kuemmerle, 2016; George *et al.*, 2021; Landholm *et al.*, 2019). Nonetheless, land use has a pronounced impact on soil microbial properties, as evidenced by a recent study conducted on the same soil samples (Kidinda *et al.*, 2023). This study demonstrated that land conversion from forest to cropland causes shifts in microbial communities driven by soil fertility, which affects SOC cycling (Kidinda *et al.*, 2023). Soil samples from less fertile forest soils exhibited fungal dominance, whereas microbial communities from more fertile cropland soils were dominated by bacteria (Kidinda *et al.*, 2023) ultimately affecting C turnover. Consequently, the influence of soil fertility proxies on microbial C mass is likely to offset the impact of mineral stabilization proxies on SOC stocks during land conversion. This could provide an additional explanation for the limited effect of mineral C stabilization under cropland compared to forest soils in our test region.

6.2.4 The unexpected effect of topography and the interplay with land use

As tropical soils still inherit their geochemical properties from their parent material despite long-lasting chemical weathering, the erosional removal of weathered topsoil layers should amplify those differences by excavating less weathered subsoil and saprolite layers with different mineral properties thus changing conditions for long-term mineral C potential (Doetterl *et al.*, 2016; Roering *et al.*, 2023; Slessarev *et al.*, 2022). However, our studies indicate that the impact of topography on soil geochemical properties and SOC dynamics is less pronounced than anticipated. This is contrary to findings that have identified topography in tropical landscapes as a key control under both forest and cropland (Chadwick and Asner, 2016; Chaplot *et al.*, 2005; Dialynas *et al.*, 2016a; Dialynas *et al.*, 2016b; Karamage *et al.*, 2016a; Karamage *et al.*, 2016b; Molina *et al.*, 2019; Turkelboom *et al.*, 2008). Instead, the impact of topography on SOC dynamics is dependent on the specific land use.

In the forest environment, lateral soil erosion fluxes are not evident due to the combined effect of a thick litter and organic layer (Figure 3.5) (Bukombe *et al.*, 2022) and canopy interception (Brandt, 1988; Li *et al.*, 2019; Rosalem *et al.*, 2019; Wilken *et al.*, 2021), which protect the soil from erosional detachment. Consequently, neither the soil geochemical properties nor SOC dynamics are influenced by topography (Figures 3.4 and 3.5; Table A.2). Instead, topography exerts an indirect influence on SOC stocks, soil Δ^{14}C and soil geochemistry, whereby well-drained landscape positions (plateaus and slopes) are separated from positions with high water saturation (footslopes and valleys) due to alluvial and riverine dynamics (Figures A.1 and A.2). Consequently, the corresponding changes in hydrological patterns lead to fluctuating redox potential, as a result of alternating dry and wet seasons in our test region (Barcellos *et al.*, 2018; Doetterl *et al.*, 2021b; Liptzin *et al.*, 2011). In combination with high Fe contents, this may promote the formation of stable aggregates (Giannetta *et al.*, 2022; Thompson *et al.*, 2006; Tong *et al.*, 2016; Waggoner *et al.*, 2017). The presence and enrichment of these stable Fe and Al-rich concretions and aggregations have been observed and identified in many tropical soils as major physico-chemical soil features (Cooper *et al.*, 2005; Martinez and Souza, 2020; Zotarelli *et al.*, 2005). These features influence biological processes and C turnover (Martinez and Souza, 2020). However, alterations in the soil redox potential can also result in the destabilization of C by the reductive dissolution of iron-bearing minerals (Bailey *et al.*, 2019; Barcellos *et al.*, 2018; Song *et al.*, 2022). In addition, soil hydrological conditions, like soil water flow along slopes and varying groundwater levels at valley bottoms, drive microbial activity thus C turnover (Cook and Orchard, 2008; Dialynas *et al.*, 2016b). Consequently, the topographical effects on SOC dynamics under erosion-free forests are constrained to alterations in hydrological soil conditions, which can result in pronounced differences in SOC stocks and pedogenic oxide content across non-valley and valley positions (Figures A.1 and A.2; Appendix A.1).

In contrast, topography induced lateral soil fluxes under cropland due to the combination of steep terrain, tillage practices, high rainfall intensity and varying crop cover (Karamage *et al.*, 2016b; Panagos *et al.*, 2017; Xiong *et al.*, 2019; Ziegler and Sutherland, 2009). Similarly to the forest sites, the impact of topography on soil geochemical properties is less pronounced than anticipated, as evidenced by the minor differences in soil properties across non-eroding, eroding and depositional cropland positions (Figure 5.6). It is surprising that these erosion-induced soil fluxes do not result in a consistent spatial and vertical redistribution of SOC stocks with different quantities and persistence across the landscape. This raises the question of the extent to which the conceptual model – viewing geomorphic transects as "soil-hillslope conveyor belts" with the creation of topsoils at eroding sites, which are C-depleted but show simultaneously dynamic C replacement, and deposition in valleys (Román-Sánchez *et al.*, 2019a; Román-Sánchez *et al.*, 2019b) – is applicable to deeply weathered tropical cropland systems. At eroding sites SOC-depleted subsoils are mixted into topsoil leading to a decrease in topsoil SOC stocks. If topsoil material is continually removed laterally, the C input from plants and the decomposition by microorganisms reach a completely different equilibrium compared to the pre-erosional state. Exposed subsoils can provide C-unsaturated reactive minerals, which further could support the stabilization of fresh C input. This process is generally understood as dynamic C replacement (Berhe *et al.*, 2012; Dialynas *et al.*, 2016a; Dialynas *et al.*, 2016b; Harden *et al.*, 1999; Kirkels *et al.*, 2014; Stallard, 1998). However, the exposure of subsoil on eroding hill slopes does not provide a more fertile or reactive matrix in our studies (Figure 5.6) to replenish diminishing soil fertility or sorb new plant C input as observed in eroding temperate soils (Chadwick and Asner, 2016; Coward *et al.*, 2017; Price *et al.*, 2005). Given the limited long-term stabilization observed in the investigated soils and the dominance of SOC with fast turnover in both the topsoil and subsoil (Figures 5.5 and 5.7), it is unlikely that readily available energy sources for microbes provided by fresh C input will accelerate the decomposition of older and formerly stabilized SOC, which represents a small fraction anyway. It can be argued that deeply weathered and low reactive soils will not be significantly affected by C priming (Blagodatskaya and Kuzyakov, 2008; Chen *et al.*, 2019; Fanin *et al.*, 2020; Hicks *et al.*, 2019; Kuzyakov and Blagodatskaya, 2015; Nottingham *et al.*, 2015). In general, a significant proportion of the eroded material is deposited in alluvial and colluvial settings (Wang *et al.*, 2015), which has the potential to result in deep burial of SOC. This is dependent on the type of deposited soil material (C-rich or C-depleted soil from hill flanks or the stability of organo – mineral complexes) (Nijs and Cammeraat, 2020), the speed of soil burial (faster burial contributing to greater conservation) (Zhao *et al.*, 2022) and the environmental conditions (water saturation and oxygen limitations) that may reduce or promote microbial decomposition to conserve labile SOC. Although our data indicates the presence of deposition at footslopes, this is not a consistent trend (Figures 5.5 and 5.7). Given that the low soil reactivity only results in small and labile SOC stocks on hillflanks, depositional footslopes will only receive C-depleted material that is unable to stabilize SOC in an efficient way. Consequently, the effectiveness of these depositional sites in conserving SOC over the long term (Oost *et al.*, 2007; VandenBygaart *et al.*, 2015) must be questioned.

As such, the conversion of forest to cropland, which results in erosion, does not lead to topography-driven patterns of SOC stocks and persistence (Figure 5.3), which is in stark contrast to what is observed in temperate cropland systems (Doetterl *et al.*, 2016; Gregorich *et al.*, 1998; Nadeu *et al.*, 2015; Oost *et al.*, 2005; Oost *et al.*, 2007; Quinton *et al.*, 2010; Wang *et al.*, 2017).

6.3 Are deeply weathered tropical soils C sources? – The role of fossil organic carbon and soil redistribution

This PhD thesis allows for a careful evaluation of whether low reactive soils function as a C sink or source. In the case of soils from undisturbed forest sites, it can be assumed that the SOC cycle is in equilibrium with regard to C input and respiratory C loss (Lal, 2005). However, it should be noted that geogenic fossil organic carbon (FOC) (Section 3.5.2) from terrestrial sediments also participates in the SOC cycle and must be considered (Hemingway *et al.*, 2018; Kalks *et al.*, 2021; Stoner *et al.*, 2023). It can be argued that the additional weathering-related release of FOC from the black shale of the mixed sedimentary region (Table 3.1), which is accessible to microbes and contributes to respiratory C losses into the atmosphere, act as a C source (Bukombe *et al.*, 2021; Hemingway *et al.*, 2018). However, microbial respiration discriminates against FOC in the presence of more available C sources (Bukombe *et al.*, 2021). Furthermore, C losses from such non-renewable C fractions occur on geological timescales, which are much longer than the average residence time of biogenic C fractions (Hemingway *et al.*, 2018). While FOC contributes to respiratory losses under forest, we assume that these are not significant enough to function as a C source.

Our study on eroding cropland, on the other hand, suggests a highly dynamic landscape with significant lateral soil fluxes that shows limited potential for long-term C stabilization (Chapter 5). This results in the fast replacement of SOC at eroding slope positions (Figure 5.5), with only a small amount of C required to compensate for C losses, given that SOC stocks are typically low due to advanced weathering (Figure 5.7). This limited mineral reactivity prevents the accumulation of higher SOC stocks with enhanced persistence in colluvial and alluvial soils (Figures 5.5 and 5.7). Furthermore, supplementary data (Figures D.3 and D.4) indicates that eroded soil material can be either translocated over a short distance and deposited within the same field parcel or transported over longer distances across the entire slope, eventually accumulating in more distal depositional sites. Consequently, footslopes and valleys may receive varying amounts of eroded soil material, depending on the specific land use patterns. As such, higher SOC stocks depend on the continuous deposition of eroded C-rich material in the absence of mineral C stabilization. A decline in the delivery of C-rich material, whether due to a loss of soil productivity or an interruption caused by field boundaries or tillage banks (Figure 5.3), probably result in a collapse of labile SOC stocks with low persistence. For example, the presence of low subsoil SOC stocks in depositional sites (Figures D.3 and D.4) may be indicative of either a reduction in deposition and the microbial decomposition of the labile C sources or the deposition of material that has already undergone a decline in C content due to degraded soils. It can be concluded that rapidly eroding and not yet fully consolidated tropical cropland systems appear to act as a C source, at least at the regional and slope scale investigated here. This highlights the vulnerability of tropical SOC stocks in sloping tropical farmland.

6.4 Beyond the case study – How do soils from other tropical regions compare?

6.4.1 What do other studies say about sorptive carbon processes in tropical soils?

It has been demonstrated that sorptive processes on reactive mineral surfaces play a pivotal role in soil C stabilization across a diverse range of ecosystems and climatic zones (Kleber *et al.*, 2021; Kramer and Chadwick, 2018; Mikutta *et al.*, 2019; Possinger *et al.*, 2020). The results demonstrate that the general SOC stabilization mechanisms are comparable to those observed in temperate soils. However, mineral C stabilization stands out in deeply weathered tropical soils, which is a consequence of the overall end-member mineralogy and low potential for C sorption.

Studies focusing on tropical soils from Puerto Rico, Ghana, and Sub-Saharan Africa (SSA) link rapid C turnover to limited mineral soil reactivity (Chiti *et al.*, 2010; Fromm *et al.*, 2024a; Hall *et al.*, 2015; Marín-Spiotta *et al.*, 2008). Interestingly, SOC stocks of tropical soils from Indonesia, Malaysian Borneo the Solomon Islands, Thailand, Cameroon, Ghana, Tanzania and SSA in general are highly correlated with pyrophosphate- and oxalate-extractable pedogenic oxides but not with the fine fraction of the soil (clay+silt) besides covering a wide degree of weathering stages including kaolinitic soils (Ashida *et al.*, 2021; Bruun *et al.*, 2010; Fromm *et al.*, 2021). These findings of rapid C cycling and the importance of pedogenic oxides in controlling SOC stocks in low reactive soil are in line with our conclusions. Contrasting findings arise from studies investigating highly weathered soils across the Amazon Basin. Here, simple variations in the quantity of low-activity 1 : 1 clay are driving significant differences in SOC stocks (Quesada *et al.*, 2020), which is not the case in our studies showing SOC stocks being unresponsive to pronounced clay content variations across test regions. However, the study shows that most of the SOC is stored in stable clay aggregates suggesting an additional level of protection against microbial decomposition within microaggregates (Quesada *et al.*, 2020) and pseudosand structures (Martinez and Souza, 2020). This finding supports our previous conclusions that the concentration of pedogenic oxides, in conjunction with clay, is a key factor in the amount of soil SOC associated with microaggregates in forest soils. Studies conducted in the Brazilian Tropics, which encompass a wide range of soil mineralogy and texture, indicate that Oxisoils may act as a significant C sink if C input could be more efficiently transferred to subsoils, which are abundant in oxalate- and DCB-extractable oxides (Souza *et al.*, 2018). However, our data do not support the existence of an effective C sink function of subsoils in our test region, as the excavation of C-depleted subsoil did not result in a greater degree of C stabilization in the investigated cropland soils. Furthermore, our data indicate a decoupling between topsoil and subsoil cycling, as evidenced by the independence of depth-trends in SOC stocks and soil Δ^{14}C from high C input (forest) or low C input (cropland) to topsoils. Furthermore, sorption experiments conducted on tropical soils have demonstrated that the mineral reactivity of the fine fraction did not differ between topsoils and subsoils (Jagadamma *et al.*, 2014). This corroborates our findings that the mineral C stabilization potential remains unaffected by lateral soil fluxes, as evidenced by the lack of change in mineral reactivity with soil depth.

Global models indicate that croplands have a large potential to sequester C by implementing better management practices (e.g. tillage reduction, applying fertilizer, return crop residues after harvest) (Fujisaki *et al.*, 2018; Ren *et al.*, 2020). Especially cropland soils from the Tropics seem to be substantially below their C sequestration potential (Abramoff *et al.*, 2021) due to climatic limitations (e.g. higher temperatures thus increased microbial C respiration) and management practices (e.g. removal of crop residues) (Georgiou *et al.*, 2022). Thus, tropical soils are to be expected to store more C if management practices are improved (Fujisaki *et al.*, 2018). However, the data obtained from our studies do not support this conclusion, as the low-reactive soils investigated have been found to have limited long-term potential for the stabilization of C input and to exhibit a high turnover rate. This highlights the difficulty in extrapolating the mineral C stabilization potential represented by C-saturation levels based solely on linear variations in the quantity of clay and silt fraction without taking the soil geochemical heterogeneity of tropical soils into account. For example, tropical Andosols exhibit a distinct mineralogy and are capable of storing considerably more SOC over the long term (Bruun *et al.*, 2010; Grant *et al.*, 2022; Marin-Spiotta *et al.*, 2011) than the investigated deeply weathered soils.

6.4.2 Does the impact of land conversion show similar patterns across tropical regions?

As previously stated, our findings indicate that the SOC stocks of deeply weathered tropical soils are unresponsive to changes in C input resulting from land conversion. This is consistent with studies on tropical SOC stocks in Papua New Guinea, which also demonstrate no impact of different land use management practices (Kukla *et al.*, 2019). Furthermore, the addition of twice the quantity of litter to tropical forests had no effect on the SOC stock (Sayer *et al.*, 2019). However, similar studies on litter manipulation experiments in highly weathered tropical forest soils have demonstrated an increase in organo – mineral association with increasing litter input (Cusack *et al.*, 2018). Other studies focusing on highly weathered soils of Tanzania suggest that under specific mineralogical combinations (low clay content but high Fe-oxide content), reactive mineral surfaces become more available by mechanical soil cultivation that even leads to an increase in mineral C stabilization (Kirsten *et al.*, 2019; Kirsten *et al.*, 2021b). Again, a global meta-analysis of data from 39 different tropical countries clearly indicates that the conversion of primary forest into cropland results in significant SOC losses (Don *et al.*, 2011). Consequently, the response of tropical soils to land conversion varies even across deeply weathered soils in tropical Africa.

6.4.3 What is the response of soils to erosional disturbances in other tropical regions?

Studies conducted in the same test region have indicated the release of old, previously stable but biolabile SOC into the modern C cycle following deforestation on sloping cropland (Drake *et al.*, 2019). This supports our interpretation that even mineral-associated SOC remains accessible to microbes. Such erosional mass fluxes in the humid Tropics and their spatial-temporal concentration are heavily dependent on land use pattern and crop rotation (Labrière *et al.*, 2015; Winowiecki *et al.*, 2021). This supports our assumption that the intricate land use patchiness resulting from smallholder subsistence farming may explain the observed inconsistent trend of topography-driven SOC stock patterns. Furthermore, studies conducted in northern Laos (Chaplot *et al.*, 2009) and southern Brazil (Vanacker *et al.*, 2019) have demonstrated the occurrence of pronounced soil rejuvenation effects and an increase in SOC stocks along cropland slopes. In contrast, our data shows such a variability in soil geochemistry and SOC stocks both on eroding slopes and stable plateau positions suggesting that lateral soil fluxes do not impact the conditions for mineral C stabilization on sloping landscapes covered by thick saprolite layers. It is noteworthy that studies from old tropical landscapes across the Hawaiian Islands (Vitousek *et* *al.*, 2003) and southern Peruvian Amazon (Chadwick and Asner, 2016) demonstrate increased rock-derived nutrient availability along slopes dissected by fluvial erosion, even in primary and old-growth forest. This is contrary to the findings of our study, which demonstrated that soil erosion has no obvious effect on soil fertility parameters regarding their pronounced variability along slopes in the investigated forest sites. This demonstrates that the response of tropical soils to erosional soil fluxes varies considerably, thereby underscoring the necessity to refrain from the ad hoc transfer of knowledge gained from other tropical regions to soils from the Afrotropics.

6.5 Conclusions and future perspectives – What have we learned and what´s next?

> *"Generalizations about tropical soils are unlikely to have wide applicability, because of the diversity of soils and the factors affecting organic matter dynamics. (...). The enormous accumulation of analytical data about tropical soils shows clearly that the quantities of organic matter in tropical soils cover a wide range."* – (Greenland *et al.*, 1992)

This thesis aimed to assess the interacting role of soil geochemistry, topography and land use as drivers for SOC stocks and soil Δ^{14}C in deeply weathered soils of the hitherto little investigated Congo and Nile Basin in the East African Rift Valley system. It is anticipated that tropical Africa will experience significant alterations to both soil biogeochemical processes and SOC cycling, with unknown consequences, given that forested landscapes are currently facing unprecedented levels of land conversion and soil degradation (Doetterl *et al.*, 2021b; UNESCO and WHC, 2010). Despite decades of recognition of their importance as a critical component in the terrestrial C cycle (Doetterl *et al.*, 2021b; Juo and Franzluebbers, 2003; Schimel *et al.*, 2015), tropical soils remain highly understudied. The majority of today's process understanding regarding biogeochemical cycling across pedo-geomorphological gradients stems from temperate soil systems. Consequently, this thesis contributes to the filling of research gaps in our understanding of the coupling between soil biogeochemistry and the responses of SOC dynamics in the context of land use change and topography-driven lateral soil fluxes in tropical (agro-)ecosystems. The findings presented here enable us to address the questions posed in the general introduction to this thesis:

How does soil parent mineralogy and its weathering stage shape the soil geochemical conditions driving SOC dynamics and how is this controlled or modified by the interaction between soil erosion and land conversion?

This research confirmed the initial hypothesis (see H1.1) that soil geochemical properties are driven by soil parent material mineralogy, even in deeply weathered tropical soils. Furthermore, the distribution and quantity of minerals depend on the initial mineralogical composition and texture of the bedrock. In accordance with the formulated hypothesis, the content of proxies for mineral C stabilization (pedogenic oxides, clay) and soil fertility (rock-derived nutrients, exchangeable bases, bray-P) varied significantly as a function of soil parent material composition (Figures 3.4 and 3.6), despite pronounced leaching processes (Table A.3). Consequently, the soil parent material leaves a long-lasting and identifiable footprint in tropical soils, which provides the geochemical stage on which mineral-related C stabilization mechanisms take place.

The thesis falsified the second part of the first hypothesis (see H1.2), namely that soil disturbance will modify soil geochemistry thus mineral-mediated stabilization of C. Although the test region exhibits steep terrain, lateral soil fluxes do not significantly impact geochemical soil properties across topographical positions under both land uses (Figures 3.4 and 5.6). The results indicated that no recent natural or anthropogenic-induced erosional processes had occurred at the investigated forest sites. Although lateral soil fluxes along slopes cannot be excluded over longer time scales (e.g. 100 to 1,000 years), the dense vegetation cover, combined with thick litter and organic layers, protects the soil from erosional detachment. However, the protective soil cover is absent in sloping cropland thus shows signs of lateral soil fluxes (Figures 5.3, 5.5 and 5.7). However, the geochemistry of the soil across the landscape positions remains largely unaltered, as the less weathered layers in closer proximity to the parent material are still covered by thick saprolite layers.

This study focused on well-developed soils where the soil parent material could not be reached even by digging soil pits with a depth of more than 3 m on steep slopes. Therefore, an overall soil and saprolite thickness of several decameters was assumed. Further research should therefore investigate the extent to which the geochemical properties of shallower cropland soils, where the parent material is already in contact with the weathering front, are affected by lateral soil fluxes. This will assist in determining whether erosional soil replenishment is either constrained by the presence of thick overlying saprolite layers or limited by other factors, such as erosion rates exceeding soil production rates (Roering *et al.*, 2023). Consequently, soil coring to the unweathered bedrock is essential to establish weathering profiles and calculate soil weathering rates (Brosens *et al.*, 2020; Burke *et al.*, 2009; Yoo and Mudd, 2008). Erosion rates may be assessed by measuring $^{239+240}$Pu fallout nuclide activity and inventory analysis, which have already been established in the test region (Wilken *et al.*, 2021). The data will help assess if weathering rates are outpaced by erosion rates, thus limiting the weathering-release of more reactive secondary minerals into the soil column. In the next step, these findings could be linked to weathering profiles of connected depositional sites that receive material from such shallower soils. This would allow for an investigation of whether potential changes in geochemical soil properties and mineral C stabilization along erosional sites, where less weathered subsoil material may already be in contact with the weathering front, are also reflected in colluvial and alluvial settings.

The data may also be used to evaluate the application of rock powder to the investigated soils for the purpose of improving C sequestration (Goll *et al.*, 2021) by providing sorptive secondary minerals, which in turn increases microaggregation and mineral C stabilization (Buss *et al.*, 2024). Furthermore, the rock powder application is regarded as a promising tool for improving soil fertility and crop yield, thus increasing C input, especially in tropical soils (Swoboda *et al.*, 2022). With regard to the limited impact of land use on the investiaged deeply weathered soils (Figures 4.3 and 4.4), the potential for positive effects of rock powder application may be constrained to the accumulation of labile SOC pools without long-term SOC stabilization. However, if the capacity of shallower soils to provide more reactive minerals is constrained due to soil erosion rates exceeding weathering rates, the enhanced weathering as a consequence of powdered rock application could be an effective instrument to enhance the mineral C stabilization potential in the test region. It is paramount that the C emissions related to the production and transportation of rock powder should not exceed the potential C sequestration in the amended soil to act as an effective C mitigation strategy. This justifies further investigation, which must also account for the interaction effects between microbial communities and C quality in order to promote conditions for C storage and prevent respiratory C losses to the atmosphere as a response to rock powder application (Kidinda *et al.*, 2023).

How does soil geochemistry interact with the effect of soil erosion and land conversion on SOC stocks and turnover?

The second hypothesis (see H2.1), specifying that SOC stocks and turnover will be driven by geochemical soil properties as a function of parent material composition, was confirmed. Nevertheless, the patterns of SOC emerging from geochemical properties differ across land use. Soils from the mafic test region exhibited higher contents of pedogenic oxides and clay compared to soils from the felsic and mixed sedimentary test sites under forest. This was found to be correlated with both higher microaggregate-associated C and total SOC stocks, which link two of the most important mineral-related C stabilization mechanisms against microbial decomposition in soil with geochemical variability retained from the parent material. In contrast, cropland SOC stocks are comparable across geochemical test sites (Figures 5.7 and B.2) despite distinct differences in soil properties (Figure 5.4. Similar, when compared across geochemical test sites, including both land uses, the SOC stocks are comparable between forest and cropland sites (Figures 4.4 and B.2). Consequently, the tropical soils under investigation do not possess sufficient reactive minerals to significantly increase SOC stocks in high-input (tropical forest) systems in comparison to low-input (cropland) systems.

This falsifies the second part of the second hypothesis (see H2.2), which states that geochemical controls will be modified by soil erosion and land conversion since they change the geochemical and environmental conditions under which mineral C stabilization takes place. This is because the investigated soils already exceed their capacity to store SOC, regardless of the amount of C input. This limited potential to stabilize C also explains that the SOC stocks in cropland soils of eroded topsoils are similar to those in non-eroding landscape positions, and that the deposition of eroded topsoil material at footslopes only slightly increases SOC stocks. However, the extent to which this weak effect of soil erosion on SOC stocks results from low reactive soils or from uncertain estimates of true soil loss remains unclear.

Consequently, further research should concentrate on capturing small-scale lateral soil fluxes at the slope scale with the aim of separating the effects of soil redistribution and soil geochemistry on SOC dynamics in cropland with complex and small-scale land use patterns. The deployment and subsequent backtracking of passive radio-frequency identification tracers (RFIDs) in conjunction with high-resolution topography measurements conducted via low-flying UAV-Sfm surveys could facilitate the identification of intricate patterns of short-term soil fluxes at the finest spatial scales (Fiener *et al.*, 2018; López-Vicente *et al.*, 2023).

In order to gain a more mechanistic process understanding of how mineral C stabilization works in the studied soils and how different soil C fractions respond to gradients in land use, topography and geochemistry, the biogeochemical quality of dissolved organic carbon (DOC) (using FT-ICR MS analysis) (Drake *et al.*, 2019) and its turnover (soil Δ^{14}C) of each soil C fraction should be analyzed. This is important because microaggregates in deeply weathered tropical soils are driven more by abiotic than biological processes compared to temperate soils (Cooper *et al.*, 2005; Denef and Six, 2005; Denef *et al.*, 2007; Martinez and Souza, 2020; Zotarelli *et al.*, 2005), which affects how mineral C stabilization in each fraction works. For example, in our study microaggregates provided additional protection to already mineral-complexed C, which is a different processes as the occlusion of coarse particulate organic matter (cPOM) often observed in temperate soils (Denef and Six, 2005; Denef and Six, 2006). Therefore, the link between functional SOC pools and stabilization mechanisms (King *et al.*, 2019; Poeplau *et al.*, 2013; Stewart *et al.*, 2008) and their response to land use change and erosion may be different in deeply weathered tropical soils compared to temperate soils. This should be combined with qualitative and quantitative analysis of the clay mineralogy and the specific surface area of sorptive minerals to track changes in mineral C stabilization in each soil fraction and relate them to the environmental gradients studied.

6.6 Final remarks

This work elucidates the role of soil parent material and geochemistry in controlling SOC dynamics in rapidly changing tropical (agro-)ecosystems. It aims to reduce uncertainties in our understanding of the terrestrial biogeochemical processes and to raise awareness that tropical soils react differently to disturbance compared to soils from the temperate zone. Thus, soil protection measurements and management practices need to adapt correspondingly and need to take local soil parent material compositions and their impact on SOC cycling into account to be most effective. This is mandatory for protecting soil resources and securing the future well-being of hundreds of millions of people and to constrain the loss of highly productive and biodiverse ecosystems providing many services of global importance (Koch *et al.*, 2013).

Furthermore, the Paris Agreement at the COP21 in 2015 brought soils as “negative emissions technologies” into focus (King *et al.*, 2018). Nevertheless, there is criticism from the soil science community that the “4 per 1000 promise” relies on a rather simplistic depiction of soil as a non-atmospheric C sink that can be easily monitored, modeled and managed (King *et al.*, 2018). However, this overlooks the actual complexity and diversity of soils. Returning to the initial knowledge gap, the majority of our current understanding is derived from temperate soils in the Northern Hemisphere, which introduces biases into contemporary biogeochemical models. In this context, the findings of this thesis indicate that the C sink function and the effectiveness of C sequestration are limited in deeply weathered soils. Therefore, in accordance with sustainability principles, it may be more beneficial to protect existing tropical SOC stocks than to attempt to restore them against the background of their limited mineralogical conditions, especially since tropical soils account for more than one-third of the world’s land area (Palm *et al.*, 2007) and, in comparison to temperate soils, may respond more rapidly to environmental changes (Fromm *et al.*, 2024b).

Bibliography

Abramoff, R. Z., Georgiou, K., Guenet, B., Torn, M. S., Huang, Y., Zhang, H., Feng, W., Jagadamma, S., Kaiser, K., Kothawala, D., Mayes, M. A., and Ciais, P. (2021). How much carbon can be added to soil by sorption? *Biogeochemistry* **152** (2-3), 127–142. DOI: 10.1007/s10533-021-00759-x.

Alcántara, V., Don, A., Vesterdal, L., Well, R., and Nieder, R. (2017). Stability of buried carbon in deep-ploughed forest and cropland soils – Implications for carbon stocks. *Sci. Rep.* **7**.(1). DOI: 10.1038/s41598-017-05501-y.

Allison, S. D. and Vitousek, P. M. (2005). Responses of extracellular enzymes to simple and complex nutrient inputs. *Soil Biol. Biochem.* **37** (5), 937–944. DOI: 10.1016/j.soilbio.2004.09.014.

Amundson, R. (2021). Factors of soil formation in the 21st century. *Geoderma* **391**. DOI: 10.1016/j.geoderma.2021.114960.

Amundson, R. (2001). The carbon budget in soils. *Annu. Rev. Earth Planet. Sci.* **29** (1), 535–562. DOI: 10.1146/annurev.earth.29.1.535.

Amundson, R., Berhe, A. A., Hopmans, J. W., Olson, C., Sztein, A. E., and Sparks, D. L. (2015). Soil and human security in the 21st century. *Science* **348**.(6235). DOI: 10.1126/science.1261071.

Angers, D., Arrouays, D., Cardinael, R., Chenu, C., Corbeels, M., Demenois, J., Farrell, M., Martin, M., Minasny, B., Recous, S., and Six, J. (2022). A well-established fact: Rapid mineralization of organic inputs is an important factor for soil carbon sequestration. *Eur. J. Soil Sci.* **73**.(3). DOI: 10.1111/ejss.13242.

Angst, G., Messinger, J., Greiner, M., Häusler, W., Hertel, D., Kirfel, K., Kögel-Knabner, I., Leuschner, C., Rethemeyer, J., and Mueller, C. W. (2018). Soil organic carbon stocks in topsoil and subsoil controlled by parent material, carbon input in the rhizosphere, and microbial-derived compounds. *Soil Biol. Biochem.* **122**, 19–30. DOI: 10.1016/j.soilbio.2018.03.026.

Angst, G., Mueller, K. E., Nierop, K. G., and Simpson, M. J. (2021). Plant- or microbial-derived? A review on the molecular composition of stabilized soil organic matter. *Soil Biol. Biochem.* **156**, 108189. DOI: 10.1016/j.soilbio.2021.108189.

Arachchige, P. S. P., Hettiarachchi, G. M., Rice, C. W., Dynes, J. J., Maurmann, L., Wang, J., Karunakaran, C., Kilcoyne, A. L. D., Attanayake, C. P., Amado, T. J. C., and Fiorin, J. E. (2018). Sub-micron level investigation reveals the inaccessibility of stabilized carbon in soil microaggregates. *Sci. Rep.* **8**.(1), 16810. DOI: 10.1038/s41598-018-34981-9.

Ashida, K., Watanabe, T., Urayama, S., Hartono, A., Kilasara, M., Ze, A. D. M., Nakao, A., Sugihara, S., and Funakawa, S. (2021). Quantitative relationship between organic carbon and geochemical properties in tropical surface and subsurface soils. *Biogeochemistry* **155** (1), 77–95. DOI: 10.1007/s10533-021-00813-8.

Assunção, S. A., Pereira, M. G., Rosset, J. S., Berbara, R. L. L., and García, A. C. (2019). Carbon input and the structural quality of soil organic matter as a function of agricultural management in a tropical climate region of Brazil. *Sci. Total Environ.* **658**, 901–911. DOI: 10.1016/j.scitotenv.2018.12.271.

Augusto, L., Achat, D. L., Jonard, M., Vidal, D., and Ringeval, B. (2017). Soil parent material — A major driver of plant nutrient limitations in terrestrial ecosystems. *Global Change Biol.* **23**.(9), 3808–3824. DOI: 10.1111/gcb.13691.

Baartman, J. E., Nunes, J. P., Masselink, R., Darboux, F., Bielders, C., Degré, A., Cantreul, V., Cerdan, O., Grangeon, T., Fiener, P., Wilken, F., Schindewolf, M., and Wainwright, J. (2020). What do models tell us about water and sediment connectivity? *Geomorphology* **367**, 107300. DOI: 10.1016/j.geomorph.2020.107300.

Bailey, K., Lloyd, F., Kearns, S., Stoppa, F., Eby, N., and Woolley, A. (2005). Melilitite at Fort Portal, Uganda: Another dimension to the carbonate volcanism. *Lithos* **85**.(1-4 SPEC. ISS.), 15–25. DOI: 10.1016/j.lithos.2005.03.019.

Bailey, V. L., Pries, C. H., and Lajtha, K. (2019). What do we know about soil carbon destabilization? *Environ. Res. Lett.* **14**.(8), 083004. DOI: 10.1088/1748-9326/ab2c11.

Barcellos, D., Cyle, K. T., and Thompson, A. (2018). Faster redox fluctuations can lead to higher iron reduction rates in humid forest soils. *Biogeochemistry* **137** (3), 367–378. DOI: 10.1007/s10533-018-0427-0.

Barker, D. S. and Nixon, P. H. (1989). High-Ca, low-alkali carbonatite volcanism at Fort Portal, Uganda. *Contrib. Mineral. Petrol.* **103**, 166–177.

Barré, P., Fernandez-Ugalde, O., Virto, I., Velde, B., and Chenu, C. (2014). Impact of phyllosilicate mineralogy on organic carbon stabilization in soils: incomplete knowledge and exciting prospects. *Geoderma* **235-236**. DOI: 10.1016/j.geoderma.2014.07.029.

Bascomb, C. L. (1968). Distribution of pyrophosphate-extractable iron and organic carbon in soils of various groups. *J. Soil Sci.* **19** (2), 251–268. DOI: 10.1111/j.1365-2389.1968.tb01538.x.

Basile-Doelsch, I., Balesdent, J., and Pellerin, S. (2020). Reviews and syntheses: The mechanisms underlying carbon storage in soil. *Biogeosciences* **17**.(21), 5223–5242. DOI: 10.5194/bg-17-5223-2020.

Baumann, M. and Kuemmerle, T. (2016). The impacts of warfare and armed conflict on land systems. *J. Land Use Sci.* **11** (6), 672–688. DOI: 10.1080/1747423X.2016.1241317.

Baumann, P., Lee, J., Frossard, E., Schönholzer, L. P., Diby, L., Hgaza, V. K., Kiba, D. I., Sila, A., Sheperd, K., and Six, J. (2021). Estimation of soil properties with mid-infrared soil spectroscopy across yam production landscapes in West Africa. *SOIL* **7**.(2), 717–731. DOI: 10.5194/soil-7-717-2021.

Beck, H. E., Wood, E. F., Mcvicar, T. R., Zambrano-Bigiarini, M., Alvarez-Garreton, C., Baez-Villanueva, O. M., Sheffield, J., and Karger, D. N. (2020). Bias Correction of Global High-Resolution Precipitation Climatologies Using Streamflow Observations from 9372 Catchments. *J. Clim.* **33**, 1299–1315. DOI: 10.1175/jcli-d-19-0332.s1.

Begill, N., Don, A., and Poeplau, C. (2023). No detectable upper limit of mineral-associated organic carbon in temperate agricultural soils. *Global Change Biol.* **29**.(16), 4662–4669. DOI: 10.1111/gcb.16804.

Beretta, A. N., Silbermann, A. V., Paladino, L., Torres, D., Bassahun, D., Musselli, R., and García-Lamohte, A. (2014). Soil texture analyses using a hydrometer: Modification of the Bouyoucos method. *Ciencia e investigación agraria* **41** (2), 25–26. DOI: 10.4067/S0718-16202014000200013.

Berhe, A. A. (2012). Decomposition of organic substrates at eroding vs. depositional landform positions. *Plant Soil* **350** (1-2), 261–280. DOI: 10.1007/s11104-011-0902-z.

Berhe, A. A., Harden, J. W., Torn, M. S., and Harte, J. (2008). Linking soil organic matter dynamics and erosion-induced terrestrial carbon sequestration at different landform positions. *J. Geophys. Res.: Biogeosci.* **113** (4). DOI: 10.1029/2008JG000751.

Berhe, A. A., Harden, J. W., Torn, M. S., Kleber, M., Burton, S. D., and Harte, J. (2012). Persistence of soil organic matter in eroding versus depositional landform positions. *J. Geophys. Res.* **117** (2). DOI: 10.1029/2011JG001790.

Berhe, A. A., Harte, J., Harden, J. W., and Torn, M. S. (2007). The significance of the erosion-induced terrestrial carbon sink. *BioScience* **57**, 337–346. URL: http://bioscience.oxfordjournals.org/.

Berkowitz, R. (2020). Tropical soils could be accelerating global warming. *Phys. Today* **73** (10), 19–20. DOI: 10.1063/PT.3.4587.

Besnard, S., Koirala, S., Weber, U., Nelson, J., Gütter, J., Herault, B., Kassi, J., A., N., Neigh, C., and Poulter, B. (2021). Mapping global forest age from forest inventories, biomass and climate data. *Earth Syst. Sci. Data*, 4881–4896.

Black, C. A. (1965). *Method of soil analysis, part 2, chemical and microbiological properties.* Ed. by A. Page. Vol. 9. J. Am. Soc. Agron., Wiley. ISBN: 9780891180722. DOI: 10.2134/agronmonogr9.2.2ed.

Blagodatskaya, E. and Kuzyakov, Y. (2008). Mechanisms of real and apparent priming effects and their dependence on soil microbial biomass and community structure: Critical review. *Biol. Fertil. Soils* **45**.(2), 115–131. DOI: 10.1007/s00374-008-0334-y.

Blagodatskaya, E., Blagodatsky, S., Khomyakov, N., Myachina, O., and Kuzyakov, Y. (2016). Temperature sensitivity and enzymatic mechanisms of soil organic matter decomposition along an altitudinal gradient on Mount Kilimanjaro. *Sci. Rep.* **6**. DOI: 10.1038/srep22240.

Blake, G. R. and Hartge, K. H. (1986). "Bulk density", pp. 0–1188. DOI: 10.2136/sssabookser5.1.2ed.c13.

Blanco, H. and Lal, R. (2023). "Tillage erosion". Springer Nature Switzerland, pp. 103–125. DOI: 10.1007/978-3-031-30341-8_6.

Borrelli, P., Alewell, C., Alvarez, P., Anache, J. A. A., Baartman, J., Ballabio, C., Bezak, N., Biddoccu, M., Cerdà, A., Chalise, D., Chen, S., Chen, W., Girolamo, A. M. D., Gessesse, G. D., Deumlich, D., Diodato, N., Efthimiou, N., Erpul, G., Fiener, P., Freppaz, M., Gentile, F., Gericke, A., Haregeweyn, N., Hu, B., Jeanneau, A., Kaffas, K., Kiani-Harchegani, M., Villuendas, I. L., Li, C., Lombardo, L., López-Vicente, M., Lucas-Borja, M. E., Märker, M., Matthews, F., Miao, C., Mikoš, M., Modugno, S., Möller, M., Naipal, V., Nearing, M., Owusu, S., Panday, D., Patault, E., Patriche, C. V., Poggio, L., Portes, R., Quijano, L., Rahdari, M. R., Renima, M., Ricci, G. F., Rodrigo-Comino, J., Saia, S., Samani, A. N., Schillaci, C., Syrris, V., Kim, H. S., Spinola, D. N., Oliveira, P. T., Teng, H., Thapa, R., Vantas, K., Vieira, D., Yang, J. E., Yin, S., Zema, D. A., Zhao, G., and Panagos, P. (2021). Soil erosion modelling: A global review and statistical analysis. *Sci. Total Environ.* **780**. DOI: 10.1016/j.scitotenv.2021.146494.

Bossio, D. A., Cook-Patton, S. C., Ellis, P. W., Fargione, J., Sanderman, J., Smith, P., Wood, S., Zomer, R. J., Unger, M. von, Emmer, I. M., and Griscom, B. W. (2020). The role of soil carbon in natural climate solutions. *Nat. Sustainability* **3**.(5), 391–398. DOI: 10.1038/s41893-020-0491-z.

Bouyoucos, G. J. (1962). Hydrometer method improved for making particle size analyses of soils. *Agron. J.* **54** (5), 464–465. DOI: 10.2134/agronj1962.00021962005400050028x.

Brandt, J. (1988). The transformation of rainfall energy by a tropical rain forest canopy in relation to soil erosion. *J. Biogeogr.* **15**.(1), 41–48.

Breugel, P. V., Kindt, R., Lillesø, J. P. B., Bingham, M., Demissew, S., Dudley, C., Friis, I., Gachathi, F., Kalema, J., Mbago, F., Moshi, H. N., Mulumba, J., Namaganda, M., Ndangalasi, H. J., Ruffo, C. K., Védaste, M., Jamnadass, R., and Graudal, L. (2020). *Potential* *natural vegetation map of Eastern Africa (Burundi, Ethiopia, Kenya, Malawi, Rwanda, Tanzania, Uganda and Zambia): Version 2.0.*

Brosens, L., Campforts, B., Robinet, J., Vanacker, V., Opfergelt, S., Ameijeiras-Mariño, Y., Minella, J. P. G., and Govers, G. (2020). Slope gradient controls soil thickness and chemical weathering in Subtropical Brazil: Understanding rates and timescales of regional soilscape evolution through a combination of field data and modeling. *J. Geophys. Res.: Earth Surf.* **125** (6). DOI: 10.1029/2019JF005321.

Bruun, T. B., Elberling, B., and Christensen, B. T. (2010). Lability of soil organic carbon in tropical soils with different clay minerals. *Soil Biol. Biochem.* **42** (6), 888–895. DOI: 10.1016/j.soilbio.2010.01.009.

Bukombe, B., Bauters, M., Boeckx, P., Cizungu, L. N., Cooper, M., Fiener, P., Kidinda, L. K., Makelele, I., Muhindo, D. I., Rewald, B., Verheyen, K., and Doetterl, S. (2022). Soil geochemistry – and not topography – as a major driver of carbon allocation, stocks, and dynamics in forests and soils of African tropical montane ecosystems. *New Phytol.* **236**.(5), 1676–1690. DOI: 10.1111/nph.18469.

Bukombe, B., Fiener, P., Hoyt, A. M., Kidinda, L. K., and Doetterl, S. (2021). Heterotrophic soil respiration and carbon cycling in geochemically distinct African tropical forest soils. *SOIL*. DOI: 10.5194/soil-7-639-2021.

Burke, B. C., Heimsath, A. M., Dixon, J. L., Chappell, J., and Yoo, K. (2009). Weathering the escarpment: chemical and physical rates and processes, south-eastern Australia. *Earth Surf. Processes Landforms* **34** (6), 768–785. DOI: 10.1002/esp.1764.

Buss, W., Hasemer, H., Ferguson, S., and Borevitz, J. (2024). Stabilisation of soil organic matter with rock dust partially counteracted by plants. *Global Change Biol.* **30** (1). DOI: 10.1111/gcb.17052.

Castellanos-Navarrete, A., Tittonell, P., Rufino, M., and Giller, K. (2015). Feeding, crop residue and manure management for integrated soil fertility management – A case study from Kenya. *Agric. Syst.* **134**, 24–35. DOI: 10.1016/j.agsy.2014.03.001.

Castillo-Figueroa, D. (2021). Carbon cycle in tropical upland ecosystems: A global review. *Web Ecol.* **21**.(2), 109–136. DOI: 10.5194/we-21-109-2021.

Cerri, C., Feller, C., Balesdent, J., Victoria, R., and Plenecassagne, A. (1985). Application du traçage isotopique naturel en 13C, à l'étude de la dynamique de la matière organique dans les sols. *C. R. Acad. Sci. II* **300**, 423–427.

Chadwick, K. D. and Asner, G. P. (2016). Tropical soil nutrient distributions determined by biotic and hillslope processes. *Biogeochemistry* **127**.(2-3), 273–289. DOI: 10.1007/s10533-015-0179-z.

Chaplot, V., Brozec, E. C. le, Silvera, N., and Valentin, C. (2005). Spatial and temporal assessment of linear erosion in catchments under sloping lands of northern Laos. *Catena* **63** (2-3), 167–184. DOI: 10.1016/j.catena.2005.06.003.

Chaplot, V., Podwojewski, P., Phachomphon, K., and Valentin, C. (2009). Soil erosion impact on soil organic carbon spatial variability on steep tropical slopes. *Soil Sci. Soc. Am. J.* **73** (3), 769–779. DOI: 10.2136/sssaj2008.0031.

Chen, C., Hall, S. J., Coward, E., and Thompson, A. (2020). Iron-mediated organic matter decomposition in humid soils can counteract protection. *Nat. Commun.* **11**.(1), 2255. DOI: 10.1038/s41467-020-16071-5.

Chen, L., Liu, L., Qin, S., Yang, G., Fang, K., Zhu, B., Kuzyakov, Y., Chen, P., Xu, Y., and Yang, Y. (2019). Regulation of priming effect by soil organic matter stability over a broad geographic scale. *Nat. Commun.* **10**.(1). DOI: 10.1038/s41467-019-13119-z.

Chenu, C. and Plante, A. T. (2006). Clay-sized organo-mineral complexes in a cultivation chronosequence: Revisiting the concept of the 'primary organo-mineral complex'. *Eur. J. Soil Sci.* **57** (4), 596–607. DOI: 10.1111/j.1365-2389.2006.00834.x.

Chiti, T., Certini, G., Grieco, E., and Valentini, R. (2010). The role of soil in storing carbon in tropical rainforests: The case of Ankasa Park, Ghana. *Plant Soil* **331** (1), 453–461. DOI: 10.1007/s11104-009-0265-x.

Cleveland, C. C. and Liptzin, D. (2007). C:N:P stoichiometry in soil: Is there a "Redfield ratio" for the microbial biomass? *Biogeochemistry* **85** (3), 235–252. DOI: 10.1007/s10533-007-9132-0.

Cook, F. J. and Orchard, V. A. (2008). Relationships between soil respiration and soil moisture. *Soil Biol. Biochem.* **40** (5), 1013–1018. DOI: 10.1016/j.soilbio.2007.12.012.

Cooper, M., Vidal-Torrado, P., and Chaplot, V. (2005). Origin of microaggregate in soils with ferralic horizons. *Sci. Agric.* **62** (3), 256–263.

Cotrufo, M. F., Ranalli, M. G., Haddix, M. L., Six, J., and Lugato, E. (2019). Soil carbon storage informed by particulate and mineral-associated organic matter. *Nat. Geosci.* **12** (12), 989–994. DOI: 10.1038/s41561-019-0484-6.

Cotrufo, M. F., Wallenstein, M. D., Boot, C. M., Denef, K., and Paul, E. (2013). The microbial efficiency-matrix stabilization (MEMS) framework integrates plant litter decomposition with soil organic matter stabilization: Do labile plant inputs form stable soil organic matter? *Glob. Change Biol.* **19** (4), 988–995. DOI: 10.1111/gcb.12113.

Coward, E. K., Ohno, T., and Plante, A. F. (2018). Adsorption and molecular fractionation of dissolved organic matter on iron-bearing mineral matrices of varying crystallinity. *Environ. Sci. Technol.* **52**.(3), 1036–1044. DOI: 10.1021/acs.est.7b04953.

Coward, E. K., Thompson, A. T., and Plante, A. F. (2017). Iron-mediated mineralogical control of organic matter accumulation in tropical soils. *Geoderma* **306**, 206–216. DOI: 10.1016/j.geoderma.2017.07.026.

Crawley, M. (2009). *The R book*. Wiley, pp. 0–942.

Curtis, P. G., Slay, C. M., Harris, N. L., Tyukavina, A., and Hansen, M. C. (2018). Classifying drivers of global forest loss. *Science* **361** (6407), 1108–1111. DOI: 10.1126/science.aau3445.

Cusack, D. F., Chadwick, O. A., Ladefoged, T., and Vitousek, P. M. (2013). Long-term effects of agriculture on soil carbon pools and carbon chemistry along a Hawaiian environmental gradient. *Biogeochemistry* **112** (1-3), 229–243. DOI: 10.1007/s10533-012-9718-z.

Cusack, D. F., Halterman, S. M., Tanner, E. V. J., Wright, S. J., Hockaday, W., Dietterich, L. H., and Turner, B. L. (2018). Decadal-scale litter manipulation alters the biochemical and physical character of tropical forest soil carbon. *Soil Biol. Biochem.* **124**, 199–209. DOI: 10.1016/j.soilbio.2018.06.005.

Cusack, D. F. and Marín-Spiotta, E. (2019). Chapter 8 - Wet tropical soils and global change. *Developments in Soil Science* **36**, 131–169. DOI: 10.1016/B978-0-444-63998-1.00008-2.

Czimczik, C. I. and Masiello, C. A. (2007). Controls on black carbon storage in soils. *Global Biogeochem. Cy.* **21**.(3). DOI: 10.1029/2006GB002798.

Dahlgren, R. A. (1994). “Quantification of allophane and imogolite, quantitative methods in soil mineralogy”. Ed. by J. E. Chairs and J. W. Stucki. Soil Sci. Soc. Am. J., pp. 430–451.

Dalzell, B. J., Fissore, C., and Nater, E. A. (2022). Topography and land use impact erosion and soil organic carbon burial over decadal timescales. *Catena* **218**, 106578. DOI: 10.1016/j.catena.2022.106578.

Davidson, E. A. and Janssens, I. A. (2006). *Temperature sensitivity of soil carbon decomposition and feedbacks to climate change.* DOI: 10.1038/nature04514.

Day, R. W. and Quinn, G. P. (1989). Comparisons of treatments after an analysis of variance in ecology. *Ecol. Monogr.* **59** (4), 433–463. DOI: 10.2307/1943075.

Degryze, S., Six, J., Paustian, K., Morris, S. J., Paul, E. A., and Merckx, R. (2004). Soil organic carbon pool changes following land-use conversions. *Global Change Biol.* **10**, 1120–1132.

Denef, K. and Six, J. (2005). Clay mineralogy determines the importance of biological versus abiotic processes for macroaggregate formation and stabilization. *Eur. J. Soil Sci.* **56**.(4), 469–479. DOI: 10.1111/j.1365-2389.2004.00682.x.

Denef, K. and Six, J. (2006). Contributions of incorporated residue and living roots to aggregate-associated and microbial carbon in two soils with different clay mineralogy. *Eur. J. Soil Sci.* **57**.(6), 774–786. DOI: 10.1111/j.1365-2389.2005.00762.x.

Denef, K., Six, J., Merckx, R., and Paustian, K. (2004). Carbon sequestration in microaggregates of no-tillage soils with different clay mineralogy. *Soil Sci. Soc. Am. J.* **68**.(6), 1935–1944. DOI: 10.2136/sssaj2004.1935.

Denef, K., Zotarelli, L., Boddey, R. M., and Six, J. (2007). Microaggregate-associated carbon as a diagnostic fraction for management-induced changes in soil organic carbon in two Oxisols. *Soil Biol. Biochem.* **39** (5), 1165–1172. DOI: 10.1016/j.soilbio.2006.12.024.

Detto, M., Muller-Landau, H. C., Mascaro, J., and Asner, G. P. (2013). Hydrological networks and associated topographic variation as templates for the spatial organization of tropical forest vegetation. *PloS One* **8**.(10). DOI: 10.1371/journal.pone.0076296.

Dewitte, O., Jones, A., Spaargaren, O., Breuning-Madsen, H., Brossard, M., Dampha, A., Deckers, J., Gallali, T., Hallett, S., Jones, R., Kilasara, M., Roux, P. L., Michéli, E., Montanarella, L., Thiombiano, L., Ranst, E. V., Yemefack, M., and Zougmore, R. (2013). Harmonisation of the soil map of Africa at the continental scale. *Geoderma* **211-212**, 138–153. DOI: 10.1016/j.geoderma.2013.07.007.

Dialynas, Y. G., Bastola, S., Bras, R. L., Billings, S. A., Markewitz, D., and B. Richter, D. de (2016a). Topographic variability and the influence of soil erosion on the carbon cycle. *Global Biogeochem. Cycles* **30**.(5), 644–660. DOI: 10.1002/2015GB005302.

Dialynas, Y. G., Bastola, S., Bras, R. L., Marin-Spiotta, E., Silver, W. L., Arnone, E., and Noto, L. V. (2016b). Impact of hydrologically driven hillslope erosion and landslide occurrence on soil organic carbon dynamics in tropical watersheds. *Water Resour. Res.* **52**.(11), 8895–8919. DOI: 10.1002/2016WR018925.

Dick, D. P., Gonçalves, C. N., Dalmolin, R. S., Knicker, H., Klamt, E., Kögel-Knabner, I., Simões, M. L., and Martin-Neto, L. (2005). Characteristics of soil organic matter of different Brazilian Ferralsols under native vegetation as a function of soil depth. *Geoderma* **124** (3-4), 319–333. DOI: 10.1016/j.geoderma.2004.05.008.

Dlugoß, V., Fiener, P., and Schneider, K. (2010). Layer-specific analysis and spatial prediction of soil organic carbon using terrain attributes and erosion modeling. *Soil Sci. Soc. Am. J.* **74** (3), 922–935. DOI: 10.2136/sssaj2009.0325.

Doetterl, S., Berhe, A. A., Arnold, C., Bodé, S., Fiener, P., Finke, P., Fuchslueger, L., Griepentrog, M., Harden, J. W., Nadeu, E., Schnecker, J., Six, J., Trumbore, S., Oost, K. V., Vogel, C., and Boeckx, P. (2018). Links among warming, carbon and microbial dynamics mediated by soil mineral weathering. *Nat. Geosci.* **11**.(8), 589–593. DOI: 10.1038/s41561-018-0168-7.

Doetterl, S., Bukombe, B., Cooper, M., Kidinda, L., D., M., Reichenbach, M., Stegmann, A., Summerauer, A., Wilken, F., and Fiener, P. (2021a). *TropSOC Database v.1.0.* DOI: https://doi.org/10.5880/FIDGEO.2021.009.

Doetterl, S., Cornelis, J.-T., Six, J., Bodé, S., Opfergelt, S., Boeckx, P., and Oost, K. V. (2015a). Soil redistribution and weathering controlling the fate of geochemical and physical carbon stabilization mechanisms in soils of an eroding landscape. *Biogeosciences* **12** (5), 1357–1371. DOI: 10.5194/bg-12-1357-2015.

Doetterl, S., Asifiwe, R. K., Baert, G., Bamba, F., Bauters, M., Boeckx, P., Bukombe, B., Cadisch, G., Cooper, M., Cizungu, L. N., Hoyt, A., Kabaseke, C., Kalbitz, K., Kidinda, L., Maier, A., Mainka, M., Mayrock, J., Muhindo, D., Mujinya, B. B., Mukotanyi, S. M., Nabahungu, L., Reichenbach, M., Rewald, B., Six, J., Stegmann, A., Summerauer, L., Unseld, R., Vanlauwe, B., Oost, K. V., Verheyen, K., Vogel, C., Wilken, F., and Fiener, P. (2021b). Organic matter cycling along geochemical, geomorphic, and disturbance gradients in forest and cropland of the African Tropics - Project TropSOC database version 1.0. *Earth Syst. Sci. Data* **13**.(8), 4133–4153. DOI: 10.5194/essd-13-4133-2021.

Doetterl, S., Bauters, M., Berhe, A. A., Chivenge, P., Finke, P., and Hauser, S. (2021c). Preface: Tropical biogeochemistry of soils in the Congo Basin and the African Great Lakes region. *SOIL* **7** (2), 1–7. DOI: 10.5194/soil-special_issue1134-preface. URL: https://doi.org/10.5194/soil-special_issue1134-preface.pdf.

Doetterl, S., Berhe, A. A., Nadeu, E., Wang, Z., Sommer, M., and Fiener, P. (2016). Erosion, deposition and soil carbon: A review of process-level controls, experimental tools and models to address C cycling in dynamic landscapes. *Earth-Sci. Rev.* **154**, 102–122. DOI: 10.1016/j.earscirev.2015.12.005.

Doetterl, S., Six, J., Wesemael, B. V., and Oost, K. V. (2012). Carbon cycling in eroding landscapes: Geomorphic controls on soil organic C pool composition and C stabilization. *Global Change Biol.* **18**.(7), 2218–2232. DOI: 10.1111/j.1365-2486.2012.02680.x.

Doetterl, S., Stevens, A., Six, J., Merckx, R., Oost, K. V., Pinto, M. C., Casanova-Katny, A., Muñoz, C., Boudin, M., Venegas, E. Z., and Boeckx, P. (2015b). Soil carbon storage controlled by interactions between geochemistry and climate. *Nat. Geosci.* **8** (10), 780–783. DOI: 10.1038/ngeo2516.

Don, A., Schumacher, J., and Freibauer, A. (2011). Impact of tropical land-use change on soil organic carbon stocks - a meta-analysis. *Global Change Biol.* **17**.(4), 1658–1670. DOI: 10.1111/j.1365-2486.2010.02336.x.

Dove, N. C., Arogyaswamy, K., Billings, S. A., Botthoff, J. K., Carey, C. J., Cisco, C., DeForest, J. L., Fairbanks, D., Fierer, N., Gallery, R. E., Kaye, J. P., Lohse, K. A., Maltz, M. R., Mayorga, E., Pett-Ridge, J., Yang, W. H., Hart, S. C., and Aronson, E. L. (2020). Continental-scale patterns of extracellular enzyme activity in the subsoil: an overlooked reservoir of microbial activity. *Environ. Res. Lett.* **15** (10), 1040a1. DOI: 10.1088/1748-9326/abb0b3.

Drake, T. W., Oost, K. V., Barthel, M., Bauters, M., Hoyt, A. M., Podgorski, D. C., Six, J., Boeckx, P., Trumbore, S. E., Ntaboba, L. C., and Spencer, R. G. (2019). Mobilization of aged and biolabile soil carbon by tropical deforestation. *Nat. Geosci.* **12** (7), 541–546. DOI: 10.1038/s41561-019-0384-9.

Dressée, P. L. C. and Lepersonne, J. (1949). *Carte Géologique 1:5000000. Institut Royal Colonial Belge Commission centrale de l'atlas général du Congo Belge et du Ruanda-Urundi, Index No. 31.*

Eby, G. N., Lloyd, F. E., and Woolley, A. R. (2009). Geochemistry and petrogenesis of the Fort Portal, Uganda, extrusive carbonatite. *Lithos* **113** (3-4), 785–800. DOI: 10.1016/j.lithos.2009.07.010.

Eswaran, H., Kimble, J., Cook, T., and Beinroth, F. H. (1992). “Soil diversity in the Tropics: Implications for agricultural development”. *Myths and Science of Soils of the Tropics*. Ed. by R. Lal and P. A. Sanchez. Vol. 29. SSSA Special Publications, pp. 1–16. DOI: 10.2136/sssaspecpub29.c1.

Eusterhues, K., Rumpel, C., Kleber, M., and Kögel-Knabner, I. (2003). Stabilisation of soil organic matter by interactions with minerals as revealed by mineral dissolution and oxidative degradation. *Org. Geochem.* **34** (12), 1591–1600. DOI: 10.1016/j.orggeochem.2003.08.007.

Evanko, C. R. and Dzombak, D. A. (1998). Influence of structural features on sorption of NOM-analogue organic acids to goethite. *Environ. Sci. Technol.* **32** (19), 2846–2855. DOI: 10.1021/es980256t.

Fang, K., Qin, S., Chen, L., Zhang, Q., and Yang, Y. (2019). Al/Fe mineral controls on soil organic carbon stock across Tibetan alpine grasslands. *J. Geophys. Res.-Biogeo.* **124** (2), 247–259. DOI: 10.1029/2018JG004782.

Fanin, N., Alavoine, G., and Bertrand, I. (2020). Temporal dynamics of litter quality, soil properties and microbial strategies as main drivers of the priming effect. *Geoderma* **377**, 114576. DOI: 10.1016/j.geoderma.2020.114576.

FAO (2006). *Guidelines for soil description, 4th edition.*

— (2014). *World references base for soil resources 2014, International soil classification system for naming soils and creating legends for soil maps.* Food and Agriculture Organization of the United Nations, pp. 0–203.

Fatumah, N., Tilahun, S. A., and Mohammed, S. (2020). Effect of tillage systems and tillage direction on soil hydrological properties and soil suspended particle concentration in arable land in Uganda. *Heliyon* **6** (12), e05616. DOI: 10.1016/j.heliyon.2020.e05616.

Feng, W., Liang, J., Hale, L. E., Jung, C. G., Chen, J., Zhou, J., Xu, M., Yuan, M., Wu, L., Bracho, R., Pegoraro, E., Schuur, E. A., and Luo, Y. (2017). Enhanced decomposition of stable soil organic carbon and microbial catabolic potentials by long-term field warming. *Glob. Change Biol.* **23** (11), 4765–4776. DOI: 10.1111/gcb.13755.

Feng, W., Plante, A. F., Aufdenkampe, A. K., and Six, J. (2014). Soil organic matter stability in organo-mineral complexes as a function of increasing C loading. *Soil Biol. Biochem.* **69**, 398–405. DOI: 10.1016/j.soilbio.2013.11.024.

Fiantis, D., Nelson, M., Shamshuddin, J., Goh, T. B., and Ranst, E. V. (2010). Determination of the geochemical weathering indices and trace elements content of new volcanic ash deposits from Mt. Talang (West Sumatra) Indonesia. *Eurasian Soil Sci.* **43**.(13), 1477–1485. DOI: 10.1134/S1064229310130077.

Fick, S. E. and Hijmans, R. J. (2017). WorldClim 2: new 1-km spatial resolution climate surfaces for global land areas. *Int. J. Climatol.* **37** (12), 4302–4315. DOI: 10.1002/joc.5086.

Fiener, P., Dlugoß, V., and Oost, K. V. (2015). Erosion-induced carbon redistribution, burial and mineralisation — Is the episodic nature of erosion processes important? *Catena* **133**, 282–292. DOI: 10.1016/j.catena.2015.05.027.

Fiener, P., Wilken, F., Aldana-Jague, E., Deumlich, D., Gómez, J., Guzmán, G., Hardy, R., Quinton, J., Sommer, M., Oost, K. V., and Wexler, R. (2018). Uncertainties in assessing tillage erosion – How appropriate are our measuring techniques? *Geomorphology* **304**, 214–225. DOI: 10.1016/j.geomorph.2017.12.031.

Finke, P., Opolot, E., Balesdent, J., Berhe, A. A., Boeckx, P., Cornu, S., Harden, J., Hatté, C., Williams, E., and Doetterl, S. (2019). Can SOC modelling be improved by accounting for pedogenesis? *Geoderma* **338**, 513–524. DOI: 10.1016/j.geoderma.2018.10.018.

Finke, P. A. and Hutson, J. L. (2008). Modelling soil genesis in calcareous loess. *Geoderma* **145** (3-4), 462–479. DOI: 10.1016/j.geoderma.2008.01.017.

Fontaine, S., Mariotti, A., and Abbadie, L. (2003). The priming effect of organic matter: a question of microbial competition? *Soil Biol. Biochem.* **35**, 837–843. DOI: 10.1016/S0038-0717(03)00123-8.

Fontaine, S., Bardoux, G., Abbadie, L., and Mariotti, A. (2004). Carbon input to soil may decrease soil carbon content. *Ecol. Lett.* **7**.(4), 314–320. DOI: 10.1111/j.1461-0248.2004.00579.x.

Friedl, M. A., Sulla-Menashe, D., Tan, B., Schneider, A., Ramankutty, N., Sibley, A., and Huang, X. (2013). MODIS Collection 5 global land cover: Algorithm refinements and characterization of new datasets. *Remote Sens. Environ.* **114**, 168–182.

Fromm, S. F. von, Doetterl, S., Butler, B. M., Aynekulu, E., Berhe, A. A., Haefele, S. M., McGrath, S. P., Shepherd, K. D., Six, J., Tamene, L., Tondoh, E. J., Vågen, T. G., Winowiecki, L. A., Trumbore, S. E., and Hoyt, A. M. (2024a). Controls on timescales of soil organic carbon persistence across sub-Saharan Africa. *Global Change Biol.* **30**. DOI: 10.1111/gcb.17089.

Fromm, S. F. von, Hoyt, A. M., Lange, M., Acquah, G. E., Aynekulu, E., Berhe, A. A., Haefele, S. M., Mcgrath, S. P., Shepherd, K. D., Sila, A. M., Six, J., Towett, E. K., Trumbore, S. E., Vägen, T. G., Weullow, E., Winowiecki, L. A., and Doetterl, S. (2021). Continental-scale controls on soil organic carbon across sub-Saharan Africa. *SOIL* **7**, 305–332. DOI: 10.5194/soil-7-305-2021.

Fromm, S. F. von, Hoyt, A. M., Sierra, C. A., Georgiou, K., Doetterl, S., and Trumbore, S. E. (2024b). Controls and relationships of soil organic carbon abundance and persistence vary across pedo-climatic regions. *Global Change Biol.* **30**.(5). DOI: 10.1111/gcb.17320.

Fujisaki, K., Chevallier, T., Chapuis-Lardy, L., Albrecht, A., Razafimbelo, T., Masse, D., Ndour, Y. B., and Chotte, J.-L. (2018). Soil carbon stock changes in tropical croplands are mainly driven by carbon inputs: A synthesis. *Agric. Ecosyst. Environ.* **259**, 147–158. DOI: 10.1016/j.agee.2017.12.008.

Fujisaki, K., Perrin, A. S., Desjardins, T., Bernoux, M., Balbino, L. C., and Brossard, M. (2015). From forest to cropland and pasture systems: A critical review of soil organic carbon stocks changes in Amazonia. *Global Change Biol.* **21**, 2773–2786. DOI: 10.1111/gcb.12906.

George, J., Adelaja, A., and Awokuse, T. O. (2021). The agricultural impacts of armed conflicts: the case of Fulani militia. *Eur. Rev. Agric. Econ.* **48** (3), 538–572. DOI: 10.1093/erae/jbaa022.

Georgiou, K., Jackson, R. B., Vindušková, O., Abramoff, R. Z., Ahlström, A., Feng, W., Harden, J. W., Pellegrini, A. F., Polley, H. W., Soong, J. L., Riley, W. J., and Torn, M. S. (2022). Global stocks and capacity of mineral-associated soil organic carbon. *Nat. Commun.* **13**. DOI: 10.1038/s41467-022-31540-9.

Gerland, P., Raftery, A. E., Ševčíková, H., Li, N., Gu, D., Spoorenberg, T., Alkema, L., Fosdick, B. K., Chunn, J., Lalic, N., Bay, G., Buettner, T., Heilig, G. K., and Wilmoth, J. (2014). World population stabilization unlikely this century. *Science* **346** (6206), 234–237. DOI: 10.1126/science.1257469.

Giannetta, B., Plaza, C., Thompson, A., Plante, A. F., and Zaccone, C. (2022). Iron speciation in soil size fractions under different land uses. *Geoderma* **418**, 115842. DOI: 10.1016/j.geoderma.2022.115842.

Giller, K. E., Delaune, T., Silva, J. V., Wijk, M. V., Hammond, J., Descheemaeker, K., Ven, G. V. de, Schut, A. G. T., Taulya, G., Chikowo, R., and Andersson, J. A. (2021). Small farms and development in sub-Saharan Africa: Farming for food, for income or for lack of better options? *Food Secur.* **13**.(6), 1431–1454. DOI: 10.1007/s12571-021-01209-0.

Goll, D. S., Ciais, P., Amann, T., Buermann, W., Chang, J., Eker, S., Hartmann, J., Janssens, I., Li, W., Obersteiner, M., Penuelas, J., Tanaka, K., and Vicca, S. (2021). Potential CO2 removal from enhanced weathering by ecosystem responses to powdered rock. *Nat. Geosci.* **14**, 545–549. DOI: 10.1038/s41561-021-00798-x.

Gorelick, N., Hancher, M., Dixon, M., Ilyushchenko, S., Thau, D., and Moore, R. (2017). Google Earth Engine: Planetary-scale geospatial analysis for everyone. *Remote Sens. Environ.* **202**, 18–27. DOI: 10.1016/j.rse.2017.06.031.

Govers, G., Vandaele, K., Desmet, P., Poesen, J., and Bunte, K. (1994). The role of tillage in soil redistribution on hillslopes. *European Journal of Soil Science* **45**.(4), 469–478. DOI: 10.1111/j.1365-2389.1994.tb00532.x.

Grant, K., Hilton, R., and Galy, V. (2023). Global patterns of radiocarbon depletion in subsoil linked to rock-derived organic carbon. *Geochem. Perspect. Lett.* **25**, 36–40. DOI: 10.7185/geochemlet.2312.

Grant, K. E., Galy, V. V., Haghipour, N., Eglinton, T. I., and Derry, L. A. (2022). Persistence of old soil carbon under changing climate: The role of mineral-organic matter interactions. *Chem. Geol.* **587**. DOI: 10.1016/j.chemgeo.2021.120629.

Grau, O., Peñuelas, J., Ferry, B., Freycon, V., Blanc, L., Desprez, M., Baraloto, C., Chave, J., Descroix, L., Dourdain, A., Guitet, S., Janssens, I. A., Sardans, J., and Hérault, B. (2017). Nutrient-cycling mechanisms other than the direct absorption from soil may control forest structure and dynamics in poor Amazonian soils. *Sci. Rep.* **7**, 45017. DOI: 10.1038/srep45017.

Greenland, D. J., Wild, A., and Adams, D. (1992). "Organic matter dynamics in soils of the Tropics - From myth to complex reality". Ed. by R. Lal and P. A. Sanchez. 29th ed. SSSA Special Publications, pp. 17–33. DOI: 10.2136/sssaspecpub29.c2.

Gregorich, E. G., Greer, K. J., Anderson, D. W., and Liang, B. C. (1998). Carbon distribution and losses: erosion and deposition effects. *Soil Till. Res.* **47**, 291–302.

Grömping, U. (2006). Relative importance for linear regression in R: The package relaimpo. *J. Stat. Softw.* **17** (1). DOI: 10.18637/jss.v017.i01.

Guggenberger, G. and Kaiser, K. (2003). "Dissolved organic matter in soil: Challenging the paradigm of sorptive preservation". *Geoderma.* Vol. 113. 3-4. Elsevier, pp. 293–310. DOI: 10.1016/S0016-7061(02)00366-X.

Guillaume, T., Damris, M., and Kuzyakov, Y. (2015). Losses of soil carbon by converting tropical forest to plantations: Erosion and decomposition estimated by δ13C. *Global Change Biol.* **21**.(9), 3548–3560. DOI: 10.1111/gcb.12907.

Hall, S. J., McNicol, G., Natake, T., and Silver, W. L. (2015). Large fluxes and rapid turnover of mineral-associated carbon across topographic gradients in a humid tropical forest: Insights from paired 14C analysis. *Biogeosciences* **12** (8), 2471–2487. DOI: 10.5194/bg-12-2471-2015.

Hall, S. J., Berhe, A. A., and Thompson, A. (2018). Order from disorder: Do soil organic matter composition and turnover co-vary with iron phase crystallinity? *Biogeochemistry* **140**.(1), 93–110. DOI: 10.1007/s10533-018-0476-4.

Han, J., Kamber, M., and Pei, J. (2012). *Data Mining. Concepts and Techniques, 3rd Edition (The Morgan Kaufmann Series in Data Management Systems).* Elsevier. Morgan Kaufmann.

Hansen, M. C., Potapov, P. V., Moore, R., Hancher, M., Turubanova, S. A., Tyukavina, A., Thau, D., Stehman, S. V., Goetz, S. J., Loveland, T. R., Kommareddy, A., Egorov, A., Chini, L., Justice, C. O., and Townshend, J. R. G. (2013). High-resolution global maps of 21st-century forest cover change. *Science* **342** (6160), 850–853. DOI: 10.1126/science.1244693.

Hao, Y., Nianpeng, H., Shenggong, L., Guirui, Y., Yang, G., and Ruomeng, W. (2016). Impact of land cover on temperature and moisture sensitivity of soil organic matter mineralization in subtropical southeastern China. *J. Resour. Ecol.* **7** (2), 85–91. DOI: 10.5814/j.issn.1674-764x.2016.02.002.

Harden, J. W., Sharpe, J. M., Parton, W. J., Ojima, D. S., Fries, T. L., Huntington, T. G., and Dabney, S. M. (1999). Dynamic replacement and loss of soil carbon on eroding cropland. *Global Biogeochem.* **13**.(4), 885–901. DOI: 10.1029/1999GB900061.

Hattori, D., Kenzo, T., Shirahama, T., Harada, Y., Kendawang, J. J., Ninomiya, I., and Sakurai, K. (2019). Degradation of soil nutrients and slow recovery of biomass following shifting cultivation in the heath forests of Sarawak, Malaysia. *For. Ecol. Manage.* **432**, 467–477. DOI: 10.1016/j.foreco.2018.09.051.

Heckman, K., Lawrence, C. R., and Harden, J. W. (2018). A sequential selective dissolution method to quantify storage and stability of organic carbon associated with Al and Fe hydroxide phases. *Geoderma* **312**, 24–35. DOI: 10.1016/j.geoderma.2017.09.043.

Heckman, K., Pries, C. E. H., Lawrence, C. R., Rasmussen, C., Crow, S. E., Hoyt, A. M., Fromm, S. F. von, Shi, Z., Stoner, S., McGrath, C., Beem-Miller, J., Berhe, A. A., Blankinship, J. C., Keiluweit, M., Marín-Spiotta, E., Monroe, J. G., Plante, A. F., Schimel, J., Sierra, C. A., Thompson, A., and Wagai, R. (2022). Beyond bulk: Density fractions explain heterogeneity in global soil carbon abundance and persistence. *Global Change Biol.* **28**.(3), 1178–1196. DOI: 10.1111/gcb.16023.

Heckman, K. and Rasmussen, C. (2018). Chapter four - Role of mineralogy and climate in the soil carbon cycle. *Developments in Soil Science* **35**, 93–110. DOI: 10.1016/B978-0-444-63865-6.00004-1.

Heckman, K., Welty-Bernard, A., Rasmussen, C., and Schwartz, E. (2009). Geologic controls of soil carbon cycling and microbial dynamics in temperate conifer forests. *Chem. Geol.* **267** (1-2), 12–23. DOI: 10.1016/j.chemgeo.2009.01.004.

Heinrich, V. H. A., Dalagnol, R., Cassol, H. L. G., Rosan, T. M., Almeida, C. T. de, Junior, C. H. L. S., Campanharo, W. A., House, J. I., Sitch, S., Hales, T. C., Adami, M., Anderson, L. O., and Aragão, L. E. O. C. (2021). Large carbon sink potential of secondary forests in the Brazilian Amazon to mitigate climate change. *Nat. Commun.* **12** (1), 1785. DOI: 10.1038/s41467-021-22050-1.

Hemelryck, H. V., Fiener, P., Oost, K. V., Govers, G., and Merckx, R. (2010). The effect of soil redistribution on soil organic carbon: An experimental study. *Biogeosciences* **7**.(12), 3971–3986. DOI: 10.5194/bg-7-3971-2010.

Hemelryck, H. V., Govers, G., Oost, K. V., and Merckx, R. (2011). Evaluating the impact of soil redistribution on the in situ mineralization of soil organic carbon. *Earth Surf. Processes Landforms* **36** (4), 427–438. DOI: 10.1002/esp.2055.

Hemingway, J. D., Hilton, R. G., Hovius, N., Eglinton, T. I., Haghipour, N., Wacker, L., Chen, M. C., and Galy, V. V. (2018). Microbial oxidation of lithospheric organic carbon in rapidly eroding tropical mountain soils. *Science* **360** (6385), 209–212. DOI: 10.1126/science.aao6463.

Hemingway, J. D., Rothman, D. H., Grant, K. E., Rosengard, S. Z., Eglinton, T. I., Derry, L. A., and Galy, V. V. (2019). Mineral protection regulates long-term global preservation of natural organic carbon. *Nature* **570**.(7760), 228–231. DOI: 10.1038/s41586-019-1280-6.

Heng, B. C. P., Sander, G. C., Armstrong, A., Quinton, J. N., Chandler, J. H., and Scott, C. F. (2011). Modeling the dynamics of soil erosion and size-selective sediment transport over nonuniform topography in flume-scale experiments. *Water Resour. Res.* **47**.(2). DOI: 10.1029/2010WR009375.

Herold, N., Schöning, I., Michalzik, B., Trumbore, S., and Schrumpf, M. (2014). Controls on soil carbon storage and turnover in German landscapes. *Biogeochemistry* **119** (1-3), 435–451. DOI: 10.1007/s10533-014-9978-x.

Hicks, L. C., Meir, P., Nottingham, A. T., Reay, D. S., Stott, A. W., Salinas, N., and Whitaker, J. (2019). Carbon and nitrogen inputs differentially affect priming of soil organic matter in tropical lowland and montane soils. *Soil Biol. Biochem.* **129**, 212–222. DOI: 10.1016/j.soilbio.2018.10.015.

Hossner, L. R. (1996). “Dissolution of total elemental analysis”. SSSA, pp. 0–1390. DOI: 10.2136/sssabookser5.3.c34.

Hunter, B. D., Roering, J. J., Almond, P. C., Chadwick, O. A., Polizzotto, M. L., and Silva, L. C. (2023). Pedogenic pathways and deep weathering controls on soil organic carbon in Pacific Northwest forest soils. *Geoderma* **436**, 116531. DOI: 10.1016/j.geoderma.2023.116531.

IBM (2019). *SPSS Statistics for Windows.*

Islam, M. R., Singh, B., and Dijkstra, F. A. (2022). Stabilisation of soil organic matter: interactions between clay and microbes. *Biogeochemistry* **160**.(2), 145–158. DOI: 10.1007/s10533-022-00956-2.

Ito, A. and Wagai, R. (2017). Data descriptor: Global distribution of clay-size minerals on land surface for biogeochemical and climatological studies. *Sci. Data* **4**.(1). DOI: 10.1038/sdata.2017.103.

Jackson, R. B., Lajtha, K., Crow, S. E., Hugelius, G., Kramer, M. G., and Piñeiro, G. (2017). The ecology of soil carbon: Pools, vulnerabilities, and biotic and abiotic controls. *Annu. Rev. Ecol. Evol. Syst.* **48**, 419–464. DOI: 10.1146/annurev-ecolsys-112414. URL: https://doi.org/10.1146/annurev-ecolsys-112414-.

Jagadamma, S., Mayes, M. A., Zinn, Y. L., Gísladóttir, G., and Russell, A. E. (2014). Sorption of organic carbon compounds to the fine fraction of surface and subsurface soils. *Geoderma* **213**, 79–86. DOI: 10.1016/j.geoderma.2013.07.030.

Jobbágy, E. G. and Jackson, R. B. (2000). The vertical distribution of soil organic carbon and its relation to climate and vegetation. *Ecol. Appl.* **10** (2), 423–436.

JPL, N. (2013). *NASA shuttle radar topography mission global 1 arc second, 201 3, distributed by NASA EOSDIS Land Processes DAAC.*

Juo, A. S. R. and Franzluebbers, K. (2003). *Tropical soils. Properties and management for sustainable agriculture.* Oxford University Press.

Kaiser, K. and Guggenberger, G. (2007). Sorptive stabilization of organic matter by microporous goethite: Sorption into small pores vs. surface complexation. *Eur. J. Soil Sci.* **58** (1), 45–59. DOI: 10.1111/j.1365-2389.2006.00799.x.

Kaiser, K. and Zech, W. (1996). Defects in estimation of aluminum in humus complexes of podzolic soils by pyrophosphate extraction. *Soil Sci.* **161** (7), 452–458. DOI: 10.1097/00010694-199607000-00005.

Kaiser, M., Zederer, D. P., Ellerbrock, R. H., Sommer, M., and Ludwig, B. (2016). Effects of mineral characteristics on content, composition, and stability of organic matter fractions separated from seven forest topsoils of different pedogenesis. *Geoderma* **263**, 1–7. DOI: 10.1016/j.geoderma.2015.08.029.

Kalks, F., Noren, G., Mueller, C. W., Helfrich, M., Rethemeyer, J., and Don, A. (2021). Geogenic organic carbon in terrestrial sediments and its contribution to total soil carbon. *SOIL* **7**.(2), 347–362. DOI: 10.5194/soil-7-347-2021.

Kalyebi, A., Macfadyen, S., Hulthen, A., Ocitti, P., Jacomb, F., Tay, W. T., Colvin, J., and Barro, P. D. (2021). Within-season changes in land-use impact pest abundance in smallholder African cassava production systems. *Insects* **12**.(3). DOI: 10.3390/insects12030269.

Karamage, F., Shao, H., Chen, X., Ndayisaba, F., Nahayo, L., Kayiranga, A., Omifolaji, J., Liu, T., and Zhang, C. (2016a). Deforestation effects on soil erosion in the Lake Kivu Basin, D.R. Congo-Rwanda. *Forests* **7** (12), 281. DOI: 10.3390/f7110281.

Karamage, F., Zhang, C., Ndayisaba, F., Shao, H., Kayiranga, A., Fang, X., Nahayo, L., Nyesheja, E. M., and Tian, G. (2016b). Extent of cropland and related soil erosion risk in Rwanda. *Sustainability* **8** (7), 609. DOI: 10.3390/su8070609.

Kassambara, A. and Mundt, F. (2020). *Factoextra: Extract and visualize the results of multivariate analysis. R Package Version 1.0.7.* URL: https://CRAN.R-project.org/package=factoextra.

Kayani, I. B., Agumas, B., Musyoki, M., Nziguheba, G., Marohn, C., Benz, M., Vanlauwe, B., Cadisch, G., and Rasche, F. (2021). Market access and resource endowment define the soil fertility status of smallholder farming systems of South-Kivu, DR Congo. *Soil Use Manage.* **37**, 353–366. DOI: 10.1111/sum.12691.

Keiluweit, M., Bougoure, J. J., Nico, P. S., Pett-Ridge, J., Weber, P. K., and Kleber, M. (2015). Mineral protection of soil carbon counteracted by root exudates. *Nat. Clim. Change* **5** (6), 588–595. DOI: 10.1038/nclimate2580.

Keulen, H. V. (2001). (Tropical) soil organic matter modelling: problems and prospects. *Nutr. Cycl. Agroecosys.* **61**, 33–39.

Khomo, L., Trumbore, S., Bern, C. R., and Chadwick, O. A. (2017). Timescales of carbon turnover in soils with mixed crystalline mineralogies. *SOIL* **3**, 17–30. DOI: 10.5194/soil-3-17-2017.

Kidinda, L. K., Doetterl, S., Kalbitz, K., Bukombe, B., Babin, D., Mujinya, B. B., and Vogel, C. (2023). Relationships between geochemical properties and microbial nutrient acquisition in tropical forest and cropland soils. *Appl. Soil Ecol.* **181**, 104653. DOI: 10.1016/j.apsoil.2022.104653.

Kidinda, L. K., Olagoke, F. K., Vogel, C., Bukombe, B., Kalbitz, K., and Doetterl, S. (2022). Microbial properties in tropical montane forest soils developed from contrasting parent material — an incubation experiment. *J. Plant Nutr. Soil Sci.* **185** (6), 807–820. DOI: 10.1002/jpln.202100274.

Kihara, J., Bolo, P., Kinyua, M., Nyawira, S., and Sommer, R. (2020). Soil health and ecosystem services: Lessons from sub-Sahara Africa (SSA). *Geoderma* **370**, 114342. DOI: 10.1016/j.geoderma.2020.114342.

Kim, D.-G., Grieco, E., Bombelli, A., Hickman, J. E., and Sanz-Cobena, A. (2021). Challenges and opportunities for enhancing food security and greenhouse gas mitigation in smallholder farming in sub-Saharan Africa. A review. *Food Secur.* **13** (2), 457–476. DOI: 10.1007/s12571-021-01149-9.

King, A. E., Congreves, K. A., Deen, B., Dunfield, K. E., Voroney, R. P., and Wagner-Riddle, C. (2019). Quantifying the relationships between soil fraction mass, fraction carbon, and total soil carbon to assess mechanisms of physical protection. *Soil Biol. Biochem.* **135**, 95–107. DOI: 10.1016/j.soilbio.2019.04.019.

King, J. K. K., Granjou, C., Fournil, J., and Cecillon, L. (2018). Soil sciences and the French 4 per 1000 Initiative—The promises of underground carbon. *Energy Res. Social Sci.* **45**, 144–152. DOI: 10.1016/j.erss.2018.06.024.

Kirkels, F., Cammeraat, L., and Kuhn, N. (2014). The fate of soil organic carbon upon erosion, transport and deposition in agricultural landscapes — A review of different concepts. *Geomorphology* **226**, 94–105. DOI: 10.1016/j.geomorph.2014.07.023.

Kirsten, M., Mikutta, R., Kimaro, D. N., Feger, K. H., and Kalbitz, K. (2021a). Aluminous clay and pedogenic Fe oxides modulate aggregation and related carbon contents in soils of the humid tropics. *SOIL* **7**, 363–375. DOI: 10.5194/soil-7-363-2021.

Kirsten, M., Kimaro, D. N., Feger, K.-H., and Kalbitz, K. (2019). Impact of land use on soil organic carbon stocks in the humid tropics of NE Tanzania. *J. Plant Nutr. Soil Sci.* **182** (4), 625–636. DOI: 10.1002/jpln.201800595.

Kirsten, M., Mikutta, R., Vogel, C., Thompson, A., Mueller, C. W., Kimaro, D. N., Bergsma, H. L. T., Feger, K.-H., and Kalbitz, K. (2021b). Iron oxides and aluminous clays selectively control soil carbon storage and stability in the humid Tropics. *Sci. Rep.* **11**.(1), 5076. DOI: 10.1038/s41598-021-84777-7.

Kleber, M., Mikutta, R., Torn, M. S., and Jahn, R. (2005). Poorly crystalline mineral phases protect organic matter in acid subsoil horizons. *Eur. J. Soil Sci.* **56** (6), 717–725. DOI: 10.1111/j.1365-2389.2005.00706.x.

Kleber, M., Bourg, I. C., Coward, E. K., Hansel, C. M., Myneni, S. C., and Nunan, N. (2021). Dynamic interactions at the mineral – organic matter interface. *Nat. Rev. Earth Environ.* **2**.(6), 402–421. DOI: 10.1038/s43017-021-00162-y.

Kleber, M., Eusterhues, K., Keiluweit, M., Mikutta, C., Mikutta, R., and Nico, P. S. (2015). “Mineral-Organic Associations: Formation, Properties, and Relevance in Soil Environments”. *Adv. Agron.* Vol. 130. Academic Press Inc., pp. 1–140. DOI: 10.1016/bs.agron.2014.10.005.

Kleber, M., Nico, P. S., Plante, A., Filley, T., Kramer, M., Swanston, C., and Sollins, P. (2011). Old and stable soil organic matter is not necessarily chemically recalcitrant: Implications for modeling concepts and temperature sensitivity. *Global Change Biol.* **17** (2), 1097–1107. DOI: 10.1111/j.1365-2486.2010.02278.x.

Knicker, H. (2011). Pyrogenic organic matter in soil: Its origin and occurrence, its chemistry and survival in soil environments. *Quatern. Int.* **243**.(2), 251–263. DOI: 10.1016/j.quaint.2011.02.037.

Knorr, W., Prentice, I. C., House, J. I., and Holland, E. A. (2005). Long-term sensitivity of soil carbon turnover to warming. *Nature* **433** (7023), 298–301. DOI: 10.1038/nature03226.

Koch, A., McBratney, A., Adams, M., Field, D., Hill, R., Crawford, J., Minasny, B., Lal, R., Abbott, L., O’Donnell, A., Angers, D., Baldock, J., Barbier, E., Binkley, D., Parton, W., Wall, D. H., Bird, M., Bouma, J., Chenu, C., Flora, C. B., Goulding, K., Grunwald, S., Hempel, J., Jastrow, J., Lehmann, J., Lorenz, K., Morgan, C. L., Rice, C. W., Whitehead, D., Young, I., and Zimmermann, M. (2013). Soil security: Solving the global soil crisis. *Global Policy* **4** (4), 434–441. DOI: 10.1111/1758-5899.12096.

Köchy, M., Hiederer, R., and Freibauer, A. (2015). Global distribution of soil organic carbon – Part 1: Masses and frequency distributions of SOC stocks for the tropics, permafrost regions, wetlands, and the world. *SOIL* **1** (1), 351–365. DOI: 10.5194/soil-1-351-2015.

Kögel-Knabner, I., Guggenberger, G., Kleber, M., Kandeler, E., Kalbitz, K., Scheu, S., Eusterhues, K., and Leinweber, P. (2008). Organo-mineral associations in temperate soils: Integrating biology, mineralogy, and organic matter chemistry. *J. Plant Nutr. Soil Sc.* **171** (1), 61–82. DOI: 10.1002/jpln.200700048.

Kome, G. K., Enang, R. K., Tabi, F. O., and Yerima, B. P. K. (2019). Influence of clay minerals on some soil fertility attributes: A review. *Open Journal of Soil Science* **9**.(9), 155–188. DOI: 10.4236/ojss.2019.99010.

Kpemoua, T. P. I., Leclerc, S., Barré, P., Houot, S., Pouteau, V., Plessis, C., and Chenu, C. (2023). Are carbon-storing soils more sensitive to climate change? A laboratory evaluation for agricultural temperate soils. *Soil Biology and Biochemistry* **183**, 109043. DOI: 10.1016/j.soilbio.2023.109043.

Kraamwinkel, C. T., Beaulieu, A., Dias, T., and Howison, R. A. (2021). Planetary limits to soil degradation. *Communications Earth and Environment* **2**.(1). DOI: 10.1038/s43247-021-00323-3.

Kramer, M. G. and Chadwick, O. A. (2018). Climate-driven thresholds in reactive mineral retention of soil carbon at the global scale. *Nat. Clim. Change* **8** (12), 1104–1108. DOI: 10.1038/s41558-018-0341-4.

Kramer, M. G., Sanderman, J., Chadwick, O. A., Chorover, J., and Vitousek, P. M. (2012). Long-term carbon storage through retention of dissolved aromatic acids by reactive particles in soil. *Global Change Biol.* **18** (8), 2594–2605. DOI: 10.1111/j.1365-2486.2012.02681.x.

Kroese, J. S., Jacobs, S. R., Tych, W., Breuer, L., Quinton, J. N., and Rufino, M. C. (2020). Tropical montane forest conversion is a critical driver for sediment supply in East African catchments. *Water Resour. Res.* **56** (10). DOI: 10.1029/2020WR027495.

Kukla, J., Whitfeld, T., Cajthaml, T., Baldrian, P., Veselá-Šimáčková, H., Novotný, V., and Frouz, J. (2019). The effect of traditional slash-and-burn agriculture on soil organic matter, nutrient content, and microbiota in tropical ecosystems of Papua New Guinea. *Land Degradation & Development* **30** (2), 166–177. DOI: 10.1002/ldr.3203.

Kumagai, T., Katul, G. G., Porporato, A., Saitoh, T. M., Ohashi, M., Ichie, T., and Suzuki, M. (2004). Carbon and water cycling in a Bornean tropical rainforest under current and future climate scenarios. *Adv. Water Resour.* **27**.(12), 1135–1150.

Kuzyakov, Y. and Blagodatskaya, E. (2015). *Microbial hotspots and hot moments in soil: Concept & review.* DOI: 10.1016/j.soilbio.2015.01.025.

Labrière, N., Locatelli, B., Laumonier, Y., Freycon, V., and Bernoux, M. (2015). Soil erosion in the humid tropics: A systematic quantitative review. *Agric. Ecosyst. Environ.* **203**, 127–139. DOI: 10.1016/j.agee.2015.01.027.

Lacrose, D. T. (2004). *Discovering knowledge in data. An introduction to data mining.* John Wiley & Sons, pp. 0–222.

Lal, R. (2005). Forest soils and carbon sequestration. *For. Ecol. Manage.* **220** (1-3), 242–258. DOI: 10.1016/j.foreco.2005.08.015.

Lan, C.-W., Lo, M. H., Chou, C., and Kumar, S. (2016). Terrestrial water flux responses to global warming in tropical rainforest areas. *Earth's Future* **4**.(5), 210–224.

Landholm, D. M., Pradhan, P., and Kropp, J. P. (2019). Diverging forest land use dynamics induced by armed conflict across the tropics. *Global Environ. Change* **56**, 86–94. DOI: 10.1016/j.gloenvcha.2019.03.006.

Laub, M., Corbeels, M., Couëdel, A., Ndungu, S. M., Mucheru-Muna, M. W., Mugendi, D., Necpalova, M., Waswa, W., Broek, M. V. de, Vanlauwe, B., and Six, J. (2023). Managing soil organic carbon in tropical agroecosystems: evidence from four long-term experiments in Kenya. *SOIL* **9**.(1), 301–323. DOI: 10.5194/soil-9-301-2023. URL: https://soil.copernicus.org/articles/9/301/2023/.

Lawrence, C. R., Harden, J. W., Xu, X., Schulz, M. S., and Trumbore, S. E. (2015). Long-term controls on soil organic carbon with depth and time: A case study from the Cowlitz River Chronosequence, WA USA. *Geoderma* **247-248**, 73–87. DOI: 10.1016/j.geoderma.2015.02.005.

Lehmann, J., Kinyangi, J., and Solomon, D. (2007). Organic matter stabilization in soil microaggregates: Implications from spatial heterogeneity of organic carbon contents and carbon forms. *Biogeochemistry* **85**.(1), 45–57. DOI: 10.1007/s10533-007-9105-3.

Levene, H. (1960). *Robust tests for equality of variances, contribution to probability and statistics essays in honor of Harold Hotelling*. Stanford University Press.

Lewis, T., Verstraten, L., Hogg, B., Wehr, B. J., Swift, S., Tindale, N., Menzies, N. W., Dalal, R. C., Bryant, P., Francis, B., and Smith, T. E. (2019). Reforestation of agricultural land in the Tropics: The relative contribution of soil, living biomass and debris pools to carbon sequestration. *Sci. Total Environ.* **649**, 1502–1513. DOI: 10.1016/j.scitotenv.2018.08.351.

Li, G., Wan, L., Cui, M., Wu, B., and Zhou, J. (2019). Influence of canopy interception and rainfall kinetic energy on soil erosion under forests. *Forests* **10**.(6). DOI: 10.3390/f10060509.

Li, Q., Wang, X., Jiang, M., Wu, Y., Yang, X., Liao, C., and Liu, F. (2017). How environmental and vegetation factors affect spatial patterns of soil carbon and nitrogen in a subtropical mixed forest in Central China. *J. Soils Sediments* **17** (9), 2296–2304. DOI: 10.1007/s11368-016-1491-5.

Li, X., McCarty, G. W., Karlen, D. L., and Cambardella, C. A. (2018). Topographic metric predictions of soil redistribution and organic carbon in Iowa cropland fields. *Catena* **160**, 222–232. DOI: 10.1016/j.catena.2017.09.026.

Li, Y., Quine, T., Yu, H., Govers, G., Six, J., Gong, D., Wang, Z., Zhang, Y., and Oost, K. V. (2015). Sustained high magnitude erosional forcing generates an organic carbon sink: Test and implications in the Loess Plateau, China. *Earth Planet. Sci. Lett.* **411**, 281–289. DOI: 10.1016/j.epsl.2014.11.036.

Liptzin, D., Silver, W. L., and Detto, M. (2011). Temporal dynamics in soil oxygen and greenhouse gases in two humid tropical forests. *Ecosystems* **14** (2), 171–182. DOI: 10.1007/s10021-010-9402-x.

Liu, J., Liang, Y., Gao, G., Dunkerley, D., and Fu, B. (2022). Quantifying the effects of rainfall intensity fluctuation on runoff and soil loss: From indicators to models. *J. Hydrol.* **607**, 127494. DOI: 10.1016/j.jhydrol.2022.127494.

Liu, J., Chen, J., Chen, G., Guo, J., and Li, Y. (2020). Enzyme stoichiometry indicates the variation of microbial nutrient requirements at different soil depths in subtropical forests. *PLoS ONE* **15** (2). DOI: 10.1371/journal.pone.0220599.

Liu, Y., He, N., Wen, X., Xu, L., Sun, X., Yu, G., Liang, L., and Schipper, L. A. (2018). The optimum temperature of soil microbial respiration: Patterns and controls. *Soil Biol. Biochem.* **121**, 35–42. DOI: 10.1016/j.soilbio.2018.02.019.

López-Vicente, M., Fujiwara, S., Onda, Y., Kozuka, S., Wakiyama, Y., and Kato, H. (2023). Combined use of UAV-SfM surveys, soil particle tracking with RFID tags and a sediment connectivity index to study plot-scale sediment transport. *Sci. Total Environ.* **891**, 164545. DOI: 10.1016/j.scitotenv.2023.164545.

Lowder, S. K., Skoet, J., and Raney, T. (2016). The number, size, and distribution of farms, smallholder farms, and family farms worldwide. *World Development* **87**, 16–29. DOI: 10.1016/j.worlddev.2015.10.041.

Lugato, E., Smith, P., Borrelli, P., Panagos, P., Ballabio, C., Orgiazzi, A., Fernandez-Ugalde, O., Montanarella, L., and Jones, A. (2018). Soil erosion is unlikely to drive a future carbon sink in Europe. *Sci. Adv.* **4**, eaau3523. DOI: 10.1126/sciadv.aau3523. URL: http://advances.sciencemag.org/.

Luo, X., Hou, E., Zhang, L., and Wen, D. (2020a). Soil carbon dynamics in different types of subtropical forests as determined by density fractionation and stable isotope analysis. *For. Ecol. Manage.* **475**. DOI: 10.1016/j.foreco.2020.118401.

Luo, Z., Luo, Y., Wang, G., Xia, J., and Peng, C. (2020b). Warming-induced global soil carbon loss attenuated by downward carbon movement. *Global Change Biol.* **26** (12), 7242–7254. DOI: 10.1111/gcb.15370.

Luo, Z., Wang, E., and Smith, C. (2015). Fresh carbon input differentially impacts soil carbon decomposition across natural and managed systems. *Ecology* **96** (10), 2806–2813. DOI: 10.1890/14-2228.1.

Lützow, M. von, Kögel-Knabner, I., Ekschmitt, K., Flessa, H., Guggenberger, G., Matzner, E., and Marschner, B. (2007). SOM fractionation methods: Relevance to functional pools and to stabilization mechanisms. *Soil Biol. Biochem.* **39** (9), 2183–2207. DOI: 10.1016/j.soilbio.2007.03.007.

Luyssaert, S., Inglima, I., Jung, M., Richardson, A. D., Reichstein, M., Papale, D., Piao, S. L., Schulze, E. D., Wingate, L., Matteucci, G., Aragao, L., Aubinet, M., Beer, C., Bernhofer, C., Black, K. G., Bonal, D., Bonnefond, J. M., Chambers, J., Ciais, P., Cook, B., Davis, K. J., Dolman, A. J., Gielen, B., Goulden, M., Grace, J., Granier, A., Grelle, A., Griffis, T., Grünwald, T., Guidolotti, G., Hanson, P. J., Harding, R., Hollinger, D. Y., Hutyra, L. R., Kolari, P., Kruijt, B., Kutsch, W., Lagergren, F., Laurila, T., Law, B. E., Maire, G. L., Lindroth, A., Loustau, D., Malhi, Y., Mateus, J., Migliavacca, M., Misson, L., Montagnani, L., Moncrieff, J., Moors, E., Munger, J. W., Nikinmaa, E., Ollinger, S. V., Pita, G., Rebmann, C., Roupsard, O., Saigusa, N., Sanz, M. J., Seufert, G., Sierra, C., Smith, M. L., Tang, J., Valentini, R., Vesala, T., and Janssens, I. A. (2007). CO2 balance of boreal, temperate, and tropical forests derived from a global database. *Global Change Biol.* **13** (12), 2509–2537. DOI: 10.1111/j.1365-2486.2007.01439.x.

Mainka, M., Summerauer, L., Wasner, D., Garland, G., Griepentrog, M., Berhe, A. A., and Doetterl, S. (2022). Soil geochemistry as a driver of soil organic matter composition: insights from a soil chronosequence. *Biogeosciences* **19**.(6), 1675–1689. DOI: 10.5194/bg-19-1675-2022.

Malik, A. A., Puissant, J., Buckeridge, K. M., Goodall, T., Jehmlich, N., Chowdhury, S., Gweon, H. S., Peyton, J. M., Mason, K. E., Agtmaal, M. V., Blaud, A., Clark, I. M., Whitaker, J., Pywell, R. F., Ostle, N., Gleixner, G., and Griffiths, R. I. (2018). Land use driven change in soil pH affects microbial carbon cycling processes. *Nat. Commun.* **9**.(1), 3591. DOI: 10.1038/s41467-018-05980-1.

Mangaza, L., Sonwa, D. J., Batsi, G., Ebuy, J., and Kahindo, J. M. (2021). Building a framework towards climate-smart agriculture in the Yangambi landscape, Democratic Republic of Congo (DRC). *Int. J. Clim. Change Strategies Manage.* **13** (3), 320–338. DOI: 10.1108/IJCCSM-08-2020-0084.

Marin-Spiotta, E., Chadwick, O. A., Kramer, M., and Carbone, M. S. (2011). Carbon delivery to deep mineral horizons in Hawaiian rain forest soils. *J. Geophys. Res.: Biogeosci.* **116** (3). DOI: 10.1029/2010JG001587.

Marín-Spiotta, E., Swanston, C. W., Torn, M. S., Silver, W. L., and Burton, S. D. (2008). Chemical and mineral control of soil carbon turnover in abandoned tropical pastures. *Geoderma* **143** (1-2), 49–62. DOI: 10.1016/j.geoderma.2007.10.001.

Marthews, T. R., Riutta, T., Menor, I. O., Urrutia, R., Moore, S., Metcalfe, D., Malhi, Y., Phillips, O., Huasco, W. H., Jaén, M. R., Girardin, C., Butt, N., Cain, R., RAINFOR, and Networks, G. (2014). *Measuring tropical forest carbon allocation and cycling: A RAINFOR-GEM field manual for intensive census plots (v3.0).*

Martinez, P. and Souza, I. F. (2020). *Genesis of pseudo-sand structure in Oxisols from Brazil – A review.* DOI: 10.1016/j.geodrs.2020.e00292.

Mathieu, J. A., Hatté, C., Balesdent, J., and Parent, É. (2015). Deep soil carbon dynamics are driven more by soil type than by climate: A worldwide meta-analysis of radiocarbon profiles. *Global Change Biol.* **21** (11), 4278–4292. DOI: 10.1111/gcb.13012.

McNally, S. R., Beare, M. H., Curtin, D., Meenken, E. D., Kelliher, F. M., Pereira, R. C., Shen, Q., and Baldock, J. (2017). Soil carbon sequestration potential of permanent pasture and continuous cropping soils in New Zealand. *Global Change Biol.* **23** (11), 4544–4555. DOI: 10.1111/gcb.13720.

Megevand, C. (2013). *Deforestation trends in the Congo Basin. Reconciling economic growth and forest protection.* World Bank, pp. 0–158.

Mehra, O. P. and Jackson, M. L. (1958). Iron oxide removal from soils and clays by a dithionite-citrate system buffered with sodium bicarbonate. *Clay. Clay Miner.* **7**, 317–327. DOI: 10.1346/CCMN.1958.0070122.

Mendez, J. C., Eynde, E. V., Hiemstra, T., and Comans, R. N. (2022). Surface reactivity of the natural metal (hydr)oxides in weathered tropical soils. *Geoderma* **406**, 115517. DOI: 10.1016/j.geoderma.2021.115517.

Mikutta, R., Kleber, M., Torn, M. S., and Jahn, R. (2006). Stabilization of soil organic matter: Association with minerals or chemical recalcitrance? *Biogeochemistry* **77** (1), 25–56. DOI: 10.1007/s10533-005-0712-6.

Mikutta, R., Schaumann, G. E., Gildemeister, D., Bonneville, S., Kramer, M. G., Chorover, J., Chadwick, O. A., and Guggenberger, G. (2009). Biogeochemistry of mineral-organic associations across a long-term mineralogical soil gradient (0.3-4100 kyr), Hawaiian Islands. *Geochim. Cosmochim. Acta* **73**.(7), 2034–2060. DOI: 10.1016/j.gca.2008.12.028.

Mikutta, R., Turner, S., Schippers, A., Gentsch, N., Meyer-Stüve, S., Condron, L. M., Peltzer, D. A., Richardson, S. J., Eger, A., Hempel, G., Kaiser, K., Klotzbücher, T., and Guggenberger, G. (2019). Microbial and abiotic controls on mineral-associated organic matter in soil profiles along an ecosystem gradient. *Sci. Rep.* **9**.(1). DOI: 10.1038/s41598-019-46501-4.

Minasny, B., Stockmann, U., Hartemink, A. E., and McBratney, A. B. (2016). "Measuring and modelling soil depth functions". Ed. by A. Hartemink and B. Minansny. Springer, pp. 225–240. DOI: 10.1007/978-3-319-28295-4_14.

Moder, K. (2016). How to keep the type I error rate in ANOVA if variances are heteroscedastic. *Austrian Journal of Statistics* **36** (3). DOI: 10.17713/ajs.v36i3.329.

Mokwunye, A. U. and Hammond, L. L. (1992). "Myths and science of fertilizer use in the Tropics". Ed. by R. Lal and P. A. Sanchez. Vol. 29. SSSA Special Publications, pp. 121–134. DOI: 10.2136/sssaspecpub29.c7.

Molina, A., Vanacker, V., Corre, M. D., and Veldkamp, E. (2019). Patterns in soil chemical weathering related to topographic gradients and vegetation structure in a high Andean tropical ecosystem. *J. Geophys. Res.: Earth Surf.* **124**.(2), 666–685. DOI: 10.1029/2018JF004856.

Moyano, F. E., Vasilyeva, N., Bouckaert, L., Cook, F., Craine, J., Yuste, J. C., Don, A., Epron, D., Formanek, P., Franzluebbers, A., Ilstedt, U., Kätterer, T., Orchard, V., Reichstein, M., Rey, A., Ruamps, L., Subke, J. A., Thomsen, I. K., and Chenu, C. (2012). The moisture response of soil heterotrophic respiration: Interaction with soil properties. *Biogeosciences* **9**.(3), 1173–1182. DOI: 10.5194/bg-9-1173-2012.

Munyakazi, F. M., Maniriho, A., Ciza, A. N., Iyoto, E. B., Lukeba, F. N., Ngerizabona, S. V., Mirindi, G. F., Namegabe, J.-L. M., and Lebailly, P. (2022). Characterization of small-scale farming as an engine of agricultural development in mountainous South Kivu, Democratic

Republic of Congo. *Asian Journal of Agriculture and Rural Development* **12**.(2), 123–129. DOI: 10.55493/5005.v12i2.4475.

Murphy, E. M., Zachara, J. M., Smith, S. C., and Phillips, J. L. (1992). The sorption of humic acids to mineral surfaces and their role in contaminant binding. *Sci. Total Environ.* **117**, 413–423.

Nadeu, E., Berhe, A. A., Vente, J. D., and Boix-Fayos, C. (2012). Erosion, deposition and replacement of soil organic carbon in Mediterranean catchments: A geomorphological, isotopic and land use change approach. *Biogeosciences* **9**.(3), 1099–1111. DOI: 10.5194/bg-9-1099-2012.

Nadeu, E., Gobin, A., Fiener, P., Wesemael, B. V., and Oost, K. V. (2015). Modelling the impact of agricultural management on soil carbon stocks at the regional scale: The role of lateral fluxes. *Global Change Biol.* **21**.(8), 3181–3192. DOI: 10.1111/gcb.12889.

Naipal, V., Ciais, P., Wang, Y., Lauerwald, R., Guenet, B., and Oost, K. V. (2018). Global soil organic carbon removal by water erosion under climate change and land use change during AD 1850–2005. *Biogeosciences* **15**.(14), 4459–4480. DOI: 10.5194/bg-15-4459-2018.

Nelson, D. W. and Sommers, L. E. (1996). "Total carbon, organic carbon, and organic matter". SSSA, pp. 0–1390. DOI: 10.2136/sssabookser5.3.c34.

Nijs, E. A. de and Cammeraat, E. L. (2020). The stability and fate of soil organic carbon during the transport phase of soil erosion. *Earth Sci. Rev.* **201**, 103067. DOI: 10.1016/j.earscirev.2019.103067.

Nottingham, A. T., Fierer, N., Turner, B. L., Whitaker, J., Ostle, N. J., McNamara, N. P., Bardgett, R. D., Leff, J. W., Salinas, N., Silman, M. R., Kruuk, L. E. B., and Meir, P. (2018). Microbes follow Humboldt: temperature drives plant and soil microbial diversity patterns from the Amazon to the Andes. *Ecology* **99** (11), 2455–2466. DOI: 10.1002/ecy.2482.

Nottingham, A. T., Gloor, E., Bååth, E., and Meir, P. (2022). Soil carbon and microbes in the warming Tropics. *Funct. Ecol.* **36** (6), 1338–1354. DOI: 10.1111/1365-2435.14050.

Nottingham, A. T., Meir, P., Velasquez, E., and Turner, B. L. (2020). Soil carbon loss by experimental warming in a tropical forest. *Nature* **584**.(7820), 234–237. DOI: 10.1038/s41586-020-2566-4.

Nottingham, A. T., Turner, B. L., Stott, A. W., and Tanner, E. V. (2015). Nitrogen and phosphorus constrain labile and stable carbon turnover in lowland tropical forest soils. *Soil Biol. Biochem.* **80**, 26–33. DOI: 10.1016/j.soilbio.2014.09.012.

Nunes, J. P., Wainwright, J., Bielders, C. L., Darboux, F., Fiener, P., Finger, D., and Turnbull, L. (2018). Better models are more effectively connected models. *Earth Surf. Processes Landforms* **43** (6), 1355–1360. DOI: 10.1002/esp.4323.

Nyakudya, I. W. and Stroosnijder, L. (2015). Conservation tillage of rainfed maize in semi-arid Zimbabwe: A review. *Soil Tillage Res.* **145**, 184–197. DOI: 10.1016/j.still.2014.09.003.

Oades, J. M. (1988). The retention of organic matter in soils. *Biogeochemistry* **5**, 35–70.

Oades, J. M. (1984). Soil organic matter and structural stability: mechanisms and implications for management. *Plant Soil* **76** (1-3), 319–337. DOI: 10.1007/BF02205590.

Obidike-Ugwu, E. O., Bege, B., Ariwaodo, J. O., and Nwafor, O. E. (2023). Land-use changes and management impact on soil quality indicators in tropical ecosystem. *Environ. Dev. Sustainability.* DOI: 10.1007/s10668-023-04026-x.

Okalebo, J. R., Gathua, K. W., and Woomer, P. L. (2002). *Laboratory methods of soil and plant analysis: A working manual.* 4th. SACRED Africa, pp. 0–131.

Olorunfemi, I. E., Olufayo, A. A., Fasinmirin, J. T., and Komolafe, A. A. (2022). Dynamics of land use land cover and its impact on carbon stocks in sub-Saharan Africa: An overview. *Environ. Dev. Sustainability* **24**.(1), 40–76. DOI: 10.1007/s10668-021-01484-z.

Oost, K. V., Govers, G., Alba, S. de, and Quine, T. A. (2006). Tillage erosion: A review of controlling factors and implications for soil quality. *Prog. Phys. Geogr.* **30** (4), 443–466. DOI: 10.1191/0309133306pp487ra.

Oost, K. V., Muysen, W. V., Govers, G., Deckers, J., and Quine, T. (2005). From water to tillage erosion dominated landform evolution. *Geomorphology* **72** (1-4), 193–203. DOI: 10.1016/j.geomorph.2005.05.010.

Oost, K. V., Quine, T. A., Govers, G., Gryze, S. D., Six, J., Harden, J. W., Ritchie, J. C., McCarty, G. W., Heckrath, G., Kosmas, C., Giraldez, J. V., Silva, J. R. M. da, and Merckx, R. (2007). The impact of agricultural soil erosion on the global carbon cycle. *Science* **318**.(5850), 626–629. DOI: 10.1126/science.1145724.

Oost, K. V., Govers, G., and Desmet, P. (2000). Evaluating the effects of changes in landscape structure on soil erosion by water and tillage. *Landscape Ecology* **15**.(6), 577–589. DOI: 10.1023/A:1008198215674.

Oost, K. V. and Six, J. (2023). Reconciling the paradox of soil organic carbon erosion by water. *Biogeosciences* **20**.(3), 635–646. DOI: 10.5194/bg-20-635-2023.

Ordway, E. M., Asner, G. P., and Lambin, E. F. (2017). Deforestation risk due to commodity crop expansion in sub-Saharan Africa. *Environ. Res. Lett.* **12**.(4). DOI: 10.1088/1748-9326/aa6509.

Öttl, L. K., Wilken, F., Juřicová, A., Batista, P. V. G., and Fiener, P. (2024). A millennium of arable land use – the long-term impact of tillage and water erosion on landscape-scale carbon dynamics. *SOIL* **10**, 281–305. DOI: 10.5194/soil-10-281-2024.

Öttl, L. K., Wilken, F., Auerswald, K., Sommer, M., Wehrhan, M., and Fiener, P. (2021). Tillage erosion as an important driver of in-field biomass patterns in an intensively used hummocky landscape. *Land Degrad. Dev.* **32** (10), 3077–3091. DOI: 10.1002/ldr.3968.

Ozlu, E. and Arriaga, F. J. (2021). The role of carbon stabilization and minerals on soil aggregation in different ecosystems. *Catena* **202**, 105303. DOI: 10.1016/j.catena.2021.105303.

Padarian, J., Stockmann, U., Minasny, B., and McBratney, A. (2022). Monitoring changes in global soil organic carbon stocks from space. *Remote Sens. Environ.* **281**, 113260. DOI: 10.1016/j.rse.2022.113260.

Palm, C., Sanchez, P., Ahamed, S., and Awiti, A. (2007). Soils: A contemporary perspective. *Annu. Rev. Environ. Resour.* **32** (1), 99–129. DOI: 10.1146/annurev.energy.31.020105.100307.

Pan, Y., Birdsey, R. A., Fang, J., Houghton, R., Kauppi, P. E., Kurz, W. A., Phillips, O. L., Shvidenko, A., Lewis, S. L., Canadell, J. G., Ciais, P., Jackson, R. B., Pacala, S. W., McGuire, A. D., Piao, S., Rautiainen, A., Sitch, S., and Hayes, D. (2011). A large and persistent carbon sink in the world's forests. *Science* **333** (6045), 988–993. DOI: 10.1126/science.1201609.

Panagos, P., Borrelli, P., Meusburger, K., Yu, B., Klik, A., Lim, K. J., Yang, J. E., Ni, J., Miao, C., Chattopadhyay, N., Sadeghi, S. H., Hazbavi, Z., Zabihi, M., Larionov, G. A., Krasnov, S. F., Gorobets, A. V., Levi, Y., Erpul, G., Birkel, C., Hoyos, N., Naipal, V., Oliveira, P. T. S., Bonilla, C. A., Meddi, M., Nel, W., Dashti, H. A., Boni, M., Diodato, N., Oost, K. V., Nearing, M., and Ballabio, C. (2017). Global rainfall erosivity assessment based on high-temporal resolution rainfall records. *Sci. Rep.* **7**.(1). DOI: 10.1038/s41598-017-04282-8.

Park, J. H., Meusburger, K., Jang, I., Kang, H., and Alewell, C. (2014). Erosion-induced changes in soil biogeochemical and microbiological properties in Swiss Alpine grasslands. *Soil Biol. Biochem.* **69**, 382–392. DOI: 10.1016/j.soilbio.2013.11.021.

Paul, S., Flessa, H., Veldkamp, E., and López-Ulloa, M. (2008). Stabilization of recent soil carbon in the humid tropics following land use changes: Evidence from aggregate fractionation and stable isotope analyses. *Biogeochemistry* **87**.(3), 247–263. DOI: 10.1007/s10533-008-9182-y.

Pauwels, J. M., Ranst, E. V., and Verloo, M. (1992). *Manuel de laboratoire de pédologie: Methods d'analyse de sols et de plantes, équipement, gestion de stocks de verrerie et de produits chimiques.*

Perrin, A. S., Fujisaki, K., Petitjean, C., Sarrazin, M., Godet, M., Garric, B., Horth, J. C., Balbino, L. C., Filho, A. S., Almeida Machado, P. L. O. de, and Brossard, M. (2014). Conversion of forest to agriculture in Amazonia with the chop-and-mulch method: Does it improve the soil carbon stock? *Agriculture, Ecosystems and Environment* **184**, 101–114. DOI: 10.1016/j.agee.2013.11.009.

Poeplau, C., Don, A., Dondini, M., Leifeld, J., Nemo, R., Schumacher, J., Senapati, N., and Wiesmeier, M. (2013). Reproducibility of a soil organic carbon fractionation method to derive RothC carbon pools. *Eur. J. Soil Sci.* **64** (6), 735–746. DOI: 10.1111/ejss.12088.

Porder, S., Paytan, A., and Vitousek, P. M. (2005). Erosion and landscape development affect plant nutrient status in the Hawaiian Islands. *Oecologia* **142** (3), 440–449. DOI: 10.1007/s00442-004-1743-8.

Possinger, A. R., Zachman, M. J., Enders, A., Levin, B. D., Muller, D. A., Kourkoutis, L. F., and Lehmann, J. (2020). Organo–organic and organo–mineral interfaces in soil at the nanometer scale. *Nat. Commun.* **11**.(1). DOI: 10.1038/s41467-020-19792-9.

Price, J. R., Velbel, M. A., and Patino, L. C. (2005). Rates and time scales of clay-mineral formation by weathering in saprolitic regoliths of the southern Appalachians from geochemical mass balance. *Geol. Soc. Am. Bull.* **117**.(5), 783. DOI: 10.1130/B25547.1.

Quesada, C. A., Paz, C., Mendoza, E. O., Phillips, O. L., Saiz, G., and Lloyd, J. (2020). Variations in soil chemical and physical properties explain basin-wide Amazon forest soil carbon concentrations. *SOIL* **6** (1), 53–88. DOI: 10.5194/soil-6-53-2020.

Quijano, L., Aldana-Jague, E., Heckrath, G., and Oost, K. V. (2021). Estimating temporal and spatial changes in soil organic carbon stocks and its controlling factors in moraine landscapes in Denmark. *Catena* **206**, 105502. DOI: 10.1016/j.catena.2021.105502.

Quinton, J. N., Govers, G., Oost, K. V., and Bardgett, R. D. (2010). The impact of agricultural soil erosion on biogeochemical cycling. *Nat. Geosci.* **3**.(5), 311–314. DOI: 10.1038/ngeo838.

Raich, J. W., Russell, A. E., Kitayama, K., Parton, W. J., and Vitousek, P. M. (2006). Temperature influences carbon accumulation in moist tropical forests. *Ecology* **87** (1), 76–87. DOI: 10.1890/05-0023.

Rasmussen, C., Heckman, K., Wieder, W. R., Keiluweit, M., Lawrence, C. R., Berhe, A. A., Blankinship, J. C., Crow, S. E., Druhan, J. L., Pries, C. E. H., Marin-Spiotta, E., Plante, A. F., Schädel, C., Schimel, J. P., Sierra, C. A., Thompson, A., and Wagai, R. (2018). Beyond clay: towards an improved set of variables for predicting soil organic matter content. *Biogeochemistry* **137**.(3), 297–306. DOI: 10.1007/s10533-018-0424-3.

RCoreTeam (2020). *A language and environment for statistical computing.*

Reichenbach, M., Fiener, P., Garland, G., Griepentrog, M., Six, J., and Doetterl, S. (2021). The role of geochemistry in organic carbon stabilization against microbial decomposition in tropical rainforest soils. *SOIL* **7** (2), 453–475. DOI: 10.5194/soil-7-453-2021.

Reichenbach, M., Fiener, P., Hoyt, A., Trumbore, S., Six, J., and Doetterl, S. (2023). Soil carbon stocks in stable tropical landforms are dominated by geochemical controls and not by land use. *Global Change Biol.* **29** (9), 2591–2607. DOI: 10.1111/gcb.16622.

Ren, W., Banger, K., Tao, B., Yang, J., Huang, Y., and Tian, H. (2020). Global pattern and change of cropland soil organic carbon during 1901-2010: Roles of climate, atmospheric chemistry, land use and management. *Geogr. Sustainability* **1** (1), 59–69. DOI: 10.1016/j.geosus.2020.03.001.

Rennert, T. (2019). Wet-chemical extractions to characterise pedogenic Al and Fe species-a critical review. *Soil Res.* **57**.(1), 1–16. DOI: 10.1071/SR18299.

Rizinjirabake, F., Nyiramana, A., Kamizikunze, T., and Mukamugema, J. (2023). Estimating soil erosion to highlight potential areas for conservation priority in Rukarara Catchment, South-

Western Rwanda. *Rwanda Journal of Engineering, Science, Technology and Environment* **5**.(1), 1–23. DOI: 10.4314/rjeste.v5i1.1.

Rodríguez-Albarracín, H. S., Demattê, J. A., Rosin, N. A., Contreras, A. E. D., Silvero, N. E., Cerri, C. E. P., Sousa Mendes, W. de, and Tayebi, M. (2023). Potential of soil minerals to sequester soil organic carbon. *Geoderma* **436**, 116549. DOI: 10.1016/j.geoderma.2023.116549.

Roering, J. J., Hunter, B. D., Ferrier, K. L., Chadwick, O. A., Yoo, K., Wackett, A. A., Almond, P. C., Silva, L., and Jellinek, A. M. (2023). Quantifying erosion rates and weathering pathways that maximize soil organic carbon storage. *Biogeochemistry* **164**.(2), 319–333. DOI: 10.1007/s10533-023-01054-7.

Román-Sánchez, A., Laguna, A., Reimann, T., Giráldez, J. V., Peña, A., and Vanwalleghem, T. (2019a). Bioturbation and erosion rates along the soil-hillslope conveyor belt, part 2: Quantification using an analytical solution of the diffusion–advection equation. *Earth Surf. Processes Landforms* **44** (10), 2066–2080. DOI: 10.1002/esp.4626.

Román-Sánchez, A., Reimann, T., Wallinga, J., and Vanwalleghem, T. (2019b). Bioturbation and erosion rates along the soil-hillslope conveyor belt, part 1: Insights from single-grain feldspar luminescence. *Earth Surf. Processes Landforms* **44** (10), 2051–2065. DOI: 10.1002/esp.4628.

Rosalem, L. M. P., Wendland, E. C., and Anache, J. A. A. (2019). Understanding the water dynamics on a tropical forest litter using a new device for interception measurement. *Ecohydrology* **12**.(2). DOI: 10.1002/eco.2058.

Rumpel, C., Amiraslani, F., Chenu, C., Cardenas, M. G., Kaonga, M., Koutika, L. S., Ladha, J., Madari, B., Shirato, Y., Smith, P., Soudi, B., Soussana, J. F., Whitehead, D., and Wollenberg, E. (2020). The 4p1000 initiative: Opportunities, limitations and challenges for implementing soil organic carbon sequestration as a sustainable development strategy. *Ambio* **49**.(1), 350–360. DOI: 10.1007/s13280-019-01165-2.

Sæther, A. H., Moen, K. L. E., Singh, B. R., Lal, R., and Kilasara, M. (1997). Soil management and topsoil thickness effects on maize for two Tanzanian soils. *J. Sustain. Agric.* **10** (1), 43–61. DOI: 10.1300/J064v10n01_06.

Šamonil, P., Phillips, J., Daněk, P., Beneš, V., and Pawlik, L. (2020). Soil, regolith, and weathered rock: Theoretical concepts and evolution in old-growth temperate forests, Central Europe. *Geoderma* **368**, 114261. DOI: 10.1016/j.geoderma.2020.114261.

Sanchez, P. A. and Logan, T. J. (1992). “Myths and science about the chemistry and fertility of soils in the Tropics”. Ed. by R. Lal and P. A. Sanchez. Vol. 29. SSSA Special Publications, pp. 35–46. DOI: 10.2136/sssaspecpub29.c3.

Sanderman, J. and Chappell, A. (2013). Uncertainty in soil carbon accounting due to unrecognized soil erosion. *Global Change Biol.* **19** (1), 264–272. DOI: 10.1111/gcb.12030.

Sanderman, J., Hengl, T., and Fiske, G. J. (2017). Soil carbon debt of 12,000 years of human land use. *Proc. Natl. Acad. Sci.* **114**.(36), 9575–9580. DOI: 10.1073/pnas.1706103114.

Sanogo, K., Birhanu, B. Z., Sanogo, S., and Ba, A. (2023). Landscape pattern analysis using GIS and remote sensing to diagnose soil erosion and nutrient availability in two agroecological zones of Southern Mali. *Agric. Food Secur.* **12**.(1), 4. DOI: 10.1186/s40066-023-00408-6.

Sayer, E. J., Lopez-Sangil, L., Crawford, J. A., Bréchet, L. M., Birkett, A. J., Baxendale, C., Castro, B., Rodtassana, C., Garnett, M. H., Weiss, L., and Schmidt, M. W. (2019). Tropical forest soil carbon stocks do not increase despite 15 years of doubled litter inputs. *Sci. Rep.* **9**.(1). DOI: 10.1038/s41598-019-54487-2.

Schaefer, C. E. G. R., Souza, J. J. L. L. de, Oliveira, F. S. de, Corrêa, G. R., and Filho, E. I. F. (2022). “The geological, geomorphological, climatic, and hydrological background of tropical regoliths and hostile subsoils: The Brazilian landmass”. *Subsoil Constraints for Crop Production.* Springer International Publishing, pp. 11–52. DOI: 10.1007/978-3-031-00317-2_2.

Schimel, D., Pavlick, R., Fisher, J. B., Asner, G. P., Saatchi, S., Townsend, P., Miller, C., Frankenberg, C., Hibbard, K., and Cox, P. (2015). Observing terrestrial ecosystems and the carbon cycle from space. *Global Change Biol.* **21** (5), 1762–1776. DOI: 10.1111/gcb.12822.

Schlüter, T. and Trauth, M. H. (2006). *Geological atlas of Africa: with notes on stratigraphy, tectonics, economic geology, geohazards and geosites of each country.* Springer, p. 272. ISBN: 9783540291442.

Schmidt, M. W., Torn, M. S., Abiven, S., Dittmar, T., Guggenberger, G., Janssens, I. A., Kleber, M., Kögel-Knabner, I., Lehmann, J., Manning, D. A., Nannipieri, P., Rasse, D. P., Weiner, S., and Trumbore, S. E. (2011). Persistence of soil organic matter as an ecosystem property. *Nature* **478** (7367), 49–56. DOI: 10.1038/nature10386.

Schneider, M. P., Scheel, T., Mikutta, R., Hees, P. V., Kaiser, K., and Kalbitz, K. (2010). Sorptive stabilization of organic matter by amorphous Al hydroxide. *Geochim. Cosmochim. Acta* **74**.(5), 1606–1619. DOI: 10.1016/j.gca.2009.12.017.

Schrumpf, M., Kaiser, K., Mayer, A., Hempel, G., and Trumbore, S. (2021). Age distribution, extractability, and stability of mineral-bound organic carbon in central European soils. *Biogeosciences* **18** (3), 1241–1257. DOI: 10.5194/bg-18-1241-2021.

Schuppli, P. A., Ross, G. J., and McKeague, J. A. (1983). The Effective Removal of Suspended Materials from Pyrophosphate Extracts of Soils from Tropical and Temperate Regions. *Soil Sci. Soc. Am. J.* **47** (5), 1026–1032. DOI: 10.2136/sssaj1983.03615995004700050037x.

Senaviratna, N. A. M. R. and Cooray, T. M. J. A. (2019). Diagnosing multicollinearity of logistic regression model. *Asian Journal of Probability and Statistics*, 1–9. DOI: 10.9734/ajpas/2019/v5i230132.

Sheng, H., Yang, Y., Yang, Z., Chen, G., Xie, J., Guo, J., and Zou, S. (2010). The dynamic response of soil respiration to land-use changes in subtropical China. *Global Change Biol.* **16** (3), 1107–1121. DOI: 10.1111/j.1365-2486.2009.01988.x.

Sheng, H., Zhou, P., Zhang, Y., Kuzyakov, Y., Zhou, Q., Ge, T., and Wang, C. (2015). Loss of labile organic carbon from subsoil due to land-use changes in subtropical China. *Soil Biol. Biochem.* **88**, 148–157. DOI: 10.1016/j.soilbio.2015.05.015.

Shi, P., Oost, K. V., and Schulin, R. (2017). Dynamics of soil fragment size distribution under successive rainfalls and its implication to size-selective sediment transport and deposition. *Geoderma* **308**, 104–111. DOI: 10.1016/j.geoderma.2017.08.038.

Shi, Z., Allison, S. D., He, Y., Levine, P. A., Hoyt, A. M., Beem-Miller, J., Zhu, Q., Wieder, W. R., Trumbore, S., and Randerson, J. T. (2020). The age distribution of global soil carbon inferred from radiocarbon measurements. *Nat. Geosci.* **13** (8), 555–559. DOI: 10.1038/s41561-020-0596-z.

Silva Oliveira, D. M. da, Paustian, K., Cotrufo, M. F., Fiallos, A. R., Cerqueira, A. G., and Cerri, C. E. P. (2017). Assessing labile organic carbon in soils undergoing land use change in Brazil: A comparison of approaches. *Ecol. Indic.* **72**, 411–419. DOI: 10.1016/j.ecolind.2016.08.041.

Silver, W. L., Ostertag, R., and Lugo, A. E. (2001). The Potential for carbon sequestration through reforestation of abandoned tropical agricultural and pasture lands. *Restor. Ecol.* **8** (4), 394–407. DOI: 10.1046/j.1526-100x.2000.80054.x.

Silver, W. L., Kueppers, L. M., Lugo, A. E., Ostertag, R., and Matzek, V. (2004). Carbon sequestration and plant community dynamics following reforestation of tropical pasture. *Ecol. Appl.* **14** (4), 1115–1127. DOI: 10.1890/03-5123.

Silver, W. L., Lugo, A. E., and Keller, M. (1999). Soil oxygen availability and biogeochemistry along rainfall and topographic gradients in upland wet tropical forest soils. *Biogeochemistry* **44**.(9), 301–328.

Simpson, R. T., Frey, S. D., Six, J., and Thiet, R. K. (2004). Preferential accumulation of microbial carbon in aggregate structures of no-tillage soils. *Soil Sci. Soc. Am. J.* **68** (4), 1249–1255. DOI: 10.2136/sssaj2004.1249.

Singh, M., Sarkar, B., Bolan, N. S., Ok, Y. S., and Churchman, G. J. (2019). Decomposition of soil organic matter as affected by clay types, pedogenic oxides and plant residue addition rates. *J. Hazard. Mater.* **374**, 11–19. DOI: 10.1016/j.jhazmat.2019.03.135.

Singh, N., Abiven, S., Torn, M. S., and Schmidt, M. W. (2012). Fire-derived organic carbon in soil turns over on a centennial scale. *Biogeosciences* **9**.(8), 2847–2857. DOI: 10.5194/bg-9-2847-2012.

Sisheber, B., Marshall, M., Mengistu, D., and Nelson, A. (2023). Detecting the long-term spatiotemporal crop phenology changes in a highly fragmented agricultural landscape. *Agricultural and Forest Meteorology* **340**. DOI: 10.1016/j.agrformet.2023.109601.

Six, J., Bossuyt, H., Degryze, S., and Denef, K. (2004). A history of research on the link between (micro)aggregates, soil biota, and soil organic matter dynamics. *Soil Till. Res.* **79** (1), 7–31. DOI: 10.1016/j.still.2004.03.008.

Six, J., Conant, R. T., Paul, E. A., and Paustian, K. (2002a). Stabilization mechanisms of soil organic matter: Implications for C-saturation of soils. *Plant Soil* **241**, 155–176.

Six, J., Elliott, E. T., and Paustian, K. (2000a). Soil macroaggregate turnover and microaggregate formation: a mechanism for C sequestration under no-tillage agriculture. *Soil Biol. Biochem.* **32**, 2099–2103. DOI: 10.1016/S0038-0717(00)00179-6. URL: www.elsevier.com/locate/soilbio.

Six, J., Paustian, K., Elliott, E. T., and Combrink, C. (2000b). Soil structure and organic matter I. Distribution of aggregate-size classes and aggregate-associated carbon. *Soil Sci. Soc. Am. J.* **64**.(2), 681–689. DOI: 10.2136/sssaj2000.642681x.

Six, J., Feller, C., Denef, K., Ogle, S. M., Moraes, J. C. de, and Albrecht, A. (2002b). Soil organic matter, biota and aggregation in temperate and tropical soils - Effects of no-tillage. *Agronomie* **22** (7-8), 755–775. DOI: 10.1051/agro:2002043.

Slessarev, E. W., Chadwick, O. A., Sokol, N. W., Nuccio, E. E., and Pett-Ridge, J. (2022). Rock weathering controls the potential for soil carbon storage at a continental scale. *Biogeochemistry* **157**.(1). DOI: 10.1007/s10533-021-00859-8.

Smith, K. S. (1999). Metal sorption on mineral surfaces: an overview with examples relating to mineral deposits. *Rev. Econ. Geol.* **6**, 161–198. DOI: 10.5382/Rev.06.07.

Song, X., Wang, P., Zwieten, L. V., Bolan, N., Wang, H., Li, X., Cheng, K., Yang, Y., Wang, M., Liu, T., and Li, F. (2022). Towards a better understanding of the role of Fe cycling in soil for carbon stabilization and degradation. *Carbon Res.* **1** (1), 5. DOI: 10.1007/s44246-022-00008-2.

Souza, I. F., Almeida, L. F. J., Jesus, G. L., Kleber, M., and Silva, I. R. (2017). The mechanisms of organic carbon protection and dynamics of C-saturation in Oxisols vary with particle-size distribution. *Eur. J. Soil Sci.* **68** (5), 726–739. DOI: 10.1111/ejss.12463.

Souza, I. F., Almeida, L. F. J., Jesus, G. L., Pett-Ridge, J., Nico, P. S., Kleber, M., and Silva, I. R. (2018). Carbon Sink Strength of Subsurface Horizons in Brazilian Oxisols. *Soil Sci. Soc. Am. J.* **82** (1), 76–86. DOI: 10.2136/sssaj2017.05.0143.

Stallard, R. F. (1998). Terrestrial sedimentation and the carbon cycle: Coupling weathering and erosion to carbon burial. *Global Biogeochem. Cycles* **12**.(2), 231–257. DOI: 10.1029/98GB00741.

Steinhof, A., Altenburg, M., and Machts, H. (2017). "Sample preparation at the Jena 14C laboratory". *Special Issue 3: Proceedings of the 22nd International Radiocarbon Conference (Part 2 of 2)*. Vol. 59. Cambridge University Press, pp. 815–830. DOI: 10.1017/RDC.2017.50.

Stewart, C. E., Plante, A. F., Paustian, K., Conant, R. T., and Six, J. (2008). Soil carbon saturation: linking concept and measurable carbon pools. *Soil Biol. Biochem.* **72** (2), 379–392. DOI: 10.2136/sssaj2007.0104.

Stone, M. M., DeForest, J. L., and Plante, A. F. (2014). Changes in extracellular enzyme activity and microbial community structure with soil depth at the Luquillo Critical Zone Observatory. *Soil Biol. Biochem.* **75**, 237–247. DOI: 10.1016/j.soilbio.2014.04.017.

Stoner, S., Trumbore, S. E., González-Pérez, J. A., Schrumpf, M., Sierra, C. A., Hoyt, A. M., Chadwick, O., and Doetterl, S. (2023). Relating mineral–organic matter stabilization mechanisms to carbon quality and age distributions using ramped thermal analysis. *Philosophical Transactions of the Royal Society A: Mathematical, Physical and Engineering Sciences* **381**.(2261). DOI: 10.1098/rsta.2023.0139.

Stucki, J. W., Goodman, B. A., and Schwertmann, U. (1988). *Iron in soils and clay minerals.* Springer, pp. 0–894.

Stuiver, M. and Polach, H. A. (1977). Discussion reporting of 14C data. *Radiocarbon* **19** (3), 355–363. DOI: 10.1017/s0033822200003672.

Summerauer, L., Baumann, P., Ramirez-Lopez, L., Barthel, M., Bauters, M., Bukombe, B., Reichenbach, M., Boeckx, P., Kearsley, E., Oost, K. V., Vanlauwe, B., Chiragaga, D., Heri-Kazi, A. B., Moonen, P., Sila, A., Shepherd, K., Mujinya, B. B., Ranst, E. V., Baert, G., Doetterl, S., and Six, J. (2021). The central African soil spectral library: a new soil infrared repository and a geographical prediction analysis. *SOIL* **7** (2), 693–715. DOI: 10.5194/soil-7-693-2021.

Swoboda, P., Döring, T. F., and Hamer, M. (2022). Remineralizing soils? The agricultural usage of silicate rock powders: A review. *Sci. Total Environ.* **807**, 150976. DOI: 10.1016/j.scitotenv.2021.150976.

Symeonakis, E. and Drake, N. (2010). 10-Daily soil erosion modelling over sub-Saharan Africa. *Environ. Monit. Assess.* **161** (1-4), 369–387. DOI: 10.1007/s10661-009-0754-7.

Tamale, J., Straaten, O. van, Hüppi, R., Turyagyenda, L. F., Fiener, P., and Doetterl, S. (2022). Soil greenhouse gas fluxes following conversion of tropical forests to fertilizer-based sugarcane systems in northwestern Uganda. *Agric. Ecosyst. Environ.* **333**, 107953. DOI: 10.1016/j.agee.2022.107953.

Tamene, L. and Le, Q. B. (2015). Estimating soil erosion in sub-Saharan Africa based on landscape similarity mapping and using the revised universal soil loss equation (RUSLE). *Nutr. Cycling Agroecosyst.* **102** (1), 17–31. DOI: 10.1007/s10705-015-9674-9.

Tamhane, A. C. (1979). A Comparison of Procedures for Multiple Comparisons of Means with Unequal Variances. *J. Am. Stat. Assoc.* **74** (366), 471–480.

Tang, J. and Riley, W. J. (2015). Weaker soil carbon-climate feedbacks resulting from microbial and abiotic interactions. *Nat. Clim. Change* **5**.(1), 56–60. DOI: 10.1038/nclimate2438.

Tanzito, G., Ibanda, P. A., Talaguma, R., and Lusanga, N. M. (2020). Slash-and-burn agriculture, the major cropping system in the region of Faradje in Democratic Republic of Congo: Ecological and socio-economic consequences. *J. Dev. Agric. Econ.* **12** (1), 25–36. DOI: 10.5897/JDAE2019.1140.

Tardy, Y. and Nahon, D. (1985). Geochemistry of laterites, stability of Al-goethite, Al-hematite, and Fe3+-kaolinite in bauxites and ferricretes: an approach to the mechanism of concretion formation. *Am. J. Sci.* **285** (10), 865–903.

Thomaz, E. L. (2013). Slash-and-burn agriculture: Establishing scenarios of runoff and soil loss for a five-year cycle. *Agric. Ecosyst. Environ.* **168**, 1–6. DOI: 10.1016/j.agee.2013.01.008.

Thompson, A., Chadwick, O. A., Boman, S., and Chorover, J. (2006). Colloid mobilization during soil iron redox oscillations. *Environ. Sci. Technol.* **40**.(18), 5743–5749. DOI: 10.1021/es061203b.

Tian, Q., Wang, D., Li, D., Huang, L., Wang, M., Liao, C., and Liu, F. (2020). Variation of soil carbon accumulation across a topographic gradient in a humid subtropical mountain forest. *Biogeochemistry* **149** (3), 337–354. DOI: 10.1007/s10533-020-00679-2.

Tian, Q., Wang, X., Wang, D., Wang, M., Liao, C., Yang, X., and Liu, F. (2017). Decoupled linkage between soil carbon and nitrogen mineralization among soil depths in a subtropical mixed forest. *Soil Biol. Biochem.* **109**, 135–144. DOI: 10.1016/j.soilbio.2017.02.009.

Tong, M., Yuan, S., Ma, S., Jin, M., Liu, D., Cheng, D., Liu, X., Gan, Y., and Wang, Y. (2016). Production of abundant hydroxyl radicals from oxygenation of subsurface sediments. *Environ. Sci. Technol.* **50** (1), 214–221. DOI: 10.1021/acs.est.5b04323.

Torn, M. S., Trumbore, S. E., Chadwick, O. A., Vitousek, P. M., and Hendricks, D. M. (1997). Mineral control of soil organic carbon storage and turnover. *Nature* **389** (6647), 170–173. DOI: 10.1038/38260.

Torres-Sallan, G., Schulte, R. P. O., Lanigan, G. J., Byrne, K. A., Reidy, B., Simó, I., Six, J., and Creamer, R. E. (2017). Clay illuviation provides a long-term sink for C sequestration in subsoils. *Sci. Rep.* **7**.(1), 45635. DOI: 10.1038/srep45635.

Totsche, K. U., Amelung, W., Gerzabek, M. H., Guggenberger, G., Klumpp, E., Knief, C., Lehndorff, E., Mikutta, R., Peth, S., Prechtel, A., Ray, N., and Kögel-Knabner, I. (2018). Microaggregates in soils. *J. Plant Nutr. Soil Sci.* **181** (1), 104–136. DOI: 10.1002/jpln.201600451.

Trumbore, S. (2009). Radiocarbon and soil carbon dynamics. *Annu. Rev. Earth Pl. Sc.* **37**, 47–66. DOI: 10.1146/annurev.earth.36.031207.124300.

Trumbore, S. (2000). Age of soil organic matter and soil respiration: radiocarbon constraints on belowground C dynamics. *Ecol. Appl.* **10** (2), 399–411. DOI: https://doi.org/10.1890/1051-0761(2000)010[0399:AOSOMA]2.0.CO;2.

Turkelboom, F., Poesen, J., Ohler, I., and Ongprasert, S. (1999). Reassessment of tillage erosion rates by manual tillage on steep slopes in northern Thailand. *Soil Tillage Res.* **51** (3-4), 245–259. DOI: 10.1016/S0167-1987(99)00041-0.

Turkelboom, F., Poesen, J., and Trébuil, G. (2008). The multiple land degradation effects caused by land-use intensification in tropical steeplands: A catchment study from northern Thailand. *Catena* **75** (1), 102–116. DOI: 10.1016/j.catena.2008.04.012.

Tyukavina, A., Hansen, M. C., Potapov, P., Parker, D., Okpa, C., Stehman, S. V., Kommareddy, I., and Turubanova, S. (2018). Congo Basin forest loss dominated by increasing smallholder clearing. *Sci. Adv.* **4** (11). DOI: 10.1126/sciadv.aat2993.

UNESCO and WHC (2010). *World Heritage in the Congo Basin.*

Valbuena, D., Tui, S. H.-K., Erenstein, O., Teufel, N., Duncan, A., Abdoulaye, T., Swain, B., Mekonnen, K., Germaine, I., and Gérard, B. (2015). Identifying determinants, pressures and trade-offs of crop residue use in mixed smallholder farms in sub-Saharan Africa and South Asia. *Agric. Syst.* **134**, 107–118. DOI: 10.1016/j.agsy.2014.05.013.

Van Oost, K., Verstraeten, G., Doetterl, S., Notebaert, B., Wiaux, F., Broothaerts, N., and Six, J. (2012). Legacy of human-induced C erosion and burial on soil–atmosphere C exchange. *Proc. Natl. Acad. Sci.* **109**, 19492–19497. DOI: 10.1073/pnas.1211162109.

Vanacker, V., Ameijeiras-Mariño, Y., Schoonejans, J., Cornélis, J. T., Minella, J. P., Lamouline, F., Vermeire, M. L., Campforts, B., Robinet, J., Broek, M. V. de, Delmelle, P., and Opfergelt, S. (2019). Land use impacts on soil erosion and rejuvenation in Southern Brazil. *Catena* **178**, 256–266. DOI: 10.1016/j.catena.2019.03.024.

VandenBygaart, A. J., Gregorich, E. G., and Helgason, B. L. (2015). Cropland C erosion and burial: Is buried soil organic matter biodegradable? *Geoderma* **239-240**, 240–249. DOI: 10.1016/j.geoderma.2014.10.011.

Veldkamp, E., Becker, A., Schwendenmann, L., Clark, D. J., and Schulte-Bisping, H. (2003). Substantial labile carbon stocks and microbial activity in deeply weathered soils below a tropical wet forest. *Global Change Biol.* **9** (8), 1171–1184. DOI: 10.1046/j.1365-2486.2003.00656.x.

Veldkamp, E., Schmidt, M., Powers, J. S., and Corre, M. D. (2020). Deforestation and reforestation impacts on soils in the Tropics. *Nature Reviews Earth & Environment* **1**.(11), 590–605. DOI: 10.1038/s43017-020-0091-5.

Verdoodt, A. and Ranst, E. V. (2003). *Land evaluation for agricultural production in the tropics. A large-scale land suitability classification for Rwanda.* Ghent University.

Vereecken, H., Schnepf, A., Hopmans, J. W., Javaux, M., Or, D., Roose, T., Vanderborght, J., Young, M. H., Amelung, W., Aitkenhead, M., Allison, S. D., Assouline, S., Baveye, P., Berli, M., Brüggemann, N., Finke, P., Flury, M., Gaiser, T., Govers, G., Ghezzehei, T., Hallett, P., Franssen, H. J. H., Heppell, J., Horn, R., Huisman, J. A., Jacques, D., Jonard, F., Kollet, S., Lafolie, F., Lamorski, K., Leitner, D., McBratney, A., Minasny, B., Montzka, C., Nowak, W., Pachepsky, Y., Padarian, J., Romano, N., Roth, K., Rothfuss, Y., Rowe, E. C., Schwen, A., Šimůnek, J., Tiktak, A., Dam, J. V., Zee, S. E. A. T. M. V. der, Vogel, H. J., Vrugt, J. A., Wöhling, T., and Young, I. M. (2016). Modeling soil processes: review, key challenges, and new perspectives. *Vadose Zone J.* **15** (5), vzj2015.09.0131. DOI: 10.2136/vzj2015.09.0131.

Vitousek, P., Chadwick, O., Matson, P., Allison, S., Derry, L., Kettley, L., Luers, A., Mecking, E., Monastra, V., and Porder, S. (2003). Erosion and the rejuvenation of weathering-derived nutrient supply in an old tropical landscape. *Ecosystems* **6**.(8), 762–772. DOI: 10.1007/s10021-003-0199-8.

Vitousek, P. M., Porder, S., Houlton, B. Z., and Chadwick, O. A. (2010). Terrestrial phosphorus limitation: mechanisms, implications, and nitrogen-phosphorus interactions. *Ecol. Appl.* **20** (1), 5–15.

Voort, T. S. V. der, Mannu, U., Hagedorn, F., McIntyre, C., Walthert, L., Schleppi, P., Haghipour, N., and Eglinton, T. I. (2019). Dynamics of deep soil carbon – insights from 14 C time series across a climatic gradient. *Biogeosciences* **16**.(16), 3233–3246. DOI: 10.5194/bg-16-3233-2019.

Wagai, R., Kajiura, M., and Asano, M. (2020). Iron and aluminum association with microbially processed organic matter via meso-density aggregate formation across soils: organo-metallic glue hypothesis. *SOIL* **6** (2), 597–627. DOI: 10.5194/soil-6-597-2020.

Wagai, R., Mayer, L. M., Kitayama, K., and Knicker, H. (2008). Climate and parent material controls on organic matter storage in surface soils: A three-pool, density-separation approach. *Geoderma* **147** (1-2), 23–33. DOI: 10.1016/j.geoderma.2008.07.010.

Wagai, R., Mayer, L. M., Kitayama, K., and Shirato, Y. (2013). Association of organic matter with iron and aluminum across a range of soils determined via selective dissolution techniques coupled with dissolved nitrogen analysis. *Biogeochemistry* **112**.(1-3), 95–109. DOI: 10.1007/s10533-011-9652-5.

Waggoner, D. C., Wozniak, A. S., Cory, R. M., and Hatcher, P. G. (2017). The role of reactive oxygen species in the degradation of lignin derived dissolved organic matter. *Geochim. Cosmochim. Acta* **208**, 171–184. DOI: 10.1016/j.gca.2017.03.036.

Wang, J., Sun, J., Xia, J., He, N., Li, M., and Niu, S. (2018). Soil and vegetation carbon turnover times from tropical to boreal forests. *Funct. Ecol.* **32** (1), 71–82. DOI: 10.1111/1365-2435.12914.

Wang, L., Huang, X., Fang, N. F., Niu, Y. H., Wang, T. W., and Shi, Z. H. (2019a). Selective transport of soil organic and inorganic carbon in eroded sediment in response to raindrop sizes and inflow rates in rainstorms. *J. Hydrol.* **575**, 42–53. DOI: 10.1016/j.jhydrol.2019.05.033.

Wang, Q., Zhao, X., Chen, L., Yang, Q., Chen, S., and Zhang, W. (2019b). Global synthesis of temperature sensitivity of soil organic carbon decomposition: Latitudinal patterns and mechanisms. *Funct. Ecol.* **33** (3), 514–523. DOI: 10.1111/1365-2435.13256.

Wang, X., Jelinski, N. A., Toner, B., and Yoo, K. (2019c). Long-term agricultural management and erosion change soil organic matter chemistry and association with minerals. *Sci. Total Environ.* **648**, 1500–1510. DOI: 10.1016/j.scitotenv.2018.08.110.

Wang, X., Toner, B. M., and Yoo, K. (2019d). Mineral vs. organic matter supply as a limiting factor for the formation of mineral-associated organic matter in forest and agricultural soils. *Sci. Total Environ.* **692**, 344–353. DOI: 10.1016/j.scitotenv.2019.07.219.

Wang, Y. P., Law, R. M., and Pak, B. (2010). A global model of carbon, nitrogen and phosphorus cycles for the terrestrial biosphere. *Biogeosciences* **7** (7), 2261–2282. DOI: 10.5194/bg-7-2261-2010.

Wang, Z., Hoffmann, T., Six, J., Kaplan, J. O., Govers, G., Doetterl, S., and Oost, K. V. (2017). Human-induced erosion has offset one-third of carbon emissions from land cover change. *Nat. Clim. Change* **7**.(5), 345–349. DOI: 10.1038/nclimate3263.

Wang, Z., Oost, K. V., and Govers, G. (2015). Predicting the long-term fate of buried organic carbon in colluvial soils. *Global Biogeochem. Cycles* **29** (1), 65–79. DOI: 10.1002/2014GB004912.

Wasner, D., Abramoff, R., Griepentrog, M., Venegas, E. Z., Boeckx, P., and Doetterl, S. (2024). The role of climate, mineralogy and stable aggregates for soil organic carbon dynamics along a geoclimatic gradient. *Global Biogeochem. Cycles* **38**.(7). DOI: 10.1029/2023GB007934.

Waters, A. G. and Oades, G. M. (1991). "Organic matter in water stable aggregates". Ed. by W. R. Wilson. Soc. Chem., pp. 163–174.

Wattel-Koekkoek, E. J. W., Buurman, P., Plicht, J. V. D., Wattel, E., and Breemen, N. V. (2003). Mean residence time of soil organic matter associated with kaolinite and smectite. *Eur. J. Soil Sci.* **54** (2), 269–278. DOI: 10.1046/j.1365-2389.2003.00512.x.

Wei, X., Shao, M., Gale, W., and Li, L. (2014). Global pattern of soil carbon losses due to the conversion of forests to agricultural land. *Sci. Rep.* **4**.(1). DOI: 10.1038/srep04062.

Weng, Y.-T., Wang, C.-C., Chiang, C.-C., Tsai, H., Song, Y.-F., Huang, S.-T., and Liang, B. (2018). In situ evidence of mineral physical protection and carbon stabilization revealed by nanoscale 3-D tomography. *Biogeosciences* **15** (10), 3133–3142. DOI: 10.5194/bg-15-3133-2018.

West, G. and Dumbleton, M. J. (1970). The mineralogy of tropical weathering illustrated by some west Malaysian soils. *Q. J. Eng. Geol. Hydroge.* **3** (1), 25–40. DOI: 10.1144/GSL.QJEG.1970.003.01.02.

Whalen, E. D., Grandy, A. S., Sokol, N. W., Keiluweit, M., Ernakovich, J., Smith, R. G., and Frey, S. D. (2022). Clarifying the evidence for microbial- and plant-derived soil organic matter, and the path toward a more quantitative understanding. *Global Change Biol.* **28** (24), 7167–7185. DOI: 10.1111/gcb.16413.

Wiaux, F., Cornelis, J. T., Cao, W., Vanclooster, M., and Oost, K. V. (2014a). Combined effect of geomorphic and pedogenic processes on the distribution of soil organic carbon quality along an eroding hillslope on loess soil. *Geoderma* **216**, 36–47. DOI: 10.1016/j.geoderma.2013.10.013.

Wiaux, F., Vanclooster, M., Cornelis, J. T., and Oost, K. V. (2014b). Factors controlling soil organic carbon persistence along an eroding hillslope on the loess belt. *Soil Biol. Biochem.* **77**, 187–196. DOI: 10.1016/j.soilbio.2014.05.032.

Wiesmeier, M., Urbanski, L., Hobley, E., Lang, B., Lützow, M. von, Marin-Spiotta, E., Wesemael, B. V., Rabot, E., Ließ, M., Garcia-Franco, N., Wollschläger, U., Vogel, H.-J., and Kögel-Knabner, I. (2019). Soil organic carbon storage as a key function of soils - A review of drivers and indicators at various scales. *Geoderma* **333**, 149–162. DOI: 10.1016/j.geoderma.2018.07.026.

Wilcke, W., Yasin, S., Abramowski, U., Valarezo, C., and Zech, W. (2002). Nutrient storage and turnover in organic layers under tropical montane rain forest in Ecuador. *Eur. J. Soil Sci.* **53** (1), 15–27. DOI: 10.1046/j.1365-2389.2002.00411.x.

Wilken, F., Ketterer, M., Koszinski, S., Sommer, M., and Fiener, P. (2020). Understanding the role of water and tillage erosion from 239+240Pu tracer measurements using inverse modelling. *SOIL* **6**, 549–564. DOI: 10.5194/soil-6-549-2020.

Wilken, F., Fiener, P., Ketterer, M., Meusburger, K., Muhindo, D. I., Oost, K. V., and Doetterl, S. (2021). Assessing soil redistribution of forest and cropland sites in wet tropical Africa using 239+240Pu fallout radionuclides. *SOIL* **7**.(2), 399–414. DOI: 10.5194/soil-7-399-2021.

Wilken, F., Sommer, M., Oost, K. V., Bens, O., and Fiener, P. (2017). Process-oriented modelling to identify main drivers of erosion-induced carbon fluxes. *SOIL* **3** (2), 83–94. DOI: 10.5194/soil-3-83-2017.

Winowiecki, L. A., Bargués-Tobella, A., Mukuralinda, A., Mujawamariya, P., Ntawuhiganayo, E. B., Mugayi, A. B., Chomba, S., and Vågen, T.-G. (2021). Assessing soil and land health across two landscapes in eastern Rwanda to inform restoration activities. *SOIL* **7** (2), 767–783. DOI: 10.5194/soil-7-767-2021.

Wischmeier, W. H. and Smith, D. D. (1978). *Predicting rainfall erosion losses: a guide to conservation planning (No. 537).*

Wood, T. E., Cavaleri, M. A., and Reed, S. C. (2012). Tropical forest carbon balance in a warmer world: A critical review spanning microbial- to ecosystem-scale processes. *Biol. Rev.* **87** (4), 912–927. DOI: 10.1111/j.1469-185X.2012.00232.x.

Xiao, H., Li, Z., Chang, X., Huang, B., Nie, X., Liu, C., Liu, L., Wang, D., and Jiang, J. (2018). The mineralization and sequestration of organic carbon in relation to agricultural soil erosion. *Geoderma* **329**, 73–81. DOI: 10.1016/j.geoderma.2018.05.018.

Xiong, M., Sun, R., and Chen, L. (2019). *A global comparison of soil erosion associated with land use and climate type.* DOI: 10.1016/j.geoderma.2019.02.013.

Xu, X., Schimel, J. P., Thornton, P. E., Song, X., Yuan, F., and Goswami, S. (2014). Substrate and environmental controls on microbial assimilation of soil organic carbon: a framework for Earth system models. *Ecol. Lett.* **17** (5), 547–555. DOI: 10.1111/ele.12254.

Yoo, K. and Mudd, S. M. (2008). Toward process-based modeling of geochemical soil formation across diverse landforms: A new mathematical framework. *Geoderma* **146** (1-2), 248–260. DOI: 10.1016/j.geoderma.2008.05.029.

You, W.-z., Zeng, D.-h., Liu, M.-g., Yun, L.-l., Ye, Y.-h., and Zhang, Y. (2010). Spatial and temporal variations of soil moisture in three types of agroforestry boundaries in the Loess Plateau, China. *J. For. Res.* **21** (4), 415–422. DOI: 10.1007/s11676-010-0091-2.

Zauyah, S., Schaefer, C. E., and Simas, F. N. (2010). “Saprolites”. *Interpretation of Micromorphological Features of Soils and Regoliths.* Elsevier, pp. 49–68. DOI: 10.1016/B978-0-444-53156-8.00004-0.

Zhang, L., Zeng, G., and Tong, C. (2011). A review on the effects of biogenic elements and biological factors on wetland soil carbon mineralization. *Acta Ecologica Sinica* **31**, 5387–5395.

Zhao, L., Fang, Q., Hou, R., and Wu, F. (2021). Effect of rainfall intensity and duration on soil erosion on slopes with different microrelief patterns. *Geoderma* **396**, 115085. DOI: 10.1016/j.geoderma.2021.115085.

Zhao, P., Doetterl, S., Wang, Z., Hoyt, A. M., Wang, E., Yu, H., Quijano, L., Fallu, D. J., Brown, A. G., Six, J., and Oost, K. V. (2022). Factors controlling SOC stability in colluvial soils under contrasting climate and soil weathering conditions. *Eur. J. Soil Sci.* **73** (5). DOI: 10.1111/ejss.13311.

Zhao, P., Doetterl, S., Wang, Z., Quijano, L., Six, J., and Oost, K. V. (2019). Soil deposition and weathering interactively controlling the stabilization of soil organic carbon. *Geophysical Research Abstracts* **21**, 2019–17318.

Zhao, X., Song, X., Li, L., Wang, D., Meng, P., and Li, H. (2024). Effect of microrelief features of tillage methods under different rainfall intensities on runoff and soil erosion in slopes. *Int. Soil Water Conserv. Res.* **12** (2), 351–364. DOI: 10.1016/j.iswcr.2023.10.001.

Ziegler, A. D. and Sutherland, R. A. (2009). Modeling soil flux by manual tillage as a nonlinear slope-dependent process. *Soil Sci. Soc. Am. J.* **73** (3), 1012–1019. DOI: 10.2136/sssaj2006.0437.

Zotarelli, L., Alves, B. J. R., Urquiaga, S., Torres, E., Santos, H. P. dos, Paustian, K., Boddey, R. M., and Six, J. (2005). Impact of tillage and crop rotation on aggregate-associated carbon in two Oxisols. *Soil Sci. Soc. Am. J.* **69**.(2), 482–491. DOI: 10.2136/sssaj2005.0482.

Appendix A

Appendix to The role of geochemistry in organic carbon stabilization against microbial decomposition in tropical rainforest soils

Table A.1: Partial correlation analysis between $\mathrm{SOC_{bulk}}$ and climate variables (Fick and Hijmans, 2017) controlling for geochemical soil properties. Zero-order correlation displays the Pearson r values when including no control variables. The controlled correlation shows the Pearson r value when controlling for DCB-extractable oxides of Al, Fe and Mn, exchangeable bases and total P.

Soil depth [cm]	Control variables	MAP [mm]	MAT [°C]	PET [mm]
0 – 10	zero-order	-0.17	0	-0.08
	DCB-extr. oxides (Al, Fe, Mn), exchangeable bases, total P	-0.16	-0.26	-0.40
30 – 40	zero-order	0.67[a]	-0.90[b]	-0.93[b]
	DCB-extr. oxides (Al, Fe, Mn), exchangeable bases, total P	-0.56	-0.03	-0.43
60 – 70	zero-order	-0.06	-0.24	-0.33
	DCB-extr. oxides (Al, Fe, Mn), exchangeable bases, total P	0	-0.13	-0.14

[a] *$p < 0.05$.* [b] *$p < 0.001$. Abbreviations: MAP, mean annual precipitation; MAT, mean annual temperature; PET, potential evapotranspiration.*

Table A.2: SOC variables grouped by soil depth, topographic position and geochemical regions (section 1: mafic; section 2: felsic; section 3: mixed). Different capital letters indicate significant differences in means ($p < 0.05$).

Section 1: mafic magmatic

Parameter	Unit	0 – 10 cm			30 – 40 cm			60 – 70 cm		
		Plateau	Sloping	Valley	Plateau	Sloping	Valley	Plateau	Sloping	Valley
C	mass%	8.54 ± 3.37 *	5.4 ± 0.59 *	8.62 ± 1.11 *	2.11 ± 0.02 *	2.55 ± 0.32 *	3.8 ± 0.66 *	1.42 ± 0.27 *	2.02 ± 0.92 *	2.62 ± 0.72 *
N	mass%	0.7 ± 0.19 *	0.55 ± 0.06 *	0.87 ± 0.12 *	0.21 ± 0.01 A	0.25 ± 0.02 A	0.38 ± 0.05 B	0.15 ± 0.01 *	0.2 ± 0.1 *	0.25 ± 0.04 *
C : N	–	11.78 ± 1.89 *	9.75 ± 0.68 *	9.92 ± 0.78 *	10.17 ± 0.23 *	10.26 ± 0.76 *	10.14 ± 1.24 *	9.61 ± 0.9 *	10.18 ± 0.92 *	10.52 ± 2.32 *
SOC_{bulk}	tC ha^{-1}	65.63 ± 25.9 *	43.07 ± 6.6 *	62.24 ± 11.41 *	25.02 ± 0.24 A	29.98 ± 3.22 A	41.22 ± 4.6 B	17.2 ± 3.2 *	25.78 ± 12.06 *	32.19 ± 9.15 *
m / s+c	–	1.43 ± 0.3 *	1.41 ± 0.45 *	1.72 ± 0.83 *	1.3 ± 0.08 *	1.13 ± 0.28 *	1.66 ± 0.5 *	1.11 ± 0.11*	0.98 ± 0.15 *	1.66 ± 1.06 *
$SOC_{>250\,\mu m}$	%	5.09 ± 2.37 *	3.62 ± 1.14 *	4.12 ± 3.38 *	1.48 ± 0.33 *	1.36 ± 0.42 *	2.18 ± 1.57 *	1.32 ± 0.03 *	1.31 ± 1.01 *	2.12 ± 1.04 *
$SOC_{53\text{ - }250\,\mu m}$	%	55.3 ± 3.38 *	55.2 ± 9.49 *	57.9 ± 12.83 *	55.63 ± 1.59 *	51.52 ± 7.26 *	60.28 ± 7.44 *	51.7 3 ± 2.54 *	48.61 ± 3.83 *	56.98 ± 16.71 *
SOC	%	39.61 ± 5.75 *	41.18 ± 8.52 *	37.98 ± 13.96 *	42.89 ± 1.47 *	47.12 ± 6.93 *	37.54 ± 6.03 *	46.95 ± 2.51 *	50.08 ± 3.76 *	40.91 ± 15.67 *

Section 2: felsic magmatic

Parameter	Unit	0 – 10 cm			30 – 40 cm			60 – 70 cm		
		Plateau	Sloping	Valley	Plateau	Sloping	Valley	Plateau	Sloping	Valley
C	mass%	4.58 ± 1.14 *	3.39 ± 0.79 *	2.99 ± 0.39 *	0.95 ± 0.07 *	0.87 ± 0.21 *	0.55 ± 0.13 *	0.55 ± 0.08 *	0.51 ± 0.12 *	0.28 ± 0.11*
N	mass%	0.45 ± 0.08 *	0.35 ± 0.07 *	0.29 ± 0.03 *	0.1 ± 0.01 *	0.09 ± 0.02 *	0.06 ± 0.01 *	0.06 ± 0.01 *	0.05 ± 0.01 *	0.03 ± 0.02*
C : N	–	10.18 ± 0.65 *	9.77 ± 0.62 *	10.31 ± 1.98 *	10.29 ± 0.04 *	10.31 ± 1.81 *	10.37 ± 0.52 *	9.57 ± 0.04 *	10.6 ± 2 *	9.89 ± 1.55 *
SOC_{bulk}	tC ha^{-1}	46.75 ± 28.49 *	44.08 ± 9.72 *	40.42 ± 8.03 *	16.41 ± 2.87 *	15.81 ± 4.61 *	9.88 ± 2.25 *	9.03 ± 1.05 *	10.32 ± 2.96 *	5.95 ± 3.26 *
m / s+c	–	1.23 ± 0.54 AB	1.37 ± 0.47 B	2.45 ± 0.39 A	0.68 ± 0.01 *	1.11 ± 0.37 *	0.72 ± 0.07 *	1.06 ± 0.28 *	1.13 ± 0.62 *	0.53 ± 0.13 *
$SOC_{>250\,\mu m}$	%	12.77 ± 6.31 *	10.15 ± 3.84 *	12.57 ± 7.94 *	5.62 ± 2.66 *	9.43 ± 9.97 *	3.71 ± 1.6 *	3.41 ± 0.47 *	8.26 ± 7.71 *	4.88 ± 2.37 *
$SOC_{53\text{ - }250\,\mu m}$	%	46.52 ± 6.42 *	50.49 ± 7.8 *	61.96 ± 7.91 *	38.14 ± 1.41 *	46.34 ± 9.4 *	40.16 ± 2.9 *	49.31 ± 6.29 *	45.34 ± 15.37 *	32.94 ± 5.73*
SOC	%	40.71 ± 12.73 AB	39.36 ± 8.45 A	25.47 ± 2.23 B	56.24 ± 1.25 *	44.22 ± 9.51 *	56.13 ± 1.47 *	47.28 ± 6.75 *	46.4± 14.02 *	62.18 ± 3.38 *

Section 3: mixed sedimentary rocks

Parameter	Unit	0 – 10 cm			30 – 40 cm			60 – 70 cm		
		Plateau	Sloping	Valley	Plateau	Sloping	Valley	Plateau	Sloping	Valley
C	mass%	6.95 ± 0.46 *	4.83 ± 1.91 *	6.3 ± 3.05 *	2.42 ± 0.15 *	2.41 ± 1.06 *	1.63 ± 0.78 *	1.36 ± 0.26 *	1.78 ± 0.86 *	2.28 ± 2.14 *
N	mass%	0.47 ± 0.06 *	0.31 ± 0.13 *	0.37 ± 0.18 *	0.15 ± 0.01 *	0.14 ± 0.07 *	0.06 ± 0.03 *	0.09 ± 0.01 *	0.09 ± 0.07 *	0.06 ± 0.05 *
C : N	–	14.84 ± 0.98 *	15.85 ± 1.86 *	17.04 ± 0.73 *	15.63 ± 1.46 A	18.63 ± 4.71 A	27.15 ± 2.98 B	15.55 ± 0.99 *	33.41 ± 37.42 *	30.29 ± 17.28 *
SOC_{bulk}	tC ha^{-1}	48.41 ± 6.59 *	41.71 ± 8.47 *	52.75 ± 30.72 *	31.08 ± 3.33 *	30.06 ± 7.42 *	26.88 ± 15.82 *	20.2 ± 4.26 *	25.74 ± 11.29 *	40.86 ± 38.35 *
m / s+c	–	0.9 ± 0.66 *	0.94 ± 0.31 *	2.97 ± 2.43 *	0.53 ± 0.08 *	0.8 ± 0.34 *	1.12 ± 0.59 *	0.85 ± 0.2 *	0.7 ± 0.69 *	1.15 ± 0.59 *
$SOC_{>250\,\mu m}$	%	6.74 ± 3.98 *	6.43 ± 7.14 *	22.19 ± 12.29 *	13.37 ± 19.44 *	6.26 ± 1.72 *	15.09 ± 9.18 *	4.41 ± 3.8 *	6.37 ± 4.6 *	10.42 ± 11.4 *
$SOC_{53\text{ - }250\,\mu m}$	%	40.18 ± 15.39 *	44.7 ± 9.46 *	52.71 ± 6.82 *	30.22 ± 8.01 *	40.16 ± 9.54 *	42.34 ± 6.19 *	43.28 ± 3.52 *	27.31 ± 20.91 *	44.56 ± 9.71 *
SOC	%	53.07 ± 17.58 *	48.87 ± 6.1 *	25.11 ± 14.87 *	56.4 ± 12.28 *	53.59 ± 8.99 *	42.57 ± 13.79 *	52.3 ± 7.28 *	49.65 ± 30.66 *	45.02 ± 18.14 *

Asterisks indicate no significant differences in means ($p > 0.05$). Means are compared across topographical positions for each depth increment in each geochemical region (plateau $n = 3$, slopes $n = 6$, valley $n = 3$).

Table A.3: Absolute and relative differences of mineral soil at plateau positions (30 – 40 cm soil depth) compared to parent material. Maximum and minimum values refer to the maximum and minimum depletion, respectively. If sample size was n = 1, the corresponding standard deviation was not applicable (N/A).

		Mafic		Felsic		Mixed	
		Soil absolute difference [ppm]	Relative difference Δ[%]	Soil absolute difference [ppm]	Relative difference Δ[%]	Soil absolute difference [ppm]	Relative difference Δ[%]
Ca	Mean ± SD	-5765 ± 5814	-99 ± 101	1443 ± N/A	1240 ± N/A	-55 ± 95	-100 ± 172
	Max	-12937	-100	1028	194	-164	-100
	Min	-75	-38	1559	N/A	0	N/A
K	Mean ± SD	161 ± 970	20 ± 603	1148 ± N/A	618 ± N/A	-248 ± 566	-32 ± 228
	Max	-1621	-65	743	126	-774	-62
	Min	984	2687	1318	8790	499	306
Mg	Mean ± SD	-10 414 ± 3417	-83 ± 33	1160 ± N/A	1015 ± N/A	587 ± 211	527 ± 36
	Max	-14333	-87	718	129	341	179
	Min	-5488	-72	1274	N/A	876	2235
Na	Mean ± SD	-519 ± 850	-63 ± 164	148 ± N/A	677 ± N/A	43 ± 59	92 ± 138
	Max	-1954	-90	102	149	-34	-53
	Min	313	375	163	2414	117	834
P	Mean ± SD	-2133 ± 1361	-58 ± 64	403 ± N/A	746 ± N/A	585 ± 201	289 ± 34
	Max	-3774	-72	223	96	333	89
	Min	186	14	450	6671	874	2583
Fe	Mean ± SD	28849 ± 25 496	32 ± 88	30867 ± N/A	284 ± N/A	87 917 ± 24 429	379 ± 28
	Max	-6967	-6	-12878	-24	56114	157
	Min	60099	85	39115	1482	121456	3486
Al	Mean ± SD	24730 ± 37287	39 ± 151	25226 ± N/A	487 ± N/A	49252 ± 5537	799 ± 11
	Max	-33553	-32	-9013	-23	41728	383
	Min	78824	307	29966	6859	55961	1514
Mn	Mean ± SD	2040 ± 1461	160 ± 72	1251 ± N/A	3126 ± N/A	168 ± 48	776 ± 29
	Max	584	34	1125	675	91	168
	Min	3273	308	1291	N/A	213	17591
Si	Mean ± SD	-16700 ± N/A	-12 ± N/A	-216070 ± N/A	-58 ± N/A	-241033 ± N/A	-67 ± N/A
	Max	-46000	-27	-256000	-62	-298700	-71
	Min	9500	8	-55900	-26	-163000	-58

A.1 Supplemented information on valley positions

The following text represents the supplementary results and short discussion on geochemical soil parameters, SOC stocks and stabilization assessed at valley positions of contrasting parent material geochemistry investigated in tropical rain mountain forest in the border region of the Congo and Nile basement. We show that, in valley positions, significant variation in the size of SOC stocks are related to changes in hydrological conditions and alluvial processes compared to non-valley positions. Geochemical differences in SOC stabilization mechanisms between regions remain in place, but are less prominent in valleys than at non-valley positions.

Table A.4: Rotated principal components and variable loadings of varimax-rotated principal component analysis for non-valley positions (rPC) ($n = 27$). Variable loadings of Pearson's r >0.5 and <-0.5 are highlighted with bold font type. The following variables contributed to the components: to describe the total element content in the soils (associated with rPC1_{nv} and rPC4_{nv}), the total reserve in base cations (TRB; sum of total Mg, Ca, K and Na), total P, metals (sum of total Fe, Al and Mn) and total Si were used. Pyrophosphate-, oxalate- and DCB-extractable phases of Al, Fe and Mn characterize the pedogenic oxides. Exchangeable acidity and bases, effective cation exchange capacity (ECEC) base saturation, CEC base saturation, pH (KCl) and bio-available P (bray-P) reflect soil fertility (associated with rPC2_{nv}). The ratio of pH / clay, ECEC base saturation / clay and CEC base saturation/clay are proxies for clay activity (associated with rPC2_{nv}). Clay, silt and sand describe the texture (associated with rPC1_{nv} and rPC3_{nv}), and several weathering indices (Al_{DCB} / Al_{t} ratio, Fe_{DCB} / Fe_{t} ratio, Al / Si ratio, Fe / Si ratio, Ca / Ti ratio and the chemical index of alteration, CIA) characterize the soil weathering stage (predominantly associated with rPC1_{nv}). $\text{SOC}_{\text{litter}}$, $\text{SOC}_{\text{organic}}$ and root input describe the C input (associated with rPC2_{nv} and rPC3_{nv}).

			rPC1_{nv}	rPC2_{nv}	rPC3_{nv}	rPC4_{nv}
	Eigenvalue		9.34	9.15	1.82	1.57
	Proportion var. (%)		0.33	0.33	0.07	0.06
	Cumulative var. (%)		0.33	0.66	0.73	0.78
	Mechanistic interpretation		solid-phase mineralogy	chemistry of the soil solution	silt content	organo – mineral complexes
	Total elements					
1	TRB	mass%	0.39	**0.83**	∼0	-0.12
2	total P	mass%	**0.83**	∼0	-0.21	∼0
3	metals ($\sum$total Fe, total Al, total Mn)	mass%	**0.95**	-0.24	∼0	∼0
4	total Si	mass%	**-0.8**	∼0	-0.38	-0.32
	Pedogenic oxides					
5	pyro.-extr. Fe, Al, Mn	mass%	∼0	-0.39	∼0	**0.82**
6	oxalate-extr. Fe, Al, Mn	mass%	**0.88**	-0.26	∼0	0.31
7	DCB-extr. Fe, Al, Mn	mass%	**0.95**	-0.19	∼0	-0.13
	Soil fertility					
8	exchangeable acidity	me / 100 g	0.31	**-0.65**	-0.13	0.27
9	exchangeable bases	me / 100 g	-0.15	**0.96**	∼0	∼0
10	ECEC base saturation	%	-0.20	**0.79**	0.33	-0.23
11	CEC base saturation	%	-0.38	**0.87**	0.21	-0.17
12	soil pH (KCl)	–	-0.24	**0.82**	0.21	∼0
13	bio available P (bray)	mg kg^{-1}	0.23	**0.5**	0.14	∼0
	Clay activity					
14	pH / clay	–	**-0.73**	**0.66**	∼0	∼0
15	ECEC base saturation / clay	–	-0.33	**0.83**	0.27	-0.17
16	CEC base saturation / clay	–	-0.41	**0.87**	0.15	-0.12
	Texture					
17	clay	%	**0.89**	-0.24	∼0	∼0
18	silt	%	-0.14	-0.39	**-0.89**	∼0
19	sand	%	**-0.76**	0.42	0.37	∼0
	Weathering					
20	Al_{DCB} / Al_{t}	–	-0.29	∼0	0.11	-0.12
21	Fe_{DCB} / Fe_{t}	–	**0.65**	∼0	∼0	0.27
22	Al / Si	–	**0.94**	∼0	0.19	-0.12
23	Fe / Si	–	**0.91**	-0.25	∼0	0.17
24	Ca / Ti	–	-0.25	**0.9**	∼0	∼0
25	CIA	%	0.44	**-0.84**	∼0	∼0
	C input					
26	$\text{SOC}_{\text{litter}}$	tC ha^{-1}	-0.26	0.19	∼0	-0.20
27	$\text{SOC}_{\text{organic}}$	tC ha^{-1}	-0.27	-0.59	-0.53	0.46
28	root input	kg m^{-3}	-0.28	0.52	-0.17	0.23

A.1.1 Supplementary results on valley positions

Pedogenic oxides

For valley positions, pyrophosphate extractable oxide mass (0.02 to 0.66 mass%) and oxalate extractable oxide mass (0.03 to 4.29 mass%) were low compared to DCB extractable oxide mass (0.11 to 10.79 mass%) (Figure A.1). In general, valley positions showed a comparable picture compared to non-valley positions (Figures 3.4 and A.1) with the exception that valley soils in the mixed sedimentary region had considerably lower amounts of pedogenic oxides at all soil depths (<0.27 mass%) compared to valley soils in the mafic and felsic region.

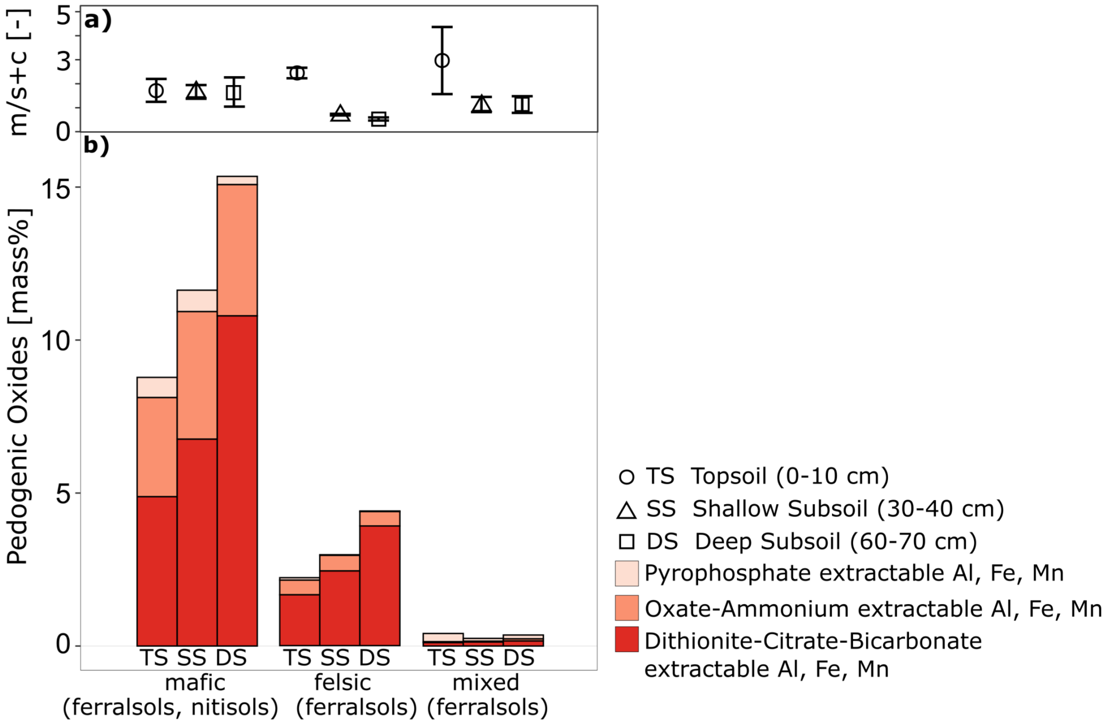

Figure A.1: (a) m / s+c ratio (n = 3 per bar) and (b) pedogenic oxide fractions of the sequential extraction across geochemical regions in valley positions (n = 1 per bar). Error bars represent standard error.

Variation in SOC properties in valley positions with geochemistry

SOC$_{bulk}$

SOC$_{bulk}$ in topsoil was not significantly different between valley and non-valley positions. However, valley positions tended to be generally higher in SOC$_{bulk}$ than their non-valley counterparts. In shallow subsoil, SOC$_{bulk}$ was significantly higher in valley positions of the mafic site (SOC$_{bulk}$: 41.2 ± 4.6 tC ha^{-1}) compared to non-valley positions (SOC$_{bulk}$: 25.0 ± 0.2 to 30.0

± 3.2 tC ha^{-1}), but no difference was found for subsoils of the felsic and mixed sedimentary region (Figures 3.5 and A.2).

Abundance of C fractions

In the felsic magmatic region, the abundance of microaggregate associated C and the ratio of m / s+c was more than twice as high in valley topsoils (m / s+c: 2.5 ± 0.4) compared to non-valley topsoils (m / s+c: 1.2 ± 0.5 to 1.4 ± 0.5) (Figs. 3a, S1a). Additionally, SOC$_{>250 \mu m}$ in topsoil of valley positions of the mixed sedimentary region was about threefold higher in valleys (22.2 ± 12.3 %) compared to the corresponding non-valley positions (6.5 ± 7.1 to 6.7 ± 4.0 %) (Figures 3.5b and A.2b), and the ratio of m / s+c exhibited a much higher variance in topsoils (Figures 3.4a, A.1a and b).

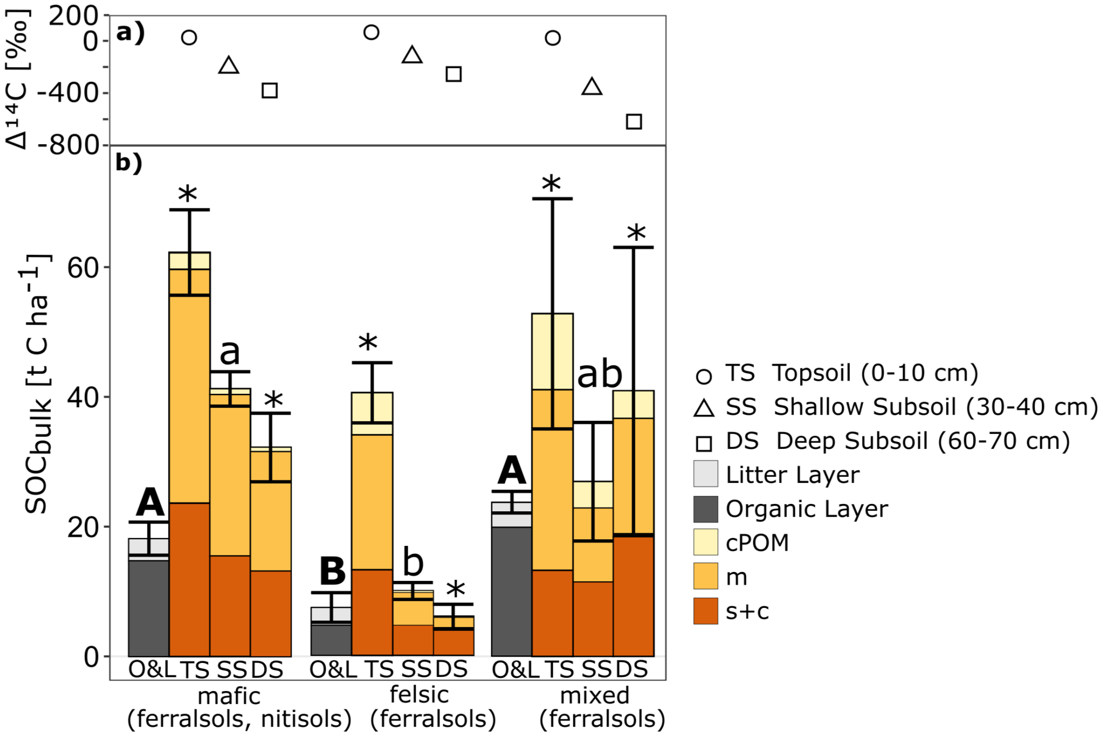

Figure A.2: (a) Δ^{14}C across geochemical regions in valley positions (n = 1 per bar). (b) SOC$_{bulk}$ and fractions across geochemical regions in valley positions (n = 3 per bar). Letters indicate significant differences between geochemical regions per soil layer. Asterisks indicate no significant differences in means (p >0.05). In case of Δ^{14}C values, error bars are smaller than symbols. cPOM – coarse particulate organic matter, m – waterstable microaggregates, s+c – free silt and clay fraction.

Changes in ^{14}C signature

Soils from all geochemical regions at valley positions were more depleted in Δ^{14}C with increasing soil depth (Figure A.1a). The Δ^{14}C ranged from 65.1 ± N / A ‰ (felsic) to 20.4 ± N / A ‰ (mixed sedimentary) in the topsoil, and -256.5 ± N / A ‰ (felsic) to -617.4 ± N / A ‰ (mixed sedimentary). The contribution of FOC to soil C in the mixed sedimentary region increased with soil depth for valley positions, ranging from 1.8 ± N / A % FOC in topsoils to 43.5 ± N / A % in subsoils (Table A.1).

Table A.5: Proportion of biogenic vs. fossil derived organic carbon (OC) in soils developed from mixed sedimentary rocks in valley positions (n = 1). Standard deviation was not applicable (N/A). FOC values in felsic and mafic soils = 0 % (data not shown).

depth increment	amount of biogenic OC (%)	amount of geogenic OC (%)
0 – 10 cm	98.2 ± N/A	1.8 ± N/A
30 – 40 cm	72.1 ± N/A	27.9 ± N/A
60 – 70 cm	56.5 ± N/A	43.5 ± N/A

Rotated principal component explained variance and loadings

For valley soils, five rPCs were determined (rPC_v) explaining 92.7 % of the variance in the valley position subset (Table A.4, Figure A.3). $rPC1_v$ (Eigenvalue 10.7, explaining 38.2 % of the variance) represents solid phase mineralogy, in which total metal oxide concentration, total P and oxalate extractable oxides concentration had strong positive loadings ($\geq$0.98), while total Si, pH / clay ratio and sand content had strong negative loadings ($\leq$-0.69). $rPC2_v$, (Eigenvalue 9.65, explaining 34.5 % of the variance) represents the chemistry of the soil solution and silt content where CEC base saturation, pH and CEC base saturation / clay ratio showed strong positive loadings ($\geq$0.92) while CIA, $SOC_{organic}$ and exchangeable acidity showed negative loadings ($\leq$-0.78). $rPC3_v$ (Eigenvalue 2.5, explaining 9 % of the variance) represents bioavailable P and Al weathering. Bioavailable P showed positive loadings (0.69), while Al_{DCB} / Al_t ratio showed negative loadings (-0.91). $rPC4_v$ (Eigenvalue 1.65, explaining 6 % of the variance) represents root input and exchangeable acidity, both having strong positive loadings ($\geq$0.55). $rPC5_v$ (Eigenvalue 1.46, explaining 5 % of the variance) represents Fe weathering and litter C stock in which both the Fe_{DCB} / Fe_t ratio and litter C stock (SOC_{litter}) had strong positive loadings ($\geq$0.66).

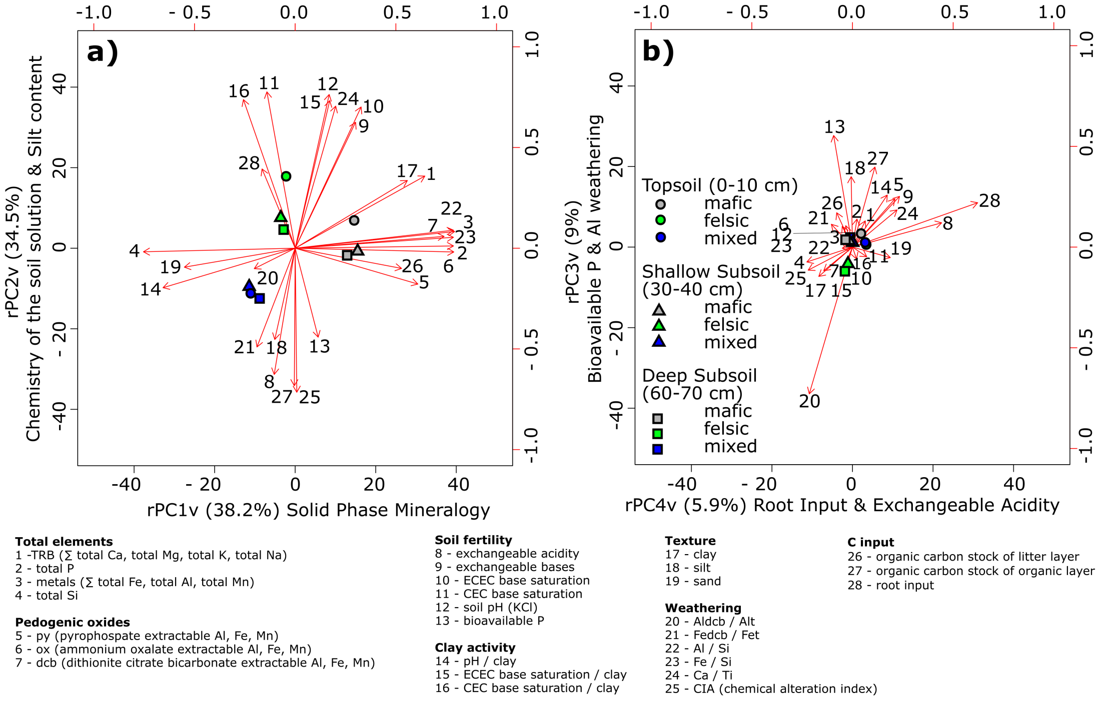

Total elements
1 -TRB (Σ total Ca, total Mg, total K, total Na)
2 - total P
3 - metals (Σ total Fe, total Al, total Mn)
4 - total Si

Pedogenic oxides
5 - py (pyrophospate extractable Al, Fe, Mn)
6 - ox (ammonium oxalate extractable Al, Fe, Mn)
7 - dcb (dithionite citrate bicarbonate extractable Al, Fe, Mn)

Soil fertility
8 - exchangeable acidity
9 - exchangeable bases
10 - ECEC base saturation
11 - CEC base saturation
12 - soil pH (KCl)
13 - bioavailable P

Clay activity
14 - pH / clay
15 - ECEC base saturation / clay
16 - CEC base saturation / clay

Texture
17 - clay
18 - silt
19 - sand

Weathering
20 - Aldcb / Alt
21 - Fedcb / Fet
22 - Al / Si
23 - Fe / Si
24 - Ca / Ti
25 - CIA (chemical alteration index)

C input
26 - organic carbon stock of litter layer
27 - organic carbon stock of organic layer
28 - root input

Figure A.3: Biplots of the varimax rotated principal component analysis. (a) $rPC1_v$ and $rPC2_v$ and (b) $rPC3_v$ and $rPC4_v$ of valley positions (N = 9). Observations cluster together based on similarities within geochemical regions and their distinction to other geochemical regions. Vector length indicates how strongly variables influence a specific rPC. The angles between vectors display the degree of auto-correlation between variables. Small angles represent positive correlations and high degree of autocorrelation, diverging angles represent negative correlations and high degree of autocorrelation, high angles indicate no correlations between variables and / or rPCs.

A.1.2 Supplementary short discussion on valley positions

Soil C stabilization driven by soil chemistry and parent material rather than topography

In contrast to our initial hypothesis that topography affects C stabilization in tropical forest soils through lateral material movements, we found no indication of this in our analysis (Table A.1). This is supported by Drake *et al.* (2019) who showed that C fluxes from pristine forest catchments within the same study area are characterized by young C from organic layers, with no indication of erosion of older, mineral stabilized C. Similarly, Wilken *et al.* (2021), using plutonium tracers to analyze soil redistribution along forest hillslopes did not detect any signs of decadal erosional processes of soils for the same sites as used in this study. Even though material fluxes due to lateral water fluxes along slopes cannot be excluded over longer time scales (e.g. 100 to 1,000 years), our results pointed to no recent natural or anthropogenic induced erosional processes in the investigated sites. However, there was a detectable effect on SOC_{bulk} between positions that are affected by riverine and alluvial dynamics with regularly high water saturation (valleys) vs. well drained positions (non-valleys), with valleys generally having higher SOC_{bulk} than their non-valley counterparts. Gleyic properties and fluvial sedimentation processes recorded in valley soils during profile description (Doetterl *et al.*, 2021b) supported this interpretation. Overall, we found that in valley positions differences in SOC variables are rather related to changes in hydrological conditions and alluvial processes than by chemical soil properties.

Appendix B

Appendix to Soil carbon stocks in stable tropical landforms are dominated by geochemical controls and not by land use

Table B.1: Iteration table for variable inflation factor (VIF) assessment.

			pedogenic oxides			texture			soil fertility			SOM quality
run	mean VIF	depth	pyro. extr. oxides (Al, Fe, Mn)	oxalate extr. oxides (Al, Fe, Mn)	DCB extr. oxides (Al, Fe, Mn)	clay	silt	sand	pH	exchangeable bases (Ca, Mg, K)	bray-P	C : N
0	16.67	+	+	+	+	+	+	+	+	+	+	+
1	7.11	+	+	+	+	+	+	-	+	+	+	+
2	5.15	+	+	+	+	+	+	-	-	+	+	+
3	2.90	+	+	+	-	+	+	-	-	+	+	+
4	2.46	+	+	+	-	+	+	-	-	+	-	+

+ represents included variables, - represents excluded variables (n = 282).

Table B.2: Stepwise linear regression including relative importance analysis for top-, sub- and deep subsoil. Topsoil includes depth increments from 0 – 10 cm, 10 – 20 cm and 20 – 30 cm. Subsoil includes depth increments from 30 – 40 cm, 40 – 50 cm and 50 – 60 cm. Deep subsoil includes depth increments from 60 – 70 cm, 70 – 80 cm, 80 – 90 cm and 90 - 100 cm.

		mineral C stabilization potential		texture		fertility	SOM quality			
response	depth	pyro. extr. oxides (Al, Fe, Mn)	oxalate extr. oxides (Al, Fe, Mn)	clay	silt	exchangeable base cations	C : N	adj. R^2	RMSE	n
SOC	topsoil	0.49*** (47 %)	0.23* (28 %)			0.26* (11 %)	0.20* (15 %)	0.41	0.60	85
	subsoil	0.94*** (71 %)		0.67*** (9 %)	0.25** (7 %)	0.46*** (5 %)	0.21** (8 %)	0.67	0.49	86
	deep subsoil	0.90*** (74 %)	-0.17’ (3 %)	0.79*** (10 %)	0.16’ (2 %)	0.56*** (5 %)	0.21** (7 %)	0.53	0.47	111

*‘ - p <0.1, * - p <0.05, ** - p <0.01, *** - p <0.001.*

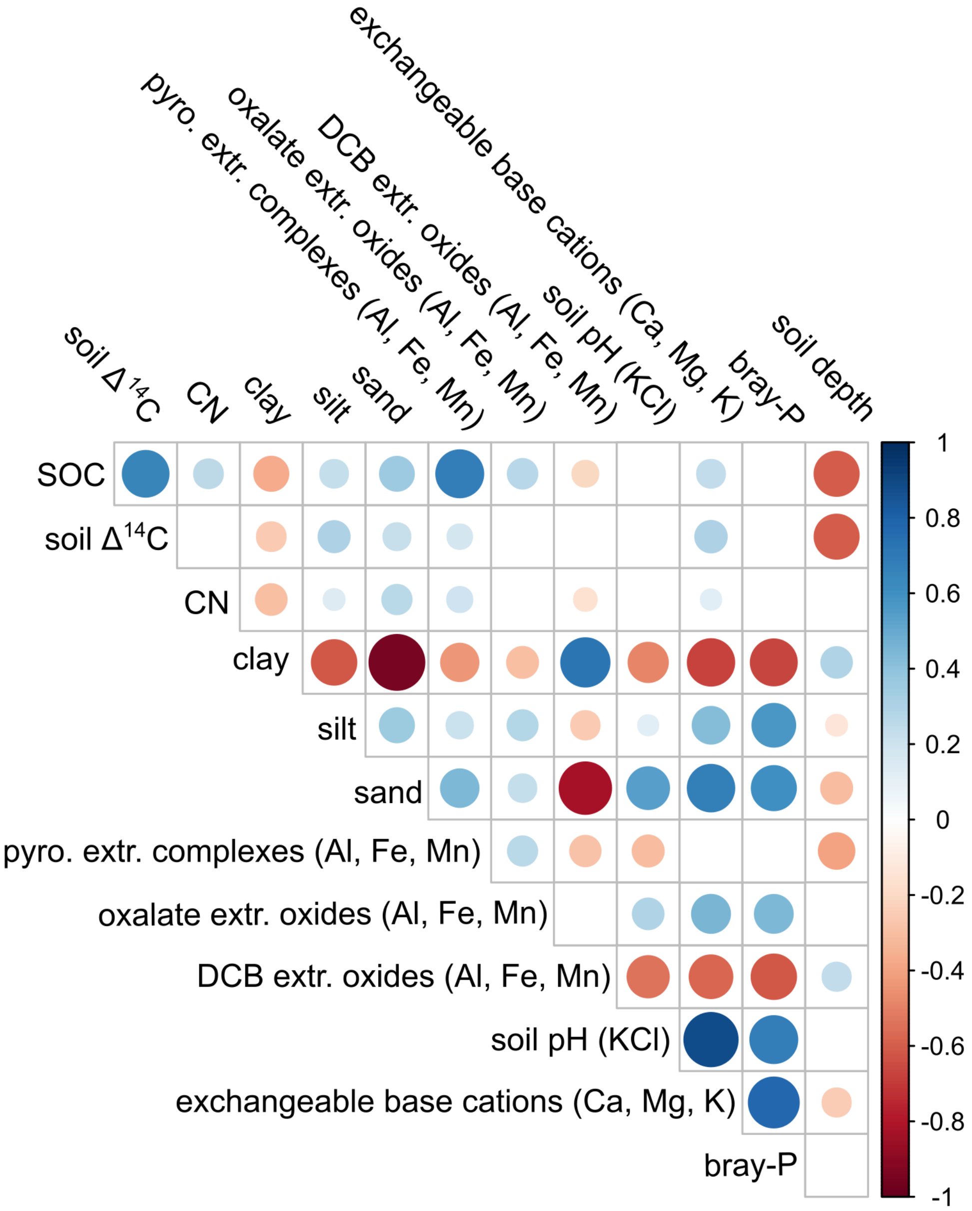

Figure B.1: Correlation matrix used for VIF assessment containing geochemical variables considered as potential predictors for SOC variables (n = 282). Size and color refer to Pearson r ($p < 0.05$). Empty cells represent non-significant correlations ($p > 0.05$).

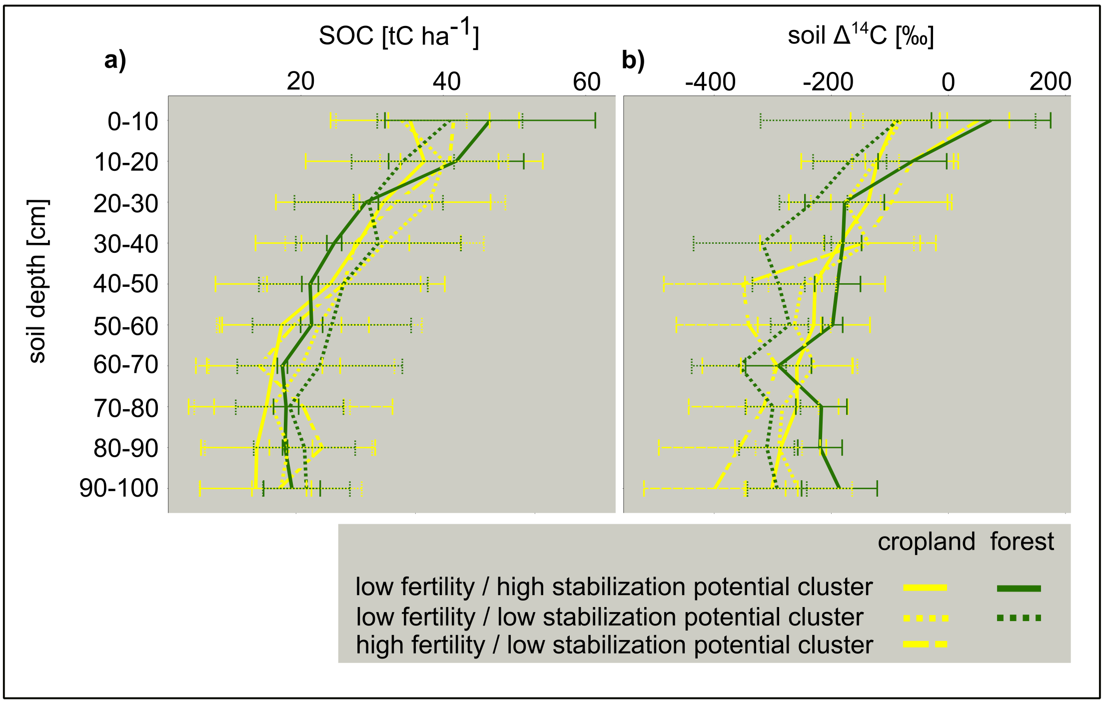

Figure B.2: Depth distribution of (a) SOC stocks and (b) soil $\Delta^{14}C$ across land use types and geochemical clusters ($n = 3 - 8$). Lines show means and error bars represent standard deviation.

Appendix C

Appendix to Weak connection of soil redistribution and soil organic carbon in the wet Tropics of Africa

Table C.1: Statistical models and their corresponding input variables used during pre-tests to explore micro-scale variability in soil geochemical and SOC properties within topographic landscape positions.

variables	units	statistical models			
		cluster analysis	multiple linear stepwise regression with relative importance analysis	random forest regression with relative importance analysis and partial dependence analysis	structural equation modelling – partial least square path analysis
SOC variables					
SOC	tC ha^{-1}	Y	Y	Y	Y
soil Δ^{14}C	‰	Y			Y
C quality					
C : N	-				Y
topography					
slope	%		Y	Y	
upslope length$_{\mathrm{culm}}$	m		Y	Y	
upslope length$_{\mathrm{boundary}}$	m		Y	Y	
upslope length$_{\mathrm{barrier}}$	m		Y	Y	
topographic landscape positions (plateau, slope, footslope / valley)	factor variable	Y			
curvature	-				Y
flow accumulation	-				Y
Stream power index	-				Y
Topographical wetness index	-				Y
Topographical position index	-				Y
texture					
clay	%		Y	Y	Y
silt	%		Y	Y	Y
sand	%				Y
pedogenic oxides					
pyro. extr. oxides (Al, Fe, Mn)	wt%				Y
oxalate. extr. oxides (Al, Fe, Mn)	wt%		Y	Y	Y
DCB. extr. oxides (Al, Fe, Mn)	wt%				Y
soil weathering					
clay : Si	-				Y
clay : Al	-				Y
Fe$_t$: Fe$_{\mathrm{DCB}}$	-				Y
total elements					
metals (Σtotal Al, Fe, Mn)	wt%				Y
TRB (Ca, Mg, K, Na)	wt%				Y
P	wt%				Y
soil fertility					
bray-P	mg kg $^{-1}$				Y
exchangeable bases (Ca, Mg, K)	meq 100g^{-1}		Y	Y	Y
CEC bases	%				Y
soil pH (KCl)	-				Y
soil depth					
soil depth	cm		Y	Y	Y

"Y" means that the variable was included in the corresponding statistical model.

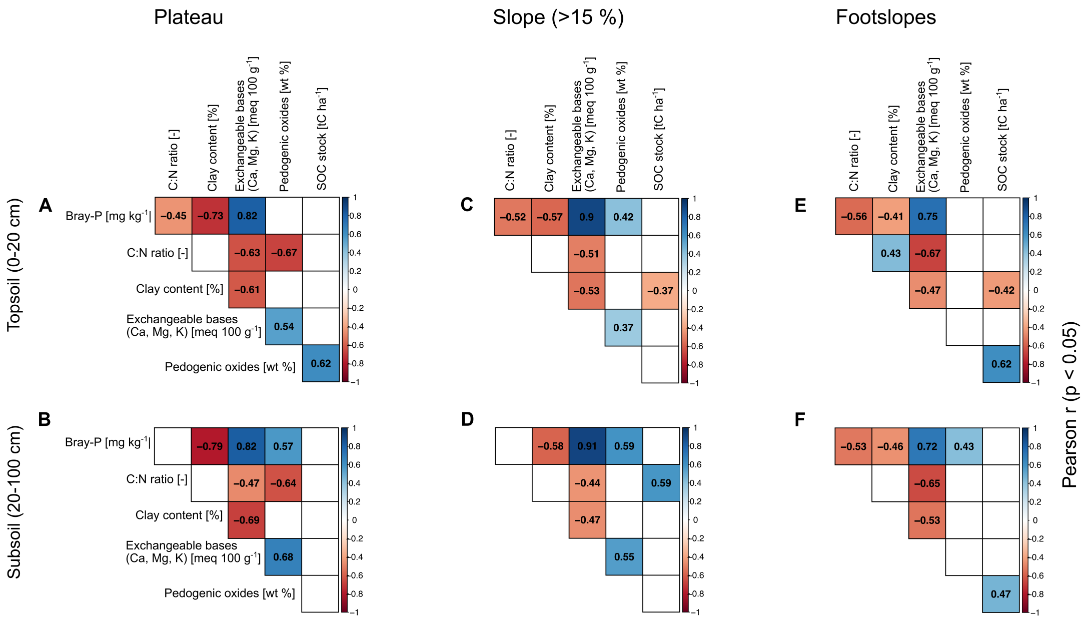

Figure C.1: Pearson correlation heatmaps regarding SOC stocks and biogeochemical properties across slope positions and depth increments.

C.1 Pre-tests for exploring micro-scale variability

The caveat of this study is the significant internal geochemical variability especially on stable plateaus (Figure 3) that should not be affected by soil redistribution in a significant way. Testing hypotheses regarding more specific influences of topography is thus challenging as the “random” noise may obliterate the signal of soil redistribution on physico-chemical and SOC properties. Thus, we conducted multiple pre-tests attempting to explain the observed variability and its relation to more complex topographic indices using several steps. In a first step, each study site was checked for topographic features (e.g. terraces, streets, field boundaries) using Google Earth Pro that may cause (bio)geochemical variability. Next, the field observation based topographic classification of each study site was double-checked using Google Earth Pro. In the next step, SOC stocks and soil Δ^{14}C data were plotted against all geochemical soil properties (data down to 1 m) and grouped by topographic classes (plateau, upper slope, midslope, footslope, valley) to check for relationships between these variables and if specific topographic classes are related with higher or lower variability. Next, to represent topography not only in a qualitative but also quantitative way, several topographic variables were calculated using Google Earth Pro combined with a shuttle radar topography mission digital elevation model (SRTM-DEM) (JPL, 2013) with a 30 m x 30 m resolution using the measurement tool in ArcMap 10.6.1 (ESRI, USA). Those variables included the upslope length until the culmination point (upslope $\text{length}_{\text{culm}}$) at each study site. In addition, to understand the potential impact of field boundaries on soil erosion, historical images (1985 – 2022) based on Landsat 4 – 8 satellite data providing multi-band surface reflectance properties were analyzed using the Google Earth Engine time-lapse function (Gorelick *et al.*, 2017). By using the measurement tool, we measured the upslope length from the center of the field to the next field boundary (upslope $\text{length}_{\text{boundary}}$). By using the time-lapse function, we checked if the field boundaries represented an average situation over several years (e.g. roads, pathways, buildings, permanent vegetation). We accounted for within-field structures with high spatio-temporal variability by measuring the upslope length from the center of the field to the next field barrier (upslope $\text{length}_{\text{barrier}}$). Field barriers (e.g. crop cover, temporal walking paths or drainage channels) are located within the investigated fields and represent the latest situation. Field boundaries and barriers should result in deposition at the upslope side and erosion at the downslope side (Figure 5.3) (Govers *et al.*, 1994; Oost *et al.*, 2000). Further, SOC variables were grouped based on these topographical classes and variables to check whether they influence the geochemical variability. Finally, we build several cluster models, non-linear random forest models with partial dependency analysis, structural equation models with path analysis and linear regression models including geochemical and topographical variables as explanatory variables for variations in SOC stocks and soil Δ^{14}C (Table C.1). This has led to a complex statistic with limited informative value since the available data cannot provide a solid explanation for the micro-variability within topographical positions in the test region. Also, the explanatory power of the topographical variables (e.g. upslope $\text{length}_{\text{culm}}$) as proxies for soil redistribution is questionable due to the high degree of land use patchiness and disrupted hydrological connectivity (see Section 5.5.1).

Thus, to analyze the impact of erosion-induced lateral soil fluxes on SOC stocks we returned to more simpler topographic landscape positions based on slope steepness (plateau, slope, footslope) to capture the effect of soil redistribution (see Section 5.3.4). We focused on analyzing the data relative to the mean of the respective plateau positions to highlight potential effects of slope gradient and slope topographic landscape position on SOC stock and geochemical soil properties. Using this data driven approach, our conclusions while being more generic are data-driven without a risk of overinterpreting potential statistical artifacts.

Appendix D

General Appendix

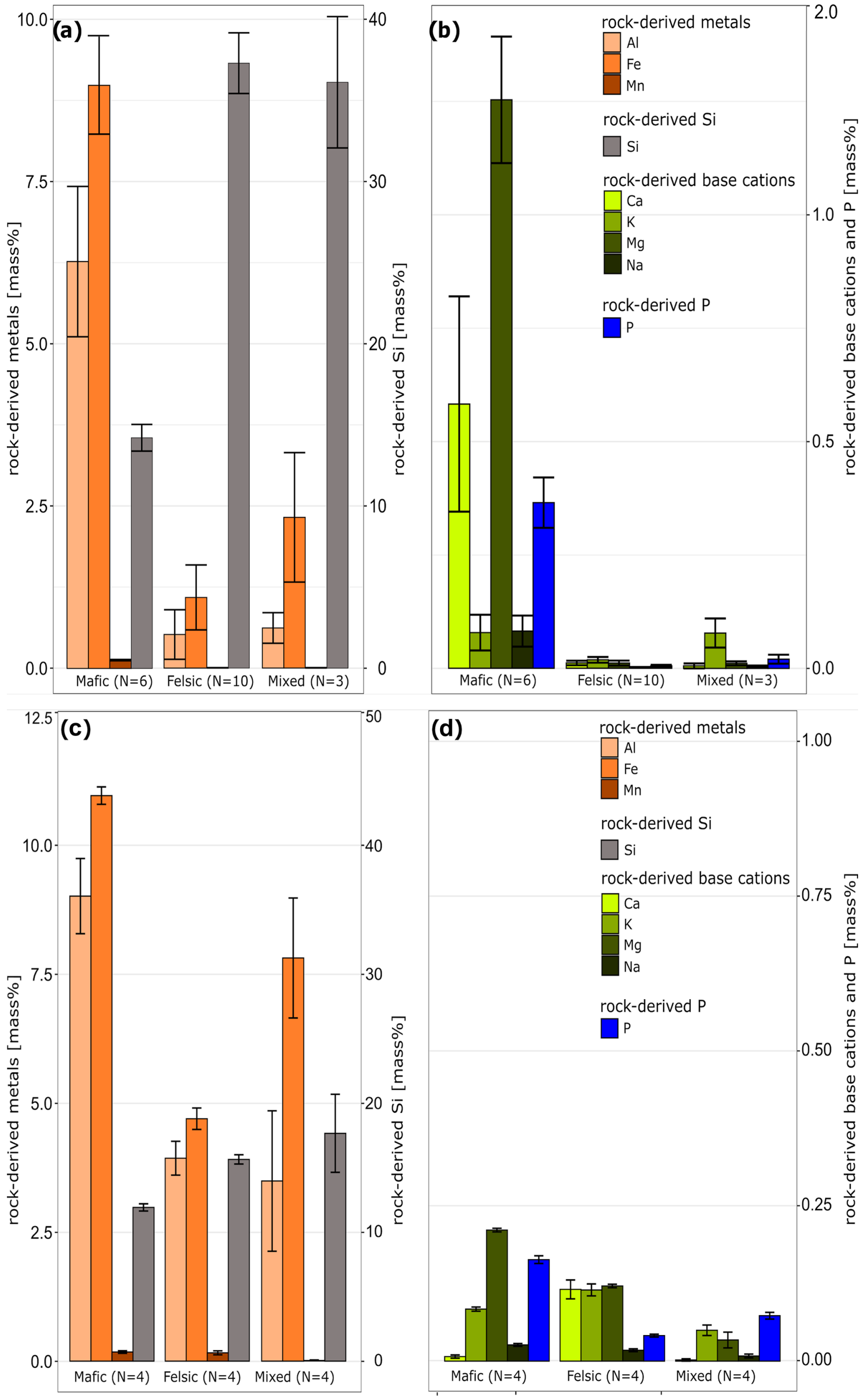

Figure D.1: Panel (a) and (b): Chemical composition of unweathered rock samples representing the parent material for soil formation in three studied geochemical regions (mean ± standard error). Panel (c) and (d): Soil chemical composition of subsoil under forest without erosional lateral soil fluxes in the three investigated geochemical test regions (mean ± standard error). Please note the difference in scale on the y axis between panels (a) and (b) respective (c) and (d). Please refer to Doetterl *et al.* (2021b) for more details.

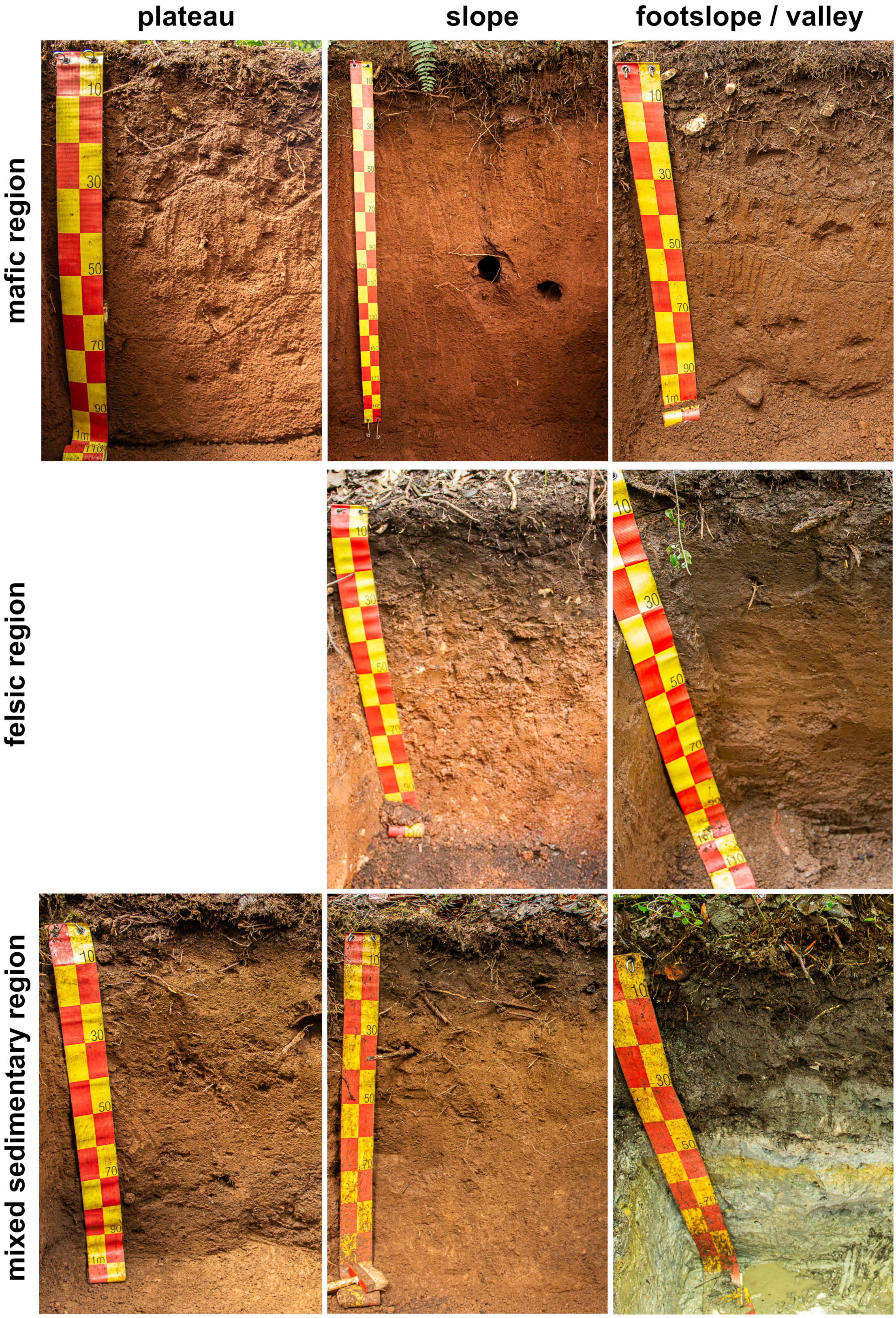

Figure D.2: Soil profiles representative for each geochemical test regions and topographical landscape position under stable, old-growth closed-canopy forests without erosional lateral soil fluxes. Please note no photograph could be taken from the plateau soil profile in the felsic test region.

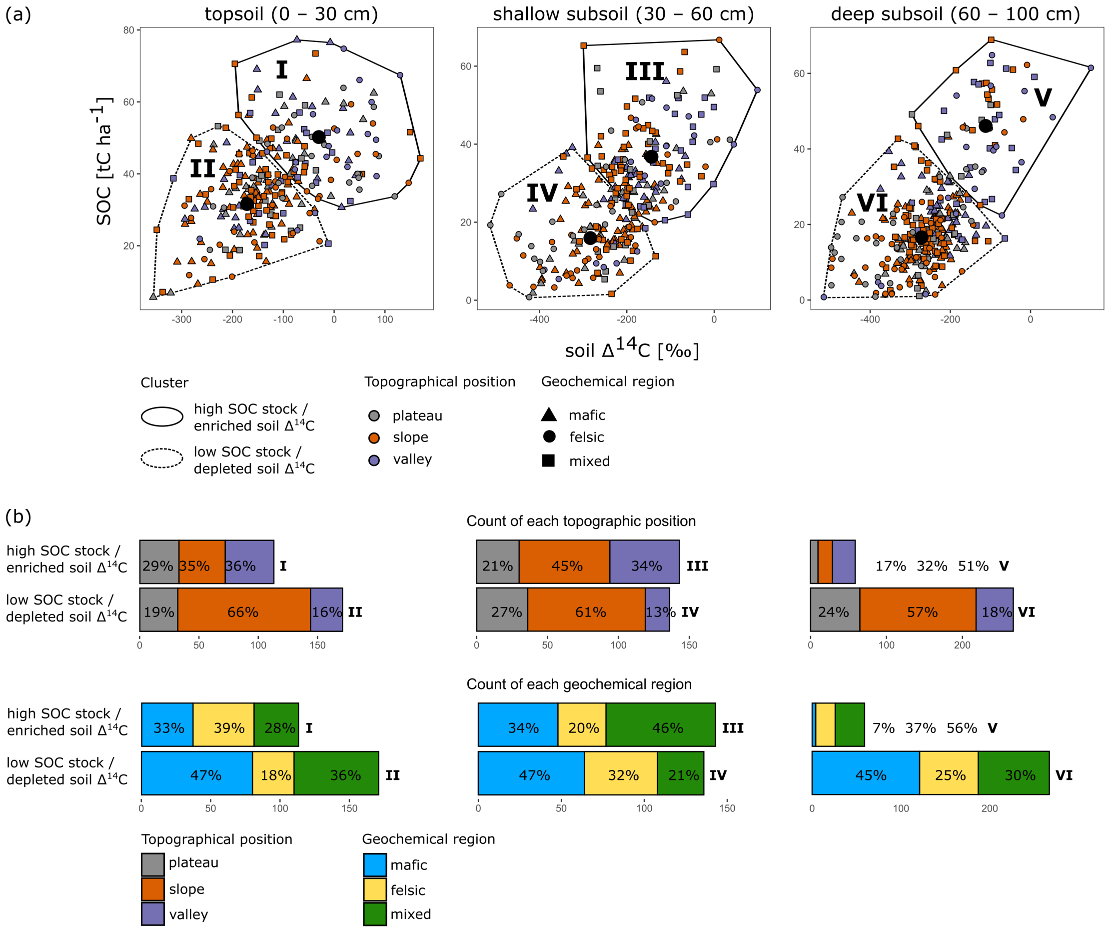

Figure D.3: Cluster analysis considering SOC stock and soil Δ^{14}C of topsoil (0 – 30 cm; n = 113 – 171), shallow subsoil (30 – 60 cm; n = 136 – 143) and deep subsoil samples (60 – 100 cm; n = 59 – 267). Panel a: The K-mean clustering results in six distinct clusters for top-, shallow sub- and deep subsoil, with respect to pairings of SOC stock and soil Δ^{14}C. Circles refer to identified clusters. The black dot in each cluster shows the center point. Colors refer to the topographic position. Symbols refer to geochemical regions. Please note that K-means clustering is based on z-score standardized data, whereas the scatter plot uses unstandardized data. Panel b: Loadings of clusters concerning data from varying topographical positions and geochemical regions. The numbers within bars show the relative amount of topographical positions and geochemical regions in each cluster. The numbers on the x-axis show the absolute amount of topographical positions and geochemical regions in each cluster. Roman numbers refer to cluster numbers.

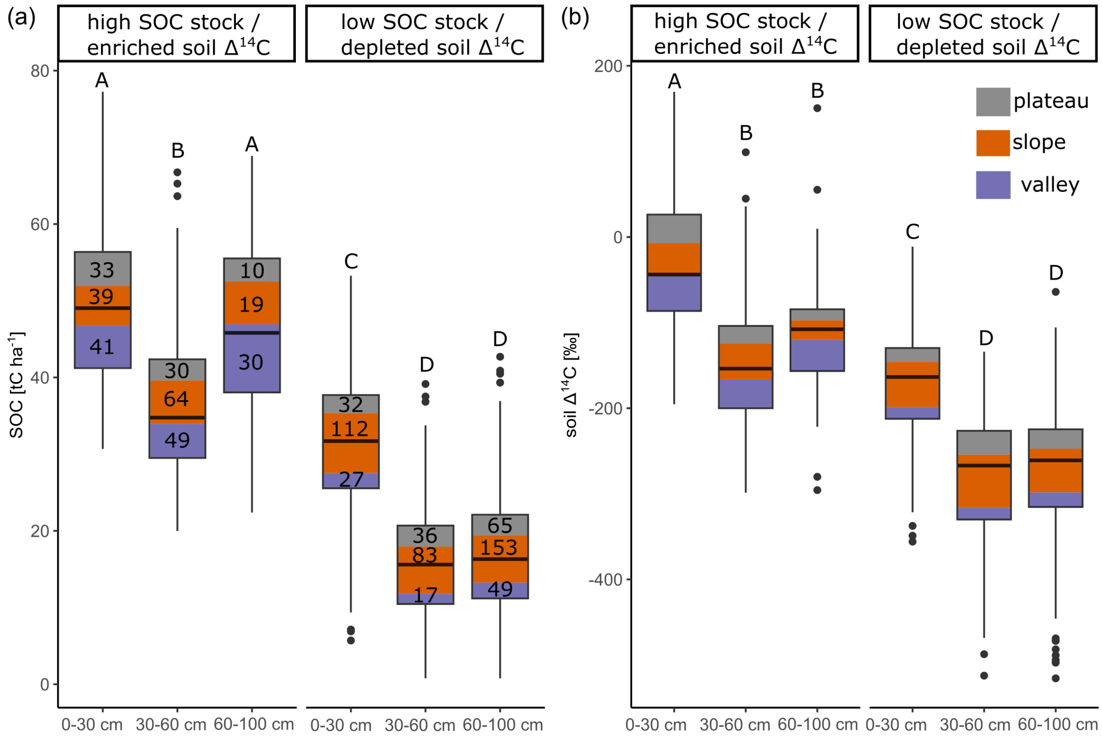

Figure D.4: Comparison of (a) SOC stocks and (b) soil Δ^{14}C across identified clusters for top-, shallow sub- and deep subsoils. The black line inside the boxplot represents the median. The upper end of the boxplot shows the third quartile and the lower end the first quartile. Whysker bars represent minimum and maxima. Black dots show extreme values. Colors refer to the amount of topographic position relative to the boxplot size and numbers refer to the absolute number of each position in the corresponding cluster. Please note that numbers in panel (a) also apply to panel (b). Letters above Whysker bars indicate significant differences in means across clusters ($p < 0.05$).

List of Figures

List of Tables

List of abbreviations

ANOVA	Analysis of variance
Al	Alumina
Bray-P	Bioavailable phosphorus
C	Carbon
Ca	Calcium
CEC	Cation exchange capacity
ECEC	Effective cation exchange capacity
cPOM	Coarse particulate organic carbon
d	Day(s)
DCB extr.	Dithionite-citrate-bicarbonate extractable
DOC	Dissolved organic carbon
DRC	Democratic Republic of the Congo
FAO	Food and Agriculture Organization of the United Nations
Fe	Iron
FOC	Fossil organic carbon
FT-IR	Fourier transform infrared
HCl	Hydrochloric acid
HNO_3	Nitric acid
ICP-OES	Inductively coupled plasma optical emission
K	Potassium
KCl	Potassium chloride
L-horizon	Litter horizon
m	Microaggregate
Ma	Million years
m.a.s.l.	Meters above sea level
MAP	Mean annual precipitation
MAT	Mean annual temperature
Mg	Magnesia
N	Nitrogen
MIR-NIR	Mid infrared-near infrared
Na	Sodium
Mn	Manganese
O-horizon	Organic horizon
OC	Organic carbon
oxalate extr.	Ammonium-oxalate extractable
P	Phosphorous
PC	Principal component
PCA	Principal component analysis
PET	Potential evapotranspiration
pyro. extr.	Pyrophosphate extractable
RMSE	Root mean square error
rPCA	Rotated principal component analysis
Si	Silica
SOC	Soil organic matter
SOM	Soil organic matter
SRO	Short-range-ordered
SRTM-DEM	Shuttle radar topography mission-digital elevation model
SSA	Sub-Saharan Africa
s+c	Silt and clay
TC	Total carbon
TN	Total nitrogen
TRB	Total reserve in base cations
TropSOC	Tropical soil organic carbon
VIF	Variation inflation factor
XRF	X-ray fluorescence

Graphical summary of the thesis

Study I: The role of geochemistry in organic carbon stabilization against microbial decomposition in tropical rainforest soils

Research questions: How does topography and geochemical properties of soil developed from different parent material affect soil organic carbon stabilization, soil carbon fractions and soil carbon turnover in tropical forest systems?

Findings: Despite long-lasting weathering, geochemical properties of soil parent material leave a footprint in tropical forest soils that affects SOC stocks, soil Δ^{14}C and mineral-related carbon stabilization mechanisms.

Study II: Soil carbon stocks in stable tropical landforms are dominated by geochemical controls and not by land use

Research question: What is the effect of parent material mineralogy and its weathering status on SOC stocks and soil C turnover modified by land conversion from tropical forest to subsidence cropland?

Findings: Due to their long weathering history, the investigated tropical soils do not provide enough reactive minerals for the stabilization of the additional C input in high input (tropical forest) compared to low-input (cropland) systems.

Methodological approach

Study design:

- Tropical forest and cropland soils
- Three parent materials
- Three topographic positions
- up to 1 m soil depth

Experiments:

- soil carbon fractions
- soil Δ^{14}C
- geochemical analysis

Study III: Weak connection of soil redistribution and soil organic carbon in the wet Tropics of Africa

Research question: What is the impact of erosion-induced lateral soil fluxes on soil organic carbon stocks and turnover in geomorphologically and geochemically diverse tropical landscapes under small-scale subsistence farming systems?

Findings: Cropland soil organic carbon stocks and turnover do not consistently adhere to classical topography-driven patterns caused by soil redistribution due the low SOC persistence of deposited SOC even in subsoils and the generally limited potential of the investigated soils to stabilize plant C inputs as SOC.

Scientific contributions of the author to the scientific community

Published in different peer-reviewed journals

Reichenbach, M., Fiener, P., Garland, G., Griepentrog, M., Six, J., and Doetterl, S.: The role of geochemistry in organic carbon stabilization against microbial decomposition in tropical rainforest soils, SOIL, 7, 453–475, https://doi.org/10.5194/soil-7-453-2021, 2021.

Reichenbach, M., Fiener, P., Hoyt, A., Trumbore, S., Six, J., and Doetterl, S.: Soil carbon stocks in stable tropical landforms are dominated by geochemical controls and not by land use. Global Change Biol., 29, 2591–2607. https://doi.org/10.1111/gcb.16622, 2023.

Reichenbach, M., Doetterl, S., Van Oost, K., Wilken, F., Muhindo, D., Bamba, F., and Fiener, P.: Low but highly variable soil organic carbon stocks across deeply weathered eroding and depositional tropical landforms, Catena, 254, 108971, https://doi.org/10.1016/j.catena.2025.108971, 2025.

Doetterl, S., Asifiwe, R. K., Baert, G., Bamba, F., Bauters, M., Boeckx, P., Bukombe, B., Cadisch, G., Cooper, M., Cizungu, L. N., Hoyt, A., Kabaseke, C., Kalbitz, K., Kidinda, L., Maier, A., Mainka, M., Mayrock, J., Muhindo, D., Mujinya, B.B., Mukotanyi, S.M., Nabahungu, L., **Reichenbach, M.**, Rewald, B., Six, J., Stegmann, A., Summerauer, L., Unseld, R., Vanlauwe, B., Van Oost, K., Verheyen, K., Vogel, C., Wilken, F., and Fiener, P.: Organic matter cycling along geochemical, geomorphic, and disturbance gradients in forest and cropland of the African Tropics – project TropSOC database version 1.0. Earth System Science Data 13: 4133–4153. https://doi.org/10.5194/essd-13-4133-2021, 2021.

Doetterl, S., Bukombe, B., Cooper, M., Kidinda, L., Muhindo, D., **Reichenbach, M.,** Stegmann, A., Summerauer, L., Wilken, F., and Fiener, P.: TropSOC Database. V. 1.0. GFZ Data Services. https://doi.org/10.5880/FIDGEO.2021.009, 2021.

Summerauer, L., Baumann, P., Ramirez-Lopez, L., Barthel, M., Bauters, M., Bukombe, B., **Reichenbach, M.,** Boeckx, P., Kearsley, E., Van Oost, K., Vanlauwe, B., Chiragaga, D., HeriKazi, A.B., Moonen, P., Sila, A., Shepherd, K., Bazirake Mujinya, B., Van Ranst, E., Baert, G., Doetterl, S., and Six, J.: The central African soil spectral library: a new soil infrared repository and a geographical prediction analysis. SOIL 7: 693–715. https://doi.org/10.5194/soil-7-693-2021, 2021.

Reviewed for different peer-reviewed journals

Chen, Y., Huang, L., Gao, J., Zhou, Z., Mehran, M., Geng, M., He, Y., Zhang, H., and Huang, J.: Long-term Chinese milk vetch incorporation promotes soil aggregate stability by affecting mineralogy and organic carbon, Soil & Tillage Research [manuscript draft], STILL-D-24-00622, 2024.

Jayasudha, M. N., Reddy, M. K., and Bargali, S. S.: Impact of cropping systems on macronutrient distribution and microbial biomass in drought affected soils, EGUsphere [preprint], https://doi.org/10.5194/egusphere-2024-40, 2024.

Kangela, A. M., Shukuru, B. N., Sharma, N. R., Mukotanyi, S. M., Imani, G., Mugumaarhama, Y., Mushagalusa, A. C., Chuma, G. B., Iragi, D. M., Bahati, D. S., Bigabwa, J. B., and Munyahali, W.: Predict soil organic carbon with environmental field inventory variables and Bayesian spatial modeling using INLA-SPDE approach in Eastern Democratic Republic of the Congo, Geoderma Regional [manuscript draft], GEODRS-D-24-00605, 2024.

Laub, M., Corbeels, M., Couëdel, A., Ndungu, S. M., Mucheru-Muna, M. W., Mugendi, D., Necpalova, M., Waswa, W., Van de Broek, M., Vanlauwe, B., and Six, J.: Managing soil organic carbon in tropical agroecosystems: evidence from four long-term experiments in Kenya, SOIL, 9, 301–323, https://doi.org/10.5194/soil-9-301-2023, 2023.

Mekuria, W., Phimister, E., Yakob, G., Tegegne, D., Moges, A., Tesfaye, Y., Melaku, D., Gerber, C., Hallett, P., and Smith, J.: Gully rehabilitation in Southern Ethiopia – value and impacts for farmers, EGUsphere [preprint], https://doi.org/10.5194/egusphere-2024-1125, 2024.

Zhanga, Q., Penga, X., and Zhuc, H.: Conquering Soil Acidification: The synergistic effects of basalt powder, lime, and PAM, EGUsphere[preprint], https://doi.org/10.5194/egusphere-2024-

1870, 2024.

Conference talks

Reichenbach, M., Fiener, P., Garland, G., Griepentrog, M., Six, J., and Doetterl, S.: Organic carbon stabilization controlled by geochemistry in tropical rainforest soils, EGU General Assembly 2021, online, 19–30 Apr 2021, EGU21-7323, https://doi.org/10.5194/egusphere-egu21-7323, 2021.

Reichenbach, M., Fiener, P., Wilken, F., Six, J., Kidinda, L., Mujinya, B., and Doetterl, S.: Soil organic carbon stocks in tropical soil systems under rainforests controlled by geochemistry, EGU General Assembly 2020, Online, 4–8 May 2020, EGU2020-12993, https://doi.org/10.5194/egusphere-egu2020-12993, 2020.

African tropical soils play a pivotal role in global biogeochemical cycles due to the carbon (C) they store and their support of one of the most productive terrestrial ecosystems worldwide. The rapid population growth in tropical Africa has led to a hotspot of modern-day land use change from old-growth forest to cropland, with potentially irreversible changes to soil geochemical properties and fertility. Our understanding of the relationships between C stabilization and geochemical properties is largely derived from studies conducted in temperate regions and tropical regions of America and Asia. However, due to profound differences in climate, landform, local parent material and soil development, the applicability of this knowledge to tropical Africa is limited. This gap in knowledge of the relationship between mineral C stabilization and geochemical properties and the mechanistic controls on C cycling in these soils is limited, which constrains our ability to predict C cycling. This work aims to present the links between mineral C stabilization and geochemical soil properties across disturbance gradients of land conversion and soil erosion in the humid African Tropics. This new insights provide directions on where future research can focus.

Universität
Augsburg
University

WATER SOIL
RESOURCES